National Library
of Canada

Acquisitions and
Bibliographic Services Branch

395 Wellington Street
Ottawa, Ontario
K1A 0N4

Bibliothèque nationale
du Canada

Direction des acquisitions et
des services bibliographiques

395, rue Wellington
Ottawa (Ontario)
K1A 0N4

Your file Votre référence

Our file Notre référence

NOTICE

The quality of this microform is heavily dependent upon the quality of the original thesis submitted for microfilming. Every effort has been made to ensure the highest quality of reproduction possible.

If pages are missing, contact the university which granted the degree.

Some pages may have indistinct print especially if the original pages were typed with a poor typewriter ribbon or if the university sent us an inferior photocopy.

AVIS

La qualité de cette microforme dépend grandement de la qualité de la thèse soumise au microfilmage. Nous avons tout fait pour assurer une qualité supérieure de reproduction.

S'il manque des pages, veuillez communiquer avec l'université qui a conféré le grade.

La qualité d'impression de certaines pages peut laisser à désirer, surtout si les pages originales ont été dactylographiées à l'aide d'un ruban usé ou si l'université nous a fait parvenir une photocopie de qualité inférieure.

Canada

BUBBLE SWARM VELOCITIES IN A FLOTATION COLUMN

Gang Shen

Department of Mining and Metallurgical Engineering
McGill University
Montreal, Canada
May, 1994

A Thesis submitted to the
Faculty of Graduate Studies and Research
in partial fulfilment of the requirements for
the degree of
Doctor of Philosophy

ISBN 0-612-00134-2

ABSTRACT

A new fast response conductivity meter was developed and tested. The "five time constant" of the meter is 0.08 s which meets the requirement for measurements under the dynamic conditions relevant to this work.

In a laboratory column, a bubble interface was created by introducing a step change of gas flow, and the rising velocity of this interface, u_{in}, was measured using a conductivity method with the new conductivity meter. A measurement of the three-dimensional bubble swarm velocity in the column was obtained by interpolation from the u_{in} measured as a function of J_{g2}/J_{g1}, where J_{g1} and J_{g2} are the superficial gas velocities before and after a step change of gas flowrate, respectively. This velocity was referred to as the hindered velocity, u_h. The buoyancy velocity, u_0, was readily determined by switching off the gas, i.e. $u_0 = u_{in}$ at $J_{g2} = 0$.

The average gas velocity, u_g, was corrected to the local average gas velocity, $u_{g,loc}$, to obtain the average gas velocity under the local pressure conditions at a given vertical position in the column. The experimental results showed that u_h was significantly less than $u_{g,loc}$ (and u_g). This is because the u_h is the three-dimensional bubble swarm velocity and $u_{g,loc}$ is the one-dimensional bubble swarm velocity. Unlike $u_{g,loc}$, the u_h was constant along the column, which was supported by theoretical momentum analysis. The u_h is proposed as the key characteristic swarm velocity of the system.

For the air - water only system in the two-dimensional domain, using parabolic models for gas holdup and liquid circulation velocity profiles over the cross section of the column, the u_h could be fitted to the experimental data. For the air - water - frother system, the u_h could not be fitted to the experimental data which is attributed to the air bubbles adopting a circulatory flow pattern.

In the air - water only system under batch operation, Nicklin's derivation (1962), i.e. $u_g=u_0+J_g$, was supported only under restrictive conditions, namely u_g and J_g must be measured at atmospheric pressure. Considering the local values, the experiments showed that $u_{g,loc}$ was not equal to $u_0+J_{g,loc}$. In the presence of frothers under batch or countercurrent operation, the experiments showed that Nicklin's derivation was not applicable even if atmospheric values of u_g and J_g were used.

RÉSUMÉ

Un nouveau conductimètre à réponse rapide a été développé et testé. Le temps de réponse de cet appareil est de 0.08 s ce qui en fait un instrument pouvant effectuer des lectures sous les conditions dynamiques relatives à ce travail.

Dans une colonne verticale de laboratoire, une interface de bulles fut créée en introduisant un changement étagé de débit du gaz. La vélocité ascendante de cette interface, u_{in}, fut mesurée par une méthode basée sur la conductivité et en utilisant le nouveau conductimètre. Une mesure de la vélocité tridimensionnelle de l'essaim de bulles dans la colonne fut obtenue par interpolation de u_{in} mesurée en fonction de J_{g2}/J_{g1}, où J_{g1} et J_{g2} sont, respectivement, les vélocités superficielles du gaz avant et après un changement étagé du débit gazeux. On réfère à cette vélocité comme étant la vécité entravée, u_h. En fermant l'entrée de gaz, la vélocité ascensionnelle ou flottabilité, u_0, fut aisément déterminée, i.e. $u_0 = u_{in}$ pour $J_{g2} = 0$.

Pour obtenir la vélocité moyenne du gaz soumis aux conditions de pression propre à sa position verticale le long de la colonne, la vélocité moyenne du gaz, u_g, fut corrigée, donnant ainsi $u_{g,loc}$, la vélocité localisée moyenne du gaz. Les résultats expérimentaux démontrent que u_h fut, de façon appréciable, moindre que $u_{g,loc}$ (et u_g). Ceci est dû à ce que u_h est la vélocité tridimensionnelle de l'essaim de bulles et que $u_{g,loc}$ en est la vélocité unidimensionnelle. Contrairement à $u_{g,loc}$, u_h est constante le long de la colonne, ce qui est corroboré par l'analyse théorique du momentum. On propose u_h comme la caractéristique clé de la vélocité de l'essaim du système.

Dans un domaine bidimensionnel, pour un système air-eau utilisant des modèles paraboliques pour les profils de vélocité de la charge retenue de gaz et de la circulation de liquide le long d'une coupe transversale de la colonne, la valeur de u_h peut être ajustée à la valeur expérimentale u_h. Pour le système air-eau-mousse, u_h n'a pu être ajustée aux données expérimentales ce qui est attribuable au fait que les bulles d'air adoptent un tracé d'écoulement circulatoire.

Dans un système air-eau pour un procédé par lots, la dérivation de Nicklin (1962), i.e. $u_g=u_0+J_g$ fut confirmée sous des conditions restrictives seulement, de sorte que u_g et J_g doivent être mesurées à pression atmosphérique. Considérant les valeurs localisées, les expériences ont montrées que $u_{g,loc}$ n'est pas égale à $u_0+J_{g,loc}$. En présence de moussant, dans un procédé à

contre-courant ou dans un procédé par lots, les expériences ont démontré que la dérivation de Nicklin n'est pas applicable même si on utilise les valeurs de u_g et J_g à pression atmosphérique.

ACKNOWLEDGEMENTS

Grateful acknowledgement is hereby made of the helpful contributions of the many whose names do not appear on the title page. First of all, I am indebted to two people:

My supervisor, Prof. J.A. Finch, for his enthusiasm, keen interest, excellent advice and constant support throughout the research program.

My wife, Zijin Xu, for her support and understanding.

As well, I gratefully acknowledge Prof. A.R. Laplante for helpful discussions and advice. Discussions with Prof. Z. Xu, Dr. C.O. Gomez and Dr. S.R. Rao are also acknowledged.

I want to thank my colleagues in the mineral processing group for their friendship and help. I also want to thank all members of the Department of Mining and Metallurgical Engineering, and specially to Mr. M. Leroux for his assistance in the laboratory.

TABLE OF CONTENTS

NOMENCLATURE

A_c cross-sectional area of column, cm^2

A_{cell} cross-sectional area of cell, cm^2 (Equation 2.3)

A_ε cross-sectional area of cell at ε_g, cm^2 (Equation 2.13)

b_g body force on unit volume of gas phase (Equation 7.59)

b_l body force on unit volume of liquid phase (Equation 7.60)

C_x relative standard deviation of variable x

C_{hg} parameter in Equation 7.48

C_t parameter in Equation 7.96

C_z parameter in Equation 7.97

C_I intercept in Equation 5.21

D diameter of column, cm

d_b bubble diameter, cm

d_{bs} Sauter mean size of bubbles, cm (Equation 5.4)

d_{bv} volume diameter of bubble, cm (Equation 5.3)

d_{max} maximum bubble size, cm (Equation 5.7)

d_{min} minimum bubble size, cm (Equation 5.6)

d_p volumetric diameter of solid particles, cm (Equation 7.69)

Eo Eötvös number (Equation 4.33)

F_b buoyancy force (Equation 4.24)

F_c gravity force of container (Equation 3.2)

F_d drag force (Equation 4.23)

F_i total force acting on balance at time i (Equations 3.2 and 3.5)

$F_{m,i}$ vertical momentum force of gas - liquid flow at time i (Equations 3.2 and 3.5)

$F_{w,i}$ gravity force of gas - liquid mixture at time i (Equations 3.2 and 3.5)

f volumetric fraction of dispersed phase (Equation 2.7)

f_g force acting on gas from liquid, per unit volume of gas (Equation 7.59)

f_l force acting on liquid from gas, per unit volume of liquid (Equation 7.60)

g gravitational acceleration, 981 cm/s^2

H parameter in Equations 4.31 and 4.32
distance from P1 to top of bubble bed, cm (Equation 5.32)
distance from top of column, m (Equation 7.3)

h depth below top of column (Equation 7.5)

h_i length of Cell i, cm (Equations 7.7 - 7.11)

I	current, A
i	current density, A/cm^2
J	correlating constant in Equation 4.29
J_f	superficial fluid velocity, cm/s (Equation 7.69)
J_g	superficial gas velocity, cm/s
$J_{g,loc}$	local superficial gas velocity, cm/s (Equation 7.4)
$J_g(\phi)$	local superficial gas velocity over the cross section of column, cm/s (Equation 7.31)
J_l	superficial liquid velocity, cm/s
j	average velocity or total local flux, cm/s
j_{gl}	drift flux of gas, cm/s
j_{l_o}	drift flux of liquid, cm/s
K	conductance, S (siemens) or mS
K_l	conductance of a liquid system (Equation 2.11)
$K(t)$	time-dependent conductance, mS (Equation 2.17)
K_w	conductance of medium, S (Equation 2.21)
K_c	conductance of two-phase system (Equation 2.12)
K_∞	actual value of conductance of medium, mS (Equation 2.17)
L	length of column, cm length of cell, cm (Equation 2.4) distance between Electrodes 7 and 6, 51 cm (Equations 3.9 and 5.10) distance from top of bubble bed to lip of column, cm (Equation 5.31)
L_c	length of cell at ε_g (Equation 2.14)
M	Morton number (Equation 4.29)
m	coefficient in Equation 4.46
m_c	coefficient in Equation 7.31
mu	momentum of system (Equation 7.52)
m_V	mass of fluid in control volume (Equation 7.57)
N	number of bubbles per unit volume of column (Equation 4.54)
N_t	number of bubbles surfacing per second (Equation 4.54)
n	constant in model of parabolic gas holdup profile (Equation 7.19)
P	pressure, dyne/cm^2 (Equation 5.32)
P_o	pressure on top of column (Equation 7.1)
P_{loc}	local pressure in column (Equation 7.1)
$P_{loc,i}$	local pressure in Cell i in column, dyne/cm^2 (Equations 7.7 - 7.11)
p	height of water (= P / (ρ_l g)), cm (Equation 5.34)

Q total volumetric flowrate, cm^3/s

Q_g volumetric flowrate of gas, cm^3/s

$Q_{g,i}$ volumetric flowrate of gas at time i (Equations 3.4 and 3.6)

Q_l volumetric flowrate of liquid, cm^3/s

$Q_{l,i}$ volumetric flowrate of liquid at time i (Equations 3.4 and 3.6)

R resistance, Ω

radius of column, cm (Equation 7.19)

R_A resistance of mixture of air bubbles and water, Ω (Equation 5.9)

R_B ratio of gas volume in $0 \leq \phi \leq \phi_B$ to total gas volume in unit height of the column (Equation 7.47)

R_{c6} resistance in Cell 6, Ω (Equation 3.10)

Re_b bubble Reynolds number

Re_p particle Reynolds number

R_w resistance of medium between two electrodes, Ω (Equation 2.18)

$R_{w,l}$ resistance of liquid between two electrodes, Ω (Equation 2.24)

$R_{w,c}$ resistance of gas - liquid mixture between two electrodes, Ω (Equation 2.24)

R_0 resistance of water, Ω (Equation 5.9)

R_1 resistance of resistor in circuit, Ω (Equation 2.18)

average resistance of mixture of air bubbles and water, Ω (Equations 3.11 and 5.22)

R_2 average resistance of water, Ω (Equations 3.12 and 5.22)

r radial distance from centre of column, cm

r_b bubble radius, cm

r_{bc} radius of curvature at front of a bubble, cm (Equation 4.28)

S control surface in Equation 7.53

S_x standard deviation of variable x

S_1 slope in Equation 5.21

S_2 slope in Equation 5.24

T time constant of conductivity meter, s (Equations 2.17 and 2.23)

period during which the interface rises from E7 to E6, s (Equations 3.9 and 5.10)

t time, s

time from moment of change in conductance, s (Equation 2.17)

time from moment of change in V_{in}, s (Equation 2.23)

t temperature, °C (Equation 3.1)

U velocity of control volume (Equation 7.54)

u_B velocity of bubbles, cm/s (Equation 4.54)

u_b bubble terminal velocity, cm/s
u_{bc} velocity of a bubble rising in a column, cm/s (Section 4.4.3)
u_{bp} terminal velocity of particles (Equation 4.46)
u_f velocity of settling front of particles in a batch system (Equation 4.46)
u_{fr} velocity of fluid relative to control volume (Equation 7.58)
u_g average gas velocity, cm/s
u_{gc} velocity of bubbles in control volume (Equation 7.74)
$u_{g,loc}$ local average gas velocity, cm/s (Equation 7.12)
u_{gj} drift velocity of gas, cm/s
u_{gl} relative velocity of gas to liquid, cm/s
u_{go} $= J_{go} / \varepsilon_{go}$, m/s (Equation 7.3)
u_{gr} velocity of gas phase relative to control volume (Equation 7.59)
$u_g(\phi)$ bubble velocity over the cross section of column, cm/s (Equation 7.31)
u_h bubble hindered velocity, cm/s
u_{in} interface velocity, cm/s
u_l average liquid velocity, cm/s
u_{lc} liquid velocity in control volume (Equation 7.65)
u_{lg} relative velocity of liquid to gas, cm/s
u_{lj} drift velocity of liquid, cm/s
u_{lr} velocity of liquid phase relative to control volume (Equation 7.60)
u_{lw} liquid circulation velocity at column wall (Equation 7.23)
$u_l(\phi)$ liquid circulation velocity (Equation 7.22)
$u_{r,c}$ relative velocity in control volume (Equation 7.74)
u_S velocity of fluid on control surface (Equation 7.53)
u_{Sr} velocity of fluid on control surface relative to control surface (Equation 7.53)
u_s slip velocity ($= u_g - u_l$), cm/s
u_{sp} slip velocity between particles and liquid, cm/s (Equation 4.47)
u_{top} velocity of top of bubble bed, cm/s (Equation 5.25)
$u_{top,v}$ velocity of top of bubble bed measured by video, cm/s (Equation 5.31)
$u_{top,p}$ velocity of top of bubble bed measured by pressure, cm/s (Equation 5.37)
$u_{top,c}$ velocity of top of bubble bed measured by conductivity method, cm/s (Equations 5.40, 5.43, 5.44, 5.45 and 5.46)
u_V velocity of fluid in control volume (Equation 7.53)
u_{Vr} velocity of fluid in control volume relative to control volume (Equation 7.54)
u_0 buoyancy velocity, cm/s
u_1 velocity of bottom of bubble swarm in Cell 6, cm/s (Equation 5.24)

$u_{1,C5}$ velocity of bottom of bubble swarm in Cell 5, cm/s (Equation 5.18)
$u_{2,C6}$ velocity of top of bubble swarm in Cell 6, cm/s (Equation 5.17)
V control volume in Equation 7.53
V_A potential on electrode A, volt (Equation 2.2)
V_B potential on electrode B, volt (Equation 2.2)
volume of each bubble (Equation 4.55)
V_a volume flowrate of liquid across A-A' in system (a) (Equation 4.57)
V_b volume flowrate of liquid across A-A' in system (b) (Equation 4.58)
average bubble volume, cm^3 (Equation 5.2)
V_{ellip} volume of an ellipsoid, cm^3 (Equation 5.1)
V_g total volume of gas in column, cm^3 (Equation 4.1)
$V_{g,i}$ volume of gas at time i (Equations 3.3 and 3.6)
$V_{l,i}$ volume of liquid at time i (Equations 3.3 and 3.6)
V_{in} AC input voltage of convertor, volt (Equation 2.23)
V_o output voltage of function generator, volt (Equation 2.19)
V_{out} DC output voltage of convertor, volt (Equation 2.23)
V_w voltage drop between two electrodes, volt (Equation 2.18)
V_l voltage drop on resistor, volt (Equation 2.18)
w_g remaining forces on gas, per unit volume of gas (Equation 7.59)
w_l remaining forces on liquid, per unit volume of liquid (Equation 7.60)
w_0 w in control volume under steady conditions (Equation 7.93)
$\bar{x}$ average value of x
$<X>$ average value of X over cross-sectional area of column (Equation 7.15)

Greek Symbols

$\alpha_{25°C}$ coefficient of conductivity variation per degree Celsius with respect to conductivity at 25°C (Equation 3.1)
β parameter in Equation 2.7
parameter in Equation 7.3
γ apparent relative conductivity
γ^* apparent relative conductance (Equation 2.15)
Δh distance between two water levels in two manometers, cm (Equation 3.19)
ΔL distance between two manometers, cm (Equation 3.19)
∇V potential gradient, volt/cm
ε_f fluid holdup (Equation 7.69)

ε_g	gas holdup
ε_{gc}	gas holdup at centre of column (Equation 7.19)
ε_{go}	gas holdup on top of column (Equation 7.1)
ε_{gw}	gas holdup at wall of column (Equation 7.19)
ε_{gi}	gas holdup in Zone i (Equation 5.25)
ε_l	liquid holdup
$\varepsilon_g(\phi)$	parabolic radial gas holdup profile (Equation 7.19)
κ	conductivity, S/cm or mS/cm
κ_m	apparent conductivity (Equation 2.7)
κ_l	conductivity of the continuous liquid phase (Equation 2.10)
κ_c	apparent conductivity of the mixture for any ε_g (Equation 2.10)
κ_1	conductivity of continuous phase (Equation 2.7)
κ_2	conductivity of dispersed phase (Equation 2.8)
$\kappa_{25°C}$	conductivity of liquid at 25°C, mS/cm (Equation 3.1)
λ	$= d_b / D$
μ_l	liquid viscosity, g/cm·s
μ_f	fluid viscosity (Equation 7.69)
μ_u	mean of population of u_0 (Equation 3.18)
μ_ε	mean of population of ε_g (Equation 3.26)
ν_M	molecular viscosity, m^2/s (Equation 7.22)
ν_t	turbulent kinematic viscosity, m^2/s (Equation 7.22)
ρ_f	density of fluid (Equation 7.58)
ρ_g	gas density, g/cm^3
ρ_l	liquid density, g/cm^3
ρ_S	density of fluid on control surface (Equation 7.53)
ρ_V	density of fluid in control volume (Equation 7.53)
σ	surface tension, dyne/cm
ΣF	sum of forces acting on system in the overall momentum equation (Equation 7.52)
ΣF_{diff}	sum of forces in direction z on control volume, per unit volume of fluid in the differential momentum equation (Equation 7.58)
τ	shear stress (Equation 7.21)
ϕ	dimensionless radial position in column ($= r/R$)
ϕ_s	sphericity of solid particles (Equation 7.69)

LIST OF FIGURES

LIST OF TABLES

LIST OF APPENDICES

CHAPTER 1

INTRODUCTION

The flotation column was patented in Canada in the early 1960s by Boutin and Tremblay (Canadian patents 680,576 and 694,547), although units of similar geometry have a much longer history (Gahl, 1916). Early descriptions of the column and testwork are given by Wheeler (1966) and Boutin and Wheeler (1967). Industrial applications of the flotation column grew slowly in the 1970s; however, since 1980 the number of new applications has been increasing rapidly (Wheeler, 1988; Finch and Dobby, 1990a). In the book by Finch and Dobby (1990a), the operating and design features of flotation columns were extensively illustrated with data from the laboratory and industrial scale.

1.1 Description of Flotation Column

A typical flotation column is illustrated schematically in Figure 1.1. Commercial units are now anywhere from 3 - 17 m in height and 0.5 - 3.0 m in diameter (either circular, square or rectangular). The side of a square column or the diameter of a circular column is used to designate column size.

The column consists of two distinct zones: the collection zone (also termed slurry, pulp or recovery zone) and the froth zone (also known as cleaning zone). These two zones are separated by an interface which defines the level or froth depth. Feed is introduced to the collection zone below the interface. Solid particles, settling downwards due to gravity, are contacted countercurrently with a bubble swarm, rising upwards from the bubble generators (spargers) located near the bottom of the column. Hydrophobic particles collide with and attach to the bubbles and are transported to the froth zone. Hydrophilic and less hydrophobic particles are removed from the bottom of the column through the tailings port. In the froth zone, wash water is added near the top of the froth to prevent the hydraulic entrainment of fine hydrophilic particles into the concentrate (Dobby and Finch, 1985; Yianatos, 1987). Usually, a net downward flow of water through the froth, called a positive bias, is maintained.

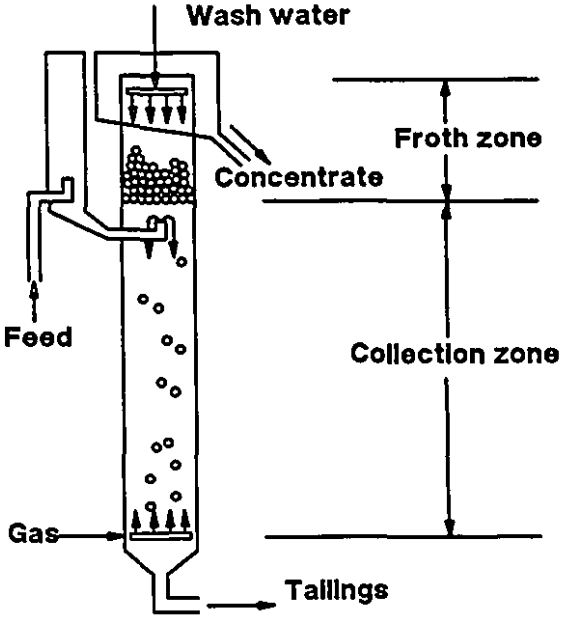

Figure 1.1 Schematic illustration of a flotation column.

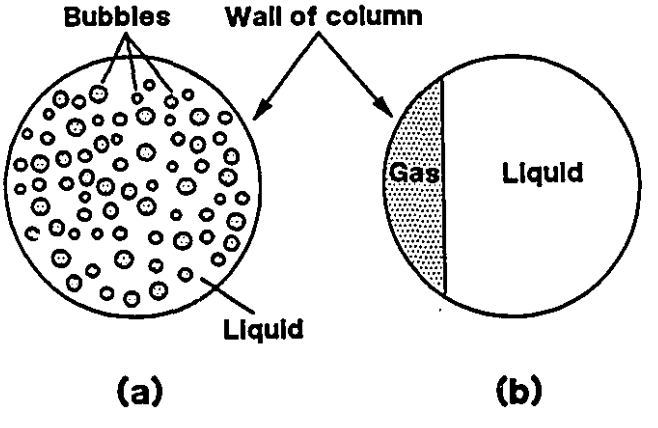

Figure 1.2 Two conditions over the cross section of the flotation column: (a) a real condition; (b) a condition for the physical meaning of the average gas velocity.

1.2 Background to Problem and Objective of Present Work

For control, a convenient division is to consider stabilizing control and optimizing control (Finch and Dobby, 1990a; 1990b). Stabilizing control, which must be established first, in the case of column flotation demands as a minimum control of level, with bias control as a useful addition; optimizing control requires control of grade and recovery (frequently unmeasured variables) according to economic criteria.

The gas rate is an important manipulated variable in the control of the flotation column. Table 1.1 is an extract of the process matrix for flotation columns presented by Finch and Dobby (1990a).

Table 1.1 Response of controlled variables (measured and unmeasured) to increase in gas rate (after Finch and Dobby, 1990a)

Manipulated Variables	Controlled variables *						
	Level	Froth depth	Bias rate	Solids in conc	Gas holdup	Grade	Recovery
Gas rate	+(-) F	-(+) F	- S	- S	+- F	- M	+- M

* where '+' indicates the controlled variable increases as gas rate is increased, '-' indicates the controlled variable decreases as gas rate is increased, S indicates a slow response, F indicates a fast response, M indicates a moderately fast response, and () indicates a steady state response if possibly different from dynamic response.

From Table 1.1, it can be seen that gas rate has a fast effect on the level. When the gas rate changes, the bubble swarm velocity is changed, and the rate of change of the level should be a function of the bubble swarm velocity. Now a basic question appears: how to measure the bubble swarm velocity in the three dimensional domain. Nicklin (1962) obtained expressions equating the bubble swarm velocity to the average gas velocity in the one dimensional domain, which will be introduced in Chapter 4. The average gas velocity, u_g, is defined as

$$u_g = \frac{J_g}{\varepsilon_g} = \frac{Q_g}{A_c \varepsilon_g} \tag{4.8}$$

where J_g is the superficial gas velocity, ε_g is the gas holdup, A_c is the cross section area of the column, and Q_g is the volume gas flowrate. Figure 1.2 (a) shows the real condition: the different sized bubbles distribute over the cross section of the column and the bubble swarm velocity should be the average of the bubble velocities. Figure 1.2 (b) illustrates the physical meaning of the average gas velocity: the gas flow individually passes through a tube which has the cross section area $A_c\varepsilon_g$. These two conditions are not necessarily equivalent.

The objective of the thesis is to develop a new method based on electrical conductivity to measure the three-dimensional bubble swarm velocity in the column and relate it to u_g. To attain the goal, a new custom-designed conductivity meter was necessary to make measurements under dynamic conditions.

1.3 Structure of Thesis

The thesis consists of eight chapters. In Chapter 1, the flotation column is introduced, and the objective and the structure of the thesis are also presented.

Chapter 2 reviews the principles and application of conductivity to process measurements in flotation columns and describes the development of a new conductivity meter.

Chapter 3 presents the equipment and experimental techniques. The computer controlled experimental procedure and data acquisition system are described. A preliminary experiment is presented to test the new conductivity meter and the experimental control system.

Chapter 4 reviews the theory of two-phase bubbly flow with particular emphasis on its application in flotation columns.

Chapter 5 presents the experimental results of the air - water only (i.e. without frother) system and the analysis of the data. The measurements of the swarm velocities - interface velocity, hindered velocity, and buoyancy velocity - are presented. The effect of the superficial gas velocity on the bubble velocity is presented. The relationship between the interface velocity and the velocity of top of the bubble bed is derived and tested.

Chapter 6 presents the experimental results and data analysis for the air - water - frother system with DF250C and DF1263 under batch and countercurrent operation conditions.

In Chapter 7 the three dimensional bubble swarm velocity in columns and its properties are discussed. The axial profiles of the gas holdup, superficial gas velocity and average gas velocity in the column are discussed.

In Chapter 8 the conclusions of the work, claims for original research, and recommendations for future work are presented.

CHAPTER 2

CONDUCTIVITY METHOD AND INSTRUMENTATION

In this chapter, the conductivity method and its application to making process measurements in flotation columns are presented. The development of a new conductivity meter for this task under dynamic conditions is described.

2.1 Conductivity Method

2.1.1 Definition of Electrical Conductivity

Electrical conductivity is defined as the ability of a substance to conduct electric current. The electrical conductivity has several equivalent terms: specific conductance (Condon, 1967; Andrews, 1970; Barrow, 1973), specific conductivity (Adamson, 1979; Kasper, 1940), and conductivity (Atkins, 1982; Levine, 1988; Braunstein and Robbins, 1971; Gilmont and Walton, 1956; Lord Rayleigh, 1892; Meredith and Tobias, 1962; Wagner, 1962). In this thesis, the term conductivity and the symbol κ will be used.

The conductivity is the proportionality constant in Ohm's law. In the three dimension domain, Ohm's law gives

$$i = -\kappa \nabla V \tag{2.1}$$

where i is the current density (A/cm^2), ∇V is the potential gradient (volt/cm), and κ is the conductivity (Ω^{-1}/cm). In fact, the conductivity is the reciprocal of the resistivity (Ω/cm) and the conductance is the reciprocal of the resistance (Ω). The unit Ω^{-1} for the conductance is written as mho (i.e. ohm spelled backwards); however, the SI name for the conductance is the siemens (S): 1 S $\equiv$ 1 Ω^{-1}. Thus the SI units of conductivity are S/m. For convenience, the cgs unit S/cm will be used in this thesis. The conductivity is an intensive property that may be thought of as the conductance of a cube of 1 cm edge, assuming the current to be perpendicular to opposite

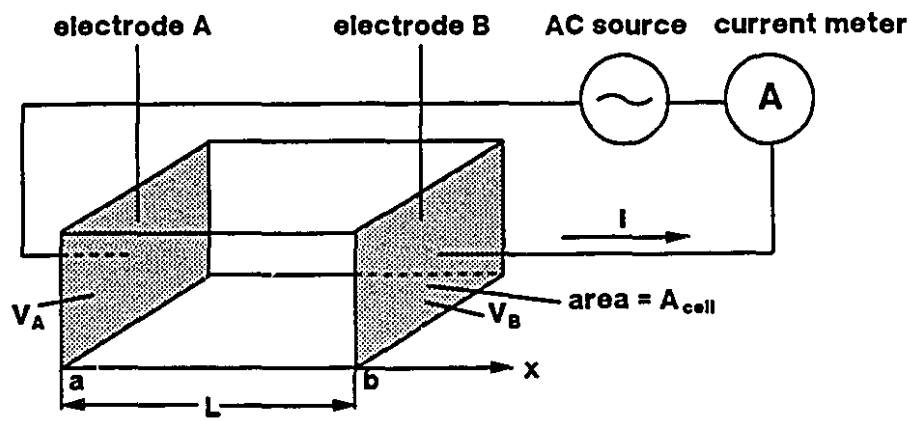

Figure 2.1 Conductivity cell and electric circuit to measure conductance of electrolyte.

faces of the cube (Braunstein and Robbins, 1971).

2.1.2 Measurement of Conductivity

All substances possess conductivity to some degree, but the magnitude varies widely, ranging from extremely low (insulators such as glass and air) to very high (silver and metals in general). The interest here is in measuring the conductivity of water containing dissolved ionic compounds, i.e. the conductivity of an electrolyte.

The resistance of an electrolyte solution can not be measured using direct current, because the changes in concentration of the electrolyte and the accumulation of electrolysis products at the electrodes change the resistance of the solution. Instead of direct current, an alternating current is used to overcome these effects.

Figure 2.1 illustrates a conductivity cell for measurement of the conductivity of an electrolyte. This cell is constructed of an insulating material with metallic pieces (usually stainless steel) on opposite faces. Using the ideal condition that the current flow is at right angles to and constrained by the area of the plates, the resistance of the electrolyte, R, is obtained from the electric circuit shown in Figure 2.1

$$R = \frac{drop\ of\ potential}{current} = \frac{V_A - V_B}{I} \tag{2.2}$$

where I is the current in the electric circuit, and V_A and V_B are the potentials on the electrodes A and B, respectively. In the case of a linear conductor, the current density on any equipotential surface is constant, hence

$$I = \int_{A_{cell}} i\, dA_{cell} = i\, A_{cell} \tag{2.3}$$

$$V_A - V_B = -\,(V_B - V_A) = -\int_a^b \nabla V\, dL = -\nabla V\,(b - a) = -\nabla V\, L \tag{2.4}$$

where A_{cell} is the cross-sectional area of the cell, L is the length of the cell, and a and b are the positions of the electrodes A and B, respectively. Substituting Equations 2.1, 2.3 and 2.4 into 2.2, yields

$$K = \frac{1}{R} = \frac{I}{V_A - V_B} = -\frac{i}{\nabla V}\frac{A_{cell}}{L} = \kappa \frac{A_{cell}}{L} \tag{2.5}$$

where K is the conductance of the electrolyte. In this equation, the term A_{cell}/L is defined as the conductivity cell constant with unit cm^{-1}. The conductivity can be calculated from the resistance

$$\kappa = \frac{1}{R}\frac{L}{A_{cell}} \tag{2.6}$$

2.1.3 Maxwell's Model

The conductivity method is a standard laboratory technique to measure the gas holdup in the gas - liquid system. Generally, the conductivity of the gas - liquid system under bubbly flow conditions (a continuous liquid phase plus one gas dispersed phase) depends on the conductivities of the two phases and their relative amounts. However, the relationship between the conductivity of the dispersion and the concentration of the dispersed phase is not linear (Maxwell, 1892).

Maxwell (1892) considered a large sphere (continuous phase) which contains many small spheres (dispersed phase) with a different conductivity. Assuming the distance between small spheres is large enough so that their effect in disturbing the path of the current may be taken as

negligible, the apparent conductivity of this large sphere is given by (Maxwell, 1892; Turner, 1976),

$$\kappa_m = \kappa_1 \frac{1 + 2\beta f}{1 - \beta f} \tag{2.7}$$

where κ_1 is the conductivity of the continuous phase, f is the volumetric fraction of the dispersed phase of conductivity κ_2, and β is given by,

$$\beta = \frac{\kappa_2 - \kappa_1}{\kappa_2 + 2\kappa_1} \tag{2.8}$$

Directly adapting this expression to a column where the mixture consists of water and dispersed air bubbles, then,

$\kappa_m = \kappa_c$, apparent conductivity of the mixture for any ε_g;

$\kappa_l = \kappa_l$, conductivity of the continuous liquid phase ($\varepsilon_g = 0$);

$\kappa_2 = 0$, conductivity of air;

$f = \varepsilon_g$, fractional gas holdup;

Thus, the gas holdup can be expressed in terms of apparent relative conductivity γ,

$$\varepsilon_g = \frac{1 - \gamma}{1 + 0.5\gamma} \tag{2.9}$$

where

$$\gamma = \frac{\kappa_c}{\kappa_l} \tag{2.10}$$

Using Maxwell's model to estimate gas holdup, the apparent relative conductivity has to be measured, which means the cell constant must be known.

Yianatos et al. (1985) developed a geometrical model based on the concept of tortuosity to estimate local gas holdup from conductance measurements in a two-phase column. In this model, the conductance of a liquid system, K_l, is

$$K_l = \kappa_l \frac{A_{cell}}{L} \tag{2.11}$$

and for a homogeneous dispersion of air bubbles in the liquid system, the conductance of the system, K_c, can be expressed by

$$K_c = \kappa \frac{A_c}{L_c} \tag{2.12}$$

where

$$A_c = A_{cell} (1 - \varepsilon_g) \tag{2.13}$$

and from the geometrical model of Yianatos et al. (1985) for the bubbling zone in a flotation column, the effective length between electrodes is given by

$$L_c = L (1 + 0.55 \varepsilon_g) \tag{2.14}$$

Combining Equations 2.11 - 2.14, the gas holdup in the bubbling zone is given by

$$\varepsilon_g = \frac{1 - \gamma^*}{1 + 0.55\gamma^*} \tag{2.15}$$

where γ^* is the apparent relative conductance given by,

$$\gamma^* = \frac{K_c}{K_c} \tag{2.16}$$

From the experiments of Yianatos (1987), Xu (1990) and Uribe-Salas (1991), it was shown that the design of electrode cell to measure the conductivity of the dispersion is very important. Uniform and parallel current lines between two opposite electrodes in the cell are essential. Once this condition is satisfied, either Equation 2.9 or 2.15 is adequate.

2.1.4 Time Constant of Conductivity Meter

Figure 2.2 illustrates a typical experimental set-up for measuring the gas holdup in a column with a commercial conductivity meter (Uribe-Salas, 1991). The output response of the commercial conductivity meter to a change in the conductance of the medium in the column is not instantaneous and follows the first order lag equation given by

$$K(t) = K_\infty (1 - e^{-t/T}) \tag{2.17}$$

where $K(t)$ is the time-dependent conductance measurement, mS; K_∞ is the actual value of conductance of the medium whose conductance is being measured, mS; t is the time from the

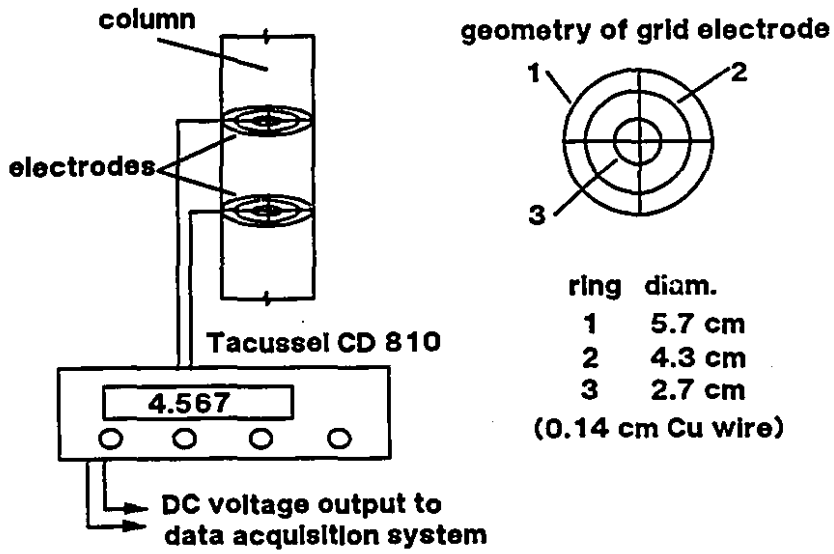

Figure 2.2 Measurement of gas holdup in a laboratory column with a conductivity meter.

moment of change in the conductance, s; and T is the time constant of the conductivity meter, s.

Uribe-Salas (1991) measured the response of a commercial conductivity meter (Tacussel, Model CD 810) to a step change in conductance from 0 to 5.25 mS and a time constant of about 0.46 s was obtained. In accordance with the first order lag model, 99% of the actual conductance value would be obtained after an elapse of time of five time constants, e.g. 2.3 s for Tacussel Model CD 810. Although this is adequate for steady state measurements, it is too long for measurements in a dynamic process.

2.2 A New Conductivity Meter

For the measurement of bubble swarm velocity in a column, a conductivity meter with a short time constant is necessary. Figure 2.3 shows the schematic diagram of a new conductivity meter designed for the present purpose. It consists of three parts:

(a) an function generator (BK Model 3011B) to generate a sine wave signal at a fixed frequency;
(b) a resistor for measuring AC current in the circuit; and
(c) an AC to DC convertor to convert an AC voltage to a DC voltage which can be read by an A/D data acquisition board.

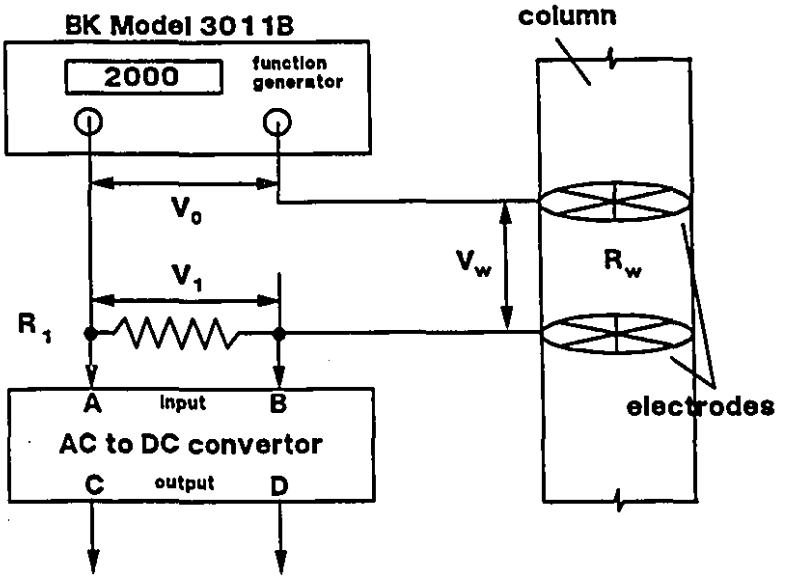

Figure 2.3 Schematic diagram of a new conductivity meter.

2.2.1 Measurement of Conductance in Column

If the input impedance of the AC to DC convertor is very large, the input current of AC to DC convertor is small enough to be neglected. From Kirchhoff's current law,

$$\frac{V_1}{R_1} = \frac{V_w}{R_w} \tag{2.18}$$

and from Kirchhoff's voltage law,

$$V_o = V_1 + V_w \tag{2.19}$$

where V_o is the output voltage of the function generator, volt; R_l is the resistance of the resistor in the circuit, ohm; V_l is the voltage drop on the resistor, volt; R_w is the resistance of the medium (i,e. the gas - liquid mixture) between two electrodes, ohm; and V_w is the voltage drop on the medium between two electrodes, volt. Substituting Equations 2.19 into 2.18, yields

$$R_w = R_1 \frac{V_o - V_1}{V_1} \tag{2.20}$$

Therefore, the conductance of the medium between two electrodes (S), K_w, can be calculated

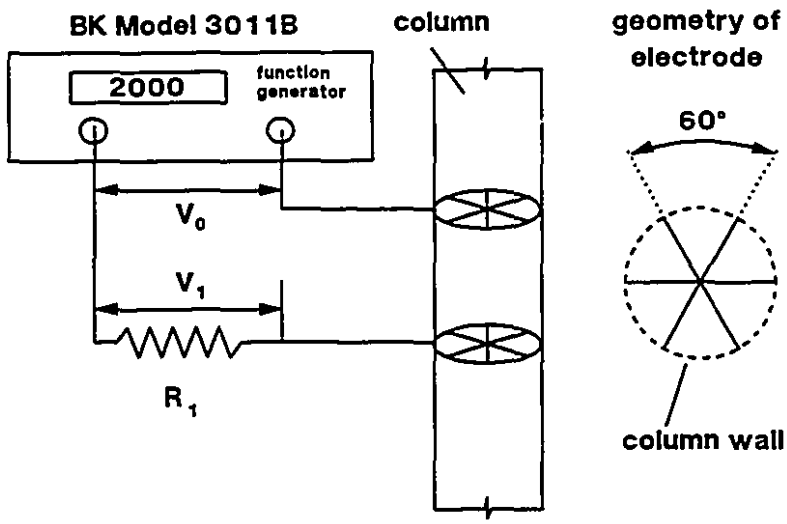

Figure 2.4 Experimental set up to evaluate effects of the frequency and voltage of V_o on the conductance of the tap water.

from the measured V_o and V_1

$$K_w = \frac{V_1}{R_1 (V_o - V_1)} \tag{2.21}$$

2.2.2 Frequency and Voltage of Output of Function Generator

For the design of the conductivity meter, the first consideration was to chose the proper frequency and voltage for V_o, i.e. the output of the function generator (Figure 2.3). Usually, a frequency of 1 KHz and voltages less than 1 V are recommended for the measurement of conductance (Cole and Coles, 1964).

To examine the effects of the frequency and voltage on the measured conductance of tap water, two experiments were carried out with the experimental set up shown in Figure 2.4. A 5.7 cm inside diameter Plexiglas column was used. Two electrodes separated 14 cm were used inside the column (25.5 cm^2). The electrodes were a "grid" design, consisting of three stainless steel wires (1.4 mm in diameter) with a cross angle between each two wires of 60° (Figure 2.4). A 4½ digital multimeter (KEITHLEY 177 Microvolt DMM) was used for the measurement of

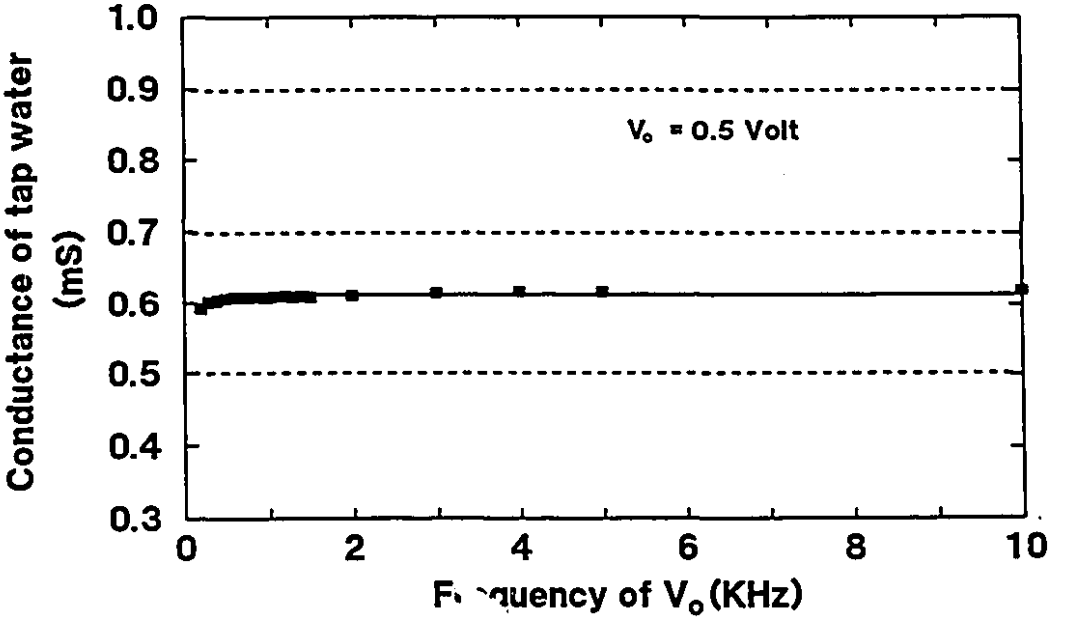

Figure 2.5 Effect of frequency of V_o on measured conductance of tap water.

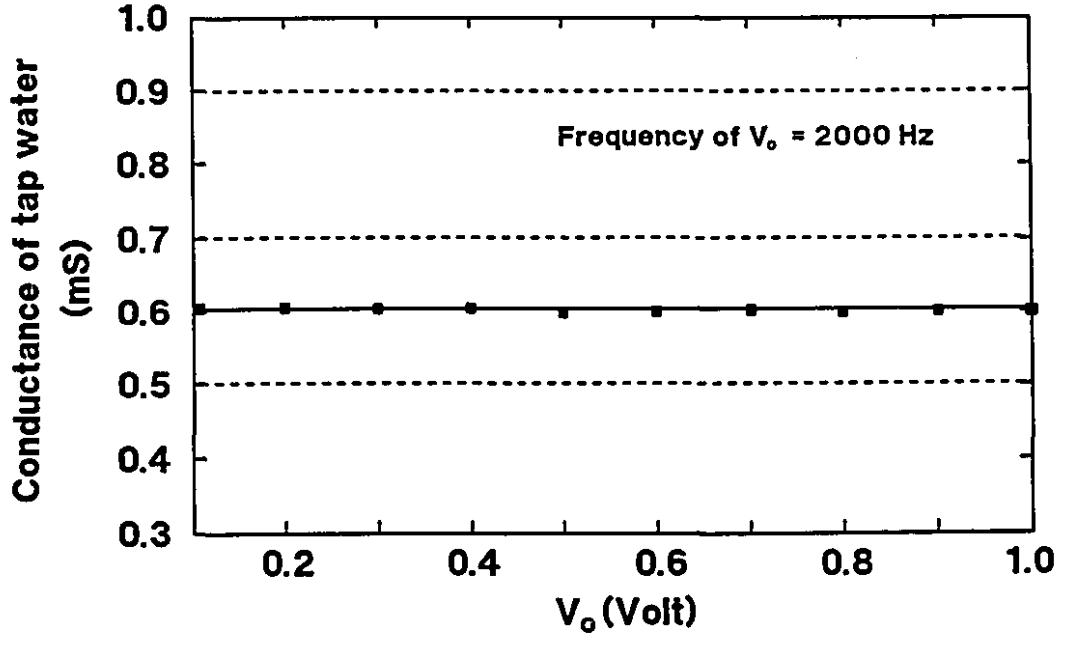

Figure 2.6 Effect of voltage of V_o on measured conductance of tap water.

V_o and V_1. The temperature of the tap water was 25.5 °C.

Substituting the measured V_o and V_1 into Equation 2.21, the values of the conductance were calculated and the results are presented in Figures 2.5 and 2.6. Figure 2.5 shows that when the frequency of V_o is larger than 600 Hz the conductance of the tap water is constant at about 0.6 mS. In Figure 2.6, at frequency = 2000 Hz, the conductance of the tap water remains constant as V_o changes in the range 0.1 - 1.0 V.

Based on the experimental results, a frequency of 2000 Hz and voltage of 0.1 - 1.0 V were selected for V_o.

2.2.3 Resistor

In order to obtain an accurate R_w, the value of resistance R_1 must be chosen properly (Figure 2.3). From theory, the optimal R_1 is equal to R_w. When this conductivity meter is used under different conditions, R_1 should be changed to match the value of R_w.

From Equation 2.20,

$$V_1 = V_o \frac{R_1}{R_1 + R_w} \tag{2.22}$$

and from Maxwell's model (Equations 2.9 and 2.10),

$$\gamma = \frac{\kappa_c}{\kappa_l} = \frac{1 - \varepsilon_g}{1 + 0.5\,\varepsilon_g} \tag{2.23}$$

As discussed in Section 2.1.3, the κ can be replaced by K because of uniform electric field between the two grid electrodes

$$\gamma = \frac{\kappa_c}{\kappa_l} = \frac{K_c}{K_l} = \frac{R_{w,l}}{R_{w,c}} \tag{2.24}$$

where $R_{w,l}$ and $R_{w,c}$ are the resistances of the liquid and the gas - liquid mixture, respectively. Substituting Equations 2.23 and 2.24 into 2.22, yields

$$V_1 = V_o \frac{R_1}{R_1 + R_{w,l} \frac{1 + 0.5\varepsilon_g}{1 - \varepsilon_g}} \tag{2.25}$$

(i) R_l is equal to $R_{w,l}$

Substituting V_o = 1.0 volt, $R_l = R_{w,l}$ = 5700 Ω, and ε_g = 0 into Equation 2.25, V_l is equal to 0.5 volt. When V_o, R_l and $R_{w,l}$ remain the same values and ε_g varies to 0.001 (i.e. 0.1%), the V_o is equal to 0.49962 volt. Here a change of 0.1% in ε_g causes the difference of 3.8 X 10^{-4} volt in V_l. The accuracy of the 12-bit A/D board is 2.44 X 10^{-4} (= $1/2^{12}$) volt for the input range of 0 - 1 volt. It can be seen that in this case the data acquisition system can read the variation of 0.1% in ε_g.

(ii) R_l is larger than $R_{w,l}$

When V_o = 1.0 volt, ε_g = 0, R_l = 5700 Ω and $R_{w,l}$ = 570 Ω, V_l is equal to 0.90909 volt by using Equation 2.25. As ε_g = 0.001, V_l is 0.90897 volt. The difference of V_l is 1.2 X 10^{-4} volt, which is less than 2.44 X 10^{-4} volt and can not be recognized by the 12-bit A/D board.

The above example shows that a large difference between R_l and $R_{w,l}$ reduces the accuracy of the measured ε_g.

2.2.4 AC to DC Convertor

For communicating with a data acquisition system, the new conductivity meter must output a DC voltage signal to an A/D board. To meet this requirement, an AC to DC convertor must be designed to transform the AC signal to a DC signal with a short response time and a unit detection ratio, where the detection ratio is defined as

$$detection\ ratio = \frac{DC\ output\ voltage}{AC\ input\ voltage} \tag{2.26}$$

(i) A diode circuit

The simplest AC to DC convertor is a diode circuit which has a diode, a capacitor and a resistor (Figure 2.7). However, Figure 2.7 shows this diode circuit has a varying detection ratio. Obviously, the diode circuit is not suitable as the AC to DC convertor in the conductivity meter.

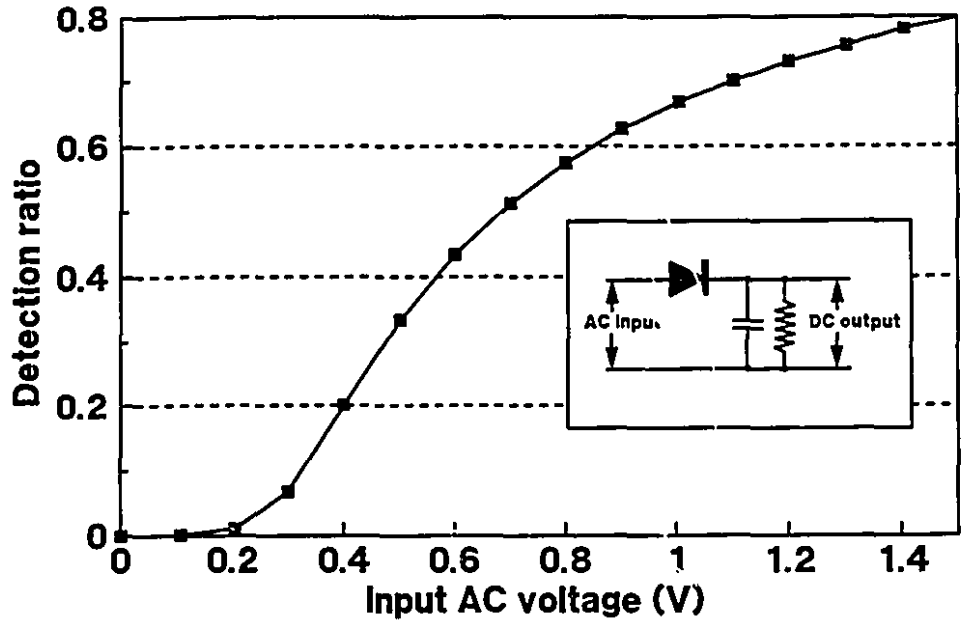

Figure 2.7 Detection ratio of diode circuit.

(ii) AC to DC convertor

Figure 2.8 shows the circuit diagram of the AC to DC convertor developed for the new conductivity meter. The detection ratio of the AC to DC convertor is equal to 1.

The convertor has two AC signal input ends: A is the input high end and B is the input low end which must be grounded; and two DC signal output ends: C is the output negative end and D is the output positive end. Note, both C and D can not be connected to the ground. When C and D are connected to an A/D data acquisition board, the A/D board must work in the differential input model not the single end model. If the A/D board works in the single end model, C or D in the AC to DC convertor will be connected to the ground by the A/D board and the conductivity meter will not work properly.

2.2.5 Response Time of AC to DC Convertor

Although computer simulation software can be used for evaluating the response time of the

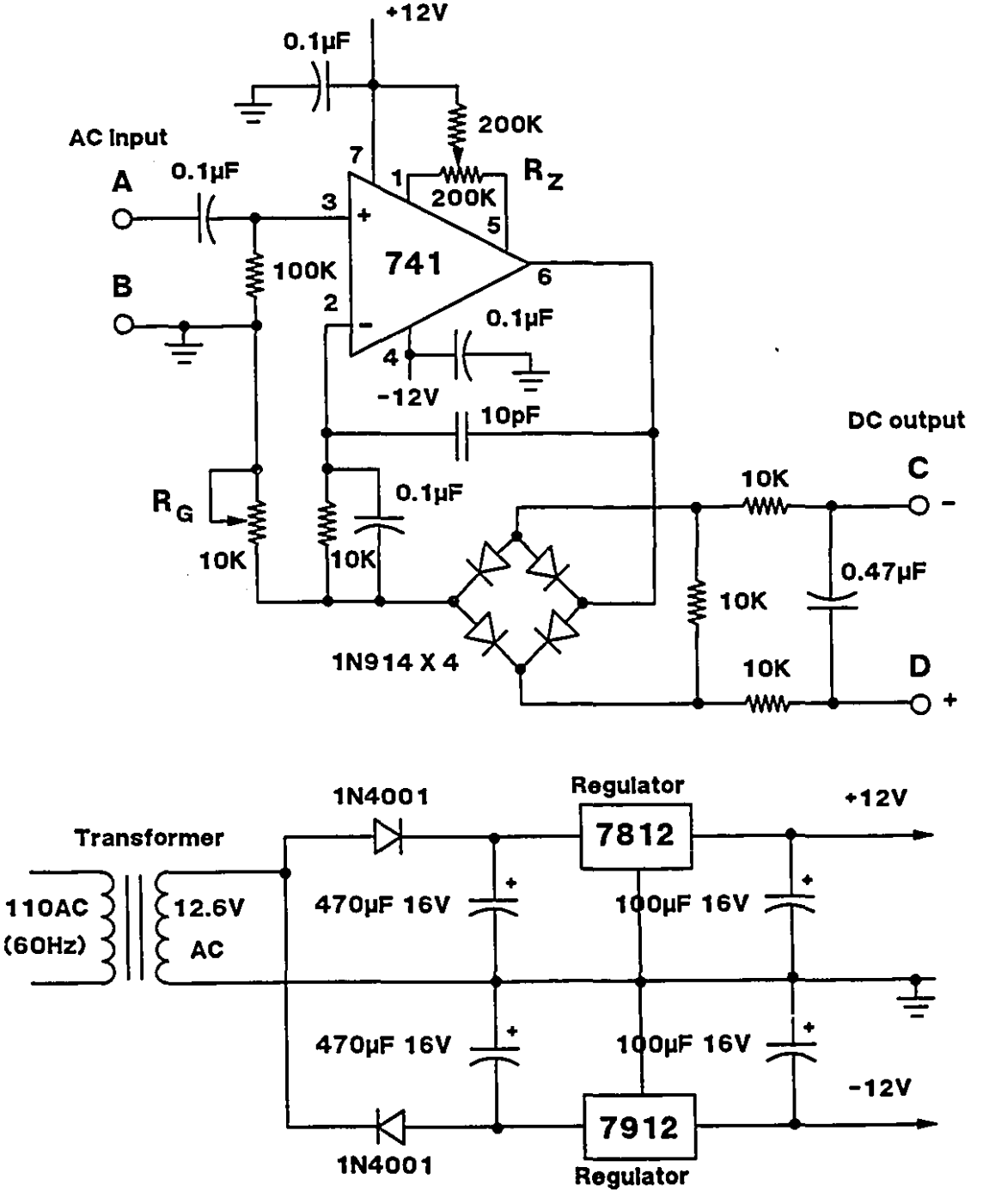

Figure 2.8 Circuit diagram of AC to DC convertor.

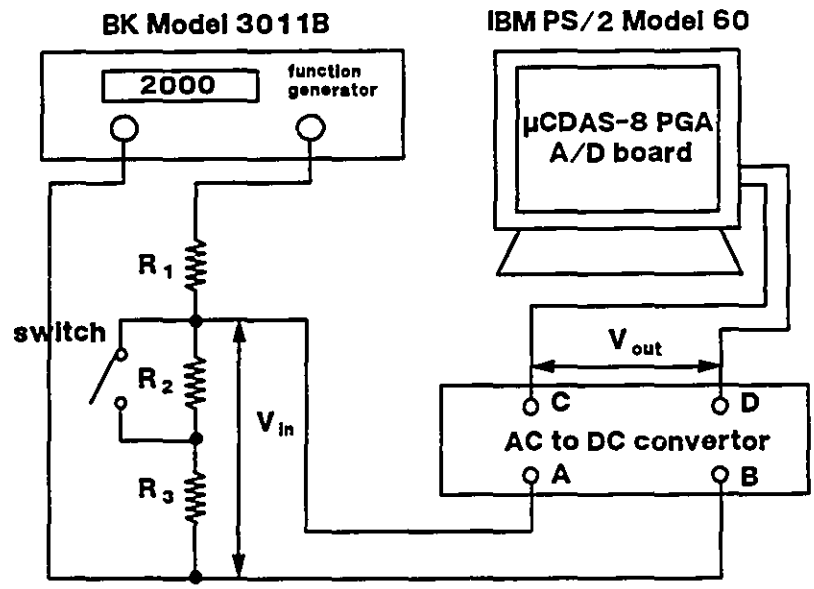

Figure 2.9 Experimental set up to measure the response time of the AC to DC convertor.

electric circuit, there is often a large difference between the measured and simulated value when using the nominal values of the components instead of the real values; for example, a nominal 10K resistor may have a real value of 10,500 ohm. Two experiments were carried out by introducing an increasing step or a decreasing step change in the input AC signals to the measured response time of the AC to DC convertor. The configuration of the experiment is shown in Figure 2.9. The V_{in} is the AC input voltage and V_{out} is the DC output voltage of the convertor.

A function generator (BK Model 3011B) was used to supply a constant AC signal. A switch circuit, which consists of a switch and three resistors R_1, R_2 and R_3, was used to produce a step change in V_{in}. A computer (IBM PS/2 Model 60) equipped by a 12-bit A/D board (μDAS-8 PGA) was used to record the output DC signal of the convertor. The data acquisition rate was 4000 samples per second.

When the switch was off, the V_{in} was 0.6 V; when the switch was on, the V_{in} was 0.06 V. The procedure of the experiment was

(a) turn off (or turn on) the switch;

(b) start the data acquisition at 0 s;

(c) turn on (or turn off) the switch;

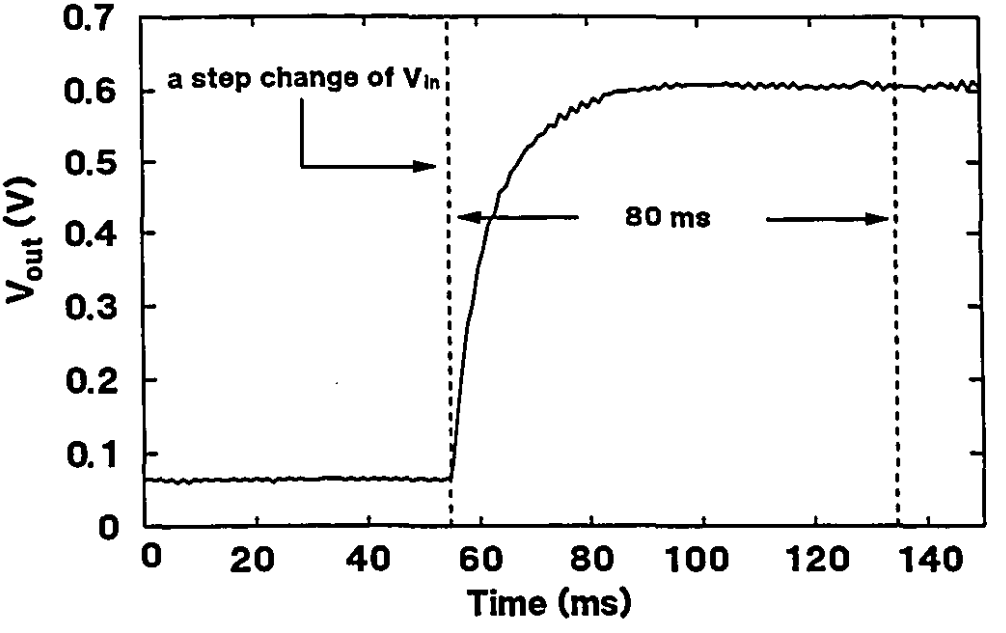

Figure 2.10 Response of V_{out} to an increasing step change of V_{in}.

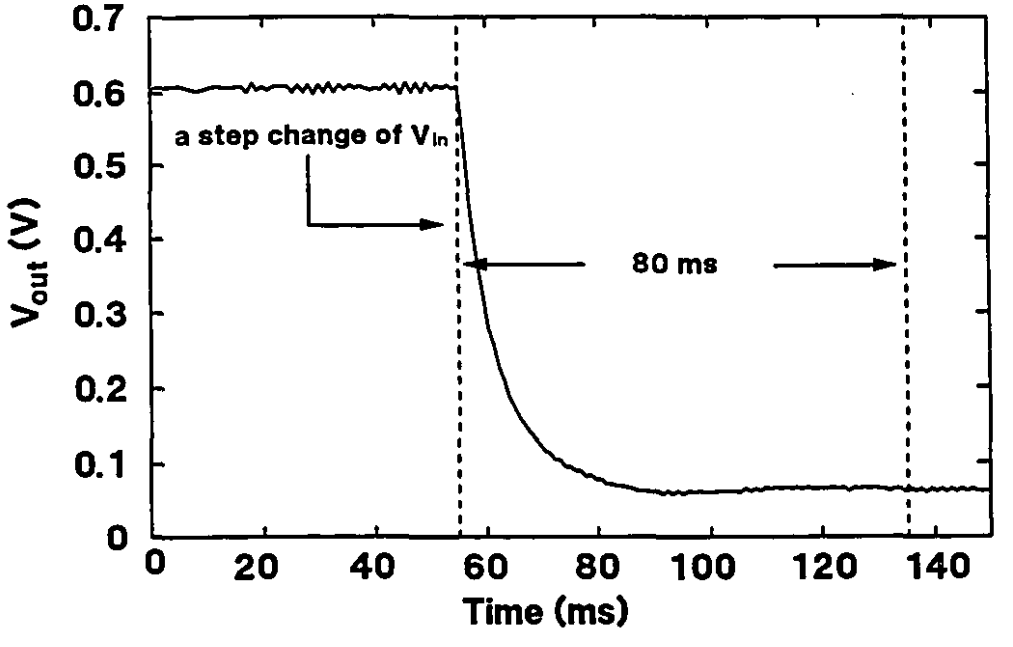

Figure 2.11 Response of V_{out} to a decreasing step change of V_{in}.

(d) stop the data acquisition at 2 s.

Figures 2.10 and 2.11 present the experimental results obtained from an increasing step change and a decreasing step change in V_{in}, respectively. The response of V_{out} to an increasing step change in V_{in} follows

$$V_{out} = V_{in} (1 - e^{-t/T}) \tag{2.27}$$

where unit for V_{in} and V_{out} is volt; t is the time from the moment of the step change in V_{in}, s; and T is the time constant of the AC to DC convertor, s. The response of V_{out} to a decreasing step change in V_{in} follows

$$V_{out} = V_{in} \ e^{-t/T} \tag{2.28}$$

The same time constant of about 0.016 s was obtained by fitting the data in Figure 2.10 into Equation 2.27 and the data in Figure 2.11 into Equation 2.28. Therefore, the "five time constant" for the AC to DC convertor is 0.08 s. This means that using this new conductivity meter each conductance measurement takes 0.08 s. Comparing with 2.3 s in the commercial conductivity meter (Tacussel Model CD 810), the response time of the newly - designed conductivity meter meets the requirement for measurements under dynamic conditions, such as the measurement of the bubble swarm velocity in columns.

2.2.6 Accuracy of AC to DC Convertor

From Figure 2.3, it can be seen that the AC to DC convertor is the key to the new conductivity meter. The accuracy of the new conductivity meter depends on the accuracy of the AC to DC convertor.

The AC to DC convertor has two adjustable resistors: R_Z is used to set the zero point, and R_G is used to adjust the gain, i.e. the detection ratio (Figure 2.8). The procedure for the calibration of the AC to DC convertor is

(a) connect the input ends A to B, and adjust R_Z until the DC voltage on the pin 6 of 741 (Figure 2.8) is equal to zero;
(b) apply a stable 0.5 V AC voltage to the input ends A and B, and adjust R_G until the DC output voltage on the output ends C and D is equal to 0.5 V.

Because of interactions inside the circuit, steps (a) and (b) need to be repeated several times.

Table 2.1 gives the evaluation of accuracy for the AC to DC convertor. The relative error of the AC to DC convertor is defined as

$$relative\ error = \frac{AC\ input\ voltage - DC\ output\ voltage}{AC\ input\ voltage} \qquad (2.29)$$

From Table 2.1, it may be observed that the relative errors are in an acceptable range, from 1.00% to -0.60%, when V_o varies in the range 0.1 - 1.0 V. In fact, the conductivity meter was used in the range V_o = 0.3 - 0.7 V in the experiments. In this case, the relative error was reduced, being in the range 0.33% to -0.29%.

Table 2.1 Evaluation of accuracy for AC to DC convertor

Input AC (V)	Output DC (V)	Relative Err.(%)
0.000	0.000	0.00
0.100	0.101	1.00
0.206	0.207	0.49
0.299	0.300	0.33
0.407	0.407	0.00
0.501	0.501	0.00
0.599	0.599	0.00
0.697	0.695	-0.29
0.801	0.797	-0.50
0.900	0.895	-0.56
1.000	0.994	-0.60

CHAPTER 3

EXPERIMENTAL TECHNIQUES

In this chapter, the experimental techniques and data acquisition system are introduced. A preliminary experiment for measuring the buoyancy velocity of a bubble swarm and the gas holdup is presented.

3.1 Experimental Techniques

A laboratory Plexiglass column, 5.7 cm in diameter and 391 cm in height, was used (Figure 3.1). A porous stainless steel sparger (hole diameter $\approx$ 50 μm, density $\approx$ 10 holes / cm^2, and surface area = 84 cm^2) installed at the bottom of the column was used to generate the air bubbles. Wash water was added at about 1.5 cm below the lip of the column through a 4 cm diameter perforated plastic distributor, and there was no feed introduced into the column. Two peristaltic pumps (Masterflex Model 7520) were used to supply and control the flows of the wash water and underflow.

The experimental techniques involved six procedures: (a) conductance measurement for the bubble swarm velocity and gas holdup, (b) liquid flowrate measurement of overflow and underflow streams, (c) liquid flowrate measurement for wash water, (d) air flowrate measurement and control, (e) pressure measurement, and (f) pump control.

3.1.1 Conductance Measurement

Figure 3.2 illustrates the conductance measurement system. Seven grid electrodes were installed in the column wall with the geometry shown in Figure 2.4. The electrode 1, i.e. E1, was located 20 cm below the lip of the column, and the distance between each two electrodes was 51 cm. The cell constant (A_{cell}/L) was equal to 0.50 for each cell.

An ERB-24 DPDT relay board was used for sequentially connecting the electrodes to the conductivity meter. The new conductivity meter was used for measuring the conductance values

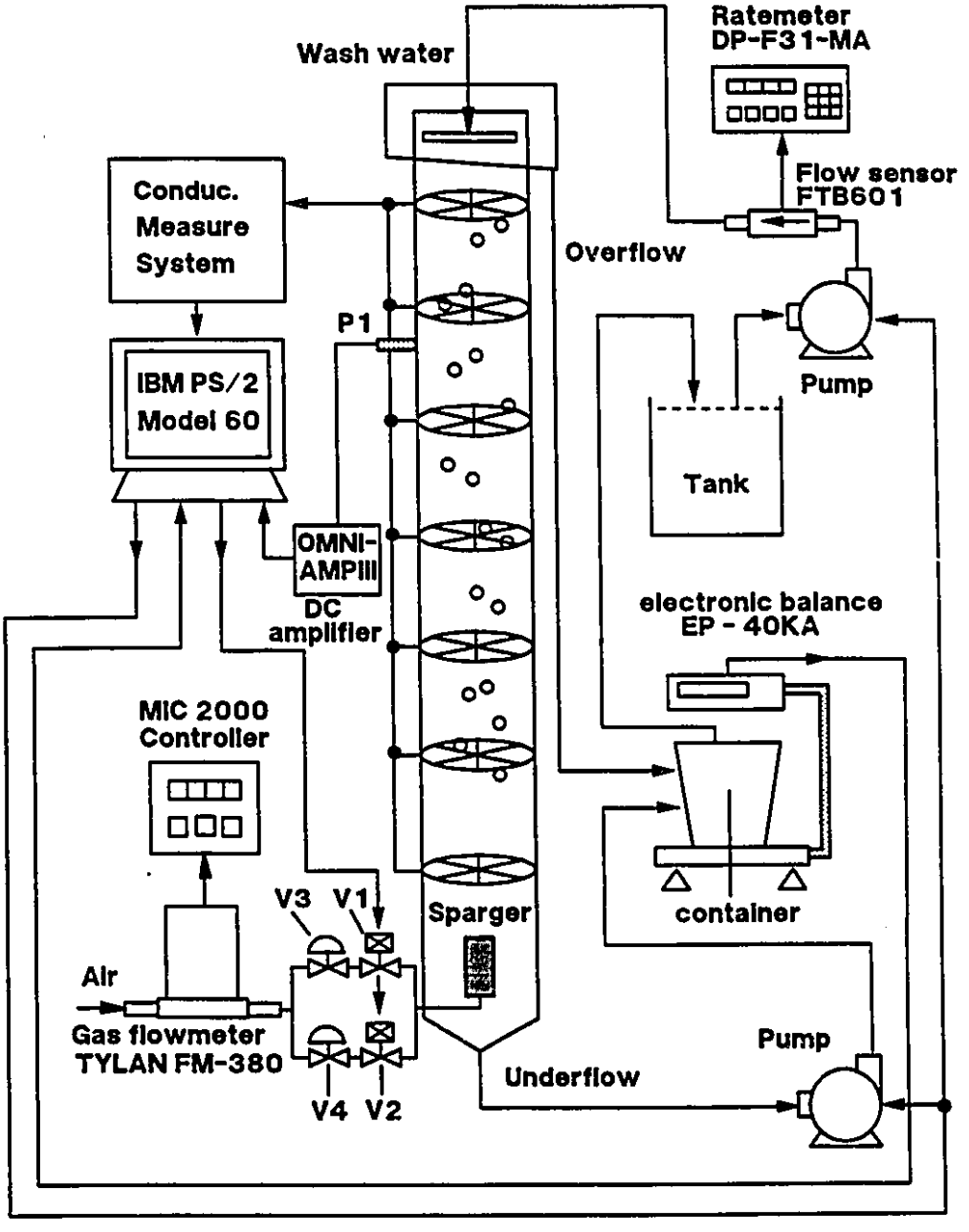

Figure 3.1 Schematic illustration of experimental set-up.

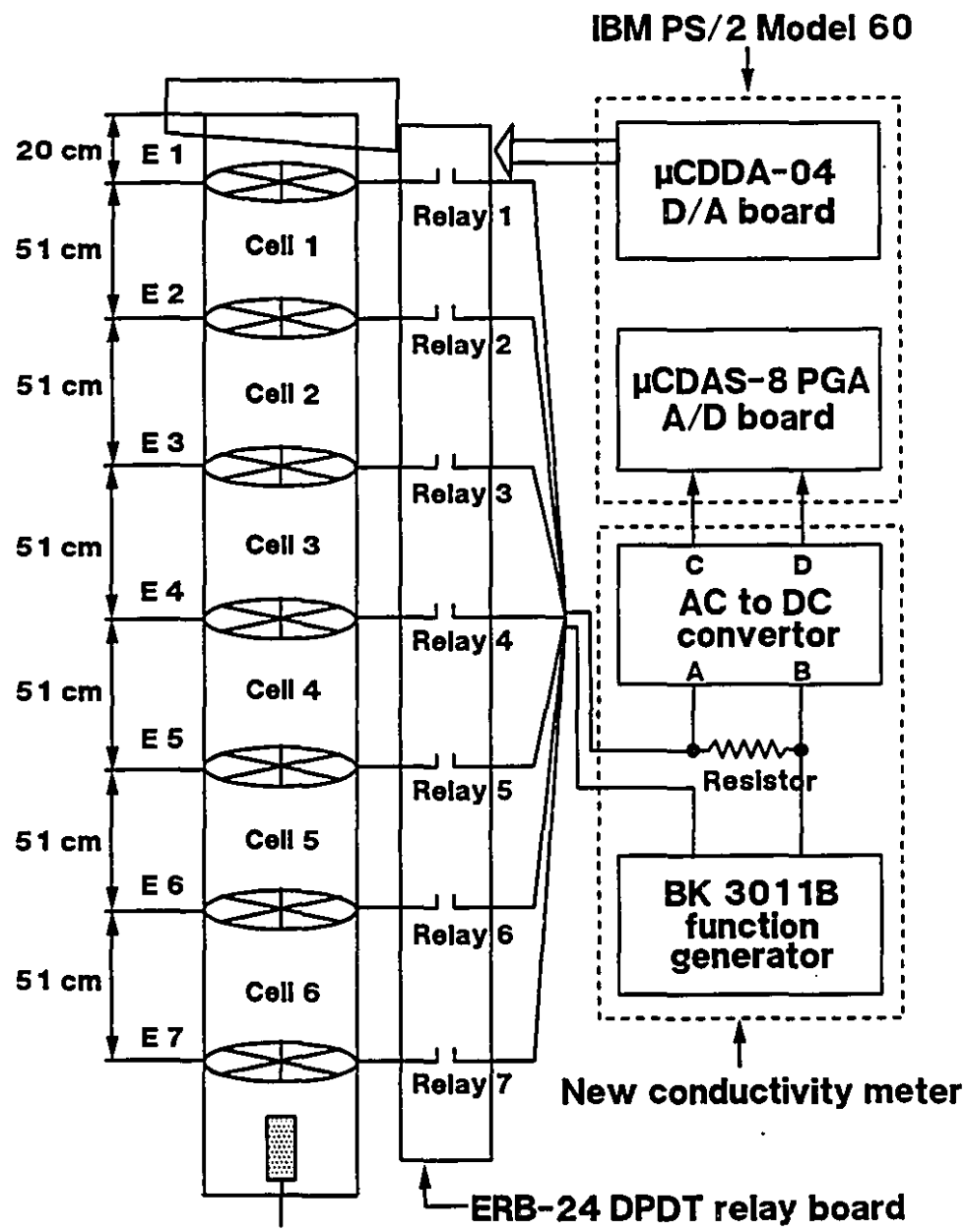

Figure 3.2 Conductance measurement system.

in Cells 1 to 6. An IBM PS/2 Model 60 computer equipped by a 12-bit μCDAS-8 PGA A/D board and a 12-bit μCDDA-04 D/A board was used for the data acquisition and the control of the relay board. The resistor used in the new conductivity meter was 5700 Ω.

(i) Effect of temperature

The conductivity of a liquid is a function of the temperature given for the region near 25°C by (Glasstone, 1930 and 1942; Condon, 1967)

$$\kappa = \kappa_{25^\circ C} [\, 1 + \alpha_{25^\circ C} (t - 25^\circ C) \,] \qquad (3.1)$$

where κ and $\kappa_{25^\circ C}$ are the conductivities (mS/cm) of the liquid at temperature t and 25°C, respectively, and $\alpha_{25^\circ C}$ is the coefficient of variation of the conductivity per degree Celsius with respect to the conductivity at 25°C.

The effect of the temperature on the performance of the cells is directly related to the effect of the conductivity. Uribe-Salas (1991) examined the effect of the temperature on the conductivity of a 0.02 M KCL solution. He pointed out that since the net effect of temperature is to vary the conductivity of the liquid according to Equation 3.1, cells whose cell constant is not affected by conductivity variations, such as the grid electrodes, will not be affected by temperature variations.

(ii) Conductance measurement procedure

The procedure for the conductance measurement was:

(a) by using μCDDA-04 D/A board, the relays 1 and 2 in the ERB-24 DPDT relay board were activated. E1 and E2, i.e. electrodes 1 and 2, was connected to the conductivity meter;

(b) a waiting period of 0.111 s, which was larger than the six time constants of the new conductivity meter (see Section 2.2.4), was counted by the computer clock;

(c) the DC output of the conductivity meter was read by the μCDAS-8 PGA A/D board, and the conductance in Cell 1 was obtained from Equation 2.21;

(d) when the steps a - c were repeated by activating relays 2 and 3, 3 and 4, 4 and 5, 5 and 6, and 6 and 7, the conductances in Cells 2, 3, 4, 5 and 6 were measured, respectively.

The collected data were stored into an ASCII file on the hard disk of the computer, which was used for data analysis after the experiments.

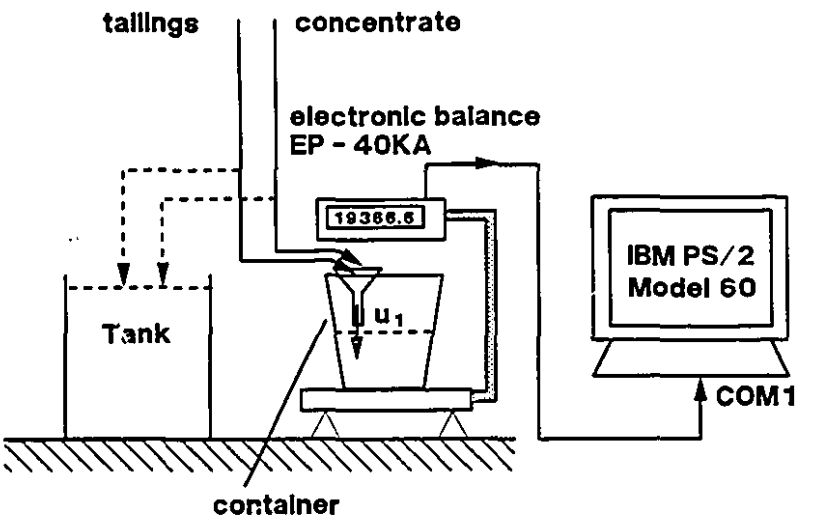

Figure 3.3 A liquid mass flowrate meter for the gas - liquid flow.

3.1.2 Liquid Flowrate Measurement for Overflow and Underflow

Accurate liquid flowrate measurement at the magnitudes of interest here is a challenge. Although some commercial flowrate meters are available, most of them are expensive and must be calibrated. A stable, inexpensive instrument is needed for the liquid flowrate measurement.

Figure 3.3 illustrates a liquid mass flowrate meter used under steady conditions. It consisted of a computer (the same as described earlier) equipped with a serial port (COM1 or COM2), and an electronic balance (EP-40KA). When the flowrates of overflow and underflow were measured, the switching between the two flows was made manually.

When the gas - liquid flow is introduced into the container (Figure 3.3), at time t_1, the total force acting on the balance, F_1, is given by

$$F_1 = F_{w,1} + F_{m,1} + F_c \tag{3.2}$$

where $F_{w,1}$ is the gravity force of the gas - liquid mixture in the container at t_1, $F_{m,1}$ is the momentum force of the gas - liquid flow in the vertical direction at t_1, and F_c is the gravity force

of the container. The $F_{w,1}$ is given by

$$F_{w,1} = \rho_l g V_{l,1} - \rho_g g V_{g,1} \tag{3.3}$$

where ρ_l and ρ_g are the densities of the liquid and gas, respectively, and $V_{l,1}$ and $V_{g,1}$ are the volumes of the liquid and gas at t_1, respectively. The $F_{m,1}$ is given by

$$F_{m,1} = \rho_l Q_{l,1} u_1 + \rho_g Q_{g,1} u_1 \tag{3.4}$$

where u_1 is the vertical velocity of the gas - liquid flow through the pipe at t_1 (Figure 3.3), and $Q_{l,1}$ and $Q_{g,1}$ are the volumetric flowrates of the liquid and gas at t_1, respectively.

At time t_2, the total force F_2 is expressed as

$$F_2 = F_{w,2} + F_{m,2} + F_c \tag{3.5}$$

The difference between F_2 and F_1 is given by

$$\begin{aligned} F_2 - F_1 &= (F_{w,2} - F_{w,1}) + (F_{m,2} - F_{m,1}) + (F_c - F_c) \\ &= [\rho_l g (V_{l,2} - V_{l,1}) + \rho_g g (V_{g,2} - V_{g,1})] \\ &\quad + (u_2 - u_1) [\rho_l (Q_{l,2} - Q_{l,1}) + \rho_g (Q_{g,2} - Q_{g,1})] \end{aligned} \tag{3.6}$$

Because $\rho_l >> \rho_g$, the terms containing ρ_g can be neglected. Assuming the gas - liquid flow is a steady flow, i.e. $u_2 = u_1$, Equation 3.6 becomes

$$F_2 - F_1 = \rho_l g (V_{l,2} - V_{l,1}) \tag{3.7}$$

Therefore, the average liquid mass flowrate during the period of $t_2 - t_1$ is given by

$$\textit{average liquid mass flowrate} = \frac{F_2 - F_1}{t_2 - t_1} \frac{1}{g} = \rho_l \frac{V_{l,2} - V_{l,1}}{t_2 - t_1} \tag{3.8}$$

For laboratory columns, the liquid flowrate is normally measured under steady conditions. By using this meter, the liquid mass flowrate can be measured in the gas - liquid flow for a laboratory column.

The full range of the electronic balance (EP-40KA) is 40 Kg and the accuracy is $\pm$ 0.5 g. The EP-40KA can continuously report the weight to a computer or a printer by sending an ASCII text through a RS-232C port on the receiving electronic equipment at a 2400 baud rate. For example, a weight of 25.366 kg is reported by an ASCII text as 25366.0 g. Comparing with

an analog DC current (4 - 20 mA) or voltage (0 - 5 Volt) signal, the digital communication technique has an advantage of nigh accuracy.

When Equation 3.8 is used for calculating the liquid mass flowrate, the measurement errors of t_1 and t_2 can be neglected because t_1 and t_2 are counted by the computer clock. The accuracy of the measured liquid mass flowrate depends on $V_{l,2}$ - $V_{l,1}$. For example, at a liquid mass flowrate of 1 Kg per minute (i.e. 1 litre per minute at ρ_l = 1 g/cm^3), if the period of t_2 - t_1 is longer than 6 s, the relative error of the measured liquid mass flow will be less than 1 %.

3.1.3 Liquid Flowrate Measurement for Wash Water

A flow sensor (FTB601) and a ratemeter (DP-F31-MA) were installed for measuring this low liquid flowrate. The flow range of FTB601 was 0.1 - 2.0 litre per minute. Because FTB601 consists of an infrared electro-optical transmitter and receiver, the flowmeter is only suitable for clear transparent fluids, which must transmit infrared light. The flow sensor (FTB601) and ratemeter (DP-F31-MA) were calibrated by the liquid mass flowmeter presented in Section 3.1.2.

3.1.4 Air Flowrate Measurement and Control

A gas mass flowmeter (TYLAN FM-380) and a microbased process controller (MIC 2000) were installed for measuring the air flow introduced into the column through the sparger (Figure 3.1). The air flowrate was displayed on the screen of MIC 2000. The full range of FM-380 was 15 standard litre per minute and it was calibrated with a wet test meter at the inlet pressure of 15 psig.

For the experiments, the air flow was divided into two parallel independent flows: the first air flow passed through a manual valve V3 and solenoid valve V1 to the sparger, and the second air flow passed through a manual valve V4 and solenoid valve V2 to the sparger. Two manual valves were used to vary the air flowrates and two solenoid valves were controlled by the computer for switching the air flows on or off. The switching time of the solenoid valve is 0.004 - 0.008 s.

3.1.5 Pressure Measurement

A pressure transducer P1 (PDCR 860 range 2.5 psig) was installed on the column wall

located 146.4 cm below the lip of the column (Figure 3.1). A DC voltage (0 - 24.65 mV) produced by P1, which was a linear function of the pressure (0 - 2.5 psig), was amplified by a DC signal amplifier (Model OMNI-AMPIII). The gain of the DC signal amplifier was 51 and the output of the amplifier was read by the A/D board.

3.1.6 Pump Control

Two Masterflex pumps (Model 7520) were used to supply and control the flows of the wash water and underflow (Figure 3.1). A DC power supply (Model U24Y101) was used to provide a 24 volt DC voltage to the D/A board, and the D/A board produced two 4 - 20 mA DC currents to control the pump speed. In the experiments, the flowrates of the two pumps were computer controlled.

3.2 Computer Control of Experiment

When experiments are conducted under dynamic conditions, such as the measurement of the bubble swarm velocity, a high accuracy is required for each operation in the experiment. In such cases, a computer control and data acquisition system is necessary. For experiments presented in this study, all procedures were controlled by the computer except the manual setting of the air flowrate and operation of the video camera.

An IBM PS/2 Model 60 computer equipped by a 12-bit μCDAS-8 PGA A/D board and a 12-bit μCDDA-04 D/A board was used (Figure 3.1). Figure 3.4 illustrates a flowsheet for the computer control and data acquisition program, which is presented in Appendix 1.

In the program, the resistances in Cells 1 - 6 were measured sequentially and the sampling rate was 1.5 samples per second per cell. Because of the computer memory used by QuickBASIC, the maximum sampling time was 20 minutes, i.e. the time for one experiment was limited to 20 minutes.

Before the computer started the data acquisition, the resistances in Cells 1 - 6, which were related to the gas holdup in Cells, were graphically displayed on the computer screen to monitor the gas holdup inside the column. After data acquisition, the measured data were checked by viewing the curves or calculating the gas holdup in each cell. The data were saved into files, which were read and analyzed by the data analysis program presented in Appendix 2.

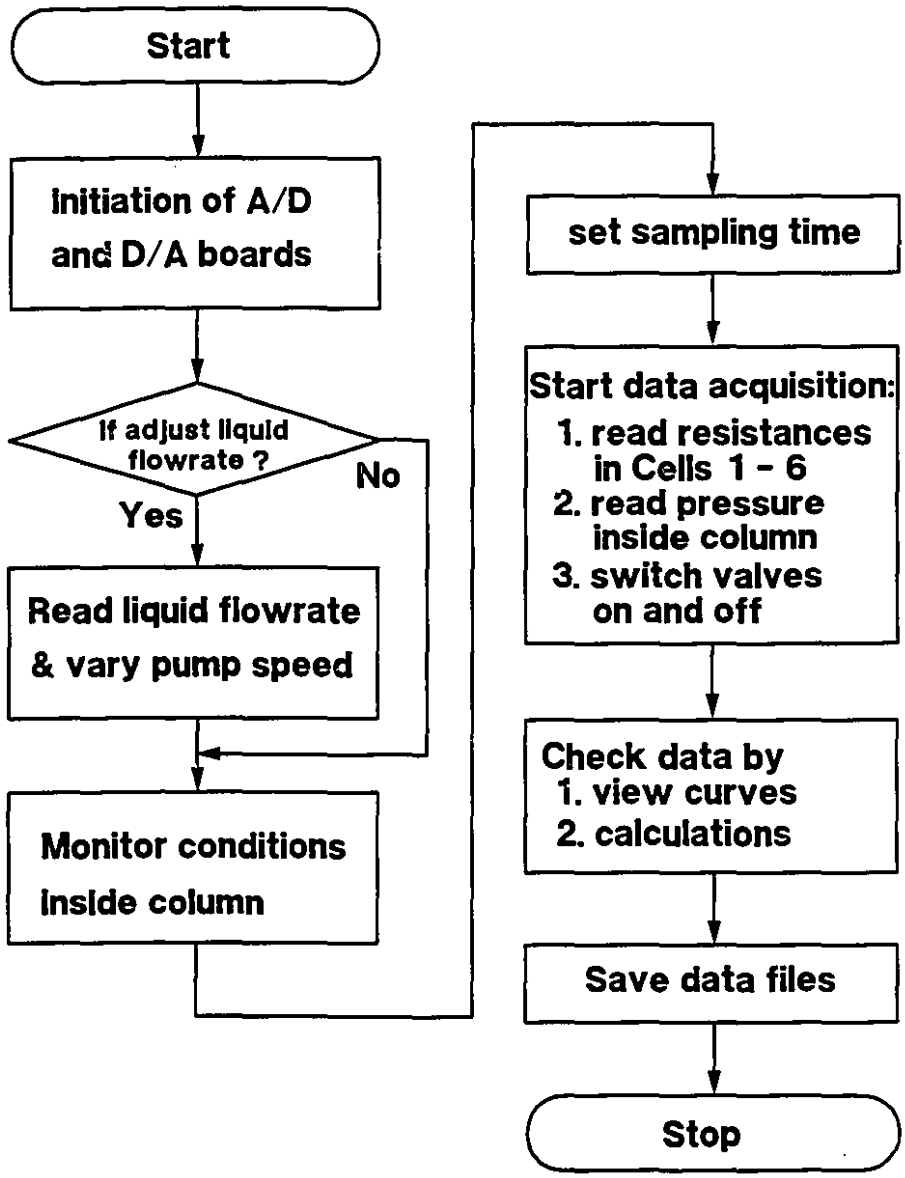

Figure 3.4 Flowsheet of the control and data acquisition program.

3.3 Preliminary Experiment in Air - Water Only System

To test the new conductivity meter and the experimental control system, the experiments were conducted with air - water only (i.e. without frother), in the batch mode to measure the buoyancy velocity of a bubble swarm and to estimate the gas holdup from Maxwell's model. The description "conductivity method" will be used to refer to parameters estimated from conductivity / conductance measurements.

3.3.1 Experimental Set Up and Procedure

Figure 3.5 (a) illustrates the experimental set up. The water manometer A located at 76 cm below the lip, and the water manometer B located at 176.5 cm below the lip of the column, were used for measuring the gas holdup inside the column. A VHS video camera was used for measuring the buoyancy velocity of a bubble swarm in the column.

The experiment was conducted by suddenly terminating the air flow. The procedure was:

(a) open Valve 1 (V1) and adjust Valve 3 (V3) to set the initial superficial gas velocity, J_g; close Valve 2 (V2) and Valve 4 (V4);
(b) wait for steady state conditions in the column;
(c) read water manometers A and B;
(c) start the video camera;
(d) at 0 s, start the data acquisition system;
(e) at 10 s, close V1;
(f) at 60 s, stop the data acquisition system;
(g) stop the video camera.

3.3.2 Measurement of Buoyancy Velocity in Cell 6

When the air flow was suddenly terminated, an interface appeared: above the interface the gas holdup was that prior to the termination of the air flow; below the interface the gas holdup was zero (Figure 3.5 (b)). By Nicklin's definition (1962), the velocity of the rising interface is the buoyancy velocity of the bubble swarm, u_0.

Figure 3.6 shows the resistance versus time in Cell 6. Before t_1, the rising interface has not reached E7 (Electrode 7) and the resistance is constant. At t_1, the resistance begins to lower

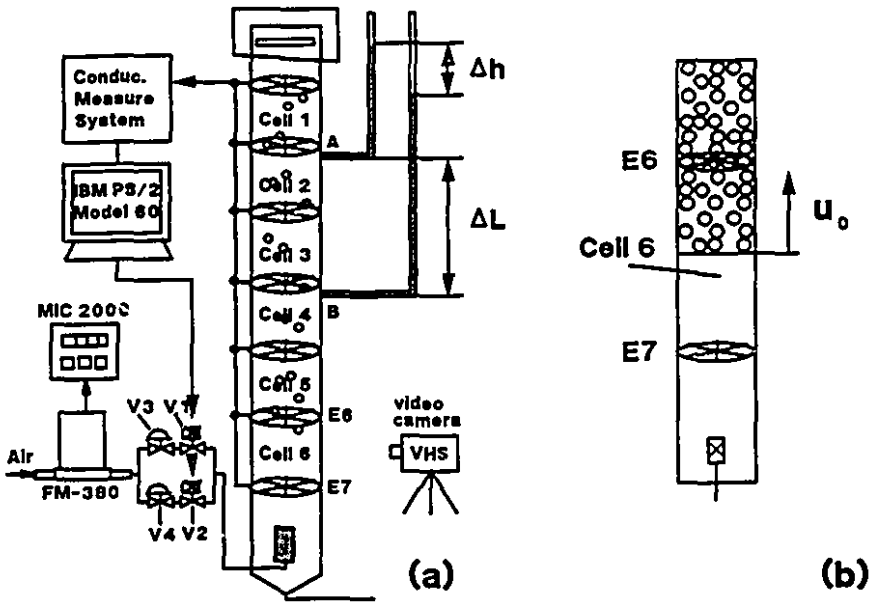

Figure 3.5 Experiment for measuring the buoyancy velocity of a bubble swarm and the gas holdup: (a) experimental set up; (b) buoyancy velocity (u_0) in the column.

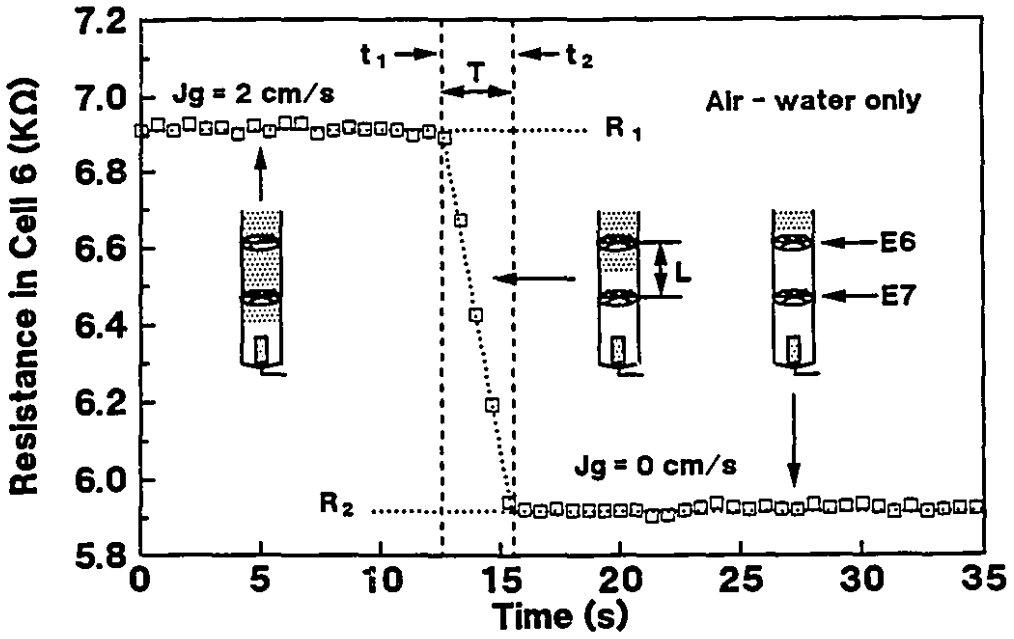

Figure 3.6 Resistance versus time in Cell 6 at J_g = 2.0 cm/s.

because the interface contacts E7. While the interface is rising from E7 to E6, the resistance in Cell 6 decreases. After t_2, the interface has left E6 and the resistance is again constant. The buoyancy velocity, u_0, can be calculated by

$$u_0 = \frac{L}{t_2 - t_1} = \frac{L}{T} \tag{3.9}$$

where L is the distance between E7 and E6 (51 cm), and T is the period during which the interface rises from E7 to E6. From Figure 3.6, it can be seen that during the period T the resistance in Cell 6, R_{c6}, is a linear function of the time, t, given by

$$R_{c6} = A + B\,t \tag{3.10}$$

where A is the intercept, and B is the slope of the line. Substituting R_1 which represents the average resistance of the mixture of the air bubbles and water, and R_2 which represents the average resistance of the water into Equation 3.10 (Figure 3.6), the t_1 and t_2 are given by

$$t_1 = (R_1 - A) / B \tag{3.11}$$

$$t_2 = (R_2 - A) / B \tag{3.12}$$

Therefore, the buoyancy velocity, u_0, can be calculated from

$$u_0 = L \frac{B}{R_2 - R_1} \tag{3.13}$$

The photography method is widely used as a standard method to evaluate the velocity of a moving object. In this experiment, a VHS video camera was used to record the image of the rising interface at a speed of 30 frames per second. By counting the number of frames in which the interface was rising through Cell 6, T was obtained, and the buoyancy velocity, u_0, was calculated by using Equation 3.9.

For the error analysis of u_0, the function

$$u_0 = \frac{L}{T} \tag{3.14}$$

was linearized by expanding it in a truncated Taylor series

$$u_0 \cong u_0(\bar{T}) + \frac{d\,u_0(\bar{T})}{dT}\,(T - \bar{T}) \tag{3.15}$$

where $\bar{T}$ is the average value of T. The variance (or square of the standard deviation) of u_0 is given by

$$S^2_{u_0} = \left[\frac{du_0}{dT}\right]^2 S^2_T = \left(-\frac{L}{\bar{T}^2}\right)^2 S^2_T \tag{3.16}$$

and the relative standard deviation of u_0 is given by

$$C_{u_0} = \frac{S_{u_0}}{\bar{u}_0} \tag{3.17}$$

The 95% confidence interval of u_0 is defined as

$$\bar{u}_0 - 2\,S_{u_0} \le \mu_u \le \bar{u}_0 + 2\,S_{u_0} \tag{3.18}$$

where μ_u is the mean of the population of u_0.

For each superficial gas velocity, J_g, ten experiments were conducted. Table 3.1 shows the agreement between buoyancy velocity obtained from the photography method, and the buoyancy velocity estimated by the conductivity method.

For evaluating the conductivity method, Table 3.1 presents the standard deviation, the relative standard deviation, and the 95% confidence interval of u_0 obtained from the error analysis of the conductivity method.

3.3.3 Measurements of Gas Holdup in Cells 2 and 3

The average gas holdup, ε_g, in Cells 2 and 3 between the two manometers (Figure 3.5 (a)), is given by (Finch and Dobby, 1990a)

$$\varepsilon_g = \frac{\Delta h}{\Delta L} \tag{3.19}$$

where Δh is the distance between the two water levels in two manometers, and ΔL is the distance between the locations of the two manometers (Figure 3.5 (a)).

Table 3.1 Experimental results and error analysis for buoyancy velocity measurements in the air - water only system

J_g (cm/s)	u_0 from video camera (cm/s)	u_0 from conductivity (cm/s)	Standard deviation (cm/s)	Relative standard deviation (%)	95% confidence interval (cm/s)
1.0	21.55	21.48	0.217	1.01	21.05 21.91
1.5	19.87	19.88	0.186	0.94	19.51 20.25
2.0	18.66	18.64	0.170	0.91	18.30 18.98
2.5	17.59	17.56	0.139	0.79	17.28 17.84
3.0	17.00	16.93	0.124	0.73	16.68 17.18

Table 3.2 Experimental results and error analysis for gas holdup measurements in the air - water only system

J_g (cm/s)	Gas holdup from pressure (%)	Gas holdup from conductivity (%)	Standard deviation (%)	Relative standard deviation (%)	95% confidence interval (%)
0	0	0	0.102		-0.20 0.20
1.0	4.52	4.40	0.112	2.55	4.18 4.62
1.5	6.70	6.80	0.112	1.65	6.58 7.02
2.0	10.05	9.88	0.163	1.65	9.55 10.21
2.5	12.22	12.39	0.162	1.31	12.07 12.71
3.0	15.58	15.35	0.140	0.91	15.07 15.63

By using the conductivity method, the gas holdup can be estimated from Maxwell's model

$$\varepsilon_g = \frac{1 - \gamma}{1 + 0.5\gamma} \tag{2.9}$$

where γ is given by

$$\gamma = \frac{R_2}{R_1} \tag{3.20}$$

where R_1 is the average resistance of the dispersion of the water and air bubbles, and R_2 is the average resistances of the water (Figure 3.6).

For the error analysis of ε_g, the function

$$\varepsilon_g = \frac{\bar{R}_1 - \bar{R}_2}{\bar{R}_1 - 0.5\,\bar{R}_2} \tag{3.21}$$

was linearized by expanding it in a truncated Taylor series

$$\varepsilon_g \equiv \varepsilon_g(\bar{R}_1, \bar{R}_2) + \frac{\partial \varepsilon_g(\bar{R}_1, \bar{R}_2)}{\partial R_1}(R_1 - \bar{R}_1) + \frac{\partial \varepsilon_g(\bar{R}_1, \bar{R}_2)}{\partial R_2}(R_2 - \bar{R}_2) \tag{3.22}$$

where $\bar{R}_1$ and $\bar{R}_2$ are the average resistance values. The variance (or square of the standard deviation) of ε_g is given by

$$S^2_{\varepsilon_g} = \left[\frac{\partial \varepsilon_g}{\partial R_1}\right]^2 S^2_{R_1} + \left[\frac{\partial \varepsilon_g}{\partial R_2}\right]^2 S^2_{R_2} \tag{3.23}$$

which gives

$$S^2_{\varepsilon_g} = \left[\frac{1.5\,R_2}{(R_1 + 0.5\,R_2)^2}\right]^2 S^2_{R_1} + \left[\frac{-1.5\,R_1}{(R_1 + 0.5\,R_2)^2}\right]^2 S^2_{R_2} \tag{3.24}$$

and the relative standard deviation of ε_g is given by

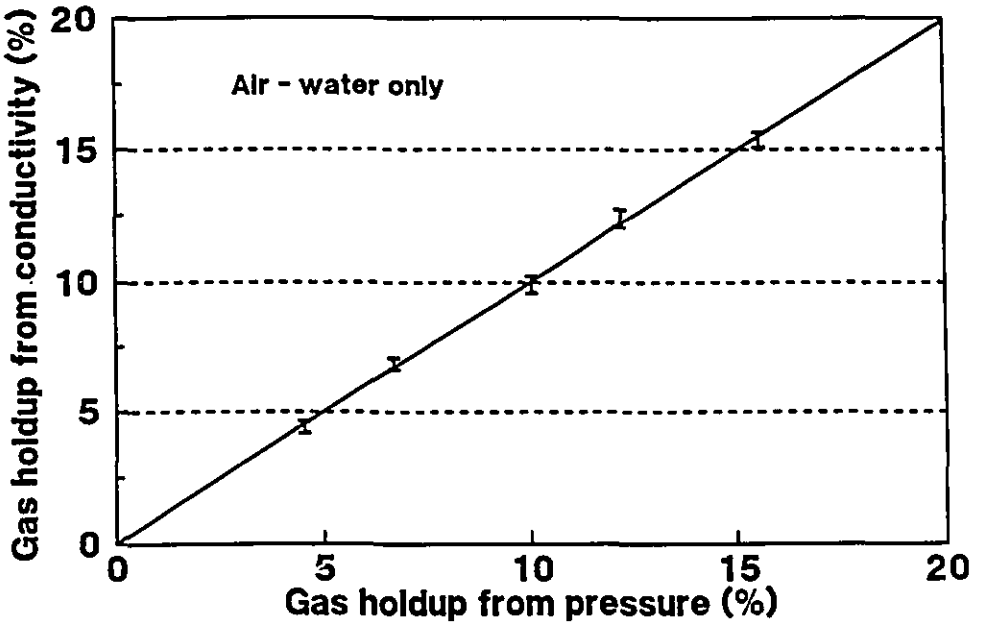

Figure 3.7 Comparison between conductivity method and pressure method, and 95% confidence interval obtained in conductivity method.

$$C_{\varepsilon_g} = \frac{S_{\varepsilon_g}}{\bar{\varepsilon}_g} \tag{3.25}$$

The 95% confidence interval of ε_g is defined as

$$\bar{\varepsilon}_g - 2\,S_{\varepsilon_g} \le \mu_\varepsilon \le \bar{\varepsilon}_g + 2\,S_{\varepsilon_g} \tag{3.26}$$

where μ_ε is the mean of the population of ε_g.

For each J_g, the measurements of R_1 and R_2 in Cells 2 and 3 were performed in ten experiments and the average values were used in the calculation of the gas holdup. Table 3.2 shows the gas holdup obtained from pressure, and the gas holdup in Cells 2 and 3 estimated by using Maxwell's model.

For the evaluation of the conductivity method, Table 3.2 presents the standard deviation, the relative standard deviation and the 95% confidence interval, which are obtained from the error analysis of the conductivity measurements. Figure 3.7 illustrates the good agreement between the conductivity method and pressure method, and the 95% confidence interval in the

conductivity method.

It is concluded that the conductivity method gives reliable buoyancy velocity and gas holdup estimations.

CHAPTER 4

TWO-PHASE BUBBLY FLOW

In this chapter, the theory of two-phase bubbly flow is reviewed with particular emphasis on its application in flotation columns.

4.1 Units and Sign Convention

The SI system of units is used in this thesis except for some cases when cgs units are used for convenience. For example, a superficial gas velocity, J_g, is expressed as 1 cm/s rather than 0.01 m/s as in the SI system. In this thesis, the sign convention for all forces and velocities is that an upward direction is positive and a downward direction is negative.

4.2 Basic Definitions

Although a detailed nomenclature is given at the beginning of the thesis, it is necessary to explain the relationships among the parameters: clear definitions are required for understanding the analysis in the following chapters.

4.2.1 Gas Holdup and Liquid Holdup

When gas is introduced into a column, part of the liquid is displaced. The volumetric fraction displaced is called the gas holdup, ε_g. The gas holdup for the whole column is called the overall gas holdup

$$overall\ gas\ holdup = \frac{V_g}{A_c L} \tag{4.1}$$

where V_g is the total volume of gas, and A_c, L are the cross-sectional area and length of the column, respectively.

The local gas holdup is defined as the average value both in space and time at a given location

$$\varepsilon_g = \frac{\int\int \varepsilon(A_c,t)\, dA_c\, dt}{\int dA_c \int dt} \tag{4.2}$$

where $\varepsilon(A_c,t)$ is the distributive function of the gas holdup over the cross-sectional area of column and time. The term ε_g is often used loosely in the literature to represent the gas holdup without mentioning whether it is an overall or local gas holdup. In this thesis, ε_g is used to represent the local gas holdup.

The liquid holdup, ε_l, is defined as

$$\varepsilon_l = 1 - \varepsilon_g \tag{4.3}$$

4.2.2 Volumetric Rates and Superficial Velocities

The volumetric rates of gas flow and liquid flow are represented by Q_g and Q_l, respectively. The total volumetric rate, Q, is given by

$$Q = Q_g + Q_l \tag{4.4}$$

The superficial gas velocity, J_g, is the volumetric flowrate of gas divided by the column cross-sectional area

$$J_g = \frac{Q_g}{A_c} \tag{4.5}$$

The units of J_g are (cm³ gas / cm² column area), or units of velocity, cm/s. In the analysis of two phase flow, J_g is also referred to as the volumetric flux of gas.

The flux is a vector quantity, but in this thesis J_g is used exclusively to represent the scalar component of gas in the direction of motion along a column. By analogy, the superficial liquid velocity, J_l, is defined as

$$J_l = \frac{Q_l}{A_c} \tag{4.6}$$

The total local flux, j, is given by

$$j = J_g + J_l = \frac{Q_g + Q_l}{A_c} \tag{4.7}$$

4.2.3 Gas Velocity, Liquid Velocity and Slip Velocity

The average gas velocity, u_g, is defined as

$$u_g = \frac{J_g}{\varepsilon_g} \tag{4.8}$$

and the average liquid velocity, u_l, is given by

$$u_l = \frac{J_l}{\varepsilon_l} = \frac{J_l}{1 - \varepsilon_g} \tag{4.9}$$

In the analysis of two phase flow, two relative velocities are defined as

$$u_{gl} = u_g - u_l \tag{4.10}$$

$$u_{lg} = u_l - u_g \tag{4.11}$$

and therefore

$$u_{gl} = -u_{lg} \tag{4.12}$$

Normally only u_{gl} is used and is defined as the slip velocity, u_s

$$u_s = u_g - u_l \tag{4.13}$$

4.2.4 Drift Velocities and Drift Fluxes

The drift velocity of gas, u_{gj}, is defined as

$$u_{gj} = u_g - j \tag{4.14}$$

By analogy, the drift velocity of liquid, u_{lj}, is defined as

$$u_{lj} = u_l - j \tag{4.15}$$

The drift flux of the gas, j_{gl}, is

$$j_{gl} = \varepsilon_g u_{gj} = \varepsilon_g (u_g - j) \tag{4.16}$$

Similarly, the drift flux of the liquid, j_{lg}, is

$$j_{lg} = (1 - \varepsilon_g) u_{lj} = (1 - \varepsilon_g)(u_l - j) \tag{4.17}$$

Substituting Equations 4.7 into 4.16 and using Equation 4.8, we have

$$j_{gl} = (1 - \varepsilon_g) J_g - \varepsilon_g J_l \tag{4.18}$$

Similarly, we obtain

$$j_{lg} = \varepsilon_g J_l - (1 - \varepsilon_g) J_g \tag{4.19}$$

Comparing Equations 4.18 with 4.19, we have

$$j_{gl} = -j_{lg} \tag{4.20}$$

This is an important property of the drift flux. Usually only j_{gl} is used and is called simply the drift flux. Normally, in the collection zone of flotation columns, j_{gl} is a positive quantity with the flow of gas upward and the flow of liquid downward.

Substituting for J_g and J_l in Equation 4.18 by using Equations 4.8 and 4.9, we get

$$j_{gl} = \varepsilon_g (1 - \varepsilon_g)(u_g - u_l) = \varepsilon_g (1 - \varepsilon_g) u_s \tag{4.21}$$

Thus the drift flux is a function of the gas holdup and slip velocity.

4.3 Flow Regimes in Columns

4.3.1 Definition of Flow Regimes

In column flotation, the collection of minerals is strongly dependent on the hydrodynamics in the collection zone. Maintaining the column in the required flow regime is essential for column control. Many researchers have worked on the definition of the flow regimes and general details can be found in Wallis (1969) and Hewitt (1982). The definitions of Wallis have been commonly accepted (Shah et al., 1982). A flow regime map is represented in Figure 4.1. In columns, as the gas rate is increased from zero, three flow regimes are encountered.

(i) Bubbly flow

This regime is characterized by a suspension of discrete bubbles in a continuous liquid. The gas bubbles are of approximately uniform size. In general the bubbly flow theory begins to fail when the gas holdup is larger than 15% (Shah et al., 1982; Whalley and Davidson, 1974). This regime is limited to a gas rate less than 5 cm/s. With the presence of frother, bubbly flow can be maintained up to a gas holdup of 35% (Xu et al., 1989; Yianatos and Finch, 1990). With special precautions, Lockett and Kirkpatrick (1975) reported that the bubbly flow regime can be realized up to a gas holdup of 66%.

(ii) Churn-turbulent flow

This regime is characterized by large bubbles rising with high velocities in the presence of small bubbles (Hills and Darton, 1976). When the gas rate increases, the bubbles get closer together and collisions occur more often (Radovich and Moissis, 1962). Some collisions lead to coalescence of bubbles and eventually to the formation of large bubbles. Figure 4.2 shows that the collision frequency increases rapidly at a gas holdup of about 30%. It means that the transition from bubbly flow to churn-turbulent flow tends to occur around this point. However, the transition may occur at a higher gas holdup ($\sim$60%) if the coalescence is prevented by frother (Whalley, 1987).

(iii) Slug flow

This regime is characterized by the coalescence of individual small gas bubbles to produce large bubbles, or slugs. Bubble slugs covering the entire cross section can be observed in columns of diameter up to 15 cm (Hills, 1976; Miller, 1980).

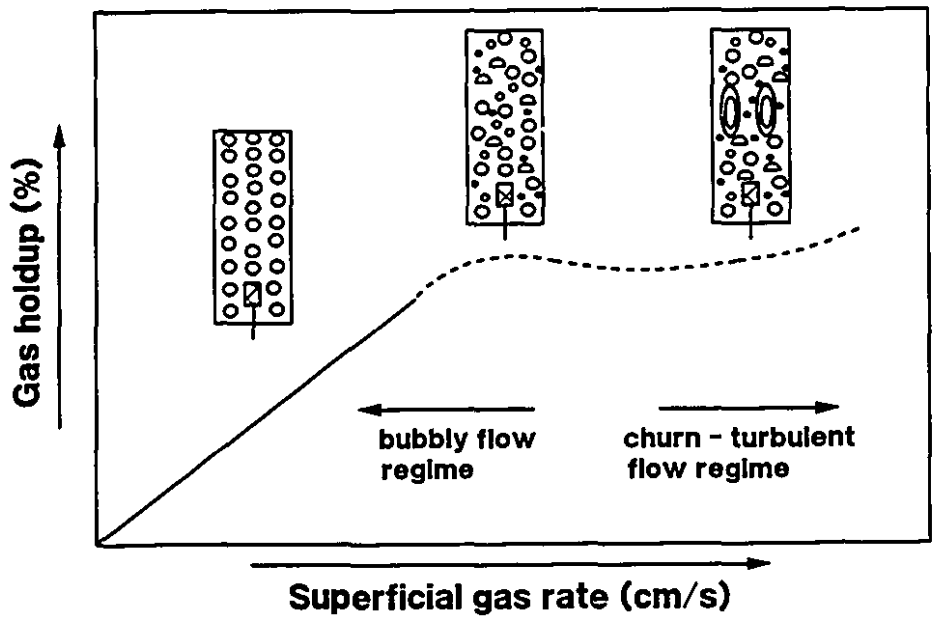

Figure 4.1 Gas holdup as a function of gas rate, general relationship (after Finch and Dobby, 1990a).

The dependence of the flow regimes on column diameter and gas rate is shown in Figure 4.3. The types of gas spargers, the physical-chemical properties of the liquid and liquid flow rate can affect the transition between flow regimes (Shah and Deckwer, 1981; Xu et al., 1989, 1990). In the operation of industrial flotation columns, performance deteriorates above a certain gas rate (Finch and Dobby, 1990a). One reason is that above this gas rate the flow regime of the collection zone transforms from bubbly flow to churn-turbulent flow. This transformation in hydrodynamic properties leads to a decrease in flotation performance. In addition to this transition, Xu et al. (1989, 1991) identified two other phenomena in the air - water - frother system which could dictate a maximum in the gas rate: loss of slurry / froth interface, and loss of positive bias. These are related to the transport upwards of water by bubbles. Consequently, bubble size as well as gas rate become factors and this is probably the case in flow transition also.

4.3.2 Determination of Flow Regimes

There are two main methods of determining the flow regimes: by sight and by instruments. The determination by eye is subjective and is only possible for flow in transparent columns. Determination by instruments has been used; for example, a gamma ray densitometer has been used to measure the mean density across the column or average gas holdup (Whalley, 1987).

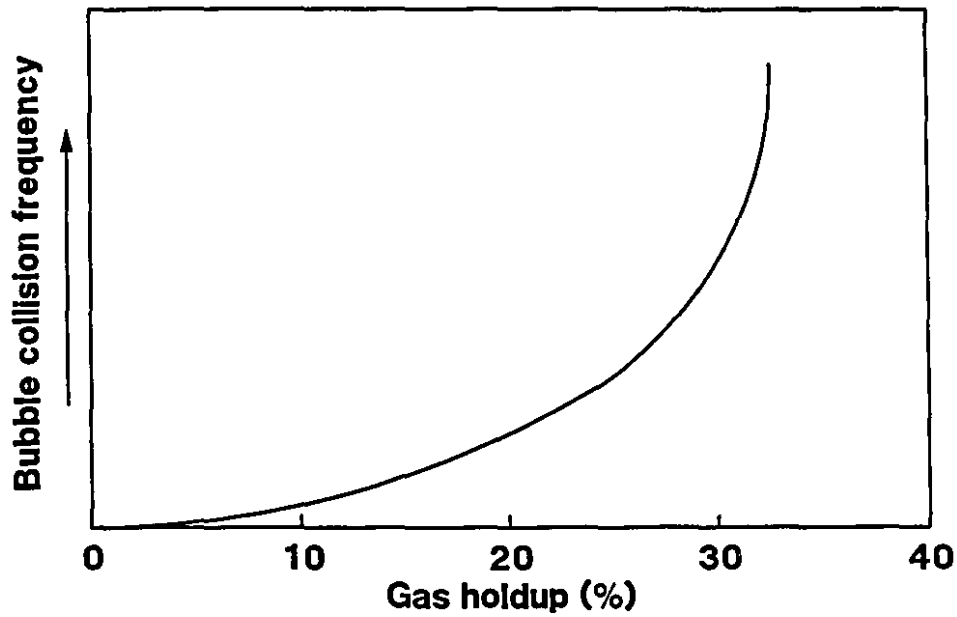

Figure 4.2 Variation of bubble collision frequency with gas holdup (after Radovich and Moissis, 1962).

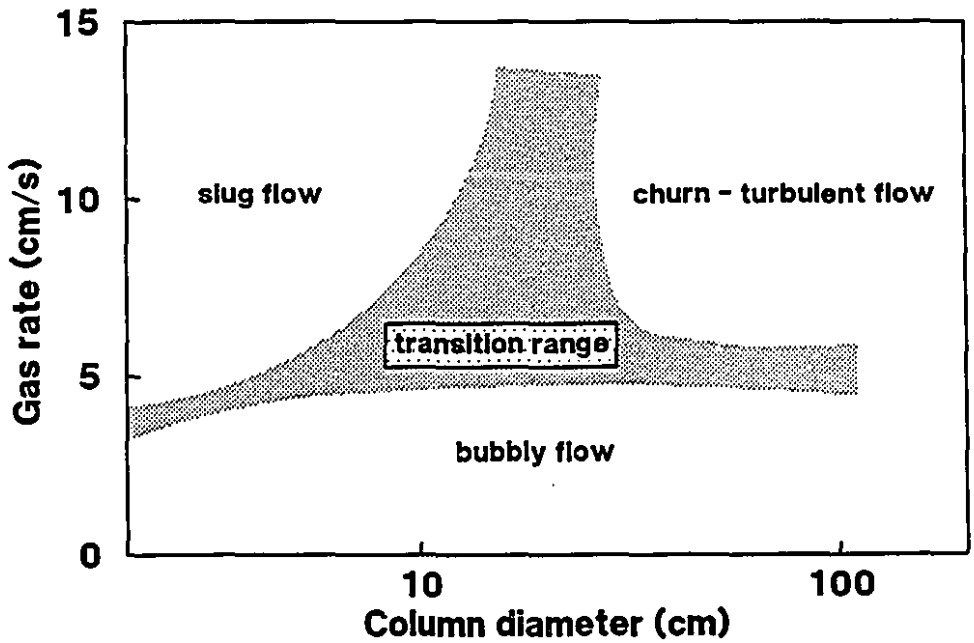

Figure 4.3 Approximate dependence of flow regimes on gas rate and column diameter (after Shah et al., 1982).

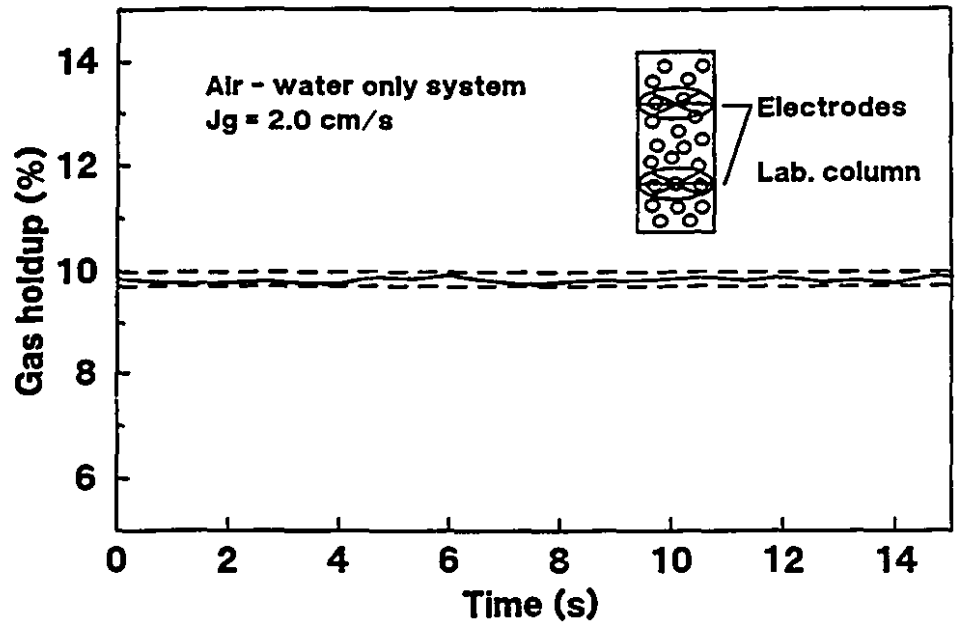

Figure 4.4 Gas holdup versus time for a laboratory column in bubbly flow regime.

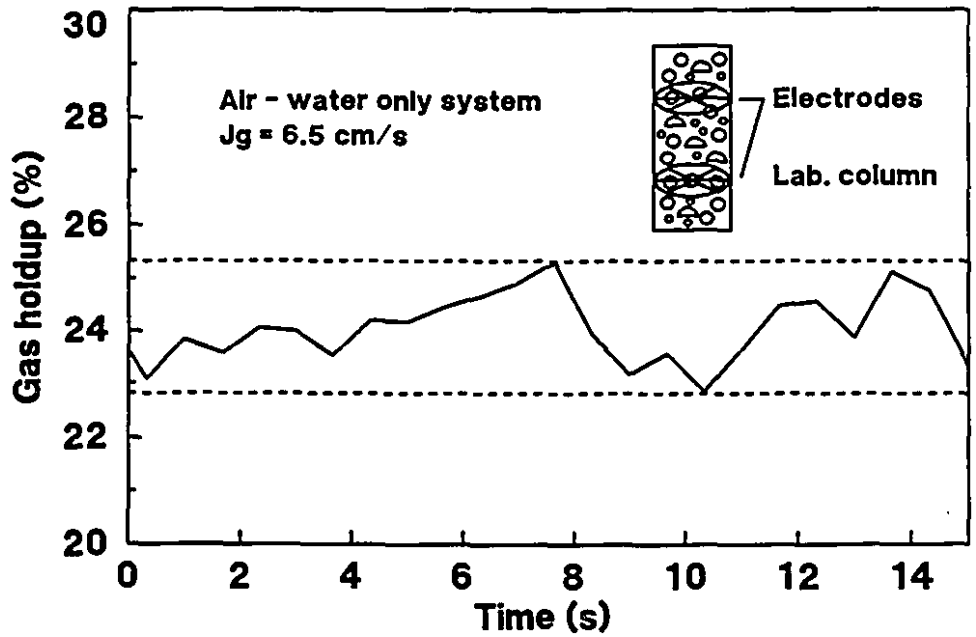

Figure 4.5 Gas holdup versus time for a laboratory column in churn-turbulent flow regime.

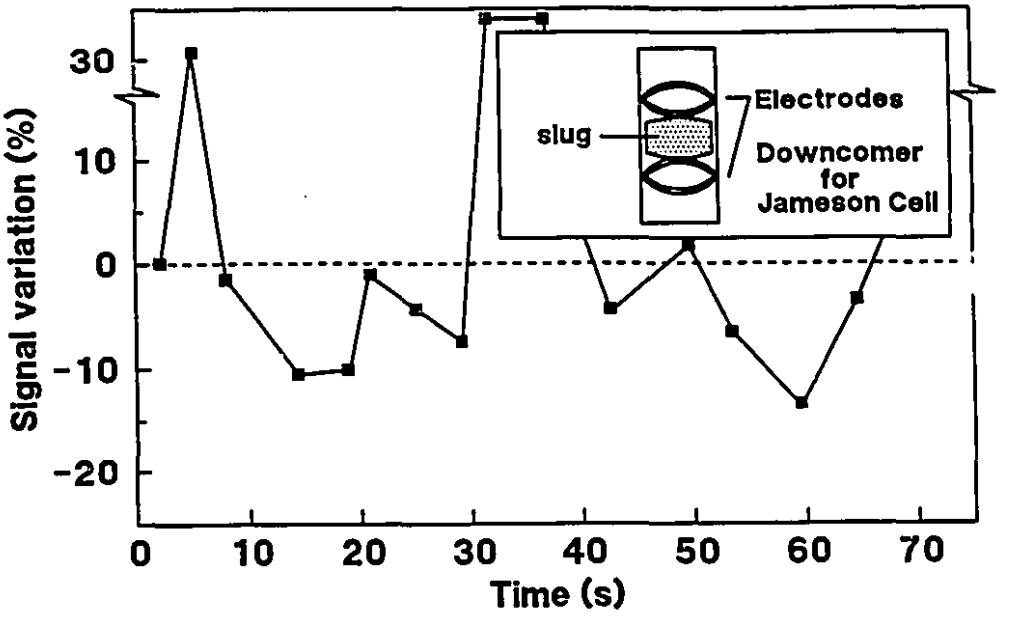

Figure 4.6 Conductivity signal variation versus time for a downcomer of Jameson Cell in slug flow regime (after Marchese,1991).

A conductivity method has been used to identify the transition point. A plot of gas holdup versus time can be used to determine the flow regimes in columns (Shen et al., 1991; Xu, 1991; Marchese, 1991; Summers, 1992). Figure 4.4 shows that a column in the bubbly flow regime gives a relatively constant gas holdup versus time. Figure 4.5 illustrates that when the column is in churn-turbulent flow the gas holdup shows wide variations. The amplitude of the variation can be used to quantify the turbulence of the flow. For a Jameson cell, if slugs pass through a conductivity cell inside the downcomer, the typical curve shown in Figure 4.6 occurs. The conductivity method not only measures the gas holdup but also gives evidence of the nature of the flow regime.

4.4 A Single Gas Bubble Rising in Liquids

4.4.1 Bubble Terminal Velocity

When a single bubble rises in a stagnant liquid of infinite dimensions, its velocity, u_b is called the bubble terminal velocity. The u_b depends on the bubble diameter and on the physical and chemical characteristics of the liquid and the gas, such as density, viscosity, surface tension, and the presence / absence of surface active agents.

The bubble Reynolds number, Re_b, is an important criterion for calculating the bubble terminal velocity and is defined as

$$Re_b = \frac{\rho_l d_b u_b}{\mu_l} \tag{4.22}$$

where ρ_l is the liquid density, μ_l is the liquid viscosity and d_b is the bubble diameter.

If the bubble is very small and the Reynolds number is less than unity, Stokes' equation can be used to calculate the bubble terminal velocity (Stokes, 1880). On the bubble, the drag force, F_d, is given by

$$F_d = 3\pi d_b u_b \mu_l \tag{4.23}$$

and the buoyancy force, F_b, is given by

$$F_b = \frac{\pi d_b^3}{6}(\rho_l - \rho_g) g \tag{4.24}$$

In order to find the bubble terminal velocity the drag force and the buoyancy force are equated and therefore

$$u_b = \frac{d_b^2 g (\rho_l - \rho_g)}{18 \mu_l} \tag{4.25}$$

In this equation, the bubble is treated as a solid sphere and it is assumed that the liquid velocity is zero at the bubble surface. However, the bubble is gaseous and the bubble surface is not stationary. When the bubble surface moves, the gas inside the bubble also moves. For u_b,

in this case, Hadamard (1911) and Rybezynski (1911) obtained the equation

$$u_b = \frac{d_b^2 g (\rho_l - \rho_g)}{18 \mu_l} \left(\frac{3 \mu_g + 3 \mu_l}{3 \mu_g + 2 \mu_l}\right) \tag{4.26}$$

where μ_g and μ_l are the gas viscosity and liquid viscosity, respectively. For $\mu_l >> \mu_g$, this equation reduces to

$$u_b = \frac{d_b^2 g (\rho_l - \rho_g)}{12 \mu_l} \tag{4.27}$$

Comparing with Stokes' equation, this equation increases u_b by 50%. However, most results of experiments show that u_b is between the values given by Equations 4.25 and 4.27.

When the bubbles are large, the shape is no longer spherical and the bubble terminal velocity does not obey Stokes' equation. If the effects of surface tension and viscosity are negligible, u_b is given by the equation of Davies and Taylor (1950):

$$u_b = \frac{2}{3}\sqrt{g r_{bc}} \tag{4.28}$$

where r_{bc} is the radius of curvature at the front of the bubble. In this case, the bubble has a spherical cap shape with an included angle of 100° and a relatively flat rear.

For bubbles of intermediate size, u_b can be calculated by the model of Clift et al. (1978) (in SI unit)

$$u_b = \frac{\mu_l}{\rho_l d_b} M^{-0.149} (J - 0.857) \tag{4.29}$$

where M is the Morton number given by

$$M = \frac{g \mu_l^4 (\rho_l - \rho_g)}{\rho_l^2 \sigma^3} \tag{4.30}$$

where σ is the surface tension and J is a correlating constant given by

$$J = 0.94 H^{0.757} \qquad (2 < H \leq 59.3) \tag{4.31}$$

and

$$J = 3.42\, H^{0.441} \qquad (H > 59.3) \tag{4.32}$$

where H is given by

$$H = \frac{4}{3} Eo\, M^{-0.149} \left(\frac{\mu_l}{\mu_w} \right)^{-0.14} \tag{4.33}$$

where Eo is Eötvös number defined as

$$Eo = \frac{g\, d_b^2 \left(\rho_l - \rho_g \right)}{\sigma} \tag{4.34}$$

This model can be used for a system where some surface - active contamination is inevitable and for the range, $M < 10^{-3}$, $Eo < 40$, $Re_b > 0.1$, and

$$\lambda \leq 0.08 + 0.02 \log_{10} Re_b \qquad (0.1 < Re_b \leq 100) \tag{4.35}$$

$$\lambda \leq 0.12 \qquad (Re_b \geq 100) \tag{4.36}$$

where

$$\lambda = \frac{d_b}{D} \tag{4.37}$$

where D is the diameter of the column.

Schiller and Naumann (1933) gave a simpler equation for $d_b < 2$ mm,

$$u_b = \frac{g\, d_b^2 \left(\rho_l - \rho_g \right)}{18\, \mu_l \left(1 + 0.15\, Re_b^{0.687} \right)} \tag{4.38}$$

For water at 20°C and a surface tension of 65 dynes/cm (a reasonable condition for flotation systems), Equation 4.38 is simplified to (Dobby et al., 1988)

$$u_b = 48.9\, d_b^{0.514} - 0.309\, d_b^{-1} \tag{4.39}$$

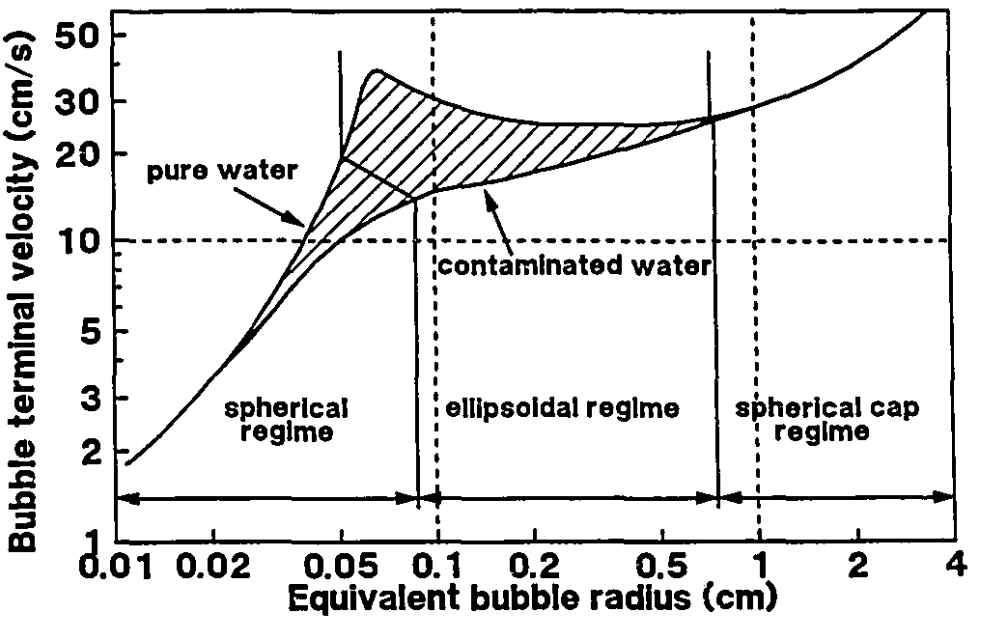

Figure 4.7 Terminal velocity of air bubbles in water at 20°C (after Clift et al., 1978).

4.4.2 Effect of Surface Contamination

Figure 4.7 illustrates the experimental terminal velocities for air bubbles rising in water. Clift et al. (1978) pointed out that some of the spread in the data results from experimental scatter but the greatest cause is surface contamination. In Figure 4.7, the two curves are based on Gaudin's work (1957) for distilled water and for water with surfactant added. It can be seen that surface - active contaminants affect the bubble terminal velocity most strongly in the ellipsoidal bubble range.

4.4.3 Effect of Containing Walls

When a bubble rises in a column, its velocity u_{bc} is generally lower than the u_b in a liquid of infinite dimensions. In a column, the ratio of u_{bc} to u_b can be expressed as a function of λ, the radio of d_b to D (Wallis, 1969).

Collins (1967) studied large inviscid bubbles and gave the following corrections:

$$\lambda < 0.125 \qquad \frac{u_{bc}}{u_b} = 1 \tag{4.40}$$

$$0.125 < \lambda < 0.6 \qquad \frac{u_{bc}}{u_b} = 1.13\, e^{-\lambda} \tag{4.41}$$

$$0.6 < \lambda \qquad \frac{u_{bc}}{u_b} = 0.496\, \lambda^{-1/2} \tag{4.42}$$

If the bubbles are treated as solid spheres in viscous fluids, Ladenburg (1907) derived

$$\frac{u_{bc}}{u_b} = (1 + 2.4\, \lambda)^{-1} \tag{4.43}$$

whereas for fluid spheres with $\mu_g << \mu_l$, Edgar (1966) obtained

$$\frac{u_{bc}}{u_b} = (1 + 1.6\, \lambda)^{-1} \tag{4.44}$$

When λ exceeds about 0.6, the bubbles behave as slugs and obey the equation

$$\frac{u_{bc}}{u_b} = 0.12\, \lambda^{-2} \tag{4.45}$$

4.5 A Swarm of Gas Bubbles Rising in Liquids

4.5.1 Relationship between u_s and u_b

When a swarm of bubbles rises in a finite liquid, the problem is more complex than for a single bubble. In this case the velocity of the bubble swarm will depend not only on the diameter of the bubbles and on the characteristics of the liquid and gas but also on the gas holdup. Several expressions have been proposed to relate the velocity of the swarm to the terminal velocity of the single bubble and to the holdup (Lockett and Kirkpatrick, 1975; Shah et al., 1982). One of the most widely accepted is that of Richardson and Zaki (1954).

From the sedimentation and fluidization of solid particles, Richardson and Zaki (1954) derived the empirical expression

$$\frac{u_f}{u_{bp}} = \varepsilon_l^{\,m} \tag{4.46}$$

where u_f is the velocity of the settling front (sedimentation case) of the particles in a batch system, u_{bp} is the terminal velocity of the particles ($\varepsilon_l \rightarrow 1$), and m is a coefficient that depends on the particle diameter and on the particle Reynolds number. A physical argument of the phenomenon gave (Richardson and Zaki, 1954)

$$u_{sp} = \frac{u_f}{\varepsilon_l} \tag{4.47}$$

where u_{sp} is the slip velocity between the particles and the fluid. Combining Equations 4.46 and 4.47, the general expression widely used in the literature is obtained

$$u_{sp} = u_{bp}\, \varepsilon_l^{\,m-1} \tag{4.48}$$

This equation has been used for gas - liquid systems

$$u_s = u_b (1 - \varepsilon_g)^{m-1} \tag{4.49}$$

It has been assumed that the values of m are a function of Reynolds number (Dobby and Finch, 1986; Dobby et al., 1988; Yianatos et al, 1988) based on the relationship of Richardson and Zaki (1954)

$$m = [\, 4.45 + 18 \left(\frac{d_b}{D}\right)]\; Re_b^{-0.1} \qquad (\, 1 < Re_b < 200 \,) \tag{4.50}$$

$$m = 4.45\; Re_b^{-0.1} \qquad (\, 200 < Re_b < 500 \,) \tag{4.51}$$

In Equation 4.49, various values of m have been used. Wallis (1962) used $m=2$ for small bubbles and $m=0$ for large bubbles (Davidson and Harrison, 1966). Bridge et al. (1964) used $m=2.39$ for small air bubbles in water following Equations 4.50 and 4.51. Turner (1966) used $m=1$ which means that u_s is not affected by ε_g. Two more complex equations are given by Marrucci (1965)

$$u_r = u_b \frac{1 - \varepsilon_g}{1 - \varepsilon_g^{n}} \tag{4.52}$$

and by Lockett and Kirkpatrick (1975)

$$u_r = u_b (1 - \varepsilon_g)^{1.5} (1 + 2.55 \varepsilon_g^{3}) \tag{4.53}$$

4.5.2 Nicklin's Derivation

Nicklin (1962) presented an analysis for the velocity of bubbles in two-phase flow and his derivation is reviewed in detail in this section. Figure 4.8 (a) illustrates steady bubbling of gas through a stagnant liquid in a column. Let there be N bubbles per unit volume of the column, uniformly spaced, each of volume V_b, and rising at a velocity u_b. Then the number of bubbles surfacing per second, N_s is equal to all those bubbles within a distance u_b of the surface

$$N_s = u_b A_c N \tag{4.54}$$

Therefore, the volume flow of gas per second, Q_g, is given by

$$Q_g = N_s V_b = u_b A_c N V_b \tag{4.55}$$

However, $N V_b$, being the volume of gas per unit volume of column, is the gas holdup, ε_g, and substituting this in Equation 4.55 gives

$$u_b = \frac{Q_g}{A_c \varepsilon_g} \tag{4.56}$$

This equals the average gas velocity, u_g, and the slip velocity, u_r, as the liquid is stationary.

Figure 4.8 (b) shows bubbles in exactly the same configuration, but rising relative to a stagnant liquid above them in a swarm of finite size. At the section A-A', the fraction of the cross sectional area occupied by gas is ε_g and bubbles rise at a velocity u_b. Here the u_r is defined as the buoyancy velocity with which the bubble swarm rises due to the difference in density between the gas and liquid. The u_r depends on the bubble size and on the gas holdup.

If downward velocities u_g and u_r are superimposed on systems (a) and (b) respectively, the

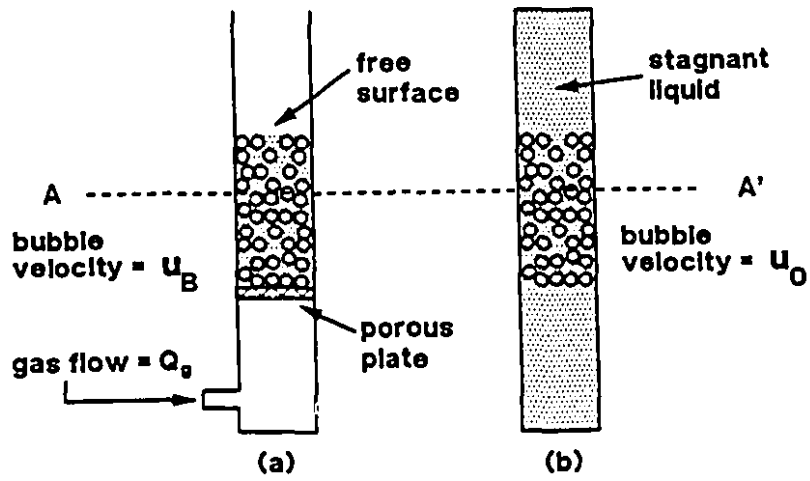

Figure 4.8 Examples of the rise of swarms of bubbles (after Nicklin, 1962).

bubbles in each case will be brought to rest. Because the two configurations are identical, and because both sets of bubbles are now stationary, it is apparent that the downward flow of liquid must be the same in each case, thereby providing a convenient basis for comparing the systems.

In system (a) initially the flow of liquid across section A-A' was zero. Because a downward velocity u_g has been imposed on the system, the volume flowrate of liquid across A-A' is given by

$$V_a = (1 - \varepsilon_g) u_g A_c \tag{4.57}$$

In system (b) from continuity the flow of liquid must be the same across all sections, and so the volume flowrate of liquid across section A-A' must equal the flowrate across any section above the bubbles. Hence,

$$V_b = u_0 A_c \tag{4.58}$$

The identity of the two systems has been demonstrated, and equating the expressions for V_a and V_b in Equations 4.57 and 4.58 gives

$$u_0 A_c = (1 - \varepsilon_g) u_g A_c \tag{4.59}$$

therefore

$$u_B = \frac{u_0}{1 - \varepsilon_g} \tag{4.60}$$

which may be rewritten as

$$\begin{aligned} u_B &= \frac{u_0}{1 - \varepsilon_g} = u_0 \frac{1 + (1 - \varepsilon_g) - (1 - \varepsilon_g)}{1 - \varepsilon_g} \\ &= u_0 \frac{1 - \varepsilon_g}{1 - \varepsilon_g} + u_0 \frac{\varepsilon_g}{1 - \varepsilon_g} = u_0 + \varepsilon_g \frac{u_0}{1 - \varepsilon_g} \\ &= u_0 + \varepsilon_g u_B = u_0 + \varepsilon_g \frac{Q_g}{\varepsilon_g A_c} \\ &= u_0 + J_g \end{aligned} \tag{4.61}$$

The slip velocity, u_s, between two phases is the same in the two systems, and is equal to the velocity of the bubbles

$$u_s = u_B = \frac{Q_g}{\varepsilon_g A_c} = \frac{u_0}{1 - \varepsilon_g} = u_0 + J_g \tag{4.62}$$

Nicklin gave a physical explanation for u_0: as the gas flows into the column, it tends to raise the entire contents of the column at a velocity Q_g/A_c, which is therefore a basic velocity given to each phase. Because of buoyancy, the gas rises faster than the basic velocity (by an amount u_0).

If there is a flow of liquid, the theory can be simply extended to give the result

$$u_B = u_0 + J_g \pm J_l \tag{4.63}$$

Note that the upward direction is positive for J_g and J_l. The slip velocity is given by

$$u_s = \frac{Q_g}{\varepsilon_g A_c} - \frac{Q_l}{(1 - \varepsilon_g) A_c} = \frac{u_0}{1 - \varepsilon_g} \tag{4.64}$$

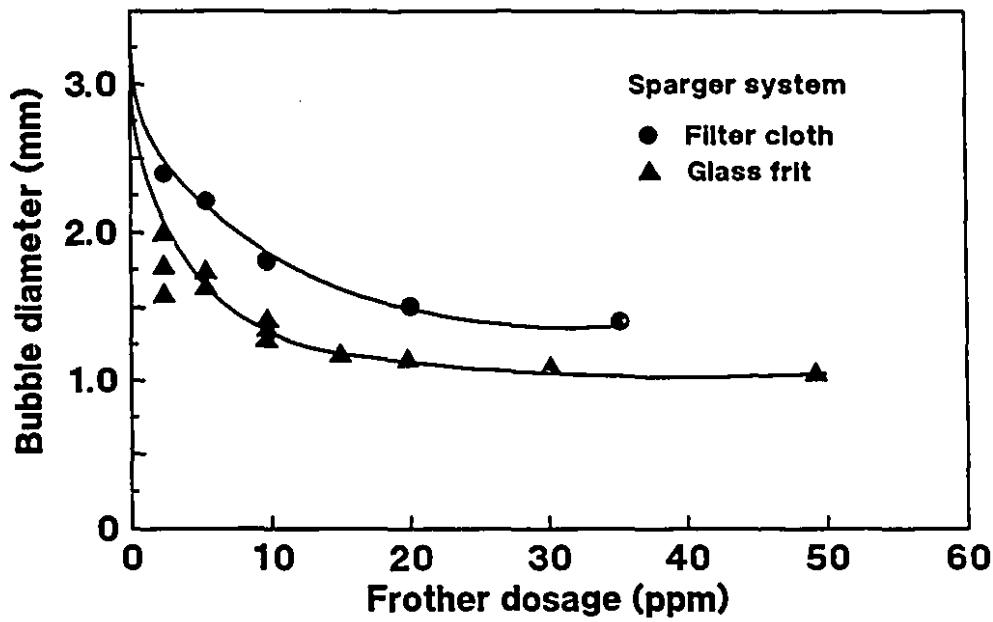

Figure 4.9 Illustration of the effect of frother (Dowfroth 250C) dosage upon d_b, J_g = 1.3 cm/s (after Flint et al., 1988).

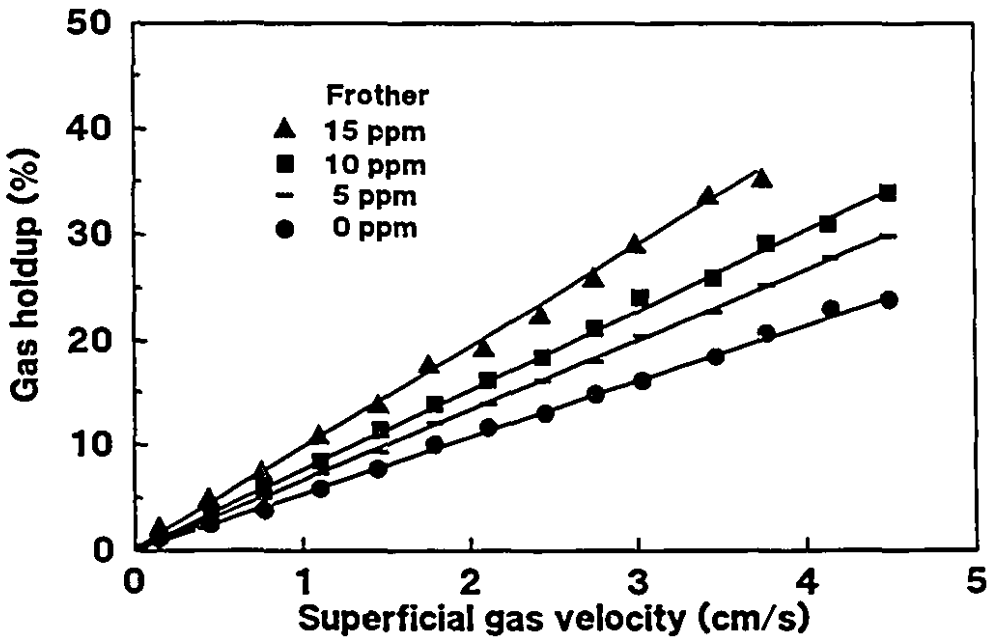

Figure 4.10 Gas holdup versus gas rate, effect of frother (Dowfroth 250C) dosage, J_l = 0.5 cm/s (after Finch and Dobby, 1990a).

4.6 Effect of Frother

The addition of frother has a pronounced impact on reducing bubble size in a swarm (Finch and Dobby, 1990a). Figure 4.9 illustrates that there is a strong effect of frother dosage at levels below about 20 ppm (Flint et al., 1988), which is similar to the trend reported by Klassen and Mokrousov (1963) for bubbles forming from a single orifice. A reduced bubble size means reduced bubble rise velocity and consequently increased gas holdup. The effect of frother concentration is illustrated in Figure 4.10, where ε_g, at a given J_g, increases significantly from 0 to 15 ppm Dowfroth 250C (Finch and Dobby, 1990a).

CHAPTER 5

AIR - WATER ONLY SYSTEM

In this chapter, the experimental results of the air - water only system (i.e. without frother) and the analysis of the data are presented. All experiments were conducted under batch conditions ($J_l = 0$).

5.1 Bubble Sizes and Bubble Size Distribution

5.1.1 Volume Diameter of Bubble d_{bv} and Mean Bubble Size d_{bs}

The bubble sizes were evaluated photographically by measuring about 1200 bubbles at various J_g at a water temperature of 21°C.

In the experiments, the shape of the bubbles was ellipsoidal. The volume of an ellipsoid is calculated from

$$V_{ellip} = \frac{4\pi}{3} a\, b\, c \tag{5.1}$$

where a, b and c are the radii on X, Z and Y axes, respectively (Figure 5.1 (a)). The major radius, a, and minor radius, b, of each bubble were measured (Figure 5.1 (b)). Assuming c is equal to a, the average bubble volume, V_b, is calculated by

$$V_b = \frac{4\pi}{3} a^2 b \tag{5.2}$$

The volume diameter of the bubble, d_{bv}, is given by

$$d_{bv} = \left[\frac{6\, V_b}{\pi}\right]^{\frac{1}{3}} \tag{5.3}$$

For a multi-bubble system, the Sauter mean size, d_{bs}, is frequently used to describe the

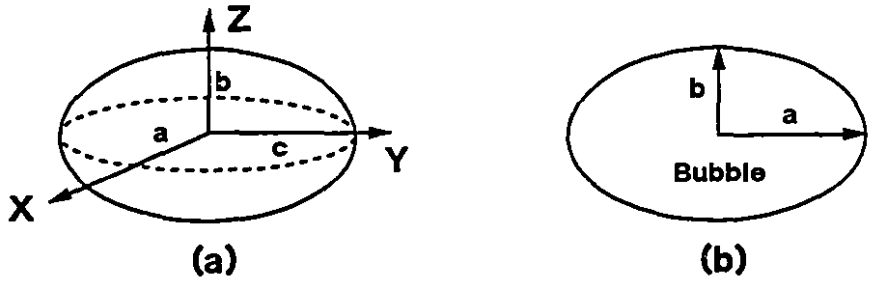

Figure 5.1 Measurement of bubbles: (a) radii of an ellipsoid; (b) measured radii a and b on a photograph.

Table 5.1 Bubble sizes at various J_g

J_g (cm/s)	d_{bs} (cm)	d_{min} (cm)	d_{max} (cm)
0.25	0.243	0.136	0.338
0.50	0.288	0.134	0.405
0.75	0.322	0.166	0.415
1.0	0.321	0.233	0.399
1.5	0.354	0.258	0.472
2.0	0.369	0.232	0.444
2.5	0.406	0.296	0.526
3.0	0.439	0.347	0.525
3.5	0.470	0.311	0.536
4.0	0.414	0.303	0.473
4.5	0.467	0.353	0.542
5.0	0.498	0.441	0.602
5.5	0.484	0.370	0.574
6.0	0.535	0.383	0.657
6.5	0.516	0.412	0.581

bubble size given by

$$d_{bs} = \frac{\sum d_{bv}^3}{\sum d_{bv}^2} \tag{5.4}$$

Table 5.1 gives the d_{bs}, d_{min} and d_{max}. Here the d_{min} is defined as the size of the smallest bubble, and the d_{max} is defined as the size of the largest bubble at the given J_g.

5.1.2 Relationships Among d_{bs}, d_{min}, d_{max} and J_g

Figure 5.2 illustrates the variation in d_{bs} with J_g. The relationship between d_{bs} and J_g is given by (in cgs units)

$$d_{bs} = 0.33\, J_g^{0.24} \tag{5.5}$$

Similarly, the relationship between d_{min} and J_g is given by

$$d_{\min} = 0.21\, J_g^{0.37} \tag{5.6}$$

and the relationship between d_{max} and J_g is given by

$$d_{\max} = 0.43\, J_g^{0.18} \tag{5.7}$$

Figure 5.3 gives two curves: one represents the relationship between d_{max} and J_g; the other represents the relationship between d_{min} and J_g. The shaded area illustrates the bubble size distribution at various J_g. Using Equations 5.5, 5.6 and 5.7, Figure 5.4 illustrates the features of the bubble size distribution. As J_g increases the d_{max}/d_{bs} decreases and d_{min}/d_{bs} increases slightly. Note that compared with d_{bs} which increases from 0.24 to 0.52 cm, the difference between d_{max} and d_{min} is almost constant for J_g from 0.25 to 6.5 cm/s. This implies that increasing J_g does not cause an absolute widening of the size distribution of bubbles.

In flotation columns, the mean bubble size and the size distribution of bubbles not only depend on the superficial gas rate J_g but also on the other physical chemical characteristics of the gas and liquid. However, an empirical relationship has been developed for correlating bubble size with gas rate (Dobby and Finch, 1986; Xu and Finch, 1989; Yianatos and Finch, 1990), namely

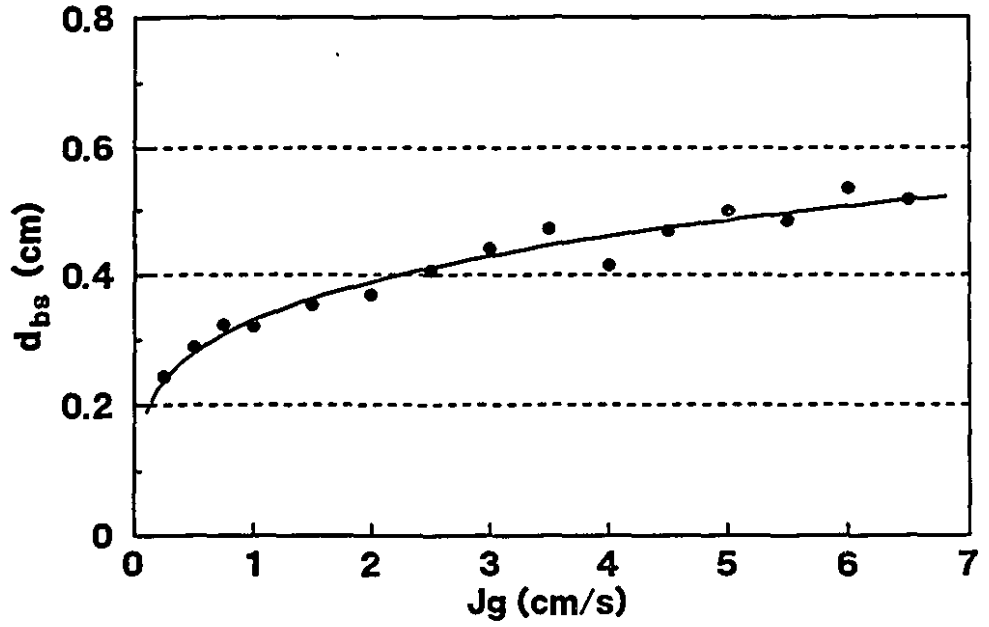

Figure 5.2 Mean bubble size d_{bs} versus J_g.

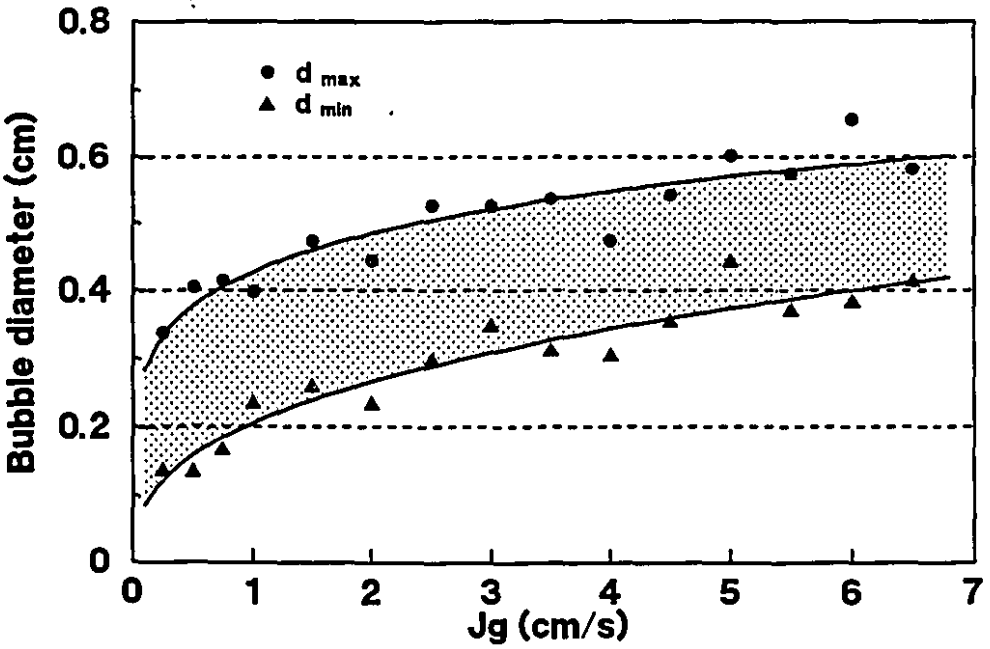

Figure 5.3 d_{max} and d_{min} versus J_g.

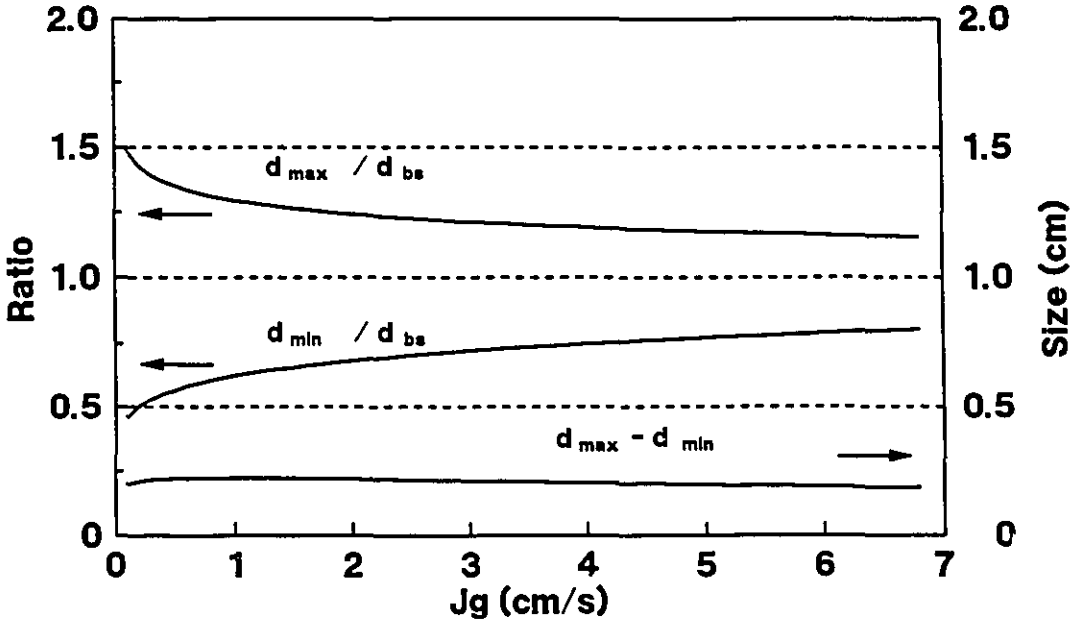

Figure 5.4 Analysis of features of the bubble size distribution.

$$d_b = C J_g^{0.25} \tag{5.8}$$

where d_b is the bubble diameter in cm and C is a fitting parameter, which is mainly dependent on the frother concentration, the sparger size and column size. Xu (1990) indicated that in cgs units, C is 0.115, 0.100, 0.085 and 0.075 with DF250C = 5, 10, 15 and 25 ppm, respectively. In this study, Equation 5.5 shows that C is 0.33 in the air - water only system with an exponent of 0.24, i.e. similar to the 0.25 exponent in Equation 5.8.

5.1.3 u_b in Air - Water Only System

When Zhou et al. (1993a; 1993b) evaluated the effects of the frothers, they found that tap water contained sufficient surface active contaminants to affect the bubble velocity. Figure 4.7 (Clift et al., 1978) illustrates that surfactants have a strong influence on the bubble terminal velocity. For bubbles between 0.2 and 0.5 cm, the bubble terminal velocities vary from 18 to 26 cm/s and the average is 21 cm/s.

5.2 Hindered Velocity of a Bubble Swarm u_h in Cell 6

5.2.1 Definition of Hindered Velocity

Figure 5.5 shows the creation and rise of a bubble front (or interface) upon introducing a step change of gas flow in a vertical column. When the gas flow is suddenly terminated as in case (a), an interface appears: above the interface the gas holdup is that prior to the termination of the gas flow; below the interface ε_g=0. By Nicklin's definition (1962), the velocity of the rising interface in case (a) is the buoyancy velocity of the bubble swarm, u_o.

In case (b) when the gas flow is not terminated completely but reduced by a certain amount, an interface is again formed. In cases (d) and (e) gas rate is increased and an interface forms, now because $\varepsilon_{g2} > \varepsilon_{g1}$. Case (c) represents the situation where gas rate is unchanged. No interface forms but it will be shown later that the velocity of the rising bubble swarm can be calculated by interpolation from the interface velocities in the other four cases.

We will define the calculated velocity of the rising bubble swarm in case (c) as, u_h, the hindered velocity of the bubble swarm. Many researchers equate the bubble swarm velocity to the average gas velocity, $u_g = J_g / \varepsilon_g$. However, we will show that the bubble swarm velocity is better equated with the hindered velocity of the bubble swarm, u_h.

5.2.2 Measurement of Interface Velocity u_{ln} in Cell 6

The experiments were carried out by introducing a step change of air flow. The procedure was:

(a) open Valve 1 (set to the initial superficial gas velocity J_{g1});
(b) wait for steady state conditions in the column;
(c) at 0 s, start the data acquisition system;
(d) at 10 s, close Valve 1 and open Valve 2 (set to the second superficial gas velocity J_{g2});
(e) at 40 s, close Valve 2;
(f) at 60 s, stop the data acquisition system.

The procedure was controlled by computer.

Figure 5.6 shows the resistance versus time in Cell 6 for an experiment in case (a). During period A, the rising interface has not reached Electrode 7 and the resistance is constant. After

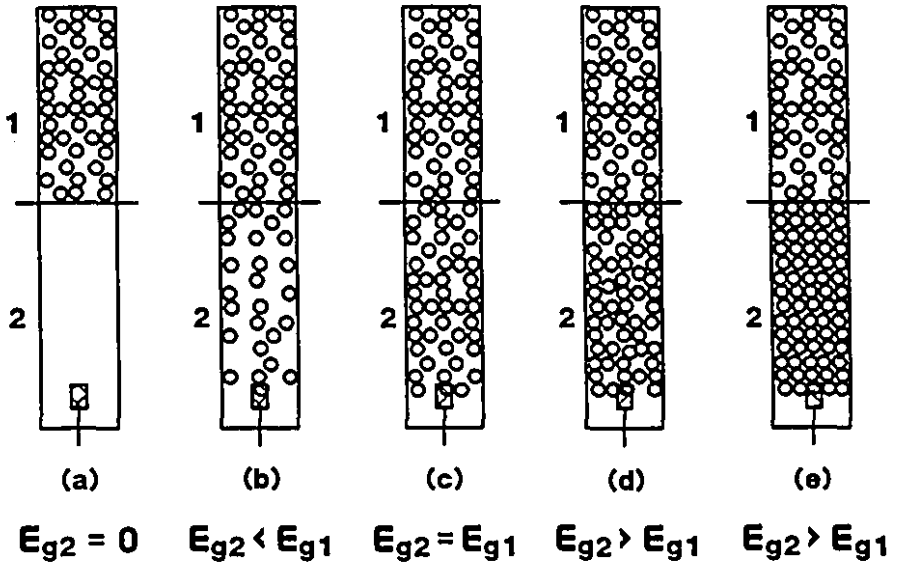

Figure 5.5 Interface formed by a step change of gas flow.

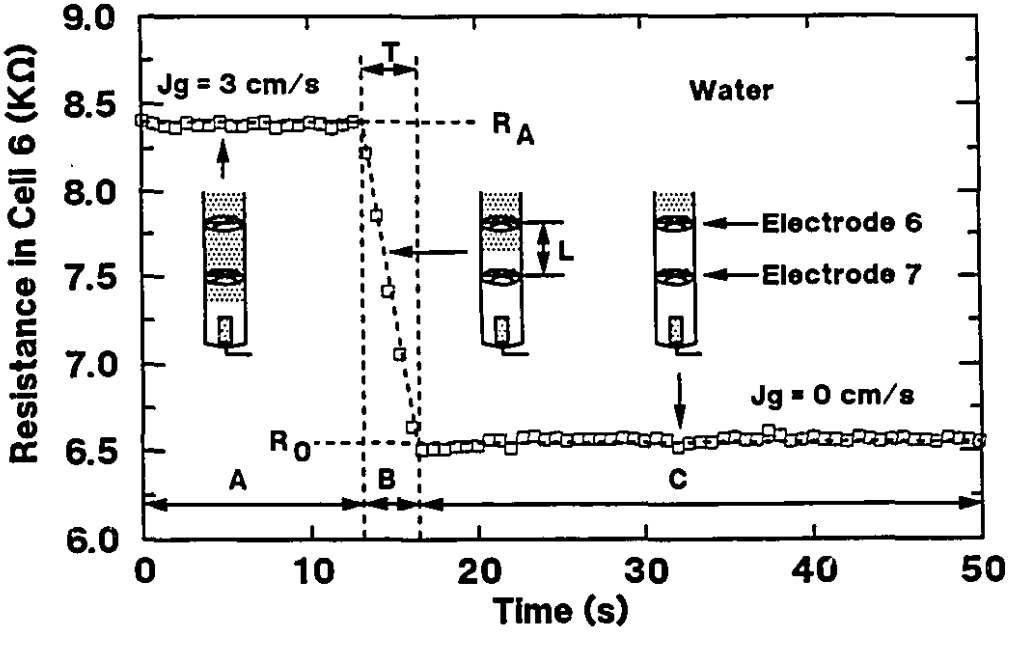

Figure 5.6 Resistance versus time in Cell 6 for case (a) in Figure 5.5.

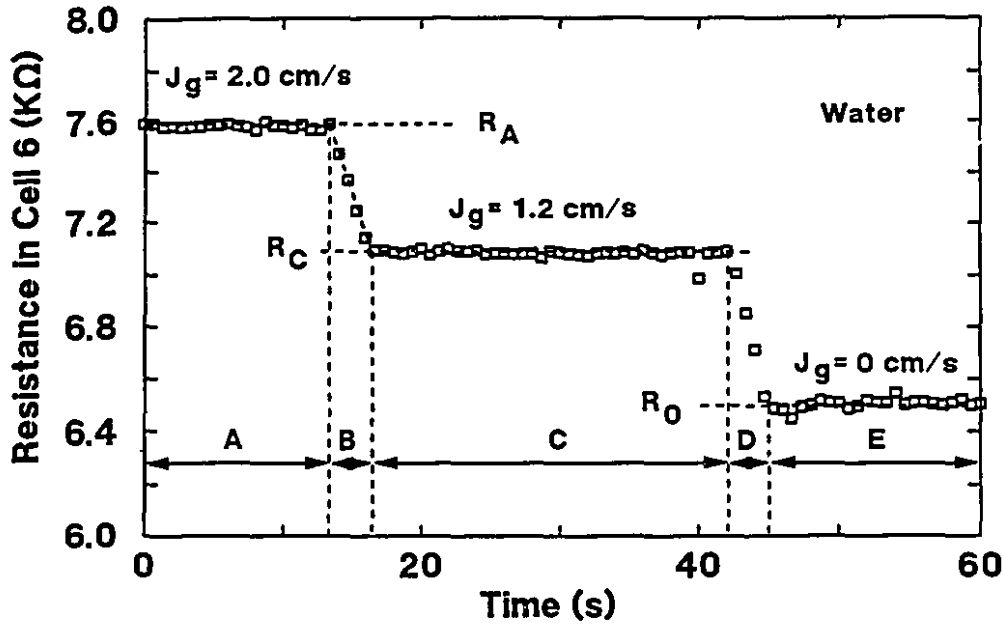

Figure 5.7 Resistance versus time in Cell 6 for case (b) in Figure 5.5.

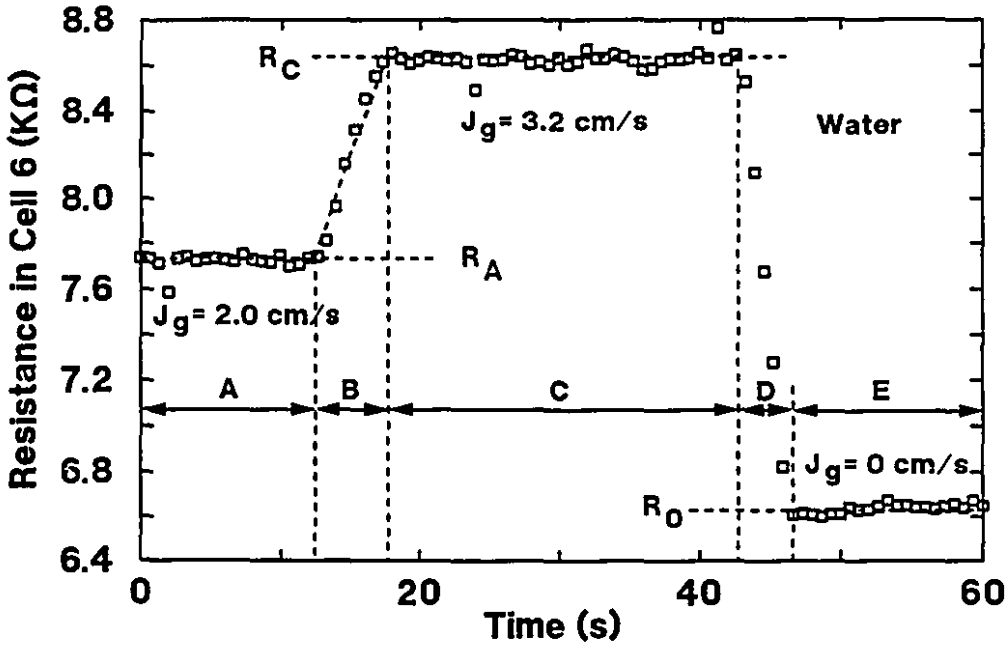

Figure 5.8 Resistance versus time in Cell 6 for case (d) or (e) in Figure 5.5.

the interface has passed Electrode 7, the resistance begins to decrease (period B). During period C the interface has left Electrode 6 and the resistance is again constant.

The resistance during period A was averaged as R_A which represents the resistance of the mixture of air bubbles and water. R_0 is the average resistance during period C which represents the resistance of the water. The gas holdup ε_g during period A can be calculated from Maxwell's model for a non-conducting dispersed phase (Finch and Dobby, 1990a; Uribe-Salas et al., 1991; Yianatos et al., 1985). For convenience, the model is written as

$$\varepsilon_g = \frac{R_A - R_0}{R_A + 0.5\,R_0} \tag{5.9}$$

The interface velocity u_{in} can be calculated by

$$u_{in} = \frac{L}{T} \tag{5.10}$$

where L is the distance between Electrodes 7 and 6 (51 cm) and T is the length of period B.

Figure 5.7 illustrates the resistance versus time in Cell 6 for case (b). All the descriptions for case (a) are applicable here with the addition of periods D and E when $J_g \rightarrow 0$. In the experiment shown in Figure 5.7, J_g was reduced from 2.0 to 1.2 cm/s. R_C and R_0 are the average resistance during periods C and E respectively. Using R_C and R_0, the gas holdup during period C can be calculated by Equation 5.9. The interface velocity in period B is determined by Equation 5.10.

Figure 5.8 illustrates the resistance versus time for case (d) or (e). In the experiment illustrated, J_g was increased from 2.0 to 3.2 cm/s. The same calculations used for Figure 5.7 are employed here. (The data obtained during period D could be used for the evaluation of the interface velocity, by treating periods C, D, and E as a new case (a).)

5.2.3 Interface Velocity u_{in} and Hindered Velocity u_h of Bubble Swarm in Cell 6

To obtain the response curve of the resistance versus time, each experiment involved hundreds data points. Because of this large quantity, a hard copy of all data has not be included. Only the analyzed results are shown here.

To form a rising interface in the column, J_g was step changed from the initial (J_{g1}) to the final (J_{g2}). Corresponding to J_{g1} and J_{g2}, ε_{g1} and ε_{g2} are defined as the gas holdup during periods A and C, respectively. Tables 5.2 - 5.6 present u_{in}, ε_{g1} and ε_{g2} at J_{g1} = 1.0, 1.5, 2.0, 2.5 and 3.0 cm/s, respectively.

(i) Linear regression for u_h

Figure 5.14 illustrates the relationship between the interface velocity and the dimensionless gas rate (J_{g2} / J_{g1}) at J_{g1} = 1.0 cm/s: a linear relation is shown. At J_{g2} / J_{g1} = 1, the interface velocity is equal to 18.2 cm/s. This velocity is the hindered velocity, i.e. the u_{in}, in case (c) of Figure 5.10. As discussed in Section 5.2.1, the bubble swarm velocity can not be measured directly by the present conductivity method. However, it can be estimated using the data analysis in Figure 5.9. To date the bubble swarm velocity has been equated with the average gas velocity, u_g. To avoid confusion, this specific interface velocity at J_{g2} / J_{g1} = 1 is defined as the bubble hindered velocity, u_h, which is, it is proposed, equated with the bubble swarm velocity. In this case, u_h is 18.2 cm/s at J_g = 1.0 cm/s. Using the same method the bubble hindered velocities are calculated for J_g = 1.5, 2.0, 2.5 and 3.0 cm/s and are shown in Figures 5.10, 5.11, 5.12 and 5.13, respectively.

(ii) Experimental errors

The relative standard deviation of u_{in} is given by

$$C_{u_{in}} = \frac{S_{u_{in}}}{\bar{u}_{in}} \tag{5.11}$$

where S_{uin} is the standard deviation of u_{in}, and $\bar{u}_{in}$ is the average value of u_{in}. The relative standard deviation of ε_g is given by

$$C_{\varepsilon_g} = \frac{S_{\varepsilon_g}}{\bar{\varepsilon}_g} \tag{3.25}$$

For all data in Tables 5.2 - 5.6, based on ten replicates for each experiment, the maximum relative standard deviation of u_{in} was 1.56%, the maximum relative standard deviation of u_0 was 1.01%, and the maximum relative standard deviation of ε_g was 2.60%.

For the linear regression of u_h, the standard errors of the estimated u_h were 0.22, 0.31, 0.18, 0.22 and 0.18 cm/s at J_{g1} = 1.0, 1.5, 2.0, 2.5 and 3.0 cm/s, respectively.

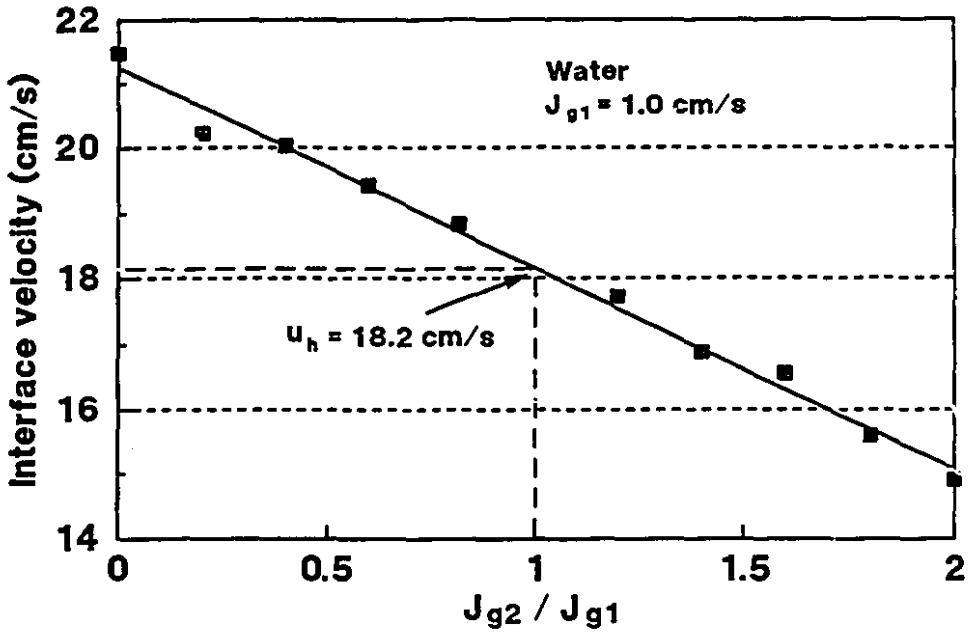

Figure 5.9 Interface velocities in Cell 6 at J_{g1} = 1.0 cm/s.

Table 5.2 Interface velocities in Cell 6 at J_{g1} = 1.0 cm/s

J_{g1} (cm/s)	J_{g2} (cm/s)	J_{g2} / J_{g1}	ε_{g1} (%)	ε_{g2} (%)	u_{in} (cm/s)
1	0	0	4.40	0	21.5
1	0.2	0.2	4.33	0.86	20.2
1	0.4	0.4	4.35	1.85	20.0
1	0.6	0.6	4.45	2.86	19.4
1	0.8	0.8	4.50	3.74	18.9
1	1.2	1.2	4.38	5.94	17.7
1	1.4	1.4	4.47	6.75	16.9
1	1.6	1.6	4.54	7.98	16.6
1	1.8	1.8	4.52	9.34	15.6
1	2.0	2.0	4.53	10.32	14.9

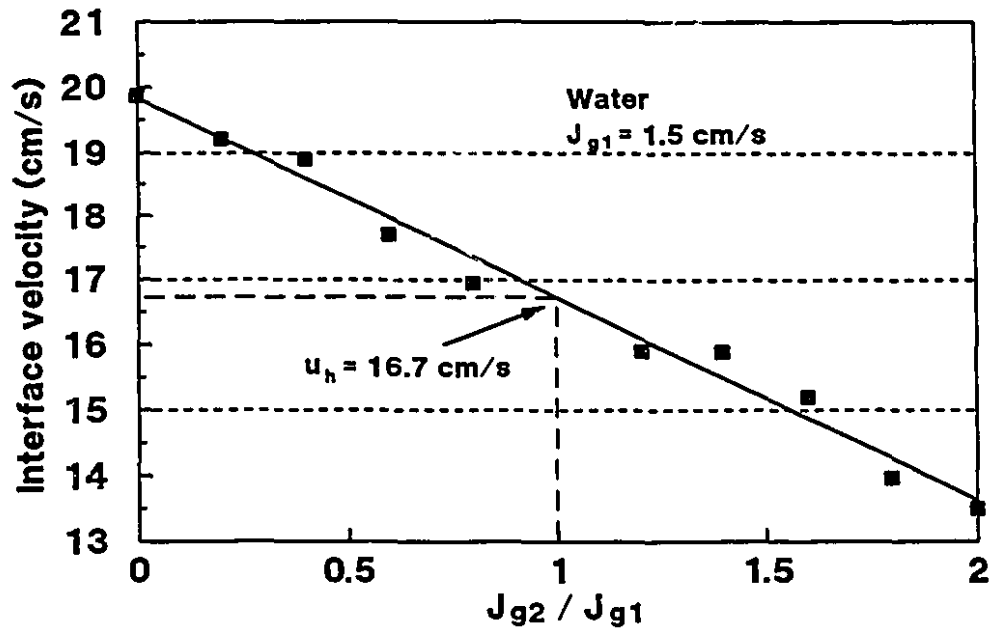

Figure 5.10 Interface velocities in Cell 6 at J_{g1} = 1.5 cm/s.

Table 5.3 Interface velocities in Cell 6 at J_{g1} = 1.5 cm/s

J_{g1} (cm/s)	J_{g2} (cm/s)	J_{g2} / J_{g1}	ε_{g1} (%)	ε_{g2} (%)	u_{in} (cm/s)
1.5	0	0	6.80	0	19.9
1.5	0.3	0.2	7.17	1.08	19.2
1.5	0.6	0.4	7.04	2.53	18.9
1.5	0.9	0.6	7.05	4.00	17.7
1.5	1.2	0.8	6.93	5.39	16.9
1.5	1.8	1.2	6.91	8.08	15.9
1.5	2.1	1.4	6.89	10.45	15.9
1.5	2.4	1.6	6.84	11.94	15.2
1.5	2.7	1.8	6.93	13.56	14.0
1.5	3.0	2.0	6.82	15.56	13.5

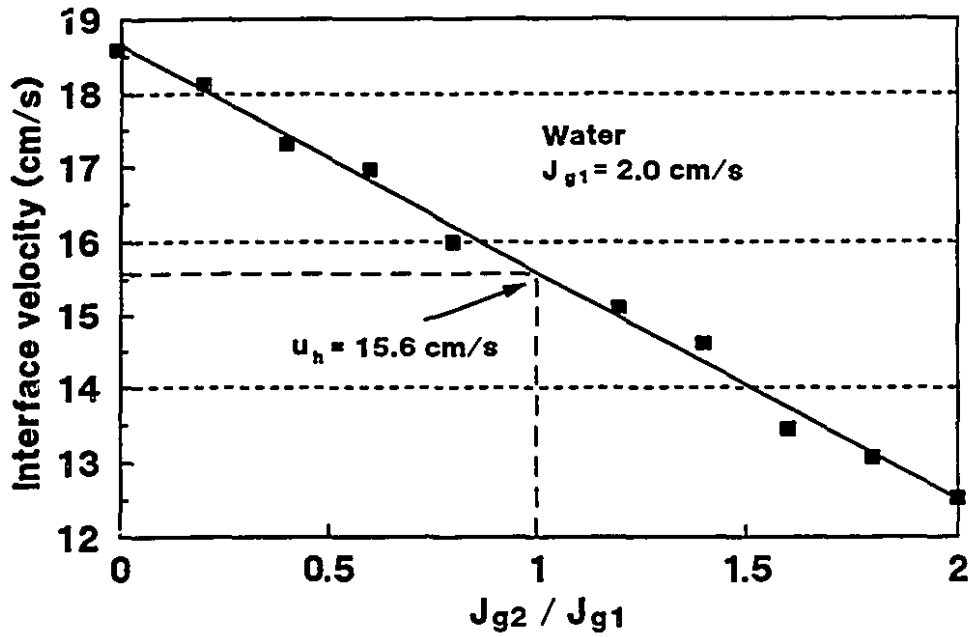

Figure 5.11 Interface velocities in Cell 6 at J_{g1} = 2.0 cm/s.

Table 5.4 Interface velocities in Cell 6 at J_{g1} = 2.0 cm/s

J_{g1} (cm/s)	J_{g2} (cm/s)	J_{g1} / J_{g2}	ε_{g1} (%)	ε_{g2} (%)	u_{in} (cm/s)
2	0	0	9.88	0	18.6
2	0.4	0.2	10.08	1.73	18.1
2	0.8	0.4	10.02	3.45	17.3
2	1.2	0.6	9.94	5.54	17.0
2	1.6	0.8	10.04	7.71	16.0
2	2.4	1.2	9.21	11.55	15.1
2	2.8	1.4	9.57	13.93	14.6
2	3.2	1.6	9.35	16.08	13.5
2	3.6	1.8	9.25	18.47	13.1
2	4.0	2.0	9.27	20.82	12.5

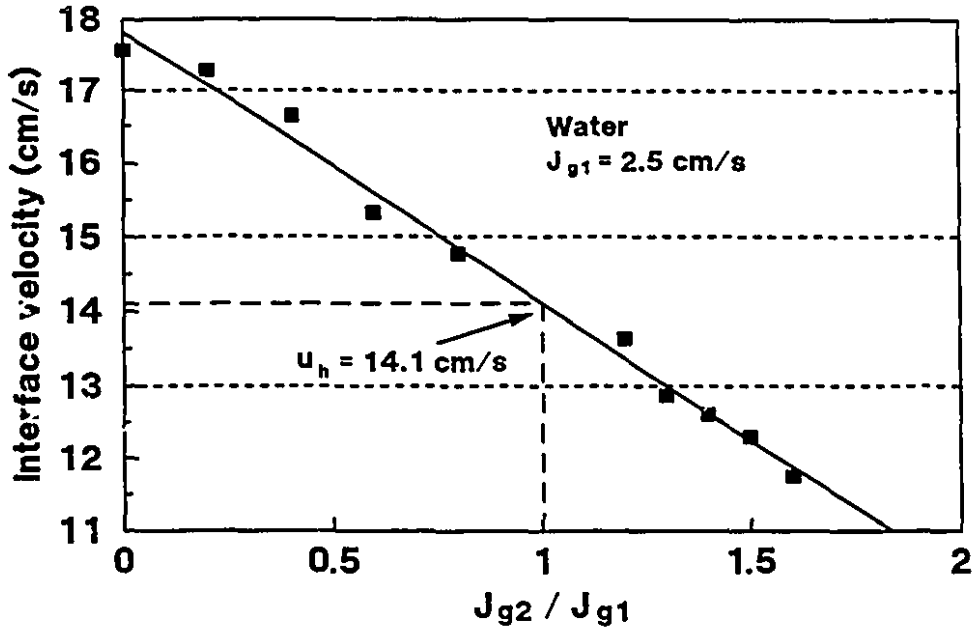

Figure 5.12 Interface velocities in Cell 6 at J_{g1} = 2.5 cm/s.

Table 5.5 Interface velocities in Cell 6 at J_{g1} = 2.5 cm/s

J_{g1} (cm/s)	J_{g2} (cm/s)	J_{g2} / J_{g1}	ε_{g1} (%)	ε_{g2} (%)	u_{in} (cm/s)
2.5	0	0	12.39	0	17.6
2.5	0.5	0.2	12.91	2.23	17.3
2.5	1.0	0.4	12.98	4.59	16.6
2.5	1.5	0.6	12.65	7.22	15.3
2.5	2.0	0.8	12.80	10.03	14.8
2.5	3.0	1.2	12.72	15.62	13.6
2.5	3.25	1.3	12.81	16.73	12.9
2.5	3.5	1.4	12.92	18.61	12.6
2.5	3.75	1.5	12.83	19.68	12.3
2.5	4.0	1.6	12.84	21.06	11.8

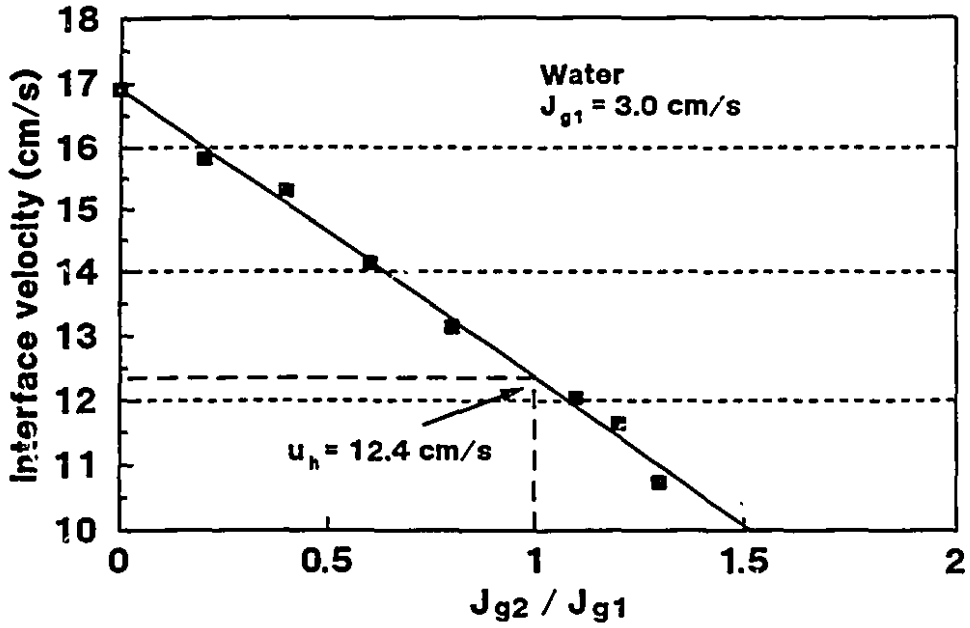

Figure 5.13 Interface velocities in Cell 6 at J_{g1} = 3.0 cm/s.

Table 5.6 Interface velocities in Cell 6 at J_{g1} = 3.0 cm/s

J_{g1} (cm/s)	J_{g2} (cm/s)	J_{g2} / J_{g1}	ε_{g1} (%)	ε_{g2} (%)	u_{in} (cm/s)
3	0	0	15.35	0	16.9
3	0.6	0.2	15.69	2.63	15.8
3	1.2	0.4	15.89	5.56	15.3
3	1.8	0.6	16.01	9.05	14.1
3	2.4	0.8	15.84	12.50	13.2
3	3.3	1.1	15.75	17.72	12.0
3	3.6	1.2	15.80	19.66	11.7
3	3.9	1.3	15.72	21.17	10.7

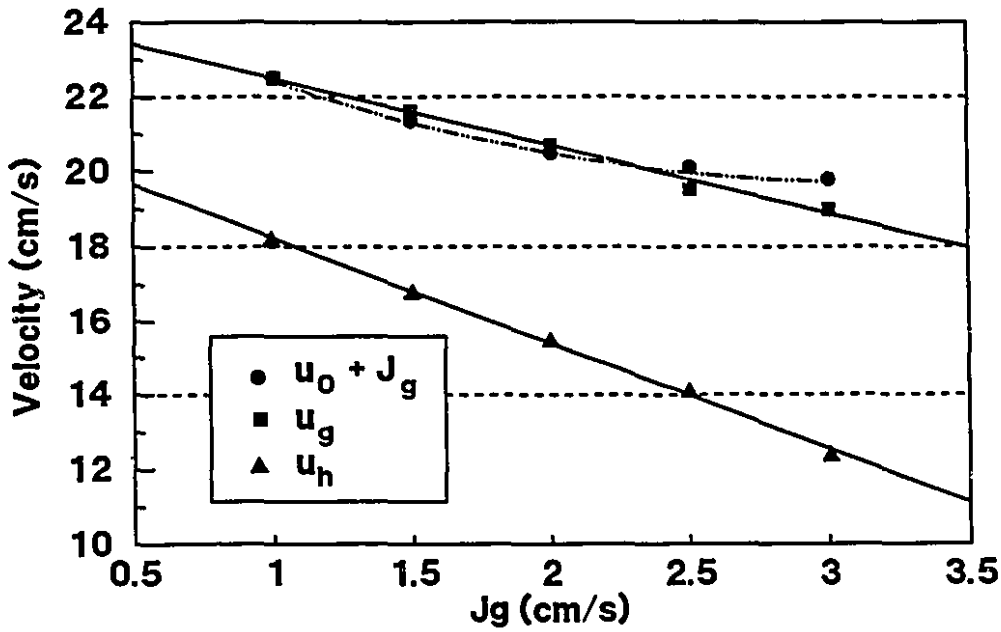

Figure 5.14 Comparison of u_g and u_h in Cell 6.

5.2.4 Relationships among u_g, u_h and J_{gl} in Cell 6

Table 5.7 shows the u_g and u_h at various J_{gl}. In Table 5.7, the u_g is calculated by $u_g = J_{gl}/\varepsilon_{gl}$. The u_0 is the measured buoyancy velocity which is equal to u_{in} at $J_{g2} = 0$. For example, the u_0 for $J_{gl} = 1.0$ cm/s is equal to 21.5 cm/s (first row in Table 5.2).

Table 5.7 Comparison among u_g, u_h and u_0+J_g in Cell 6 *

J_{gl}	1.0	1.5	2.0	2.5	3.0
ε_{gl}(%)	4.44	6.94	9.66	12.79	15.76
u_g	22.5	21.6	20.7	19.5	19.0
$u_0 + J_{gl}$	22.5	21.4	20.6	20.1	19.9
u_h	18.2	16.7	15.6	14.1	12.4

* all velocities are cm/s.

Assuming u_h is a linear function of J_{gl}, as Figure 5.14 suggests, an empirical model is

$$u_h = 21.1 - 2.84 J_{gl} \tag{5.12}$$

where the units are in cgs. Figure 5.14 illustrates that the difference between u_g and u_0+J_g is quite small. It establishes that Nicklin's concept can be applied to the data obtained in Cell 6 in the bubble column. However, the difference between u_g and u_h is significant and increases as J_{gl} increases.

5.2.5 Relationship between u_{in} and u_h in Cell 6

To explore the relation between u_{in} and u_h, the dimensionless velocity (u_{in}/u_l) versus the dimensionless gas rate (J_{g2}/J_{gl}) is shown in Figure 5.15. It indicates that the slope of the curve is a function of the initial gas rate, J_{gl}. Table 5.8 gives the slopes at various J_{gl}.

Table 5.8 Slopes at various J_{gl}

J_{gl} (cm/s)	1.0	1.5	2.0	2.5	3.0
Slope	-0.1700	-0.1854	-0.1976	-0.2631	-0.3688

The equation relating the slope and J_{gl} is given by

$$slope = -0.170 - 0.00162\, J_{gl}^{4.4} \tag{5.13}$$

Figure 5.16 shows that the above equation gives an acceptable fit. From inspection of Figure 5.20, the linear relation between u_{in}/u_h and J_{g2}/J_{gl} can be taken as

$$\frac{u_{in}}{u_h} = A \frac{J_{g2}}{J_{gl}} + B \tag{5.14}$$

where A and B are the slope and intercept of the linear equation, respectively. When $J_{gl}/J_{g2} = 1$, u_{in}/u_h is equal to 1 and thus

$$B = 1 - A \tag{5.15}$$

Substituting Equations 5.15 in 5.14, yields

$$u_{in} = u_h \left[1 + A \left(\frac{J_{g2}}{J_{gl}} - 1 \right) \right] \tag{5.16}$$

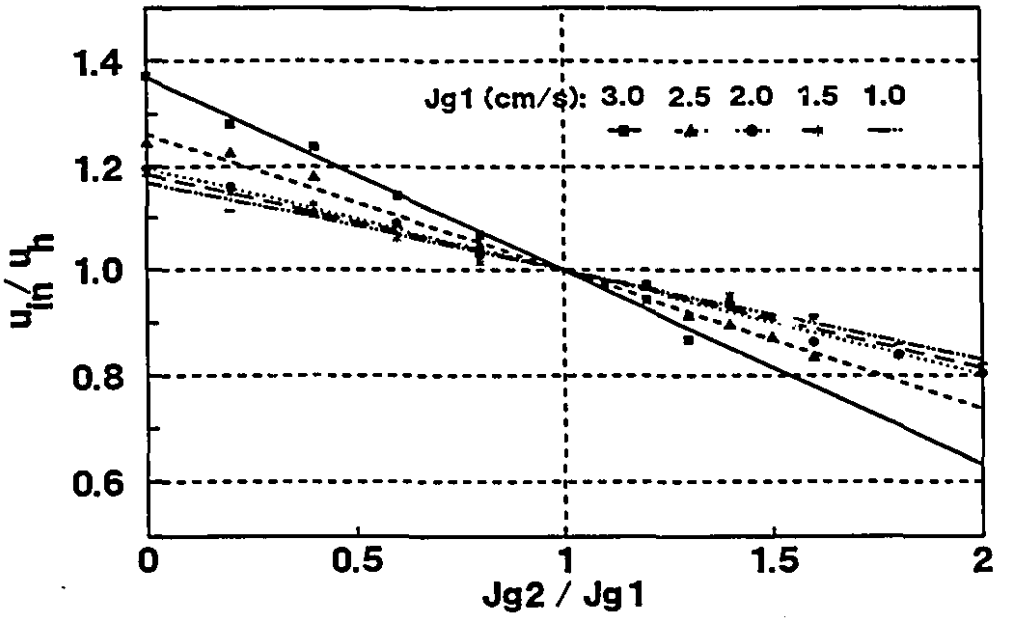

Figure 5.15 Dimensionless velocity versus dimensionless gas rate.

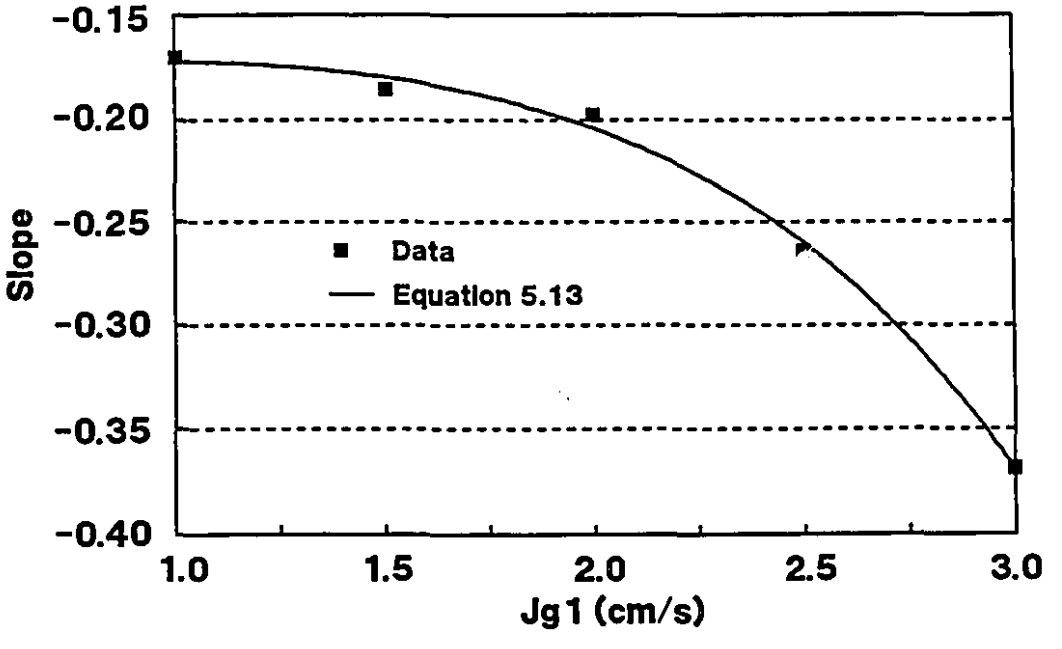

Figure 5.16 Curve fitting for the slope and J_{g1}.

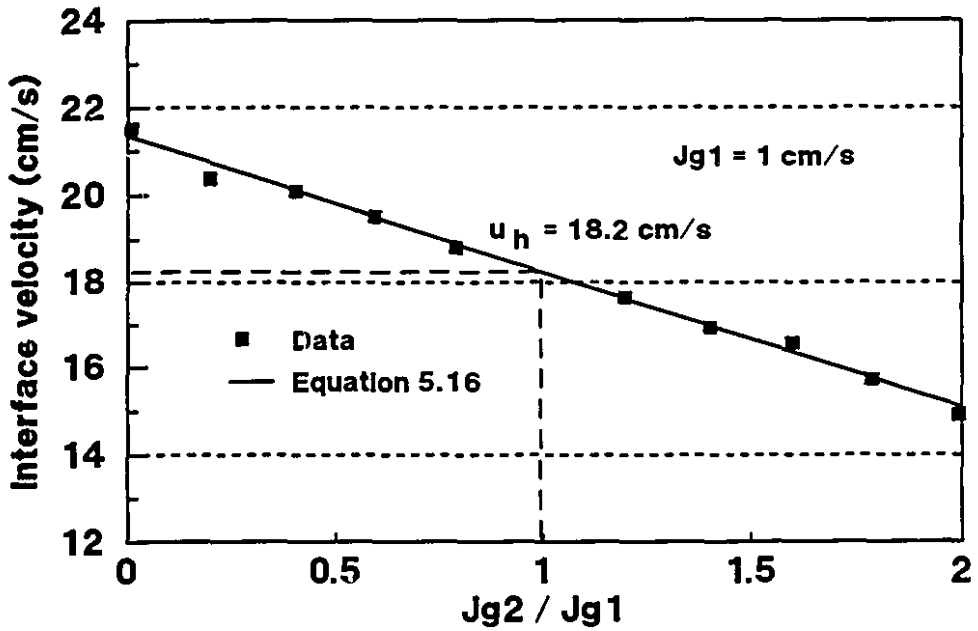

Figure 5.17 Comparison of model and measured u_{in} in Cell 6 at J_{gl} = 1.0 cm/s.

where u_h and A, to recall, are

$$u_h = 21.1 - 2.84 J_{gl} \tag{5.12}$$

$$A = -0.170 - 0.00162 J_{gl}^{4.4} \tag{5.13}$$

The model applies to water only under bubbly flow conditions (J_g < 4 cm/s) and batch operation. Figure 5.17 illustrates that the model shows good agreement with the measured u_{in} at J_{gl} = 1.0 cm/s. Using Equation 5.16, u_{in} can be evaluated from u_h and J_g. This suggests that for a particular column the hindered velocity, u_h, should be a characteristic parameter of the system.

5.3 Buoyancy Velocity of a Bubble Swarm u_0 in Cell 6

5.3.1 Definition of Buoyancy Velocity

The buoyancy velocity, u_0, is the velocity with which the bubble swarm rises due to the difference in density between the gas and liquid. It depends on the bubble size and gas holdup, and on the properties of the system. Figure 5.18 illustrates two ways in which an interface can be created to measure velocities: (a) by stopping the gas flow, and (b) by introducing an air pulse. In case (b) there are two velocities: u_2 is the velocity of the top interface and u_1 is the velocity of the bottom interface. In Figure 5.18 u_0 is defined as the buoyancy velocity.

5.3.2 Measurements of u_1 and u_2

Nicklin (1962) measured the u_0 and u_1 shown in Figure 5.18. He assumed that u_1 was equal to u_0 although no proof was offered. The goal of the experiments in this section was to measure u_1 and u_2 and to find the relationships among u_1, u_2 and the buoyancy velocity, u_0, measured in Section 5.2.

A set of experiments was carried out by introducing air pulses of varying duration into the column. The duration of the air pulse was determined by the open-time of the air valve. All experiments were made at J_g = 2.0 cm/s under steady conditions and J_l = 0. As an example, for air pulse duration of 0.44 second, the procedure was:

(a) set J_g = 2.0 cm/s and switch off air flow;
(b) wait for all air bubbles to leave the liquid;
(c) start the data acquisition system at 0 s;
(d) switch on the air valve at 10 s;
(e) switch off the air valve at 10.44 s;
(f) stop the data acquisition system at 40 s.

The procedure was controlled by computer.

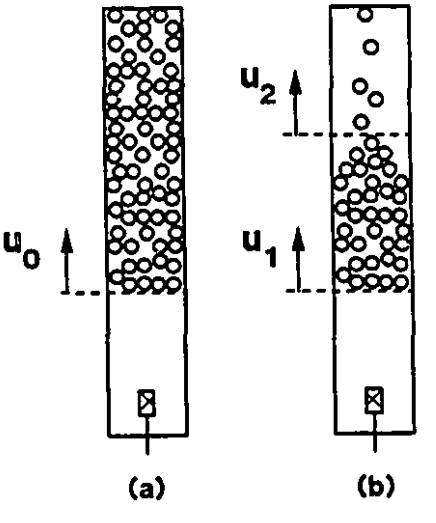

Figure 5.18 Velocities of a bubble swarm: (a) gas switched off; (b) gas switched on then off.

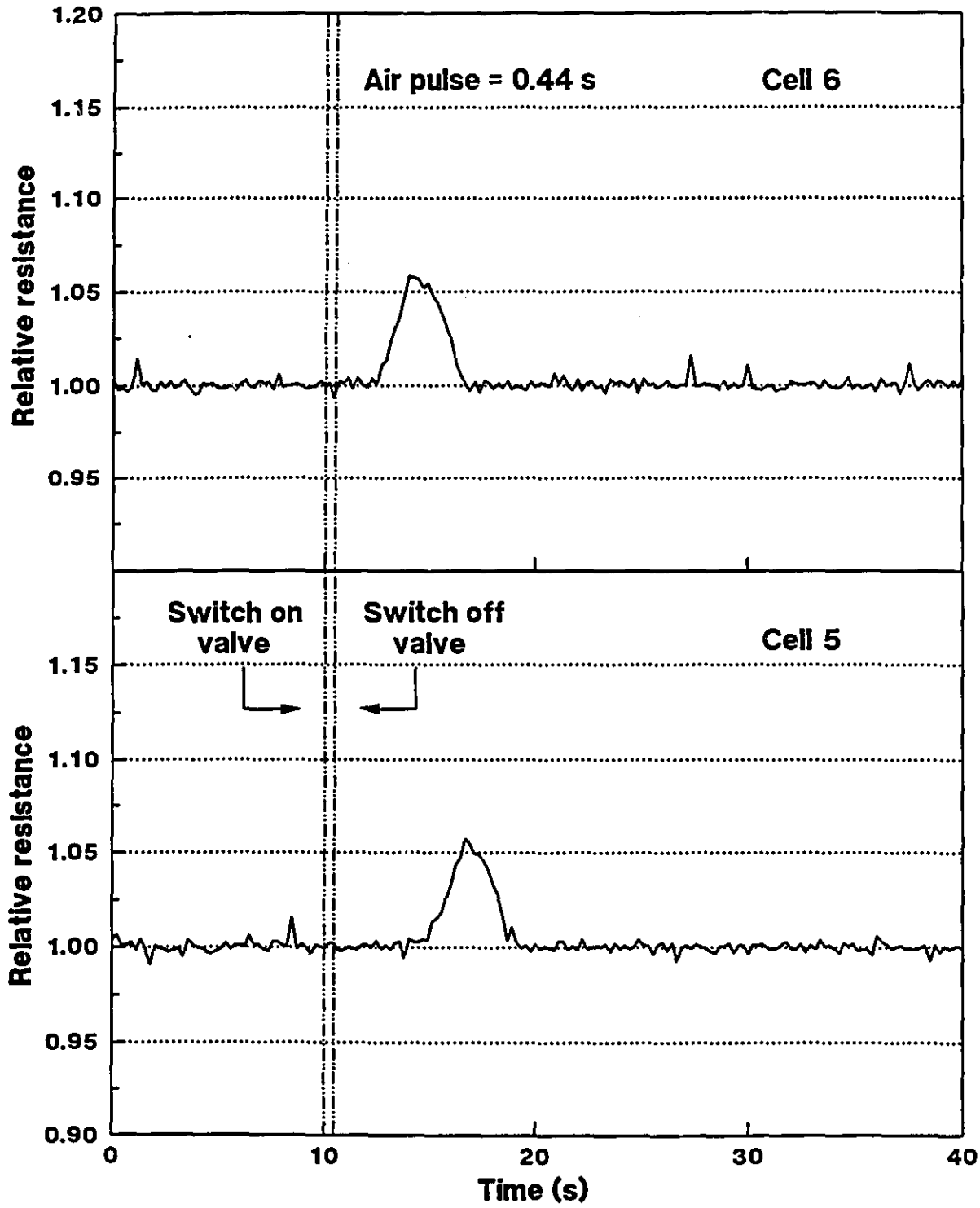

Figure 5.19 Relative resistance versus time at air pulse = 0.44 s.

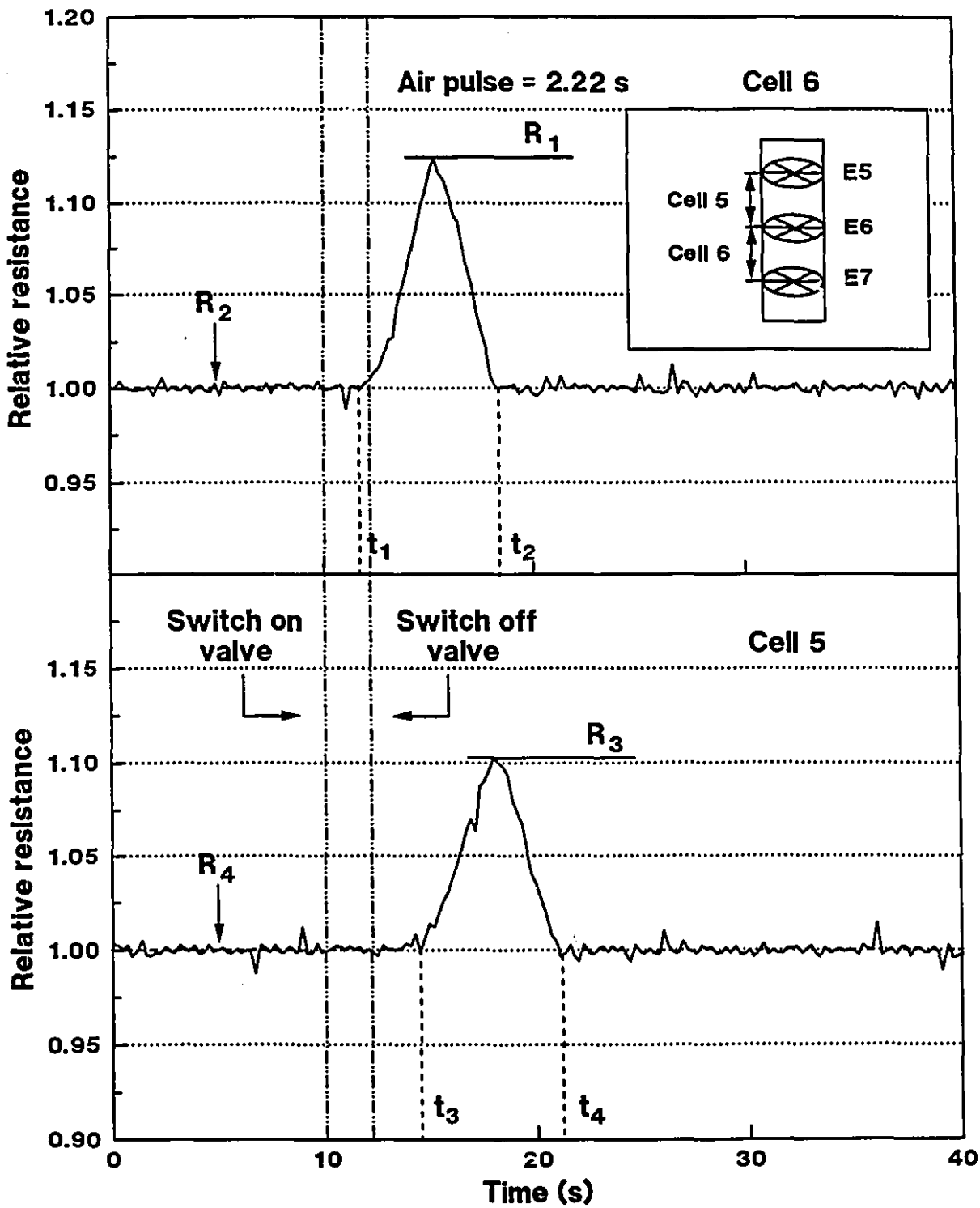

Figure 5.20 Relative resistance versus time at air pulse = 2.22 s.

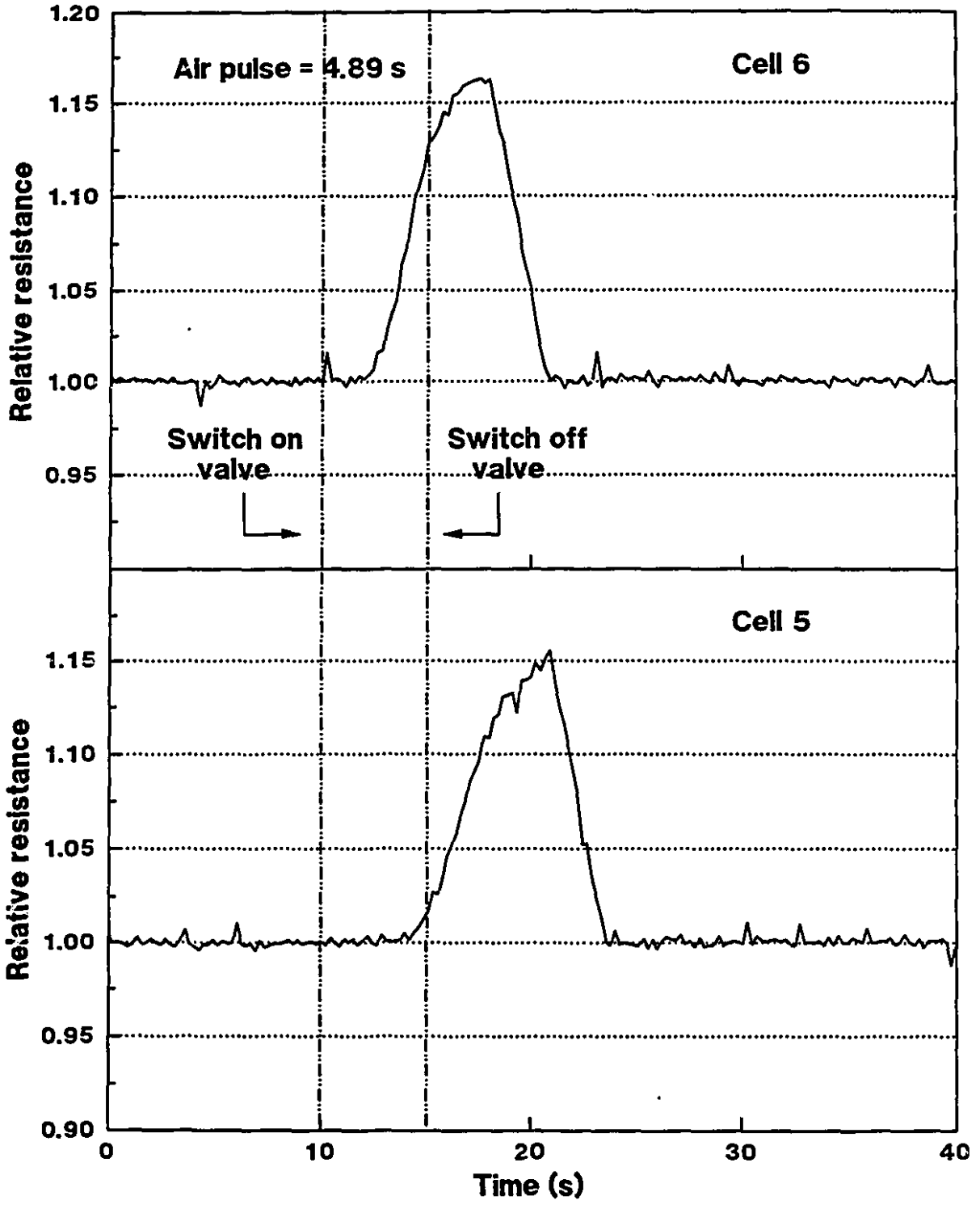

Figure 5.21 Relative resistance versus time at air pulse = 4.89 s.

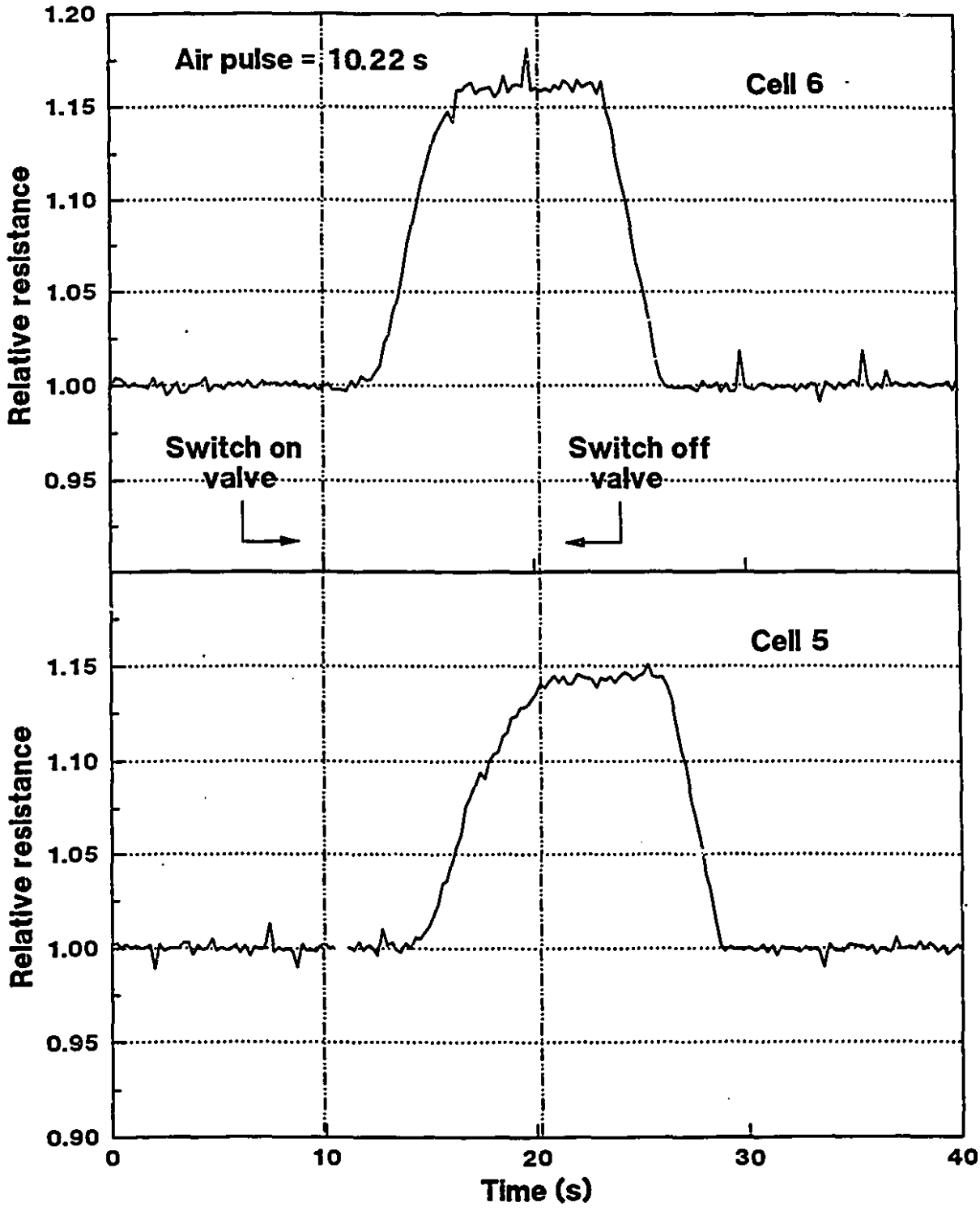

Figure 5.22 Relative resistance versus time at air pulse = 10.22 s.

5.3.3 Results and Analysis

Figures 5.19 - 5.22 show results for air pulse = 0.44, 2.22, 4.89 and 10.22 seconds, respectively. (To eliminate the unit of resistance, Figures 5.19 - 5.22 use a relative resistance on the Y-axis, where R_2 is set as 1 for Cell 6 and R_4 is set as 1 for Cell 5.) Even at air pulse = 0.44 s, data were recorded clearly (Figure 5.19) although the total number of air bubbles injected was quite low. Figure 5.21 illustrates the condition where the bubble swarm just fills the cell (note the flattening of the peak in Cell 6).

Data in Figure 5.20 can be used to illustrate the calculations. When the air pulse was introduced into the column, the top of the bubble swarm first touched Electrode 7 (E7) at t_1 and then touched Electrode 6 (E6) at t_3. The bottom of the bubble swarm left E6 at t_2 and then left E5 at t_4. The distance between two electrodes is 51 cm. Consequently the velocity of the top of the bubble swarm in Cell 6, $u_{2,C6}$, is given by

$$u_{2,C6} = \frac{51}{t_3 - t_1} \tag{5.17}$$

and the velocity of the bottom of the bubble swarm in Cell 5, $u_{1,C5}$, is given by

$$u_{1,C5} = \frac{51}{t_4 - t_2} \tag{5.18}$$

with units of cm/s. From t_1, t_2, t_3 and t_4, we can obtain $u_{1,C5}$ and $u_{2,C6}$.

In Figure 5.20, R_2 was the average resistance of the water without air bubbles in Cell 6, and R_1 was the maximum resistance as air bubbles passed through the cell. The maximum gas holdup in Cell 6, $\varepsilon_{g,m6}$, was calculated by substituting R_2 and R_1 into Maxwell's equation. Similarly R_4 and R_3 were used to calculate the maximum gas holdup in Cell 5, $\varepsilon_{g,m5}$.

Based on six replicates for each experiment, the maximum relative standard deviation was 5.36% for the $u_{2,C6}$ and $u_{1,C5}$ shown in Table 5.9, and the maximum relative standard deviation was 5.85% for the $\varepsilon_{g,m6}$ and $\varepsilon_{g,m5}$ shown in Table 5.10.

Table 5.9 gives the $u_{2,C6}$ and $u_{1,C5}$ at the various durations of the air pulses. From Section 5.1, the single bubble terminal velocity, u_b, is about 21 cm/s. However, Figure 5.23 shows $u_{2,C6}$ decreases as the air pulse increases, asymptotically approaching 25.5 cm/s. The difference

Table 5.9 $u_{2,cs}$ and $u_{1,cs}$ versus duration of air pulse

Duration of air pulse (s)	$u_{2,cs}$ (cm/s)	$u_{1,cs}$ (cm/s)
0.44	34.9	21.1
0.89	34.0	20.9
1.33	31.9	19.2
2.22	28.8	18.1
3.11	28.9	18.6
4.00	28.3	18.5
4.89	26.0	18.8
6.67	25.6	18.9
10.22	25.5	18.6

Table 5.10 $\varepsilon_{g,m6}$ and $\varepsilon_{g,m5}$ versus duration of air pulse

Duration of air pulse (s)	$\varepsilon_{g,m6}$ (%)	$\varepsilon_{g,m5}$ (%)
0.44	2.02	2.02
0.89	3.79	3.67
1.33	5.32	4.56
2.22	7.58	6.38
3.11	9.38	7.81
4.00	9.51	8.59
4.89	9.79	9.38
6.67	9.91	9.34
10.22	9.88	9.09

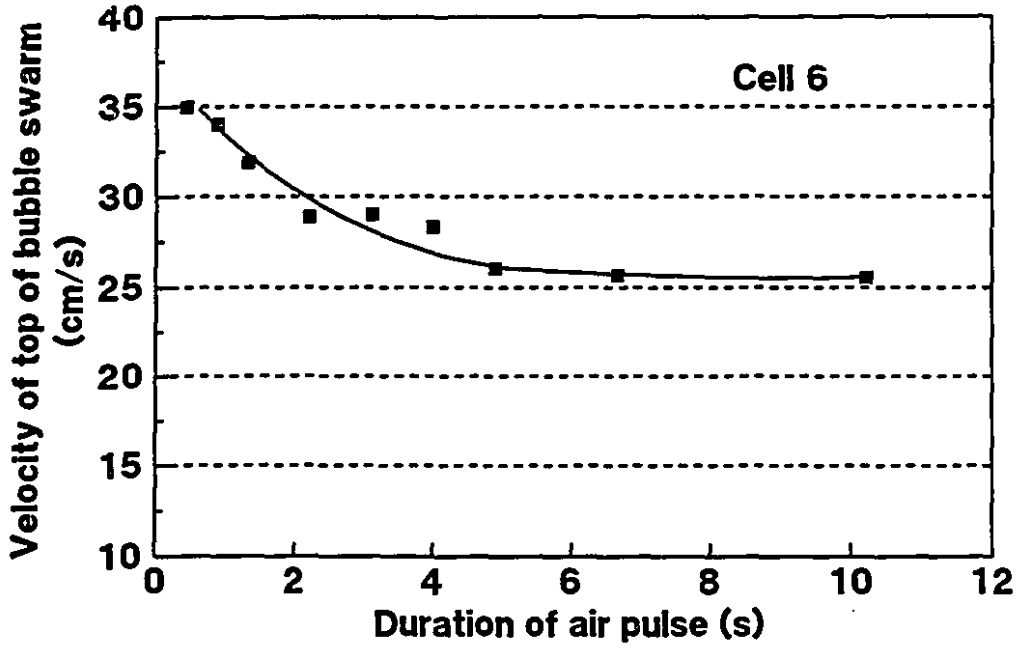

Figure 5.23 Velocity of top of bubble swarm in Cell 6, $u_{2,CS}$.

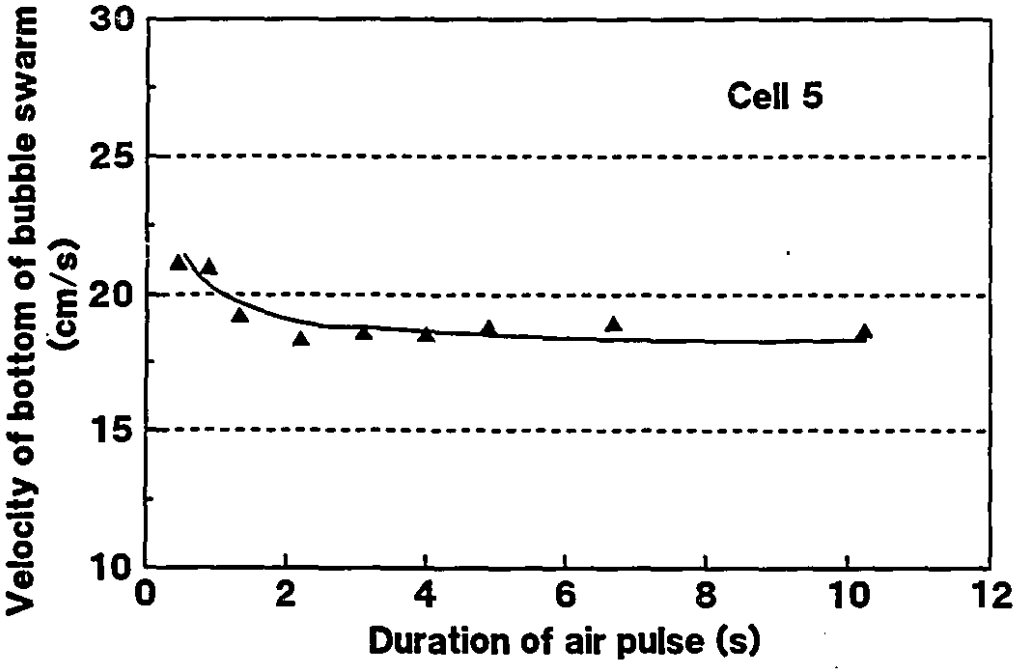

Figure 5.24 Velocity of bottom of bubble swarm in Cell 5, $u_{1,CS}$.

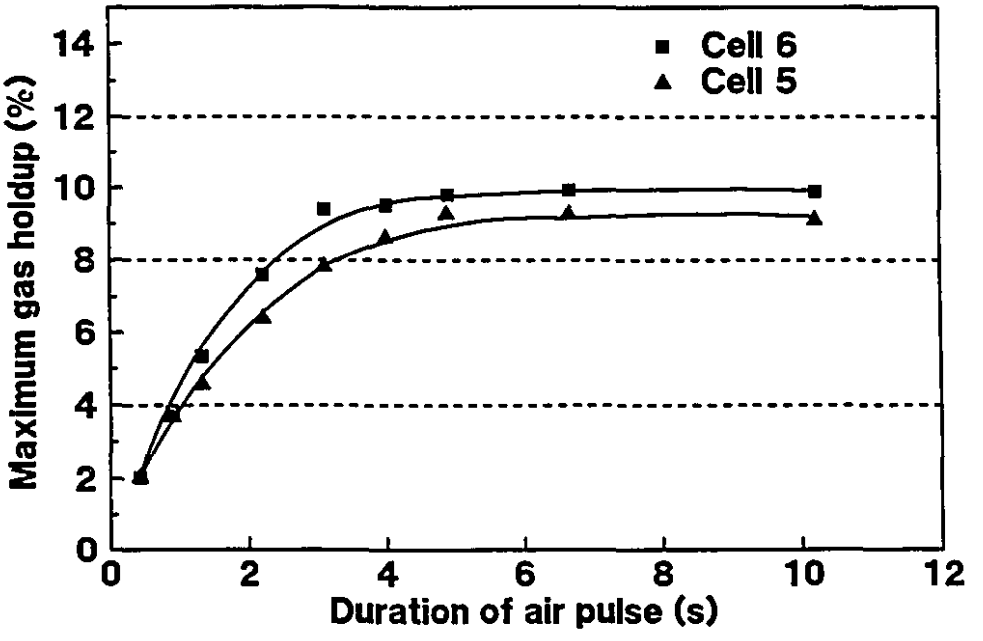

Figure 5.25 Maximum gas holdups in Cells 6 and 5 as a function of air pulse duration.

between $u_{2,C6}$ and u_b is contributed by the liquid circulation in the column which will be discussed in Chapter 7.

Figure 5.24 illustrates the relation between $u_{1,C5}$ and the air pulse duration. When the duration of the air pulse was greater than 5 s, $u_{1,C5}$ attained a value between 18.5 and 18.9 cm/s. In Table 5.4 of Section 5.2.3, u_0 was 18.6 cm/s in Cell 6 under the same conditions as $u_{1,C5}$ (J_{g1} = 2.0 cm/s and J_{g2} = 0 cm/s). Assuming no difference between Cells 6 and 5, we equate $u_{1,C6}$ with $u_{1,C5}$. Comparing u_0 with $u_{1,C5}$, we agree with Nicklin's assumption that u_l is equal to u_0.

Table 5.10 compares the maximum gas holdups between Cells 6 and 5 at various durations of the air pulse. Note, gas holdup is perhaps better described as gas content as gas bubbles are not distributed evenly. In Figure 5.25, $\varepsilon_{g,m6}$ is always larger than $\varepsilon_{g,m5}$. When the air pulse duration was larger than 5 s, the difference of between $\varepsilon_{g,m6}$ and $\varepsilon_{g,m5}$ became a constant. This would indicate an axial profile of gas holdup in the column.

5.4 Effect of J_g on Bubble Velocity

5.4.1 Nicklin's Experiment

Nicklin (1962) measured the effect of J_g on the bubble velocity by interrupting the gas flow. Figure 5.26 shows gas flow being stopped for a short period (case (a)) and restarted at the previous flow rate (case (b)). Nicklin pointed out that from continuity the liquid velocity, u_l, across the section A - A', should be

$$u_l = J_g \tag{5.19}$$

and so the velocity of the bottom of the upper swarm of bubbles, u_1, should be

$$u_1 = u_0 + u_l = u_0 + J_g \tag{5.20}$$

Nicklin assumed that u_l was equal to the velocity of the bubbles and obtained data that agreed with Equation 5.20.

5.4.2 Measurement of Effect of J_g

A set of experiments was carried out by varying the restarting time of the air flow. The goal of the experiments was to measure the change in the velocity of the bottom of the upper swarm in Cell 6 before and after the air flow was restarted. The computer-controlled procedure was:

(a) set J_g and wait for the steady state operation of the cclumn;
(b) start the data acquisition system at 0 s;
(c) switch off the air valve at 10 s;
(d) switch on the air valve at the designed restarting time;
(e) stop the data acquisition and switch off the air valve at 40 s.

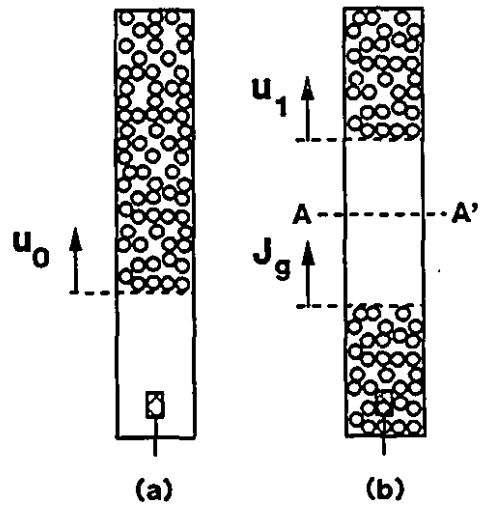

Figure 5.26 Velocities of the bottom of the upper swarm (a) gas switched off; (b) then gas switched on.

Figure 5.27 (b) shows the plot of the resistance versus time in a conceptual measurement and

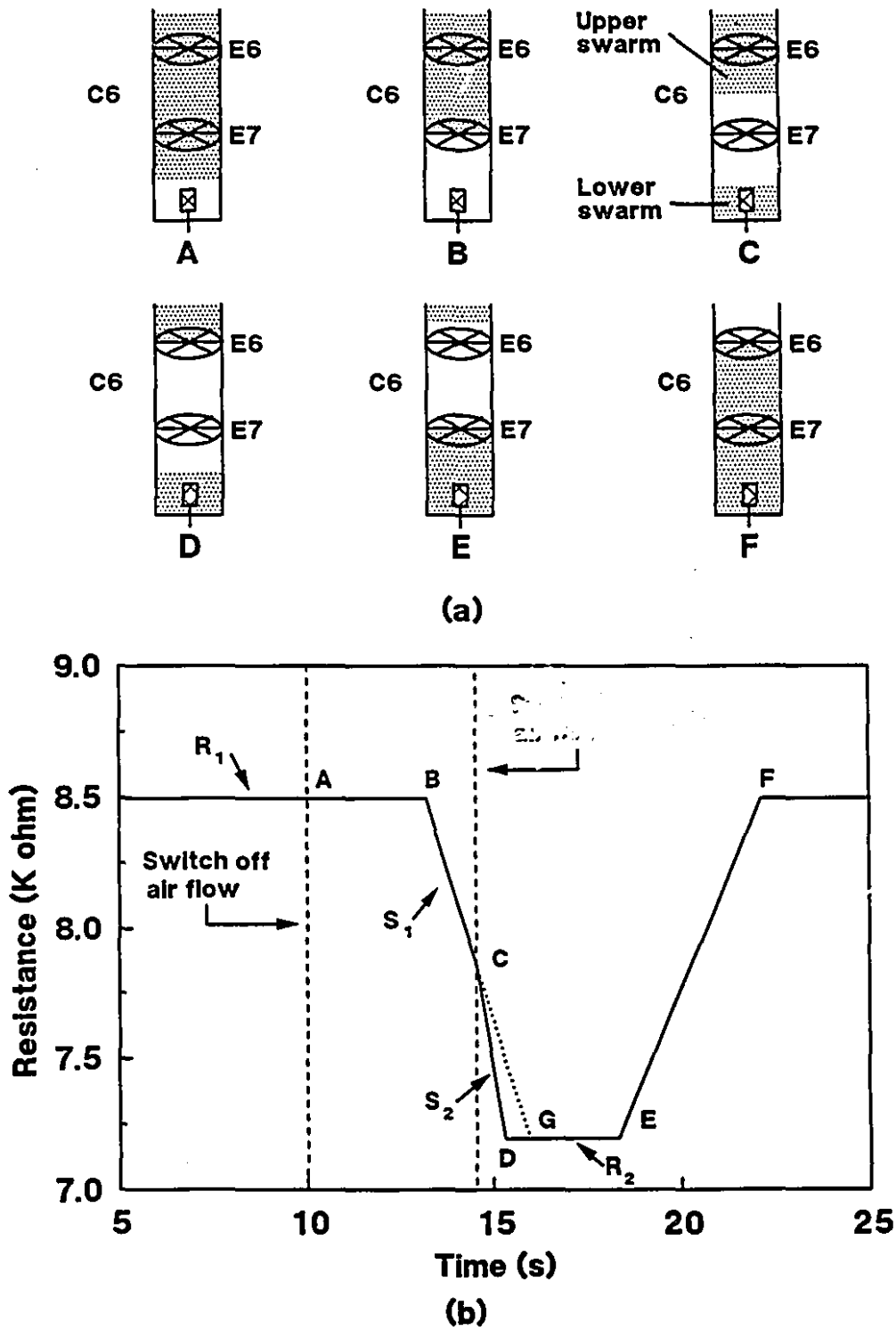

Figure 5.27 Conceptual measurement of u_1 (the velocity of the bottom of the upper swarm) (a) corresponding conditions for (b); (b) curve of resistance versus time.

Figure 5.27 (a) illustrates the corresponding cases A to F:

(A) the air flow was stopped;
(B) the bottom of the upper swarm left Electrode 7 (E7) and the resistance began to reduce in Cell 6 (C6);
(C) the air flow was restarted and a gap between the bottom of the upper swarm and the top of the lower swarm was formed;
(D) the bottom of the upper swarm left E6 and the top of the lower swarm did not reach E7;
(E) the top of the lower swarm reached E7 and the resistance began to increase in C6;
(F) the top of the lower swarm reached E6.

In Figure 5.27 (b), R_1 is the resistance of the dispersion of liquid and bubbles and R_2 is the resistance of the liquid in Cell 6. The slope, S_1, of the line B−C corresponds to the buoyancy velocity, u_0. In this case u_0 is equal to the velocity of the bottom of the upper swarm before the air flow is restarted. Linear regression was used to calculate S_1

$$R = S_1 \cdot t + C_1 \tag{5.21}$$

where R is the resistance, t is the time and C_1 is the intercept. Substituting R_1 in Equation 5.21, t_B can be obtained, the time when the bottom of the upper swarm leaves E7. The dashed line C−G, i.e. the extension of the line B−C, shows what the plot of the resistance versus time would have been if the velocity of the bottom of the upper swarm had not changed. Substituting R_2 to Equation 5.21, t_G can be obtained. The difference between t_G and t_B is given by

$$t_G - t_B = \frac{R_2 - C_1}{S_1} - \frac{R_1 - C_1}{S_1} = \frac{R_2 - R_1}{S_1} \tag{5.22}$$

Consequently, u_0 can be calculated by

$$u_0 = \frac{L}{t_G - t_B} = \frac{51}{t_G - t_B} = \frac{51}{R_2 - R_1} S_1 \tag{5.23}$$

The slope, S_2, of the line C−D corresponds to u_1, which is the velocity of the bottom of the upper swarm after the air flow is restarted. The relationship between u_1 and S_2 is given by

$$u_1 = \frac{51}{R_2 - R_1} S_2 \tag{5.24}$$

In Equations 5.23 and 5.24, the difference between R_2 and R_1 is a constant for a certain J_g. It can be seen that there is a linear relationship between the slope and the velocity of the bottom

of the upper swarm. If Nicklin's assumption is right, the velocity of the bottom of the upper swarm should increase from u_0 to $(u_0 + J_g)$ due to the restarted air flow. Consequently, S_2 should be greater than S_1 as shown in Figure 5.27 (b).

5.4.3 Results and Analysis

The first set of experiments was carried out at J_g = 2.0 cm/s i.e., under bubbly flow conditions. Figures 5.28 - 5.33 show the results for the restarting time = 16.2, 15.3, 14.4, 13.6, 12.7 and 11.8 s, respectively. It can be seen that there was no case where the slope changed significantly upon restarting the air flow (Figure 5.34). The data in Table 5.11 show that there is no difference between u_0 and u_1 at J_g = 2.0 cm/s. Based on eight replicates for each experiment, the maximum relative standard deviation was 1.26% for u_0 and u_1 shown in Table 5.11.

Table 5.11 u_0 and u_1 at J_g = 2.0 cm/s

Restarting time (s)	16.2	15.3	14.4	13.6	12.7	11.8
u_0 (cm/s)	18.7	18.6	18.7	18.8	-	-
u_1 (cm/s)	-	18.7	18.7	18.6	18.8	18.6

In this case the increment in velocity J_g is only 2.0 cm/s on u_0 = 18 cm/s (or about 11%). A larger difference was therefore tested, J_g = 5.0 cm/s. Figures 5.35 - 5.40 show the results for the restarting time = 18.2, 17.6, 16.9, 16.2, 15.6 and 14.9 s, respectively. In these experiments, turbulence was clearly observed in the column. Figure 5.41 illustrates that there was an increase in slope (i.e. increase in velocity) after the air flow was restarted: Table 5.12 shows that the differences between u_0 and u_1, however, are much smaller than suggested by Nicklin's assumption. Based on eight replicates for each experiment, the maximum relative standard deviation was 1.38% for u_0 and u_1 shown in Table 5.12.

Table 5.12 u_0 and u_1 at J_g = 5.0 cm/s

Restarting time (s)	18.2	17.6	16.9	16.2	15.6	14.9
u_0 (cm/s)	13.9	13.8	13.9	13.7	13.9	-
u_1 (cm/s)	-	13.9	14.1	14.5	14.9	15.0

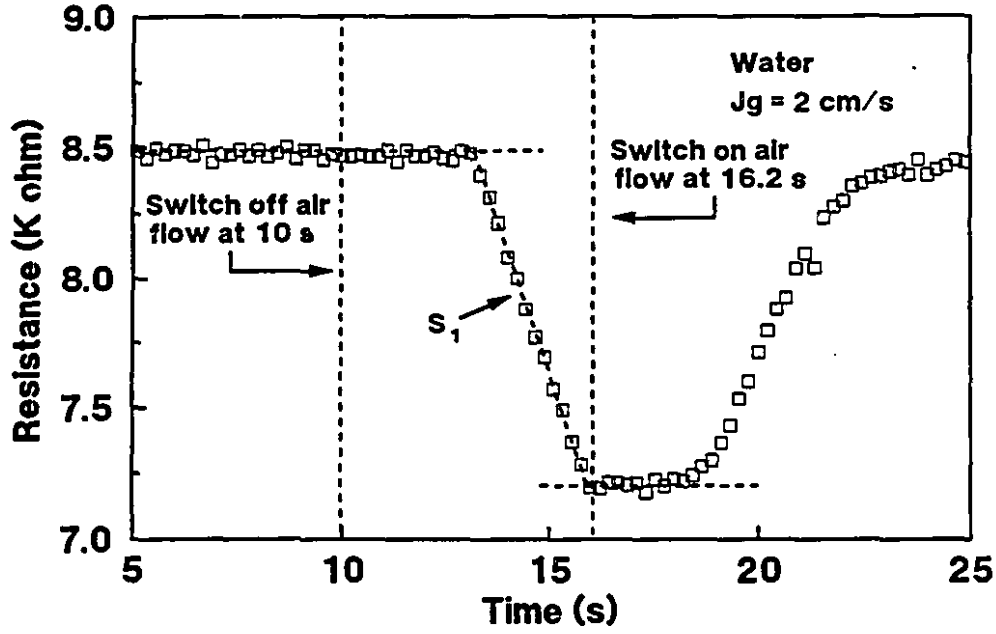

Figure 5.28 Resistance versus time at restarting time = 16.2 s and J_g = 2.0 cm/s.

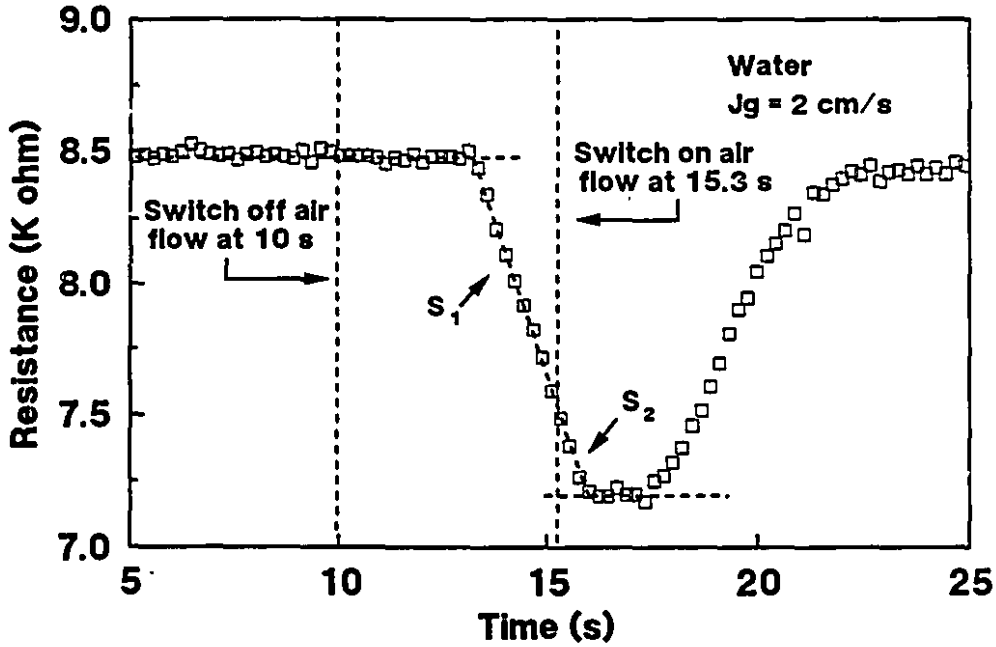

Figure 5.29 Resistance versus time at restarting time = 15.3 s and J_g = 2.0 cm/s.

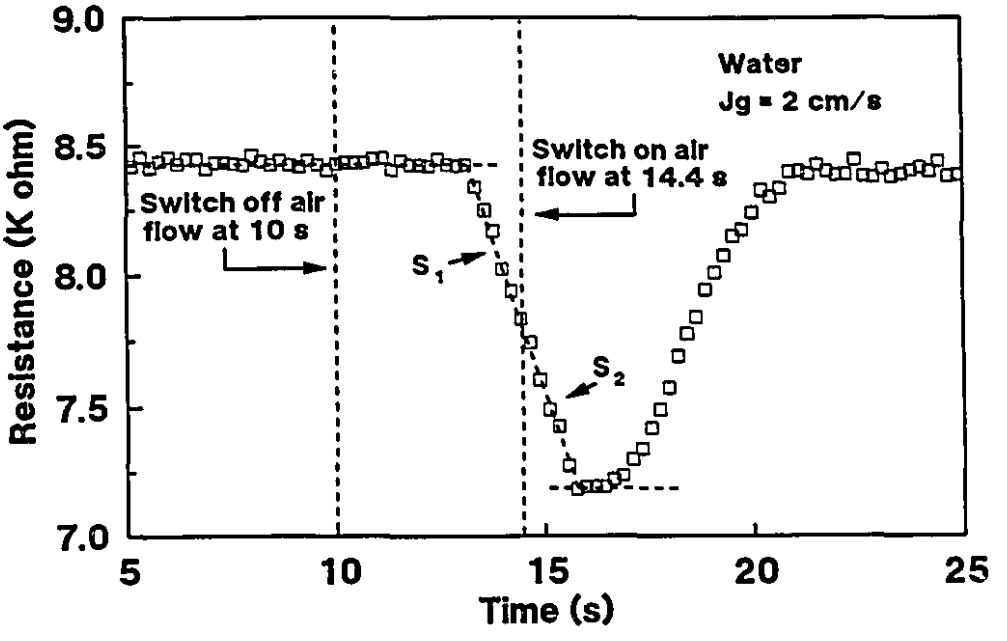

Figure 5.30 Resistance versus time at restarting time = 14.4 s and J_g = 2.0 cm/s.

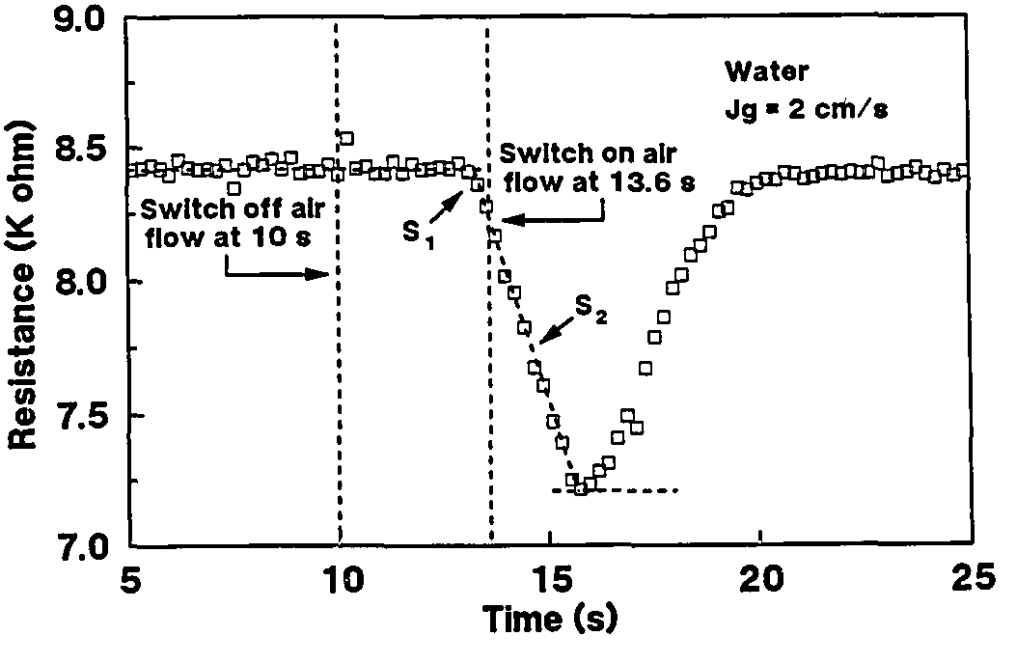

Figure 5.31 Resistance versus time at restarting time = 13.6 s and J_g = 2.0 cm/s.

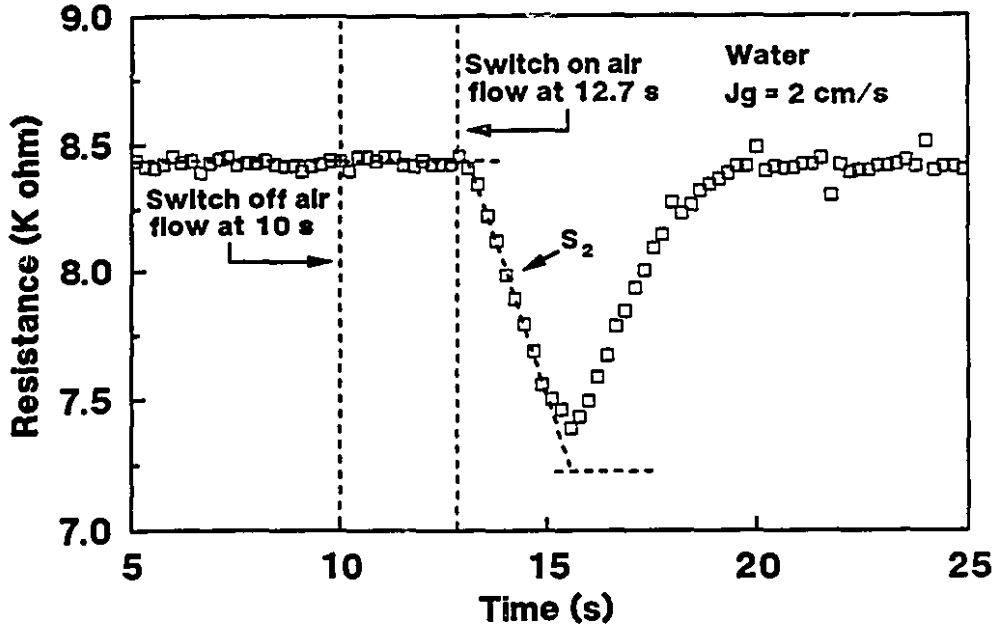

Figure 5.32 Resistance versus time at restarting time = 12.7 s and J_g = 2.0 cm/s.

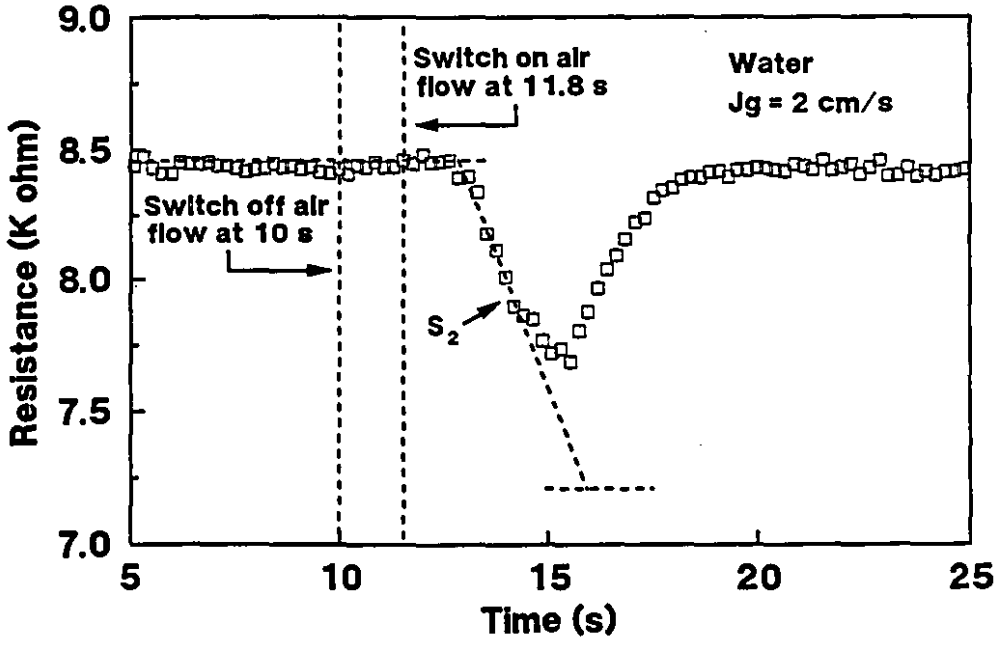

Figure 5.33 Resistance versus time at restarting time = 11.8 s and J_g = 2.0 cm/s.

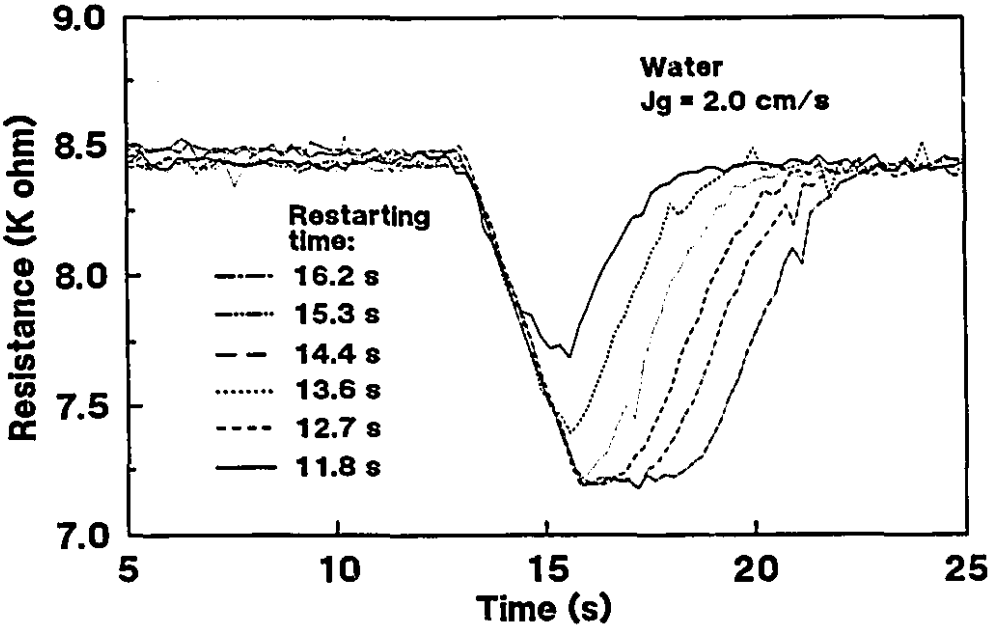

Figure 5.34 Comparison among slopes of curves at J_g = 2.0 cm/s.

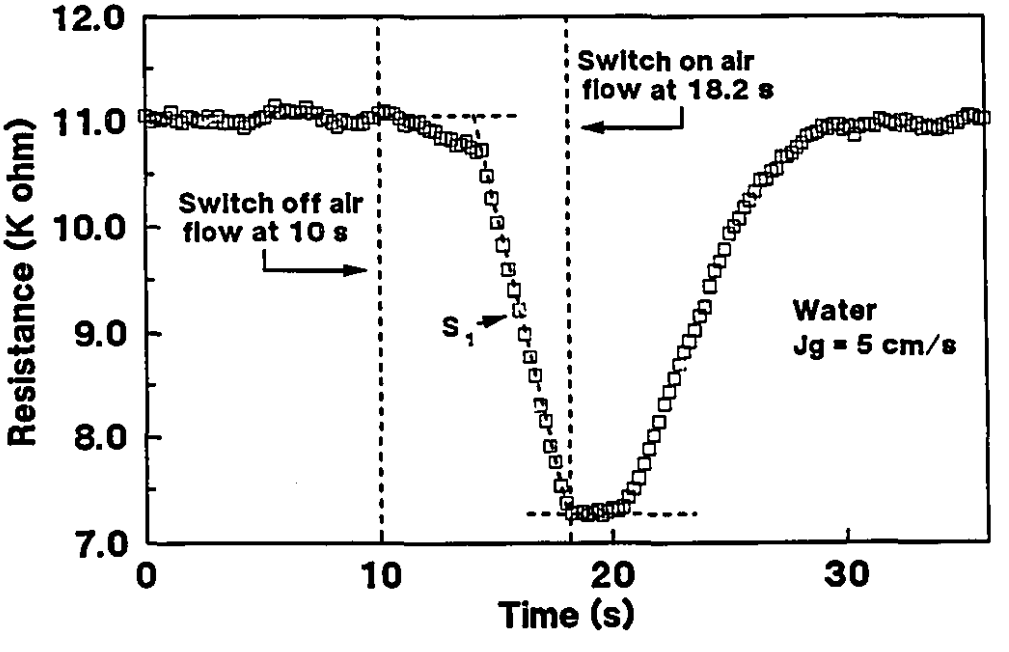

Figure 5.35 Resistance versus time at restarting time = 18.2 s and J_g = 5.0 cm/s.

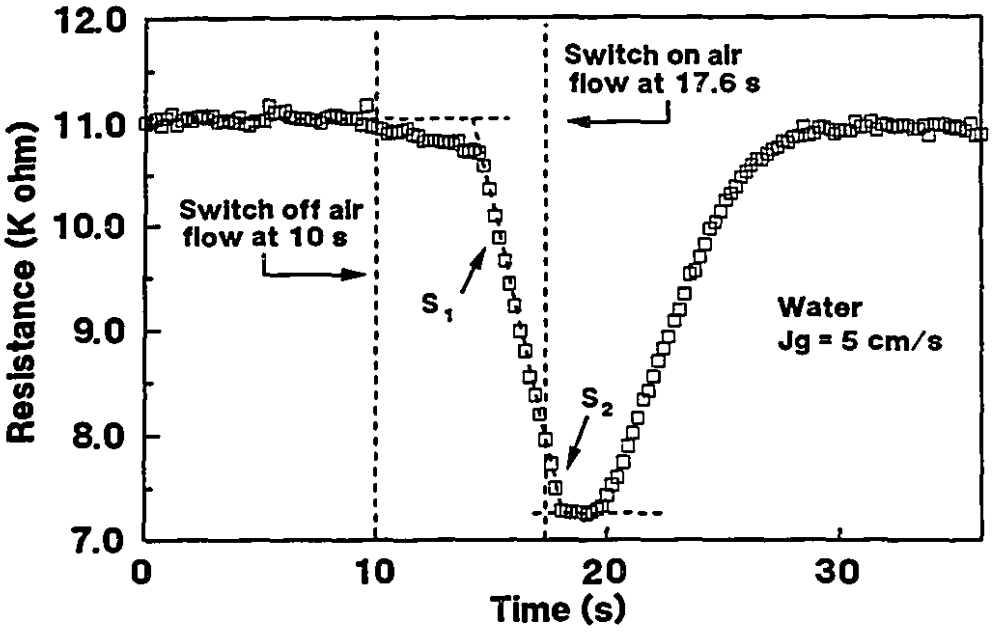

Figure 5.36 Resistance versus time at restarting time = 17.6 s and J_g = 5.0 cm/s.

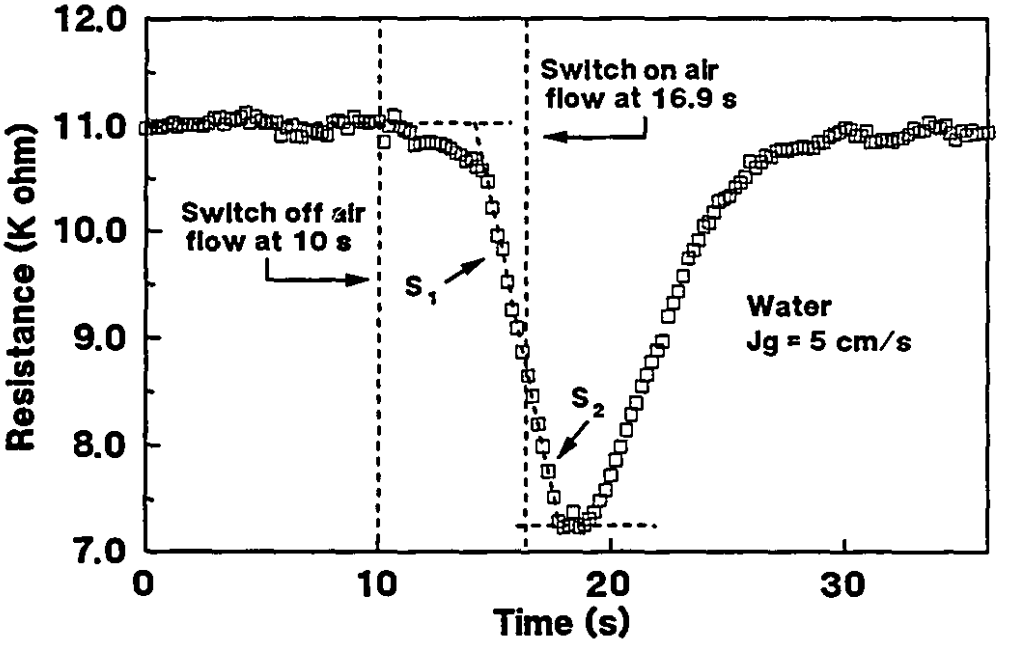

Figure 5.37 Resistance versus time at restarting time = 16.9 s and J_g = 5.0 cm/s.

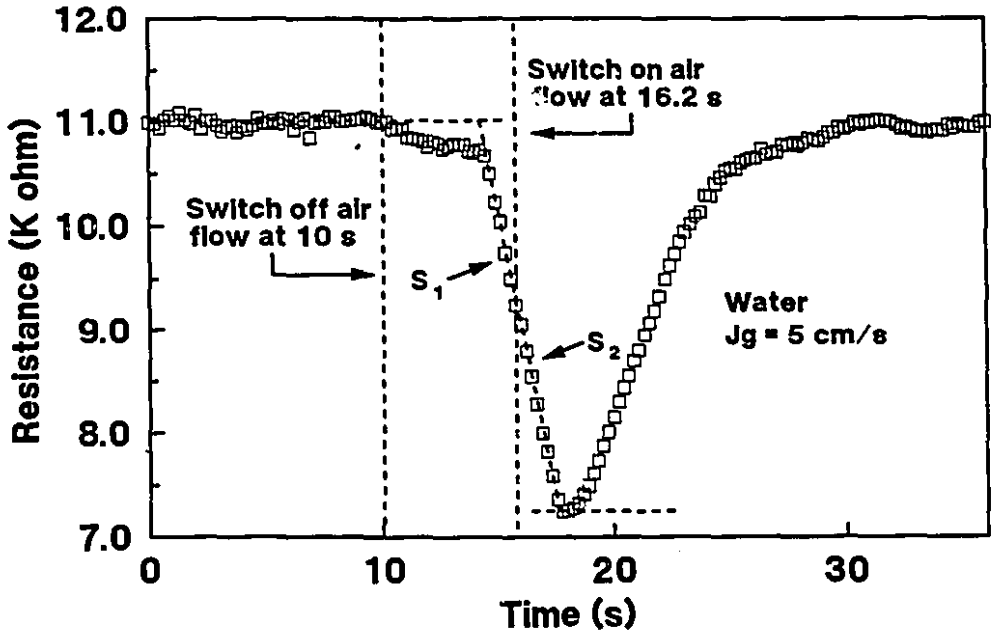

Figure 5.38 Resistance versus time at restarting time = 16.2 s and J_g = 5.0 cm/s.

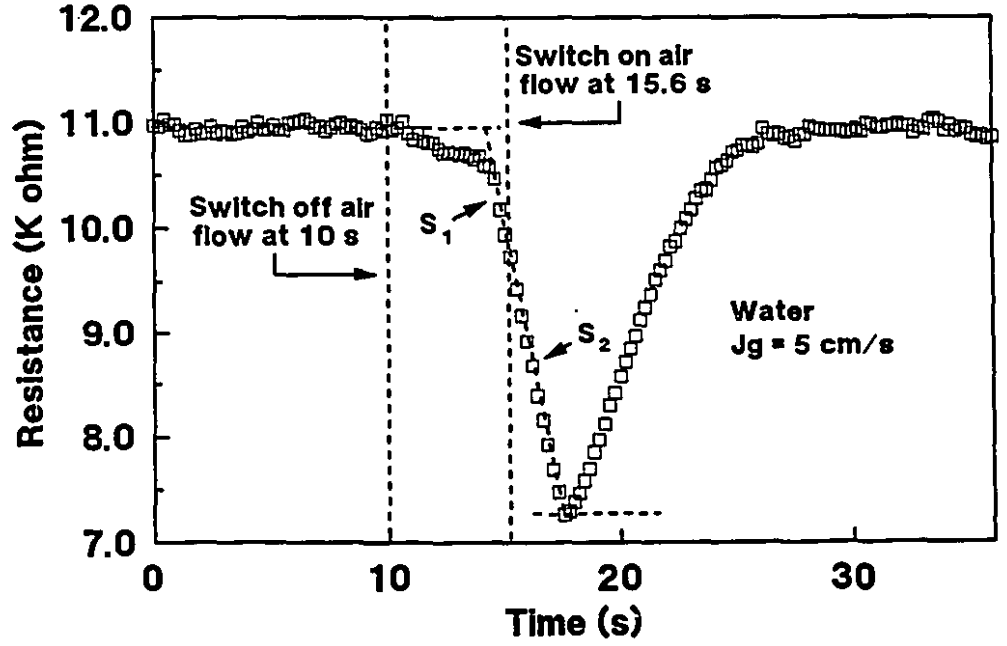

Figure 5.39 Resistance versus time at restarting time = 15.6 s and J_g = 5.0 cm/s.

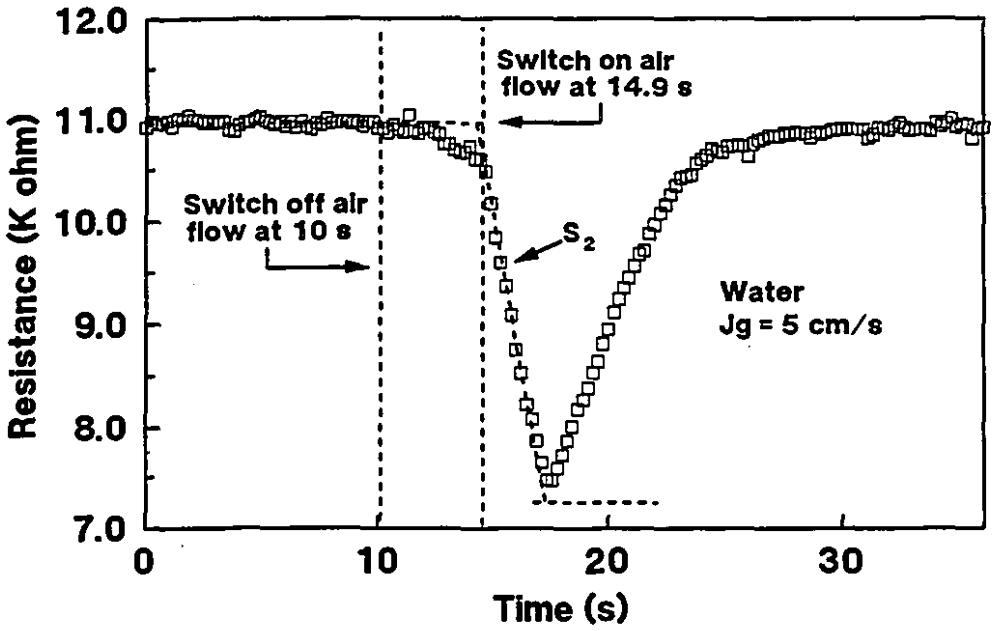

Figure 5.40 Resistance versus time at restarting time = 14.9 s and J_g = 5.0 cm/s.

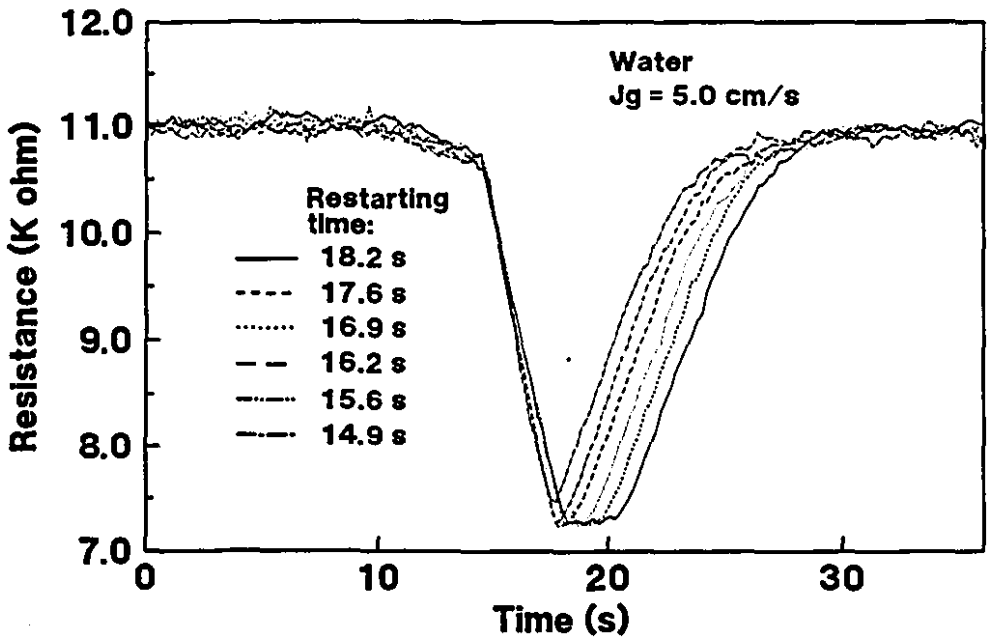

Figure 5.41 Comparison among slopes of curves at J_g = 5.0 cm/s.

5.5 Axial Profile of Swarm Velocity

In Section 5.2, the interface velocity, u_{in}, in Cell 6 was discussed in detail. The hindered velocity, u_h, was calculated by interpolation of u_{in}. In this section, the axial profiles of u_{in} and u_h in the column will be examined.

5.5.1 Measurement of u_{in} in Cells 5 - 2

The distances from the centre of Cells 6, 5, 4, 3 and 2 to the top of the column are 300.5, 249.5, 198.5, 147.5 and 96.5 cm, respectively. The interface velocity, u_{in}, was measured in Cells 5, 4, 3 and 2 with the same conductivity method which was used in Cell 6. Note Cell 1 was not included in the analysis as it often did not remain in full. The detailed results and analysis are given in 48 tables in Appendix 3.

Figures 5.42, 5.44, 5.46, 5.48 and 5.50 show u_{in} for each cell as a function of J_{g2} / J_{gl} for J_{gl} = 1.0, 1.5, 2.0, 2.5 and 3.0 cm/s, respectively. From these diagrams, it can be seen that the interface moves differently for $J_{g2} / J_{gl} < 1$ and $J_{g2} / J_{gl} > 1$: for Cells 5 - 2, the linear relationship between u_{in} and J_{g2} / J_{gl}, which was obtained in Cell 6 (see Section 5.2), remains acceptable for $J_{g2} / J_{gl} < 1$; for $J_{g2} / J_{gl} > 1$, however, u_{in} increases gradually from Cell 5 to 2. An interesting feature is that this increasing u_{in} appears to approach but not exceed the u_h of Cell 6. For example, Figure 5.46 shows that u_{in} in Cell 2 at J_{g2} / J_{gl} = 1.2, 1.4, 1.6, 1.8 and 2.0 is 18.2, 18.2, 18.1, 18.1 and 18.0 cm/s, respectively. These values are equal or very close to u_h (18.2 cm/s) in Cell 6 for J_{gl} = 2.0 cm/s. The implication of this feature will be discussed later.

5.5.2 Characteristic of System: u_h

Figures 5.43, 5.45, 5.47, 5.49 and 5.51 compare u_h obtained in Cell 6 with u_h evaluated in Cells 5 - 2 at J_{gl} = 1.0, 1.5, 2.0, 2.5 and 3.0 cm/s, respectively. Although the linear relationship between u_{in} and J_{g2} / J_{gl} is not applicable for Cells 5 - 2, the interpolated values of u_h in Cells 5 - 2 agree with u_h obtained in Cell 6. It suggests that the hindered velocity, u_h, is a characteristic parameter of the system no matter where it is measured. Consequently, Equation 5.12 obtained for Cell 6 (see Section 5.2.4) can be used for the entire column

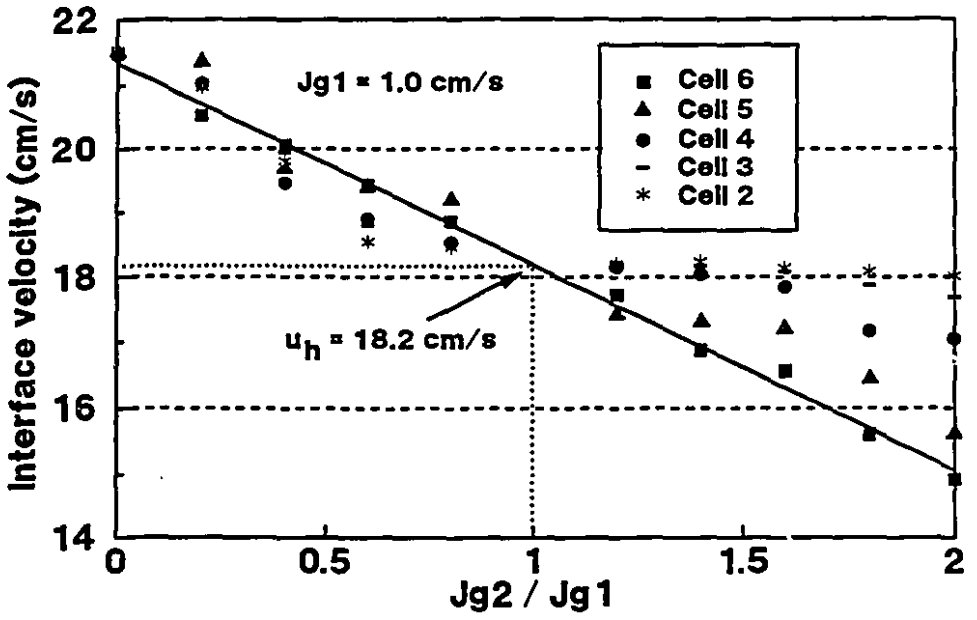

Figure 5.42 Measurement of u_{in} in Cells 6, 5, 4, 3 and 2 at J_{g1} = 1.0 cm/s. The u_h quoted is for Cell 6 from Section 5.2.

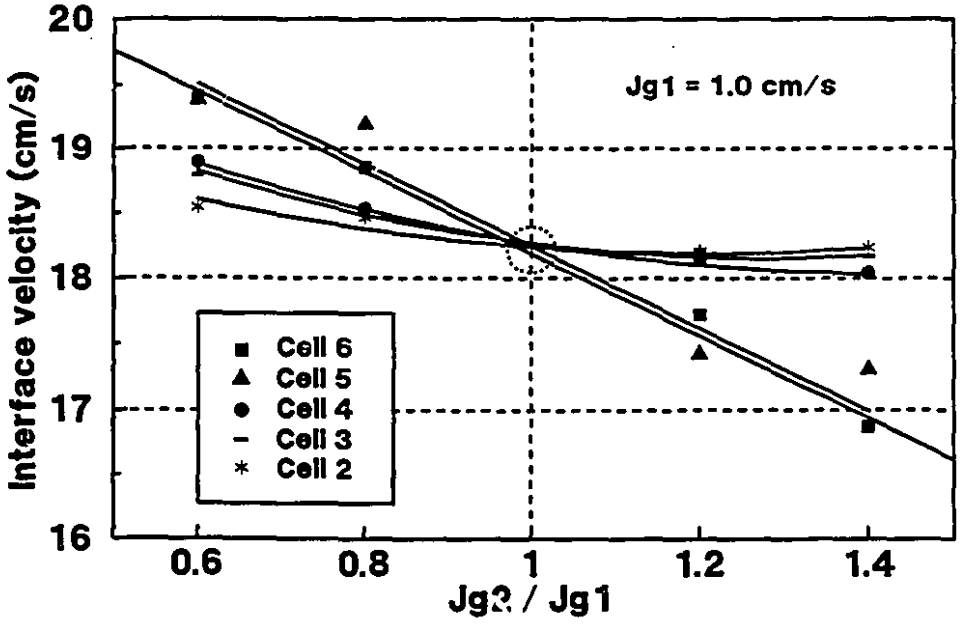

Figure 5.43 Evaluation of u_h with u_{in} in different cells at J_{g1} = 1.0 cm/s.

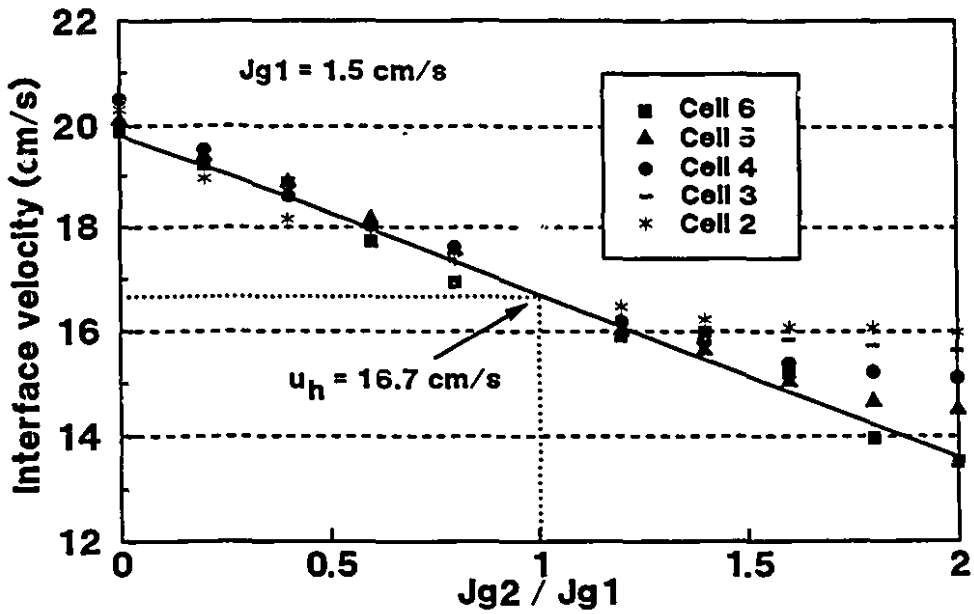

Figure 5.44 Measurement of u_{in} in Cells 6, 5, 4, 3 and 2 at J_{g1} = 1.5 cm/s. The u_h quoted is for Cell 6 from Section 5.2.

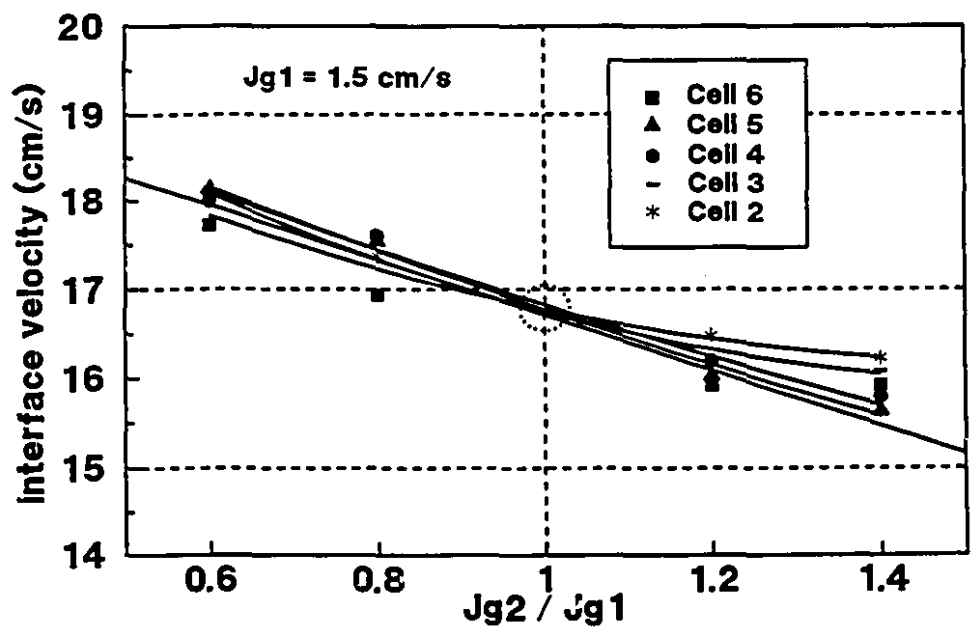

Figure 5.45 Evaluation of u_h with u_{in} in different cells at J_{g1} = 1.5 cm/s.

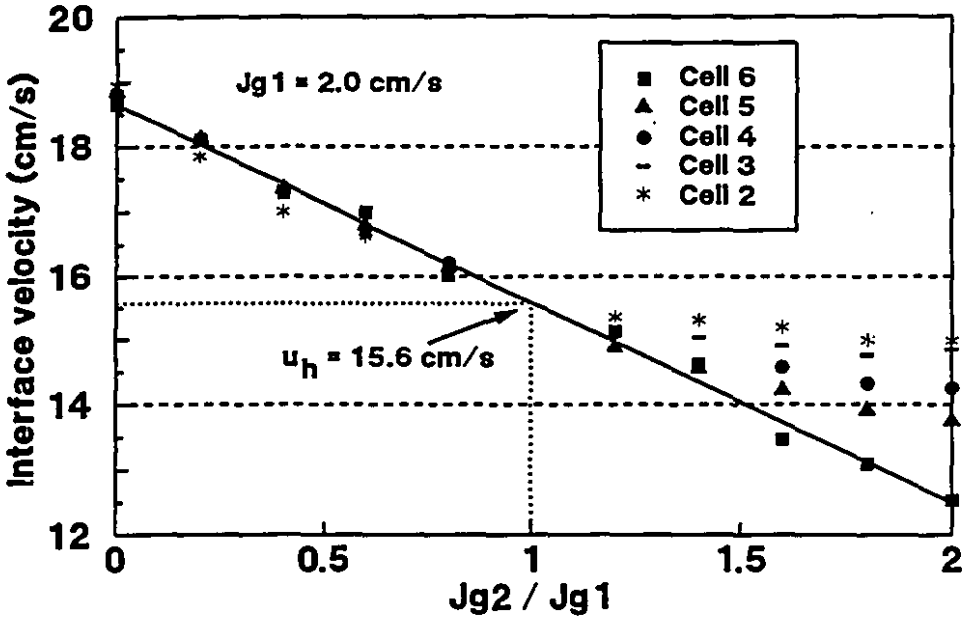

Figure 5.46 Measurement of u_{in} in Cells 6, 5, 4, 3 and 2 at $J_{gl} = 2.0$ cm/s. The u_h quoted is for Cell 6 from Section 5.2.

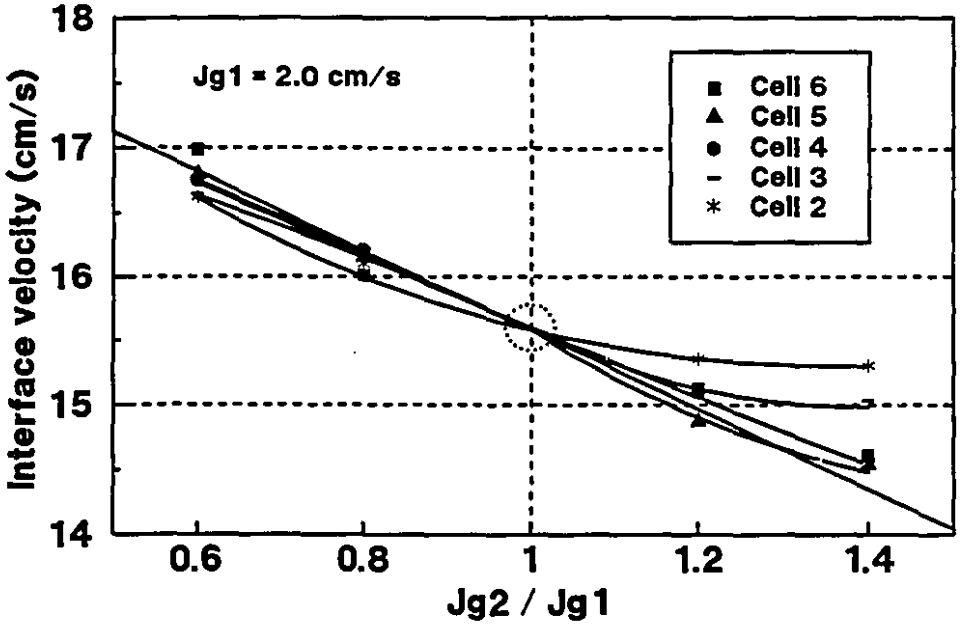

Figure 5.47 Evaluation of u_h with u_{in} in different cells at $J_{gl} = 2.0$ cm/s.

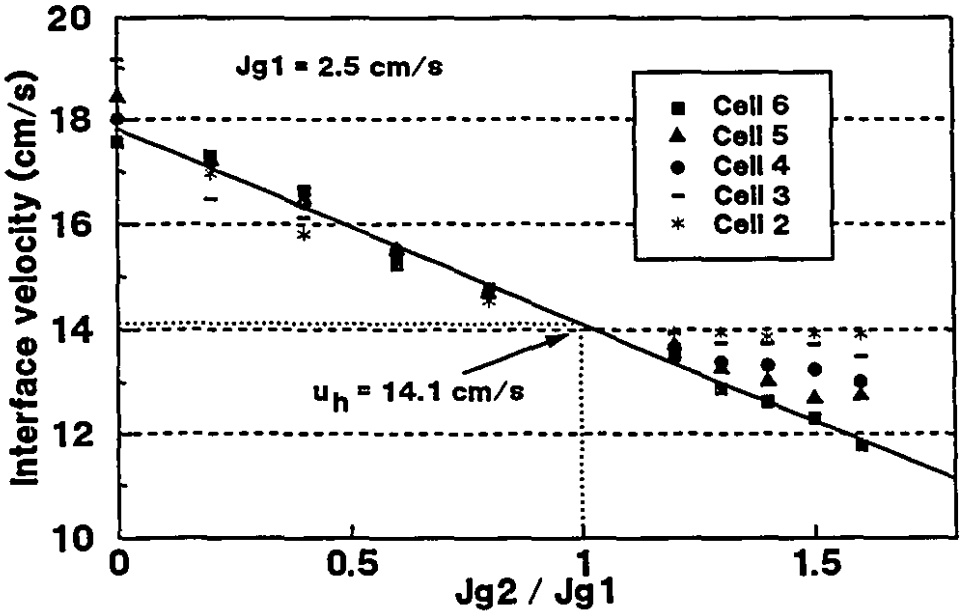

Figure 5.48 Measurement of u_{in} in Cells 6, 5, 4, 3 and 2 at J_{g1} = 2.5 cm/s. The u_h quoted is for Cell 6 from Section 5.2.

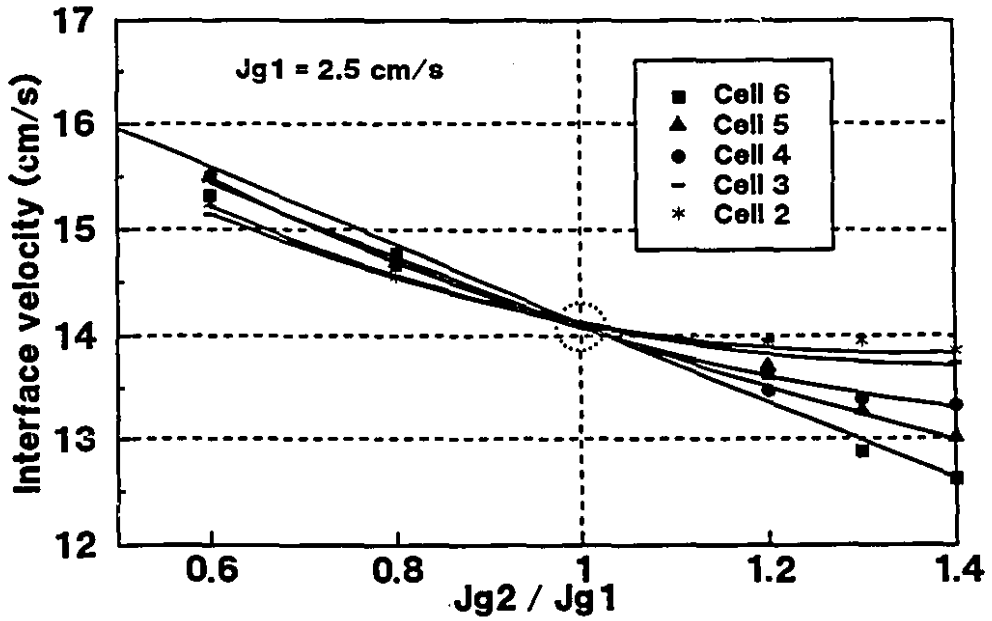

Figure 5.49 Evaluation of u_h with u_{in} in different cells at J_{g1} = 2.5 cm/s.

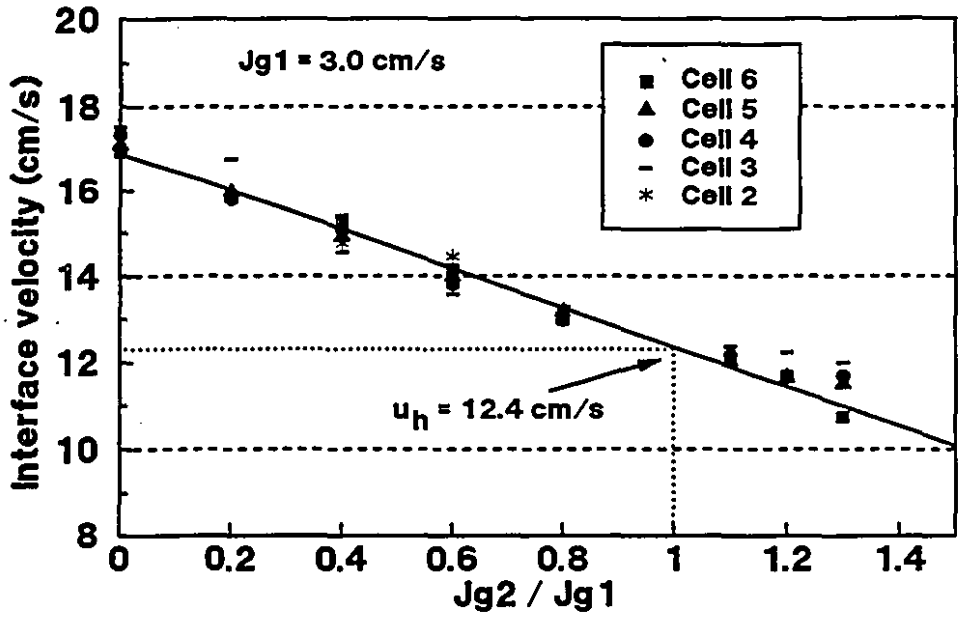

Figure 5.50 Measurement of u_{in} in Cells 6, 5, 4, 3 and 2 at J_{gf} = 3.0 cm/s. The u_h quoted is for Cell 6 from Section 5.2.

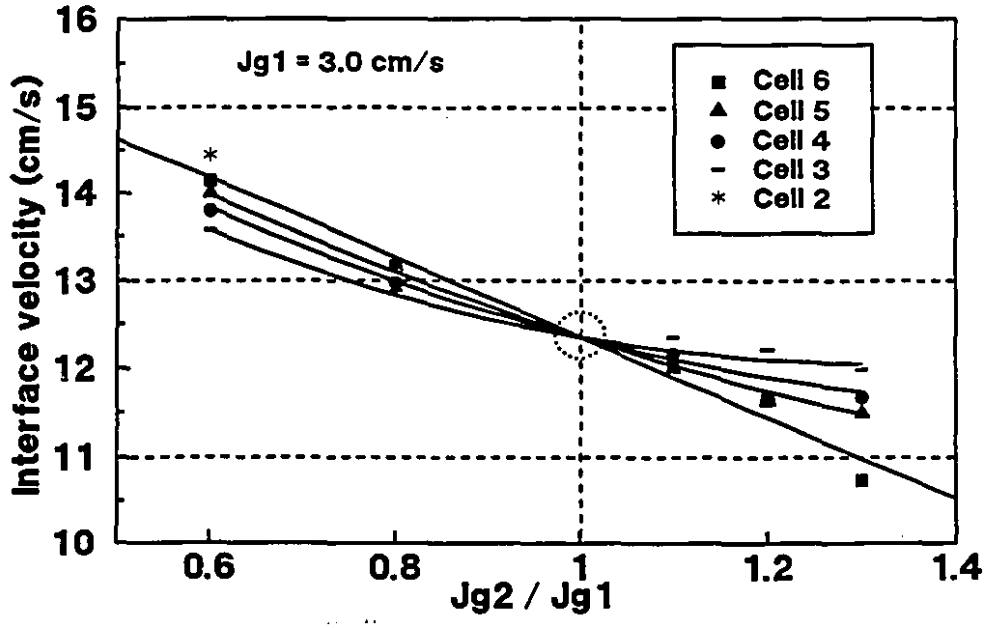

Figure 5.51 Evaluation of u_h with u_{in} in different cells at J_{gf} = 3.0 cm/s.

$$u_h = 21.1 - 2.84\, J_{gl} \tag{5.12}$$

In Section 5.2.5, the relationship between u_{in} and u_h was obtained for Cell 6 ($0 < J_g < 4$ cm/s)

$$u_{in} = u_h \left[1 + A \left(\frac{J_{g2}}{J_{gl}} - 1 \right) \right] \tag{5.16}$$

where

$$A = -0.170 - 0.00162\, J_{gl}^{4.4} \tag{5.13}$$

In Figures 5.42 - 5.51, A is the slope of the straight line for u_{in} versus J_{g2} / J_{gl} in Cell 6. Because of the non - linear relationship between J_{g2} / J_{gl} and u_{in} in Cells 5 - 2, A becomes a quite complex function of J_{gl} and J_{g2}. One approach may be to use Equations 5.16 and 5.13 over a narrow range of J_{g2} / J_{gl} for the entire column to avoid this complex function of A.

In practice, in flotation columns the gas rate is normally changed over a narrow range to avoid excessive interactions. Therefore, it is not necessary to develop a model to cover a wide range of J_{g2} / J_{gl}. From Figures 5.43, 5.45, 5.47, 5.49 and 5.51, it can be seen that the curves are close to a straight line in the range $0.90 < J_{g2} / J_{gl} < 1.10$. In this range Equation 5.13 can be used with a small error. With the limitation of $0.90 < J_{g2} / J_{gl} < 1.10$, the model (Equations 5.16, 5.12 and 5.13) can be used to predict u_{in} for a column under bubbly flow conditions ($J_g < 4$ cm/s) and batch operation.

5.6 Velocity of Top of Bubble Bed u_{top}

In column flotation, stabilizing control demands as a minimum control of level, i.e. pulp / froth interface position (Finch and Dobby, 1990a). Floats and pressure - based methods are generally used for level measurement. In this section, the relationship between u_{in} and u_{top}, which could be used to *predict* the level variation due to a change in the air flowrate, will be discussed.

5.6.1 Relationship Between u_{in} and u_{top}

In the batch system, u_{top} is defined as the velocity of the top of the bubble bed (Figure 5.52 (a)). Here the upward direction is positive for u_{in} and u_{top}. When the interface B-B' rises in the column, the increment of liquid in Zone 2 should be equal to the decrement of liquid in Zone 1. The mass balance of the liquid, across the interface B-B' in unit time, is given by

$$u_{in} (1 - \varepsilon_{g2}) A_c \rho_l = u_{in} (1 - \varepsilon_{g1}) A_c \rho_l - u_{top} (1 - \varepsilon_{g1}) A_c \rho_l \qquad (5.25)$$

where ε_{g1} is the gas holdup in Zone 1 and ε_{g2} is the gas holdup in Zone 2 (Figure 5.52 (a)). The left hand side of Equation 5.25 is the volumetric increment of the liquid in Zone 2 and the right hand side is the volumetric decrement of the liquid in Zone 1 in unit time. The first term of the right hand side is the contribution to the volumetric decrement of the liquid in Zone 1 due to the motion of the interface B-B' and the second term is the contribution due to the motion of the top of the bubble bed. The simplified equation is

$$u_{in} (1 - \varepsilon_{g2}) = u_{in} (1 - \varepsilon_{g1}) - u_{top} (1 - \varepsilon_{g1}) \qquad (5.26)$$

Consequently, the relationship between u_{in} and u_{top} is given by

$$u_{top} = \frac{\varepsilon_{g2} - \varepsilon_{g1}}{1 - \varepsilon_{g1}} u_{in} \qquad (5.27)$$

In the absence of a froth, in a bubble column the u_{in} is always positive, u_{top} is negative when $\varepsilon_{g2} < \varepsilon_{g1}$ and positive when $\varepsilon_{g2} > \varepsilon_{g1}$. There are four cases relevant to the present experiments:

(a) $\varepsilon_{g2} = 0$: the u_{top} is downward and its magnitude is

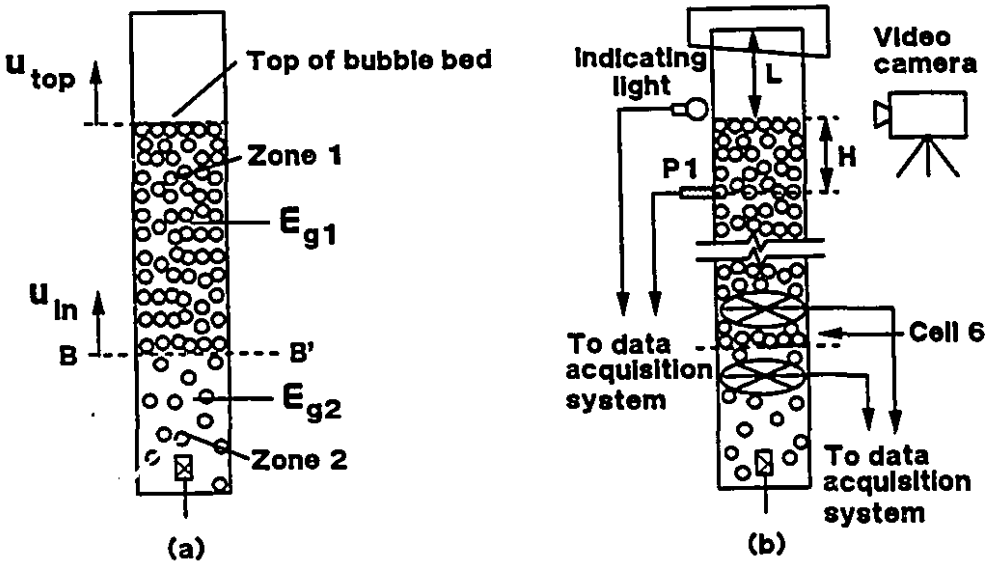

Figure 5.52 Measurement of u_{top}: (a) mass balance of liquid on interface B-B'; (b) configuration of experiment.

$$|u_{top}| = u_{in} \frac{\varepsilon_{g1}}{1 - \varepsilon_{g1}} = u_0 \frac{\varepsilon_{g1}}{1 - \varepsilon_{g1}} \tag{5.28}$$

which agrees with Nicklin's derivation (1962). In this case the u_{in} is equal to the buoyancy velocity, u_0.

(b) $\varepsilon_{g2} < \varepsilon_{g1}$: the u_{top} is downward and its magnitude is

$$|u_{top}| = u_{in} \frac{\varepsilon_{g1} - \varepsilon_{g2}}{1 - \varepsilon_{g1}} \tag{5.29}$$

(c) $\varepsilon_{g2} > \varepsilon_{g1}$: the u_{top} is upward and its magnitude is

$$|u_{top}| = u_{in} \frac{\varepsilon_{g2} - \varepsilon_{g1}}{1 - \varepsilon_{g1}} \tag{5.30}$$

(d) $\varepsilon_{g2} = \varepsilon_{g1}$: the u_{top} is equal to zero.

5.6.2 Measurement of u_{top}

To examine Equation 5.27, two methods were used to measure u_{top}: a video recording method and a pressure method. Figure 5.52 (b) illustrates the configuration of the experiment. When the resistance signals were measured in Cell 6, the pressure was also read by the transducer (P1) and the actual location of the top of the bubble bed was recorded by the video camera. The procedure was:

(a) open Valve 1 (set to the initial superficial gas velocity J_{g1});
(b) wait for steady state operation of the column;
(c) start the video camera manually;
(d) at 0 s, start the data acquisition system and switch on the indicating light;
(e) at 10 s, close Valve 1 and open Valve 2 (set to the second superficial gas velocity J_{g2});
(f) at 40 s, close Valve 2;
(g) at 60 s, stop the data acquisition system and switch off the indicating light;
(h) stop the video camera manually.

The procedure was controlled by computer except for the operation of the video camera. To measure u_{top}, the time marks generated by the video camera were recorded on the video tape frame by frame and these time marks were independent of the clock of the computer. In an experiment, as the computer switches on the indicating light at 10 s, the light and the time mark at that moment are recorded together on the video tape. Therefore, the two clock systems, the time mark of the video camera and the clock of the computer, are linked by the indicating light.

5.6.3 Results and Analysis

(i) $u_{top,v}$

The $u_{top,v}$ is defined as the velocity of the top of the bubble bed measured by the video recording method. The data were taken by reading the location of the top of the bubble bed versus the time marks on the video tape. Figure 5.53 illustrates that there was a linear relationship between the location of the top of the bubble bed and time. In Figure 5.53, L is the distance from the top of the bubble bed to the top of the column (Figure 5.52 (b)). The $u_{top,v}$ is given by

$$u_{top,v} = \frac{dL}{dt} \tag{5.31}$$

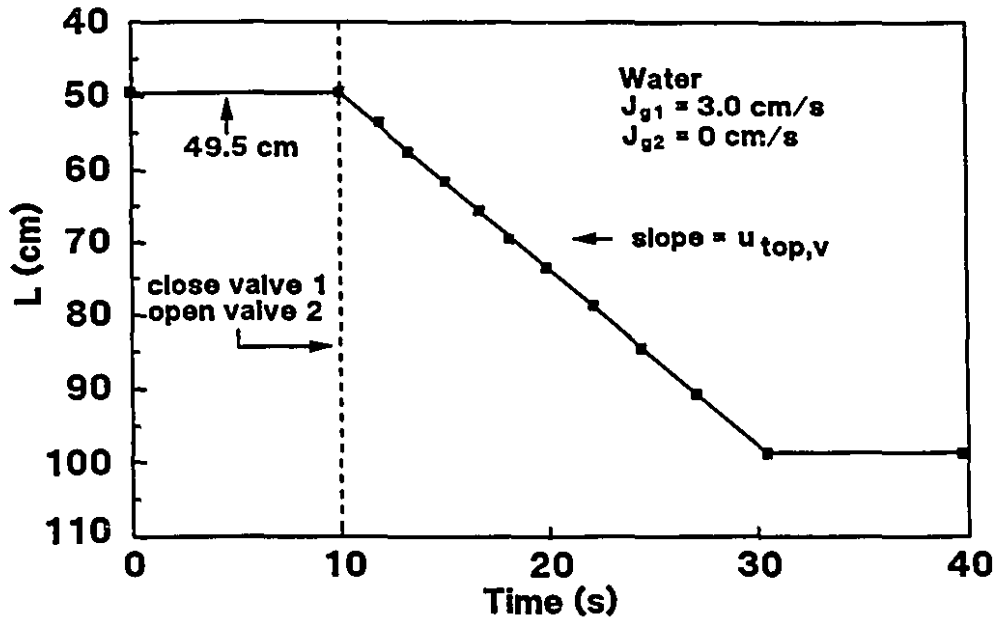

Figure 5.53 Location of top of bubble bed recorded by video versus time at J_{g1} = 3.0 cm/s and J_{g2} = 0 cm/s.

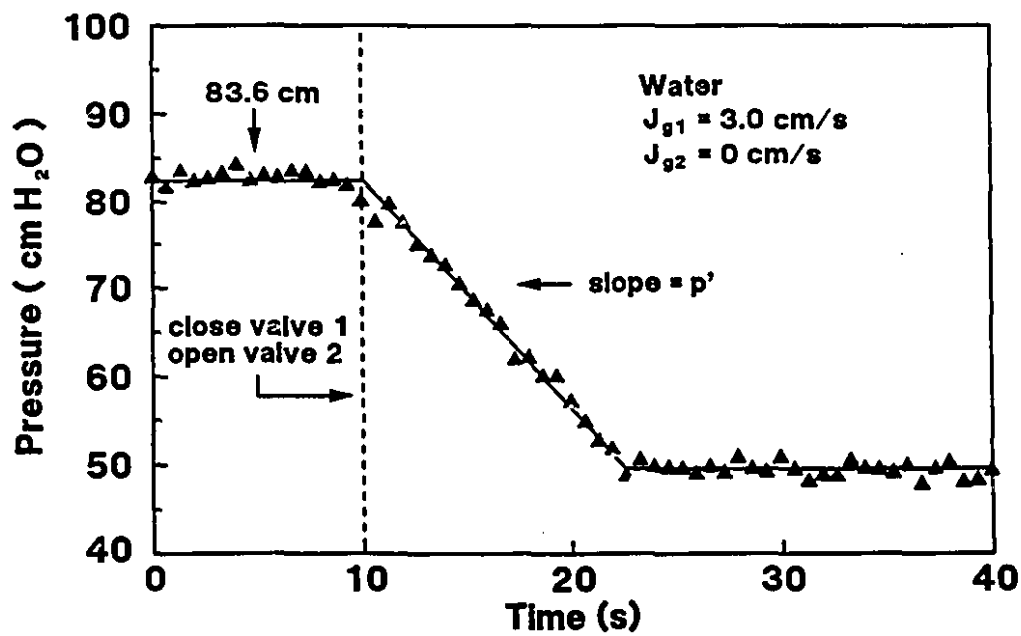

Figure 5.54 Pressure read by P1 versus time at J_{g1} = 3.0 cm/s and J_{g2} = 0 cm/s.

(ii) $u_{top,p}$

The velocity of the top of the bubble bed also can be estimated by the pressure method. The gauge pressure read by P1 is given by

$$P = H g [\rho_l (1 - \varepsilon_{gl}) + \rho_g \varepsilon_{gl}] \tag{5.32}$$

where H is the distance from P1 to the top of the bubble bed (Figure 5.52 (b)) and P is the pressure with units of dynes/cm^2. Because $\rho_l >> \rho_g$, ignoring ρ_g yields

$$P = H g \rho_l (1 - \varepsilon_{gl}) \tag{5.33}$$

Setting $p = P / (\rho_l g)$ with the unit of cm, we obtain

$$p = H (1 - \varepsilon_{gl}) \tag{5.34}$$

The first derivative of p with respect to t (time) is given by

$$\begin{aligned} p' = \frac{dp}{dt} &= (1 - \varepsilon_{gl}) \frac{d}{dt} (H) + H \frac{d}{dt} (1 - \varepsilon_{gl}) \\ &= (1 - \varepsilon_{gl}) \frac{dH}{dt} - H \frac{d\varepsilon_{gl}}{dt} \end{aligned} \tag{5.35}$$

Assuming ε_{gl} is constant in Zone 1, Equation 5.35 becomes

$$p' = (1 - \varepsilon_{gl}) \frac{dH}{dt} \tag{5.36}$$

The $u_{top,p}$ is defined as the velocity of the top of the bubble bed measured by the pressure given by

$$u_{top,p} = \frac{dH}{dt} = \frac{p'}{1 - \varepsilon_{gl}} \tag{5.37}$$

Figure 5.54 illustrates that there was a linear relationship between the pressure read by P1 and time.

The distance from P1 to the top of the column, i.e. $L + H$, is 147.0 cm. From Figures 5.53 and 5.54, it can be seen that L was 49.5 cm and p was 83.6 cm at $J_{gl} = 3.0$ cm/s. Substituting H (= 147.0 - L) and p into Equation 5.34, ε_{gl}, between P1 and the top of the bubble bed, can be calculated

$$\varepsilon_{g1} = \frac{H - p}{H} = \frac{(147.0 - 49.5) - 83.6}{147.0 - 49.5} = 0.143 \quad (5.38)$$

Then the relationship between $u_{top,p}$ and p' is given by

$$u_{top,p} = \frac{p'}{1 - \varepsilon_{g1}} = \frac{p'}{1 - 0.143} = 1.17\, p' \quad (5.39)$$

(iii) $u_{top,c}$

Substituting u_{in}, ε_{g1} and ε_{g2} into Equation 5.27, the calculated velocity of the top of the bubble bed, u_{top}, can be obtained: in this calculation, u_{in}, ε_{g1} and ε_{g2} were measured by the conductivity method and thus u_{top} is symbolized by $u_{top,c}$, in general, and specifically by $u_{top,c6}$, $u_{top,c5}$ etc. for u_{in} measured in Cell 6, Cell 5 etc..

Table 5.13 shows $u_{top,c6}$, $u_{top,v}$ and $u_{top,p}$ at $J_{g1} = 3.0$ cm/s. Figure 5.55 illustrates three linear relationships:

$$u_{top,c6} = -3.02 + 2.96 \frac{J_{g2}}{J_{g1}} \quad (5.40)$$

$$u_{top,v} = -2.39 + 2.38 \frac{J_{g2}}{J_{g1}} \quad (5.41)$$

$$u_{top,p} = -2.50 + 2.47 \frac{J_{g2}}{J_{g1}} \quad (5.42)$$

with units of cm/s. The three equations give results close to zero at $J_{g2}/J_{g1} = 1$ (as expected). Among $u_{top,c6}$, $u_{top,v}$ and $u_{top,p}$, remember the $u_{top,v}$ is the actual velocity of the top of the bubble bed.

Comparing $u_{top,p}$ and $u_{top,c6}$ with $u_{top,v}$, we see that the difference between $u_{top,v}$ and $u_{top,p}$ is smaller than the difference between $u_{top,v}$ and $u_{top,c6}$. The key is which ε_g should be used. For $u_{top,p}$, $\varepsilon_{g1} = 14.3$ %, near the top of the bubble bed, was used. This ε_{g1} is close to the average value of the gas holdups in Cells 6 - 2, i.e. 14.80 %.

From measurements of u_{in} and ε_g in Section 5.5, it can be seen that the ε_g in Cell 6 is larger

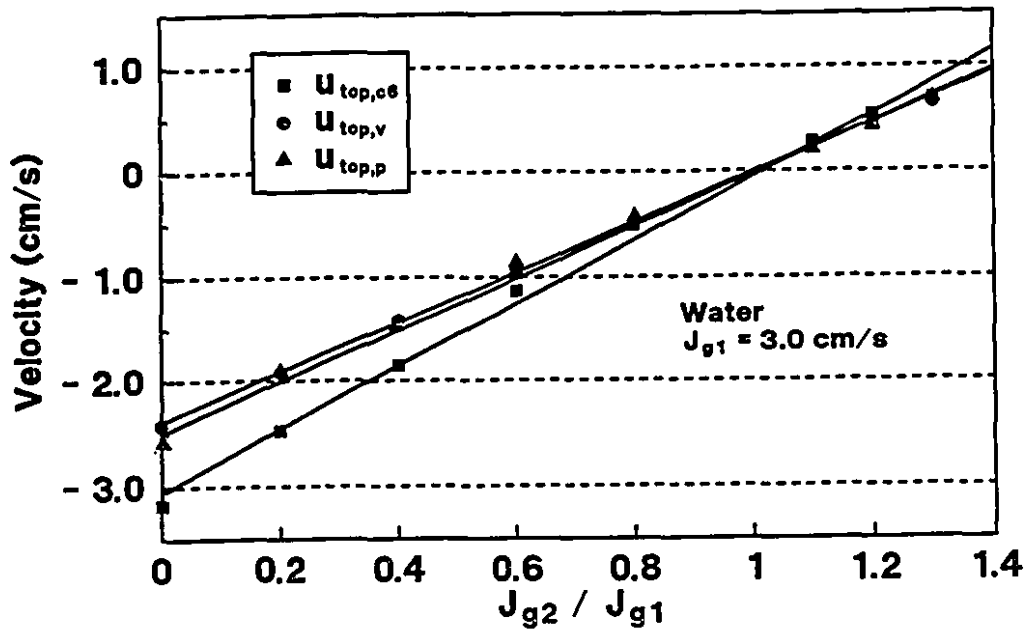

Figure 5.55 Comparison among $u_{top,c6}$, $u_{top,v}$ and $u_{top,p}$.

Table 5.13 $u_{top,c6}$, $u_{top,v}$ and $u_{top,p}$ at J_{g1} = 3.0 cm/s

J_{g1} (cm/s)	J_{g2} (cm/s)	u_{in} (cm/s)	$u_{top,c6}$ (cm/s)	$u_{top,v}$ (cm/s)	$u_{top,p}$ (cm/s)
3.00	0.00	16.93	-3.07	-2.42	-2.64
3.00	0.60	15.83	-2.45	-1.92	-1.95
3.00	1.20	15.29	-1.88	-1.41	-1.51
3.00	1.80	14.13	-1.17	-0.94	-0.88
3.00	2.40	13.17	-0.52	-0.49	-0.42
3.00	3.30	12.02	0.28	0.28	0.15
3.00	3.60	11.65	0.53	0.48	0.41
3.00	3.90	10.73	0.69	0.65	0.70

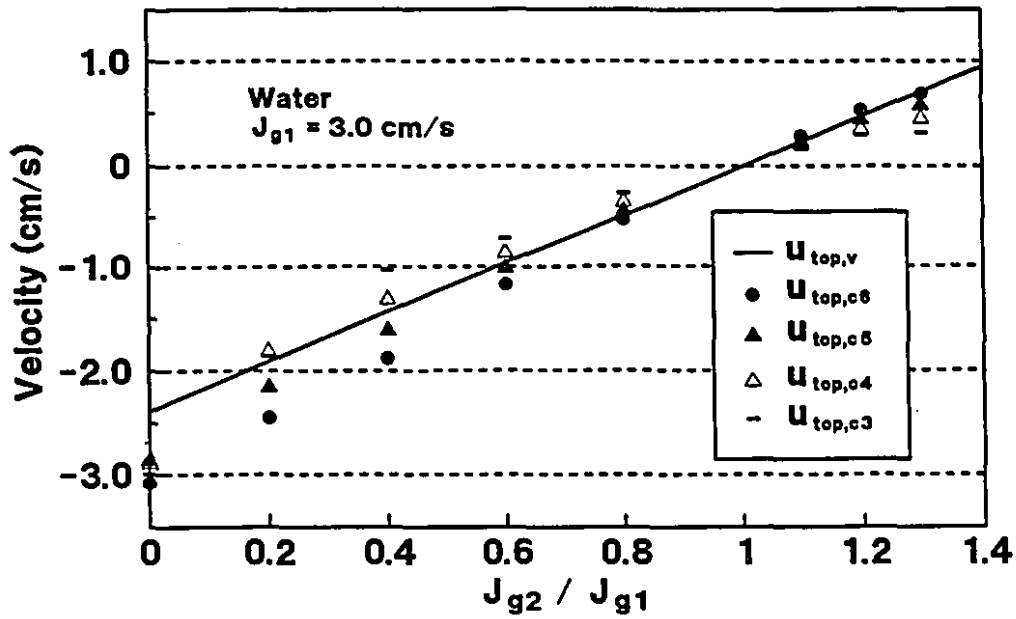

Figure 5.56 Comparison among $u_{top,c6}$ - $u_{top,c3}$ and $u_{top,v}$

Table 5.14 $u_{top,c5}$, $u_{top,c4}$ and $u_{top,c3}$ at J_{g1} = 3.0 cm/s

J_{g1} (cm/s)	J_{g2} (cm/s)	$u_{top,c5}$ (cm/s)	$u_{top,c4}$ (cm/s)	$u_{top,c3}$ (cm/s)
3.00	0.00	-2.86	-2.88	-2.99
3.00	0.60	-2.16	-1.82	-1.86
3.00	1.20	-1.62	-1.32	-1.03
3.00	1.80	-1.01	-0.86	-0.71
3.00	2.40	-0.44	-0.35	-0.26
3.00	3.30	0.23	0.20	0.16
3.00	3.60	0.44	0.35	0.29
3.00	3.90	0.58	0.45	0.32

than that in Cells 5 - 2 (see Tables 41 - 48 in Appendix 3). In this case, an axial gas holdup profile in the column contributes to the difference between $u_{top,c6}$ and $u_{top,v}$. Table 5.14 gives the $u_{top,c}$'s in Cells 5, 4 and 3 at J_{gl} = 3.0 cm/s and Figure 5.56 compares $u_{top,c6}$, $u_{top,c5}$, $u_{top,c4}$ and $u_{top,c3}$ with $u_{top,v}$. For Cells 6 - 3, the difference between $u_{top,c}$ and $u_{top,v}$ at J_{g2}/J_{gl}=0 is obviously larger than for the other J_{g2}/J_{gl} values. In the absence of the data at J_{g2}/J_{gl}=0, the three linear relationships to present $u_{top,c5}$, $u_{top,c4}$ and $u_{top,c3}$ are

$$u_{top,c5} = -2.59 + 2.53 \frac{J_{g2}}{J_{gl}} \tag{5.43}$$

$$u_{top,c4} = -2.16 + 2.10 \frac{J_{g2}}{J_{gl}} \tag{5.44}$$

$$u_{top,c3} = -1.95 + 1.89 \frac{J_{g2}}{J_{gl}} \tag{5.45}$$

with units of cm/s. It is clear that the $u_{top,c}$ is sensitive to the location of the cell in the column. If the average of $u_{top,c5}$ and $u_{top,c4}$ is used for fitting, the relationship is given by

$$u_{top,(c5+c4)/2} = -2.38 + 2.31 \frac{J_{g2}}{J_{gl}} \tag{5.46}$$

Comparing Equation 5.46 with 5.41, It can be seen that the best location for the conductance cell to obtain $u_{top,c}$ is in between Cell 5 and Cell 4 in this column.

From the control point of view, the conductance cell should be set close to the sparger to obtain $u_{top,c}$ as early as possible. However, the analysis of the results indicates this may give a poor prediction of u_{top}. One approach may be to use a factor to correct $u_{top,c}$: for $u_{top,c6}$, a factor of 0.8 corrects $u_{top,c6}$ to $u_{top,v}$ within a small error. This factor should be a function of the properties of the system. With the limitation of $0.90 < J_{g2} / J_{gl} < 1.10$, the $u_{top,c6}$ can be used even without the factor because the difference between $u_{top,v}$ and $u_{top,c6}$ is quite small in this narrow range (Figures 5.55 and 5.56).

CHAPTER 6

AIR - WATER - FROTHER SYSTEM

In this chapter, four sets of experiments are presented: (a) batch operation with Dowfroth 250C (DF250C) = 10 ppm; (b) batch operation with DF250C = 20 ppm; (c) countercurrent operation with DF250C = 20 ppm; (d) batch operation with Dowfroth 1263 (DF1263) = 20 ppm. The properties of the frothers DF250C and DF1263 are given in Appendix 4.

6.1 Experiments with DF250C = 10 ppm

All experiments with DF250C = 10 ppm were conducted under batch operation ($J_l = 0$) at room temperature.

6.1.1 Procedure of Experiment

The procedure was controlled by computer:

(a) open Valve 1 (set to J_{g1});
(b) wait for steady state operation of the column;
(c) at 0 s, start the data acquisition system;
(d) at 10 s, close Valve 1 and open Valve 2 (set to J_{g2});
(e) close Valve 2;
(f) stop the data acquisition system.

Depending on the interface velocity, the time for an experiment was 1 - 3 minutes.

6.1.2 u_{in} and u_h in Cell 6

Figures 6.1 and 6.2 illustrate the experiments for the same cases (a) and (b) in Figure 5.5, respectively. The rising interface was still readily detected and its velocity, u_{in}, could be measured by the conductivity method.

The interface velocity, u_{in}, and the gas holdup, ε_g, were calculated by using Equations 5.9 and 5.10. Tables 6.2 - 6.6 present the u_{in}, ε_{g1} and ε_{g2} in Cell 6 at J_{g1} = 0.25, 0.5, 0.75, 1.0 and

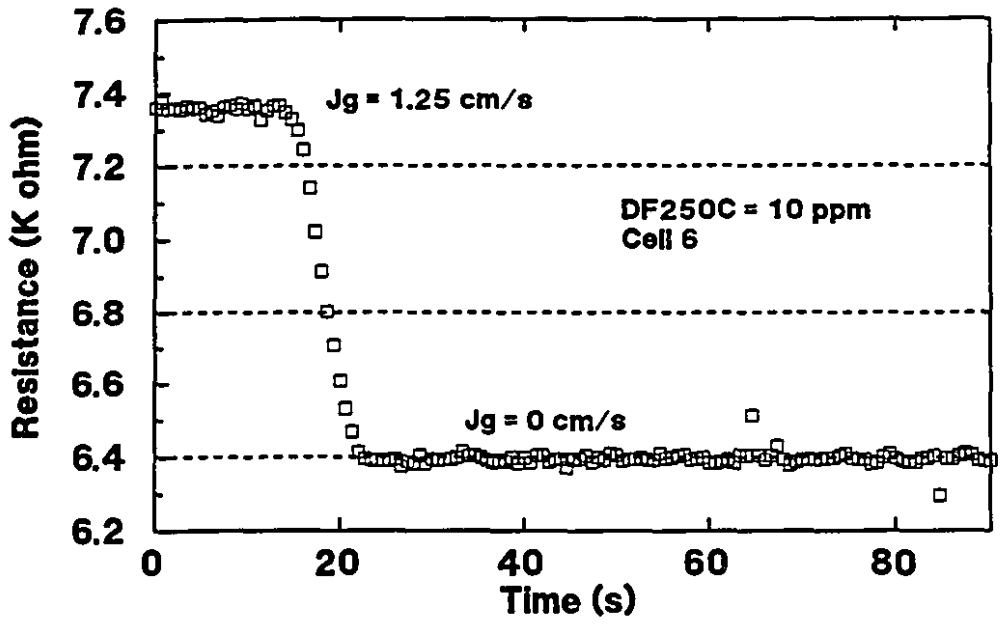

Figure 6.1 Resistance versus time in Cell 6 for case (a) in Figure 5.5 with DF250C = 10 ppm.

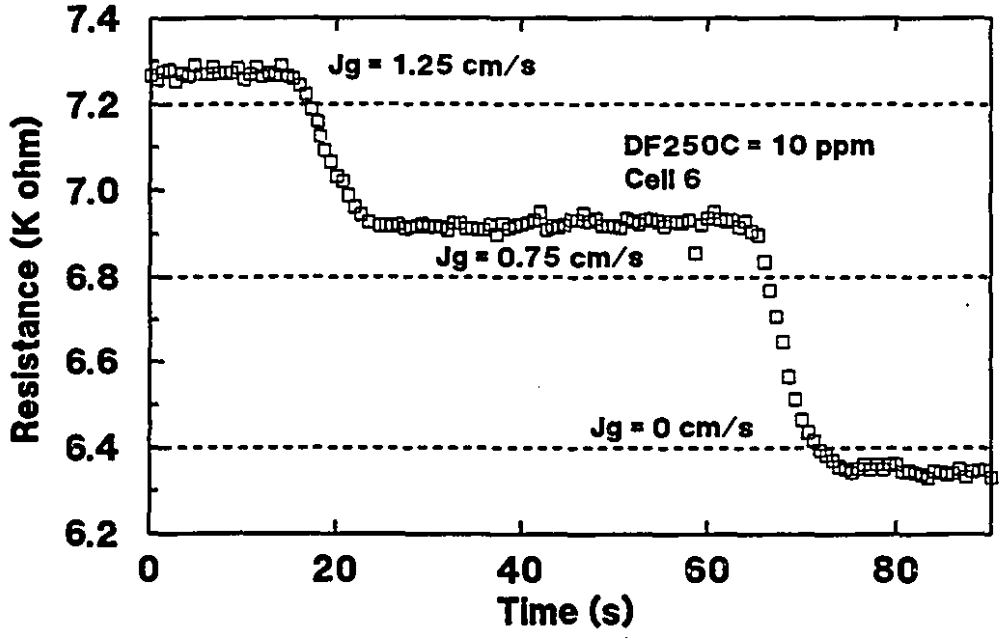

Figure 6.2 Resistance versus time in Cell 6 for case (b) in Figure 5.5 with DF250C = 10 ppm.

1.25 cm/s, respectively. The linear regressions for u_h at J_{gl} = 0.25, 0.5, 0.75, 1.0 and 1.25 cm/s are shown in Figures 6.3 - 6.7, respectively.

Based on ten replicates for each experiment, the maximum relative standard deviation for u_{in} was 1.45%, the maximum relative standard deviation for u_0 was 1.16%, and the maximum relative standard deviation for ε_g was 2.33% for data shown in Tables 6.2 - 6.6. The standard errors of the estimated u_h were 0.09, 0.14, 0.12, 0.18 and 0.05 cm/s at J_{gl} = 0.25, 0.5, 0.75, 1.0 and 1.25 cm/s, respectively.

Table 6.1 shows the comparison among u_g, u_h and u_0+J_g in Cell 6 at various J_{gl}. Figure 6.8 illustrates that as J_g increases u_g increases and u_h varies in the range of 5.1 - 6.0 cm/s. In Figure 6.8, it is evident that a large difference exists between u_g and u_0+J_g. It means that Nicklin's

Table 6.1 Comparison among u_g, u_h and u_0+J_g in Cell 6 (DF250C = 10 ppm) *

J_{gl}	0.25	0.50	0.75	1.00	1.25
ε_{gl} (%)	2.05	3.82	5.28	6.83	8.38
u_g	12.2	13.1	14.2	14.6	14.9
$u_0 + J_g$	5.7	7.4	8.7	8.7	9.0
u_h	5.1	5.8	6.0	5.5	5.5

* All velocities are cm/s.

derivation, $u_g = u_0 + J_g$, is not applicable in the presence of the frother DF250C = 10 ppm under batch operation.

Figure 6.9 illustrates that the model used for the air - water only system can also be applied in this case

$$u_{in} = u_h \left[1 + A \left(\frac{J_{g2}}{J_{gl}} - 1 \right) \right] \qquad (5.16)$$

where u_h is a function of J_{gl}

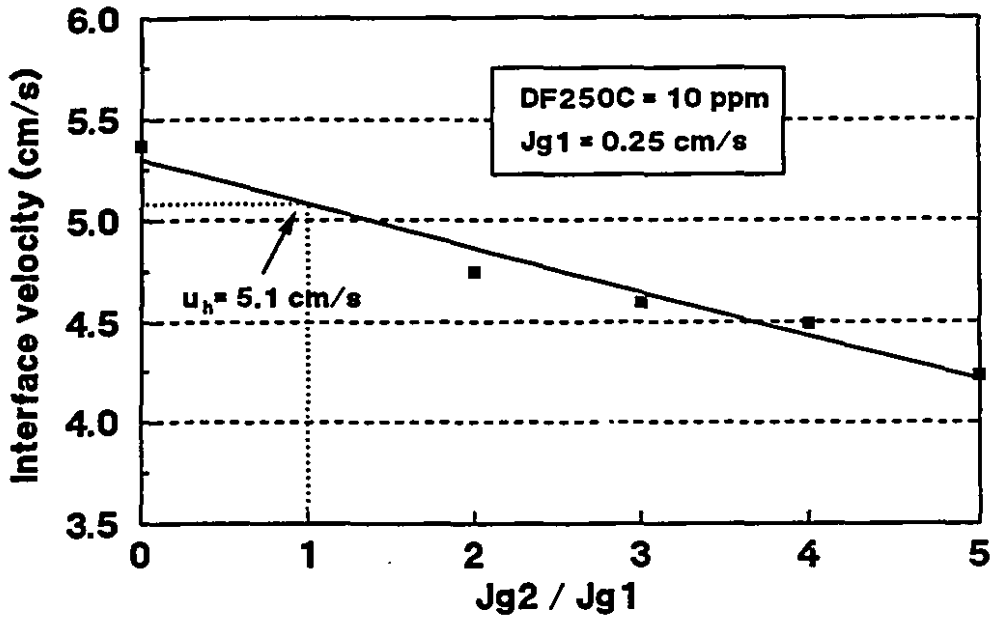

Figure 6.3 u_{in} and u_h in Cell 6 at J_{g1} = 0.25 cm/s with DF250C = 10 ppm.

Table 6.2 Measurement of u_{in} in Cell 6 at J_{g1} = 0.25 cm/s with DF250C = 10 ppm

J_{g1} (cm/s)	J_{g2} (cm/s)	J_{g2} / J_{g1}	ε_{g1} (%)	ε_{g2} (%)	u_{in} (cm/s)
0.25	0	0	2.03	0	5.4
0.25	0.50	2.0	2.12	3.92	4.8
0.25	0.75	3.0	2.07	5.46	4.6
0.25	1.00	4.0	2.01	6.71	4.5
0.25	1.25	5.0	2.02	8.10	4.2

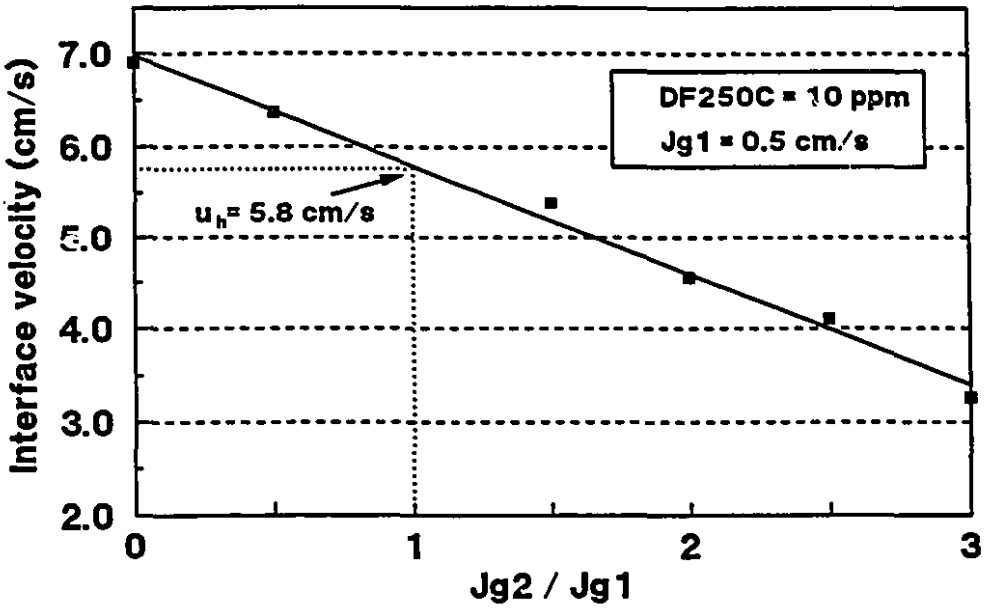

Figure 6.4 u_{in} and u_h in Cell 6 at J_{g1} = 0.5 cm/s with DF250C = 10 ppm.

Table 6.3 Measurement of u_{in} in Cell 6 at J_{g1} = 0.50 cm/s with DF250C = 10 ppm

J_{g1} (cm/s)	J_{g2} (cm/s)	J_{g2} / J_{g1}	ε_{g1} (%)	ε_{g2} (%)	u_{in} (cm/s)
0.50	0	0	3.85	0	6.9
0.50	0.25	0.5	3.81	2.00	6.4
0.50	0.75	1.5	3.89	5.28	5.4
0.50	1.00	2.0	3.79	6.64	4.6
0.50	1.25	2.5	3.80	8.50	4.1
0.50	1.50	3.0	3.78	9.69	3.3

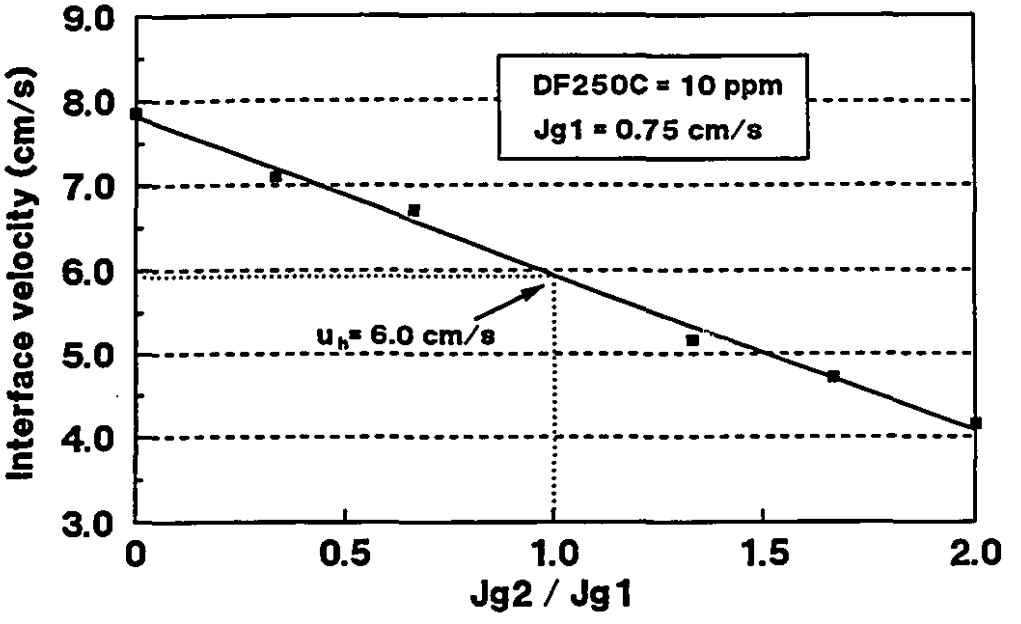

Figure 6.5 u_{in} and u_h in Cell 6 at J_{g1} = 0.75 cm/s with DF250C = 10 ppm.

Table 6.4 Measurement of u_{in} in Cell 6 at J_{g1} = 0.75 cm/s with DF250C = 10 ppm

J_{g1} (cm/s)	J_{g2} (cm/s)	J_{g2} / J_{g1}	ε_{g1} (%)	ε_{g2} (%)	u_{in} (cm/s)
0.75	0	0	5.30	0	7.9
0.75	0.25	0.33	5.26	1.90	7.1
0.75	0.50	0.67	5.24	3.70	6.7
0.75	1.00	1.33	5.33	6.89	5.2
0.75	1.25	1.67	5.25	7.87	4.7
0.75	1.50	2.00	5.31	9.60	4.2

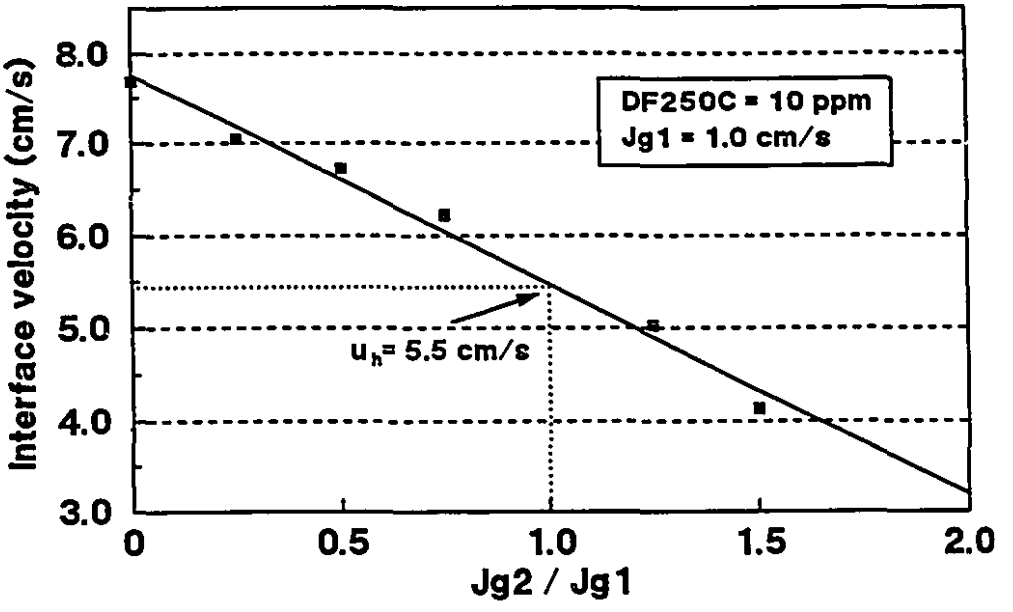

Figure 6.6 u_{in} and u_h in Cell 6 at J_{g1} = 1.0 cm/s with DF250C = 10 ppm.

Table 6.5 Measurement of u_{in} in Cell 6 at J_{g1} = 1.0 cm/s with DF250C = 10 ppm

J_{g1} (cm/s)	J_{g2} (cm/s)	J_{g2} / J_{g1}	ε_{g1} (%)	ε_{g2} (%)	u_{in} (cm/s)
1.00	0	0	6.80	0	7.7
1.00	0.25	0.25	6.84	2.18	7.0
1.00	0.50	0.50	6.85	3.65	6.7
1.00	0.75	0.75	6.79	5.15	6.2
1.00	1.25	1.25	6.89	9.00	5.0
1.00	1.50	1.50	6.81	10.18	4.1

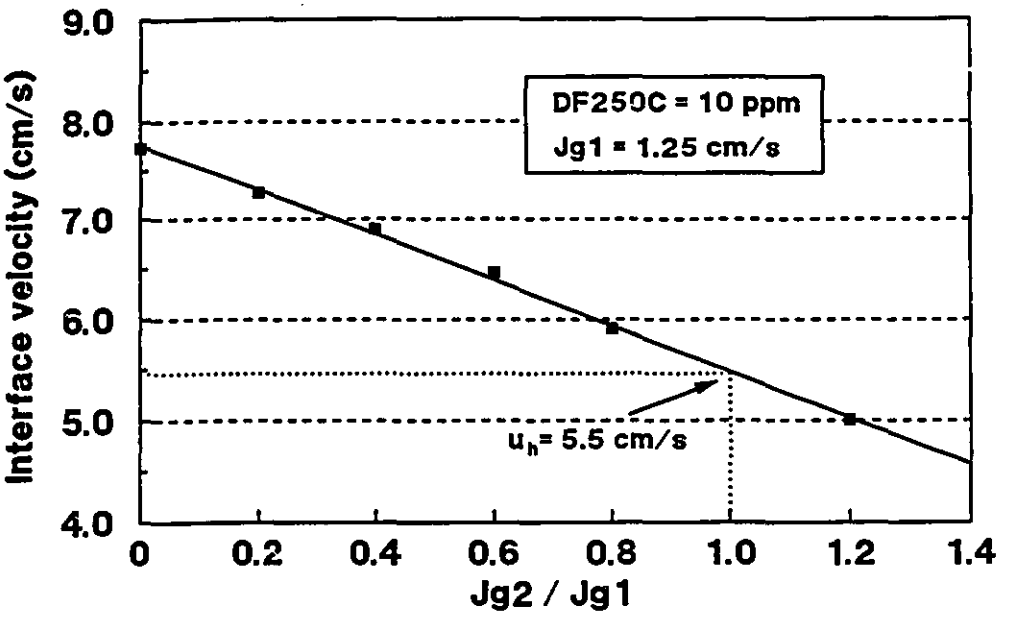

Figure 6.7 u_{in} and u_h in Cell 6 at J_{g1} = 1.25 cm/s with DF250C = 10 ppm.

Table 6.6 Measurement of u_{in} in Cell 6 at J_{g1} = 1.25 cm/s with DF250C = 10 ppm

J_{g1} (cm/s)	J_{g2} (cm/s)	J_{g2} / J_{g1}	ε_{g1} (%)	ε_{g2} (%)	u_{in} (cm/s)
1.25	0	0	8.35	0	7.7
1.25	0.25	0.20	8.42	2.17	7.3
1.25	0.50	0.40	8.37	3.93	6.9
1.25	0.75	0.60	8.40	5.24	6.5
1.25	1.00	0.80	8.33	7.02	5.9
1.25	1.50	1.20	8.41	9.16	5.0

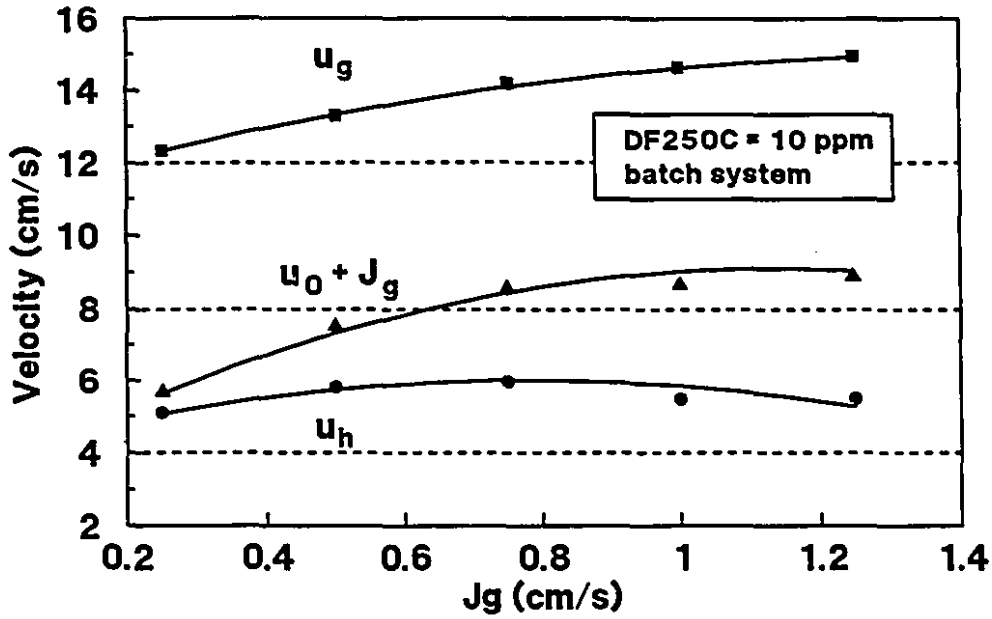

Figure 6.8 Comparison among u_g, u_h and u_0+J_g in Cell 6 (DF250C = 10 ppm).

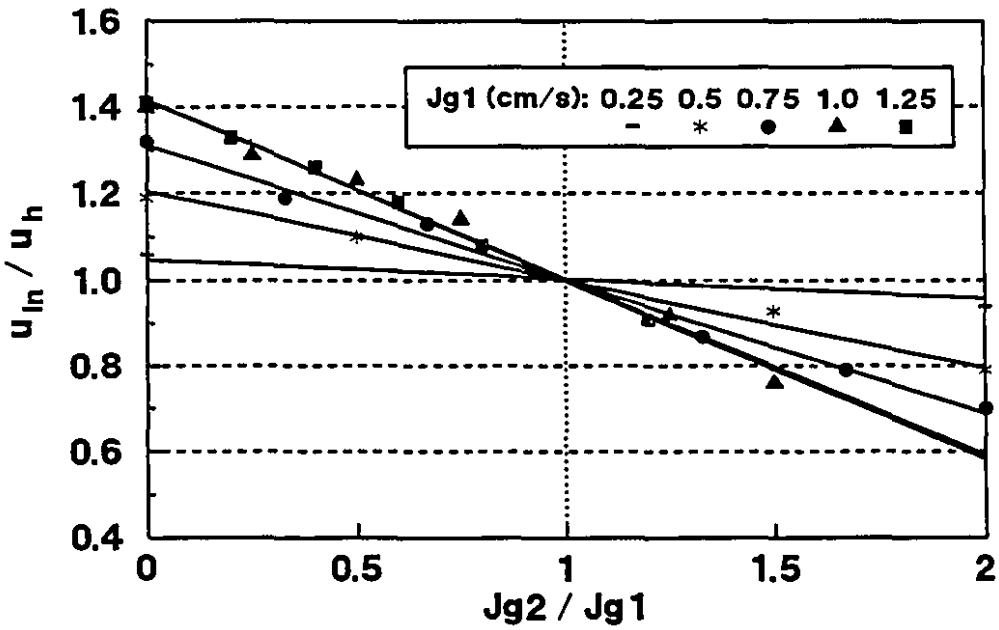

Figure 6.9 Dimensionless velocity versus dimensionless gas rate (DF250C = 10 ppm).

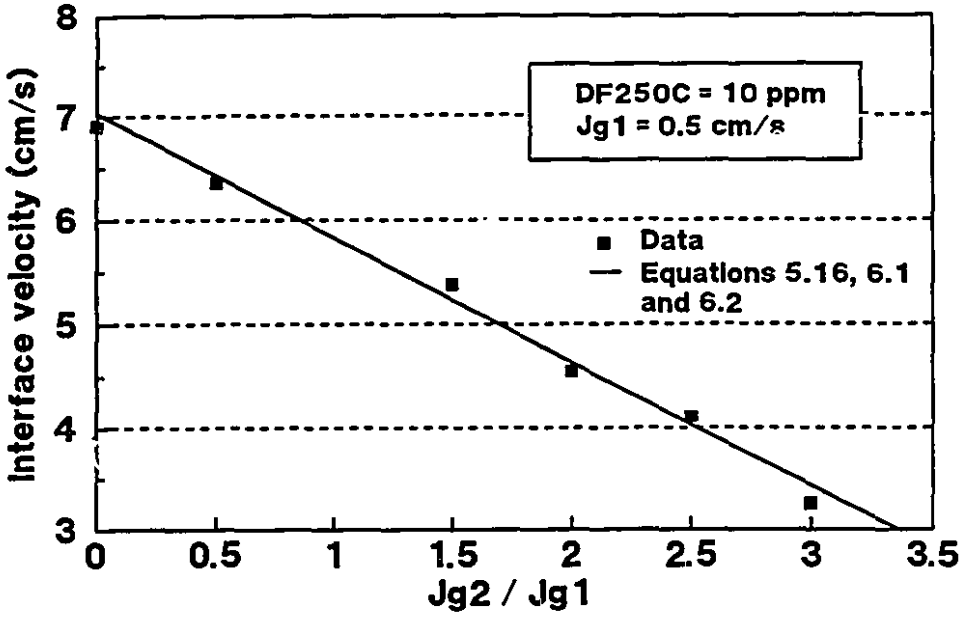

Figure 6.10 Example of model fit: model and measured u_{in} in Cell 6 at J_{gl} = 0.5 cm/s with DF250C = 10 ppm.

$$u_h = 3.23 + 9.99\,J_{gl} - 11.6\,J_{gl}^2 + 3.95\,J_{gl}^3 \tag{6.1}$$

and A also is a function of J_{gl}

$$A = 0.167 - 0.928\,J_{gl} + 0.365\,J_{gl}^2 \tag{6.2}$$

In Cell 6, the model applies to the condition $0.25 < J_g < 1.25$ cm/s under batch operation with DF250C = 10 ppm. Figure 6.10 shows a model fit with the measured u_{in} at J_{gl} = 0.5 cm/s.

6.1.3 Axial Profile of u_{in} with DF250C = 10 ppm

With DF250C = 10 ppm, the u_{in} was measured in Cells 4 and 2 with the same conductivity method used in Cell 6. Figures 6.11 - 6.15 illustrate the axial profile of u_{in} in the column at J_{gl} = 0.25, 0.50, 0.75, 1.0 and 1.25 cm/s, respectively. In these Figures, the curve shows the linear regression for u_{in} in Cell 6.

It can be seen that u_{in} varies slightly from Cell 2 to Cell 6 and u_h is constant along the column. With the restriction $0.9 < J_{g2} / J_{gl} < 1.1$, Equations 5.16, 6.1 and 6.2 obtained from Cell 6 can be used for the entire column.

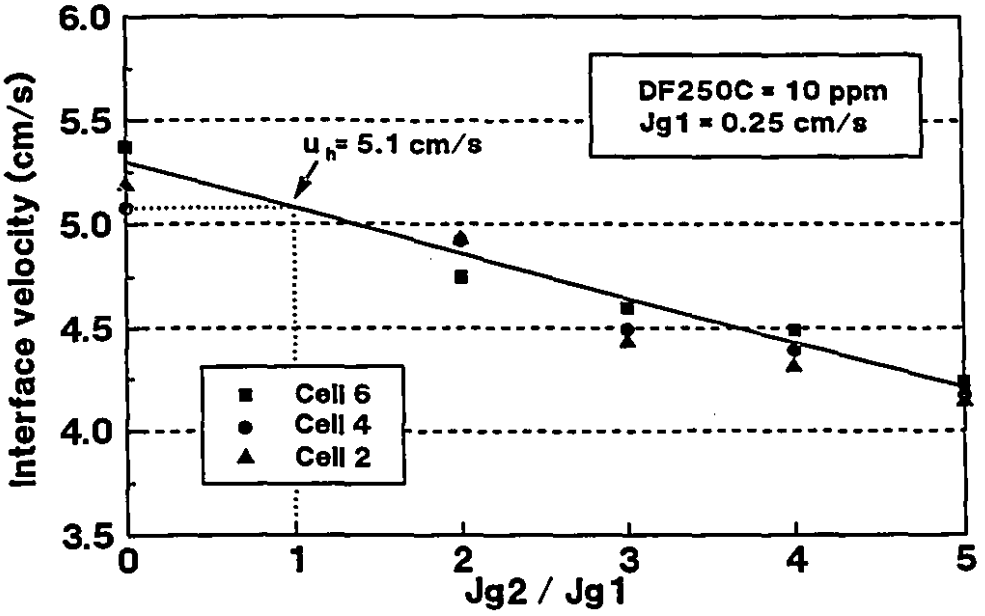

Figure 6.11 Measurement of u_{in} in Cells 6, 4 and 2 at J_{gl} = 0.25 cm/s with DF250C = 10 ppm. The u_h quoted is for Cell 6.

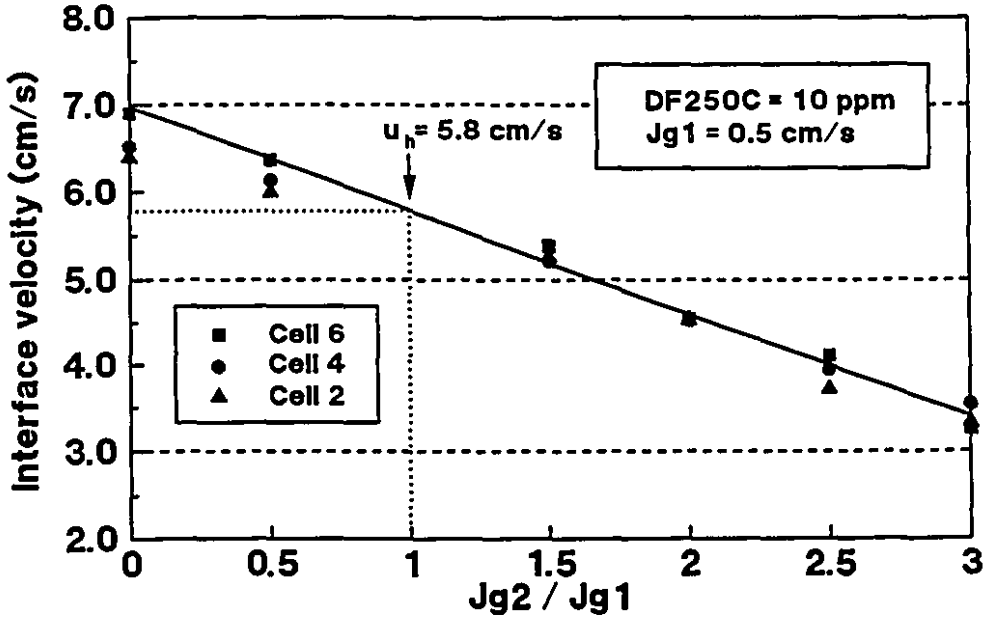

Figure 6.12 Measurement of u_{in} in Cells 6, 4 and 2 at J_{gl} = 0.50 cm/s with DF250C = 10 ppm. The u_h quoted is for Cell 6.

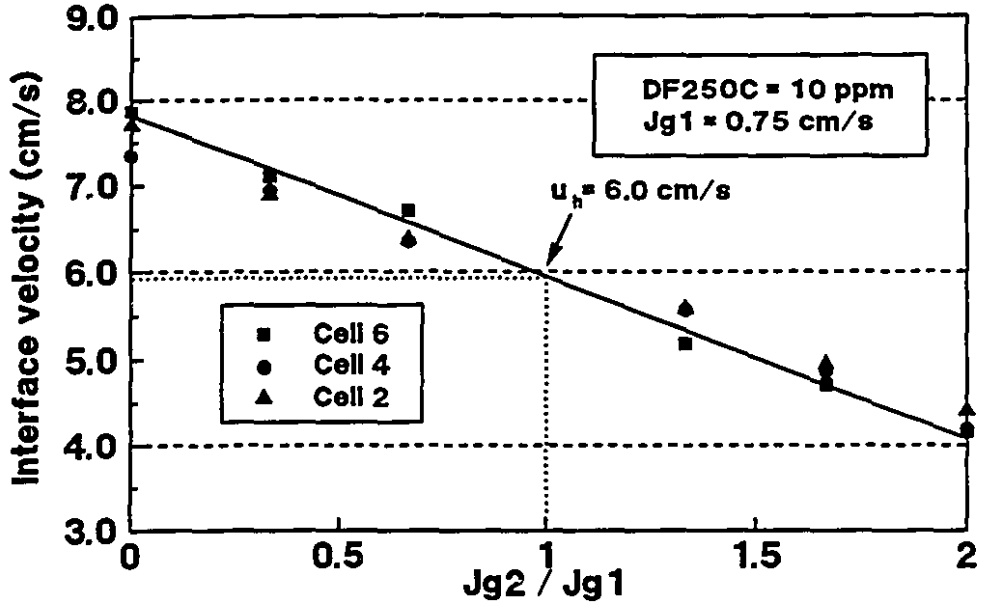

Figure 6.13 Measurement of u_{in} in Cells 6, 4 and 2 at J_{gl} = 0.75 cm/s with DF250C = 10 ppm. The u_h quoted is for Cell 6.

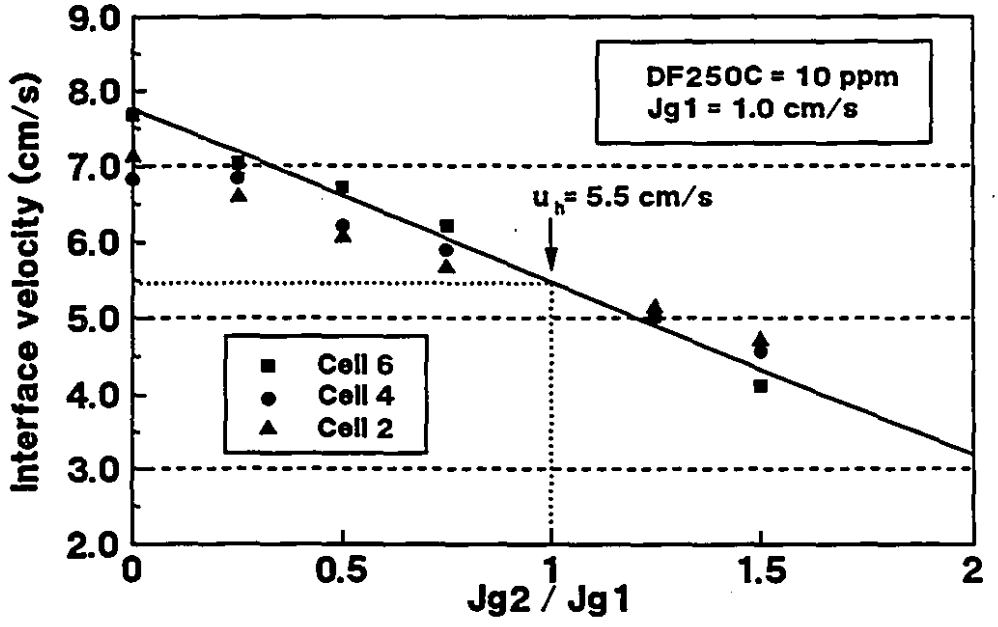

Figure 6.14 Measurement of u_{in} in Cells 6, 4 and 2 at J_{gl} = 1.0 cm/s with DF250C = 10 ppm. The u_h quoted is for Cell 6.

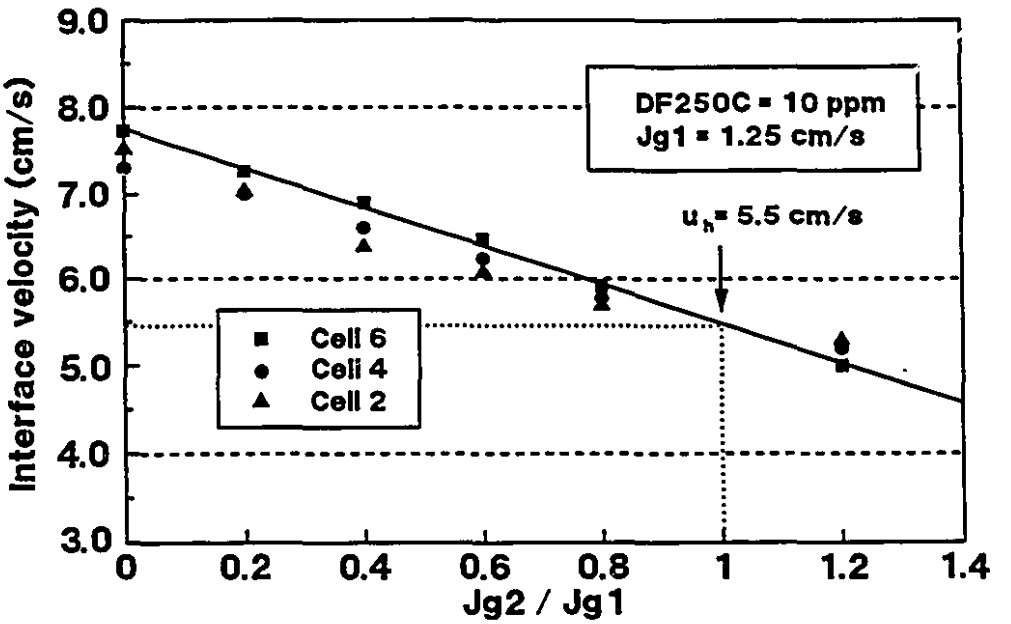

Figure 6.15 Measurement of u_{in} in Cells 6, 4 and 2 at J_{gl} = 1.25 cm/s with DF250C = 10 ppm. The u_h quoted is for Cell 6.

6.2 Experiments with DF250C = 20 ppm in Batch System

The experiments presented in this section were carried out under batch operation ($J_l = 0$) at room temperature with DF250C = 20 ppm. The procedure of the experiment was the same as that described in Section 6.1.1.

6.2.1 u_{ln} and u_h in Cell 6 in Batch System

Figures 6.16 and 6.17 illustrate the experiments with DF250C = 20 ppm for the same cases (a) and (b) in Figure 6.10, respectively. The rising interface formed by a step change of the gas flow was still readily detected.

As shown in Section 5.2, the ε_g and u_{in} were calculated by using Equations 5.9 and 5.10. Tables 6.8 - 6.12 show the u_{in} and ε_g in Cell 6 at J_{gl} = 0.5, 0.75, 1.0, 1.25 and 1.5 cm/s, respectively. Figures 6.18 - 6.22 illustrate the linear regressions for u_h at J_g = 0.5, 0.75, 1.0, 1.25 and 1.5 cm/s, respectively.

For data shown in Tables 6.8 - 6.12, based on ten replicates for each experiment, the maximum relative standard deviation for u_{in} was 1.40%, the maximum relative standard deviation for u_0 was 1.26%, and the maximum relative standard deviation for ε_g was 2.25%. The standard errors of the estimated u_h were 0.06, 0.05, 0.08, 0.08 and 0.11 cm/s at J_{gl} = 0.5, 0.75, 1.0, 1.25 and 1.5 cm/s, respectively.

Table 6.7 shows u_g, u_h and u_0+J_g in Cell 6 at various J_{gl} in the batch system. In Figure 6.23,

Table 6.7 Comparison among u_g, u_h and u_0+J_g in Cell 6 (DF250C = 20 ppm) *

J_{gl}	0.50	0.75	1.00	1.25	1.50
ε_{gl} (%)	4.05	6.36	8.50	11.70	13.01
u_g	12.3	11.8	11.8	10.7	11.5
$u_0 + J_{gl}$	4.5	5.4	6.6	7.2	8.4
u_h	3.1	3.0	3.9	4.5	5.0

* All velocities are cm/s.

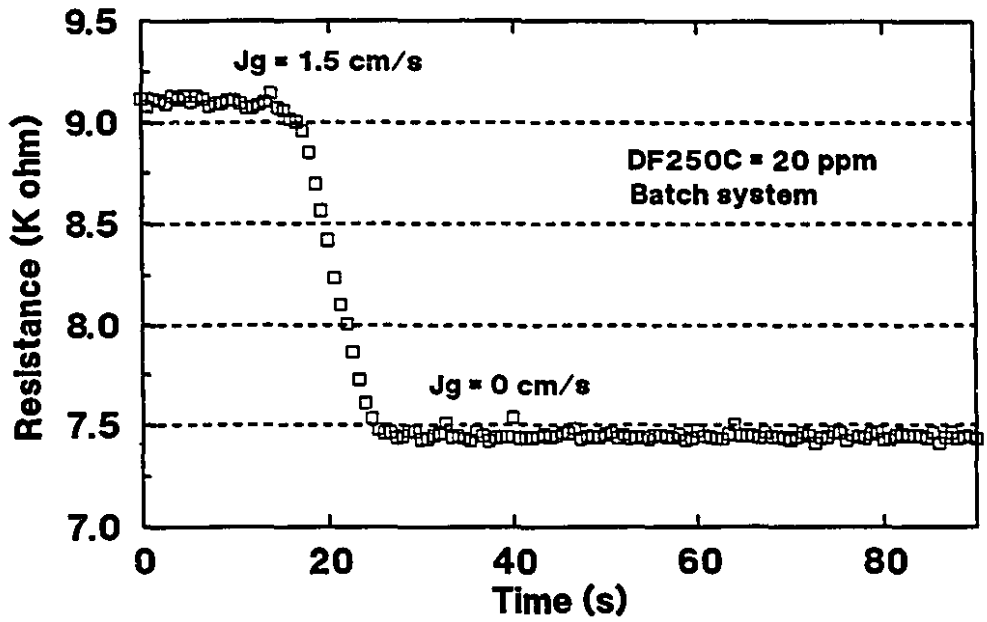

Figure 6.16 Resistance versus time in Cell 6 for case (a) in Figure 5.5 with DF250C = 20 ppm.

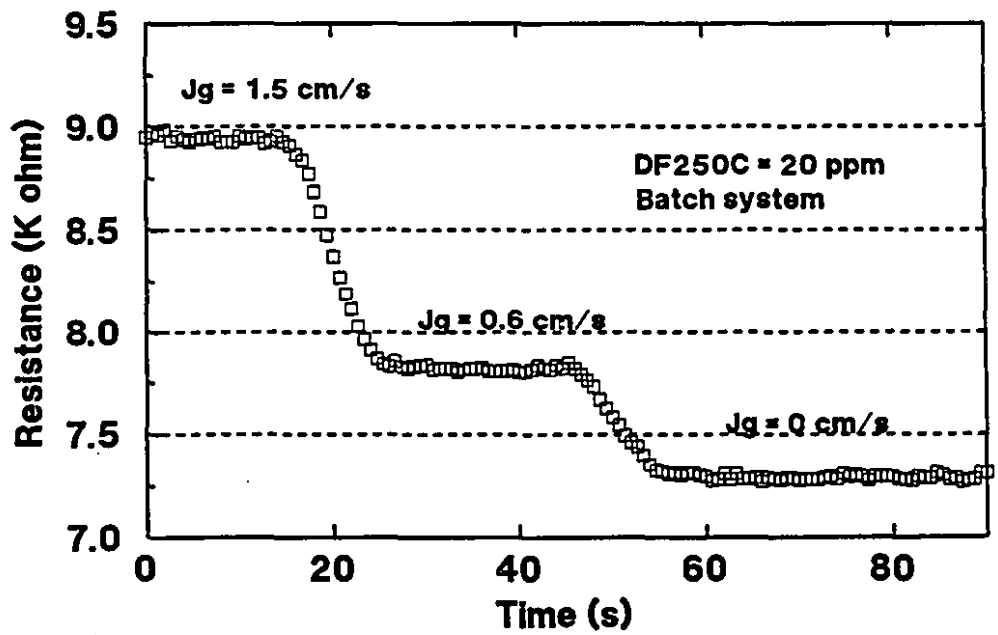

Figure 6.17 Resistance versus time in Cell 6 for case (b) in Figure 5.5 with DF250C = 20 ppm.

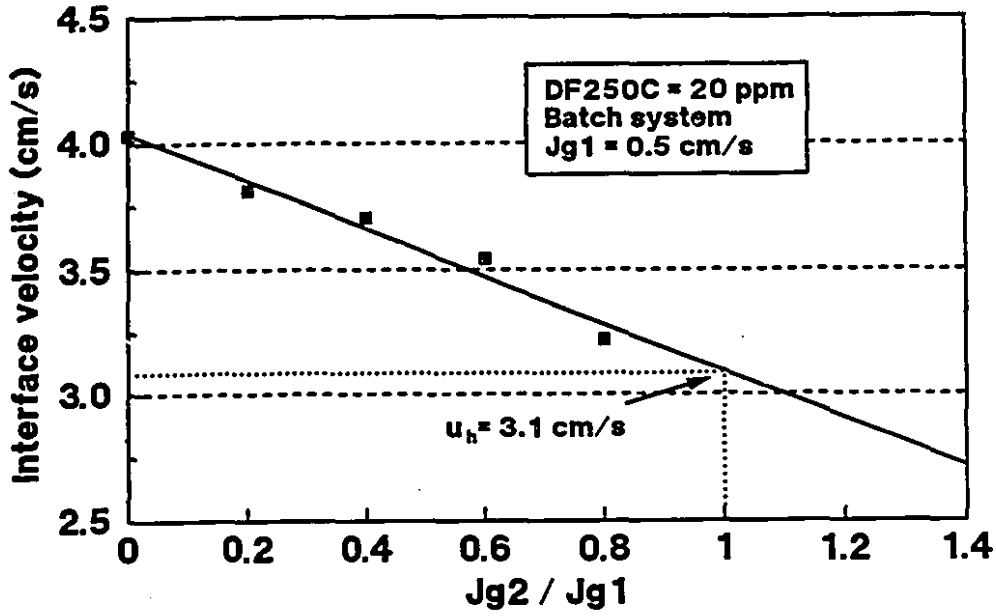

Figure 6.18 Interface velocities in Cell 6 at J_{g1} = 0.5 cm/s with DF250C = 20 ppm.

Table 6.8 Measurement of u_{in} in Cell 6 at J_{g1} = 0.5 cm/s with DF250C = 20 ppm

J_{g1} (cm/s)	J_{g2} (cm/s)	J_{g2} / J_{g1}	ε_{g1} (%)	ε_{g2} (%)	u_{in} (cm/s)
0.5	0	0	4.10	0	4.0
0.5	0.1	0.2	4.01	0.96	3.8
0.5	0.2	0.4	4.03	1.96	3.7
0.5	0.3	0.6	4.08	2.61	3.5
0.5	0.4	0.8	4.03	3.32	3.2

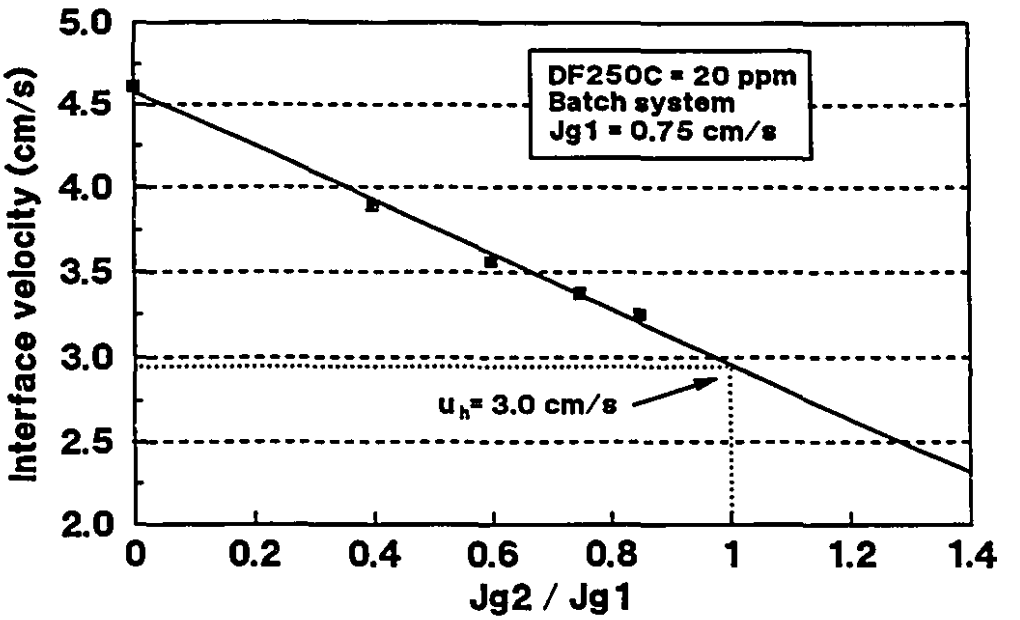

Figure 6.19 Interface velocities in Cell 6 at J_{gl} = 0.75 cm/s with DF250C = 20 ppm.

Table 6.9 Measurement of u_{in} in Cell 6 at J_{gl} = 0.75 cm/s with DF250C = 20 ppm

J_{gl} (cm/s)	J_{g2} (cm/s)	J_{g2} / J_{gl}	ε_{gl} (%)	ε_{g2} (%)	u_{in} (cm/s)
0.75	0	0	6.39	0	4.6
0.75	0.30	0.40	6.35	2.52	3.9
0.75	0.45	0.60	6.40	3.55	3.6
0.75	0.56	0.75	6.30	4.45	3.4
0.75	0.64	0.85	6.36	5.15	3.3

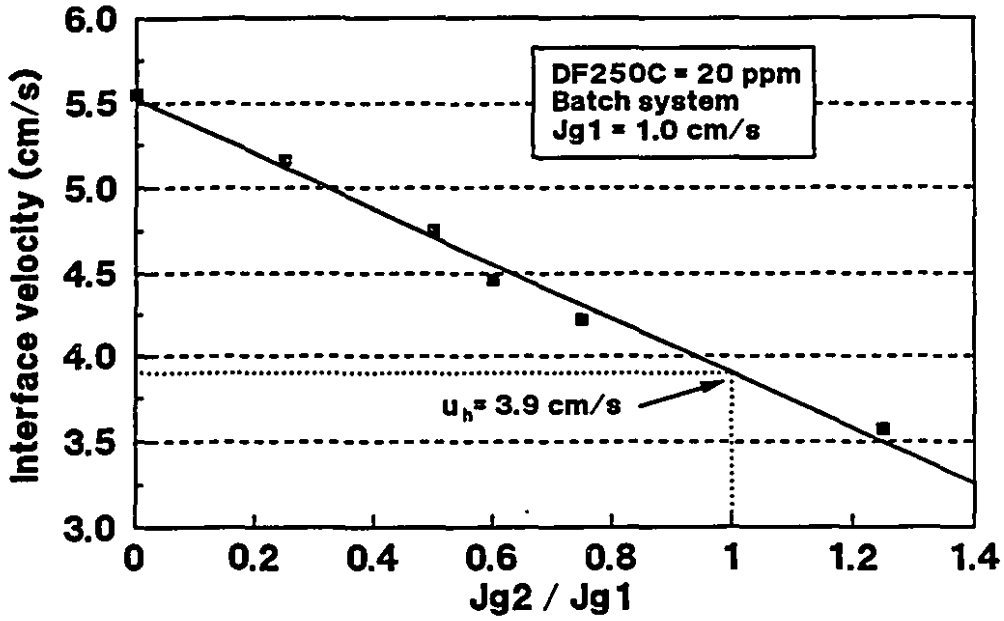

Figure 6.20 Interface velocities in Cell 6 at J_{g1} = 1.0 cm/s with DF250C = 20 ppm.

Table 6.10 Measurement of u_{in} in Cell 6 at J_{g1} = 1.0 cm/s with DF250C = 20 ppm

J_{g1} (cm/s)	J_{g2} (cm/s)	J_{g2} / J_{g1}	ε_{g1} (%)	ε_{g2} (%)	u_{in} (cm/s)
1	0	0	8.46	0	5.6
1	0.25	0.25	8.52	2.11	5.2
1	0.50	0.50	8.49	3.96	4.8
1	0.60	0.60	8.55	4.87	4.5
1	0.75	0.75	8.45	6.53	4.2
1	1.25	1.25	8.53	11.63	3.6

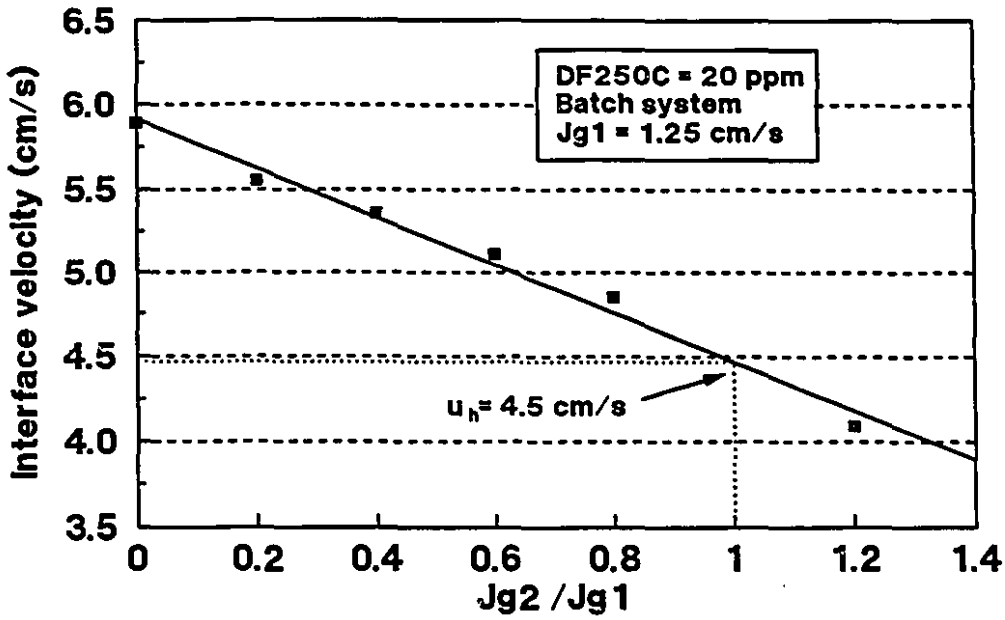

Figure 6.21 Interface velocities in Cell 6 at J_{g1} = 1.25 cm/s with DF250C = 20 ppm.

Table 6.11 Measurement of u_{in} in Cell 6 at J_{g1} = 1.25 cm/s with DF250C = 20 ppm

J_{g1} (cm/s)	J_{g2} (cm/s)	J_{g2} / J_{g1}	ε_{g1} (%)	ε_{g2} (%)	u_{in} (cm/s)
1.25	0	0	11.78	0	5.9
1.25	0.25	0.2	11.66	2.10	5.6
1.25	0.50	0.4	11.71	4.08	5.4
1.25	0.75	0.6	11.69	5.92	5.1
1.25	1.00	0.8	11.65	9.36	4.9
1.25	1.50	1.2	11.70	13.06	4.1

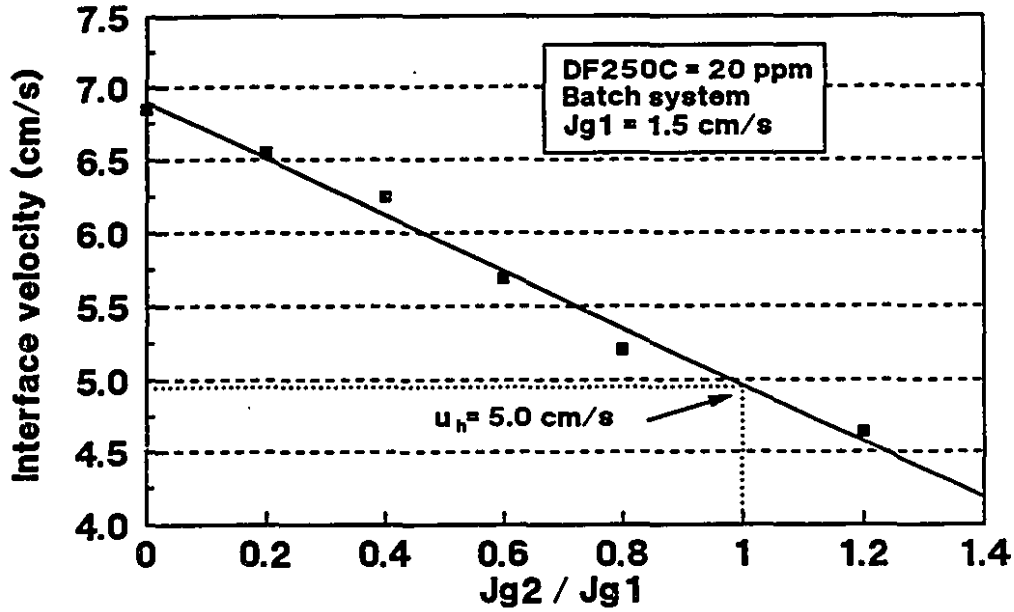

Figure 6.22 Interface velocities in Cell 6 at J_{g1} = 1.5 cm/s with DF250C = 20 ppm.

Table 6.12 Measurement of u_{in} in Cell 6 at J_{g1} = 1.5 cm/s with DF250C = 20 ppm

J_{g1} (cm/s)	J_{g2} (cm/s)	J_{g2} / J_{g1}	ε_{g1} (%)	ε_{g2} (%)	u_{in} (cm/s)
1.5	0	0	13.10	0	6.9
1.5	0.3	0.2	12.96	2.42	6.6
1.5	0.6	0.4	12.98	4.66	6.3
1.5	0.9	0.6	13.00	7.51	5.7
1.5	1.2	0.8	13.05	10.50	5.2
1.5	1.8	1.2	12.96	13.84	4.6

it can be seen that the u_g increases as $J_{gl} > 1.5$ cm/s. Figure 6.23 illustrates that the u_g decreases and u_h increases as J_g increases in the range 0 - 1.25 cm/s. By Nicklin's derivation, u_g should be equal to u_0+J_g but Figure 6.23 shows a large difference between them. Combining with the results shown in Figure 6.10, it is evident that Nicklin's derivation is not applicable in the presence of the frother.

Figure 6.24 illustrates that Equation 5.16 is again applicable

$$u_{in} = u_h \left[1 + A \left(\frac{J_{g2}}{J_{gl}} - 1 \right) \right] \tag{5.16}$$

where u_h is a function of J_{gl}

$$u_h = -14.1 + 4.61\, J_{gl}^{-1} + 18.7\, J_{gl} - 5.33\, J_{gl}^2 \tag{6.3}$$

and A also is a function of J_{gl}

$$A = -7.36 + 1.99\, J_{gl}^{-1} + 7.33\, J_{gl} - 2.38\, J_{gl}^2 \tag{6.4}$$

The model corresponds to the condition $0.5 < J_g < 1.25$ cm/s under batch operation with DF250C = 20 ppm. Figure 6.25 illustrates that the model fit to the measured u_{in} in Cell 6 at $J_{gl} = 1.0$ cm/s.

6.2.2 Axial Profile of u_{in} with DF250C = 20 ppm

With DF250C = 20 ppm, the u_{in} was measured in Cells 4 and 2. Figures 6.26 - 6.30 illustrate the axial profile of u_{in} in the column at $J_{gl} = 0.50$, 0.75, 1.0, 1.25 and 1.5 cm/s, respectively.

The diagrams illustrate that u_h is constant in the column and u_{in} varies over a small range from Cell 2 to Cell 6. With the limitation $0.9 < J_{g2} / J_{gl} < 1.1$, Equations 5.16, 6.3 and 6.4 obtained from Cell 6 can be used for the entire column.

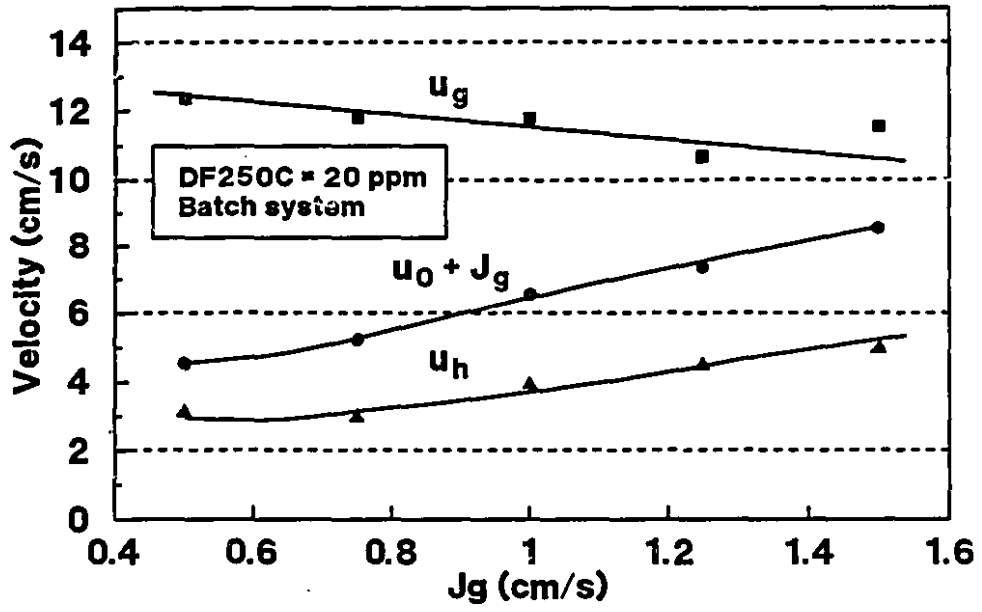

Figure 6.23 Comparison among u_g, u_h and u_0+J_g in Cell 6 in batch system with DF250C = 20 ppm.

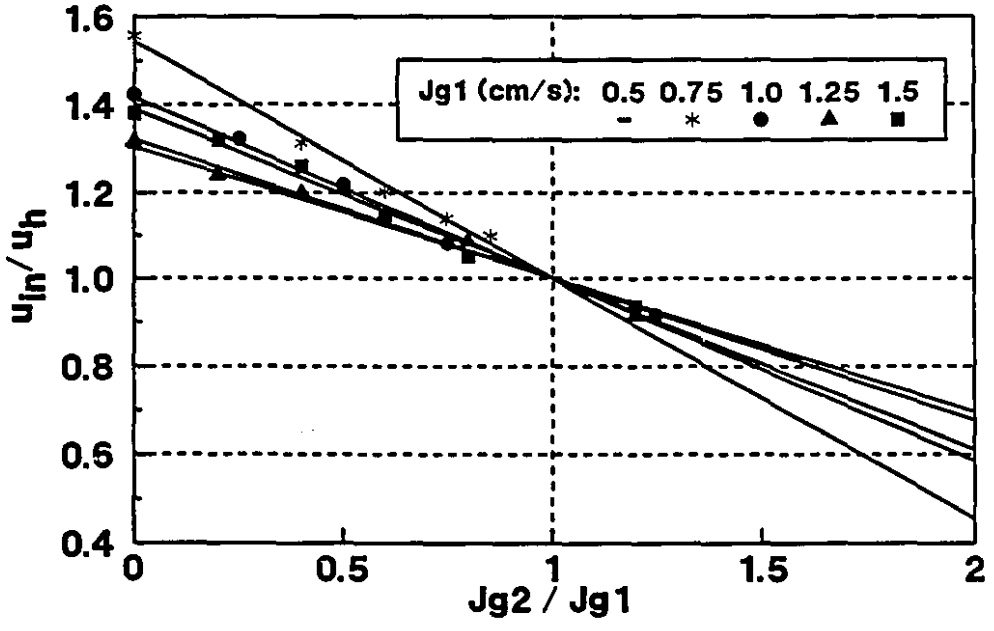

Figure 6.24 Dimensionless velocity versus dimensionless gas rate (DF250C = 20 ppm).

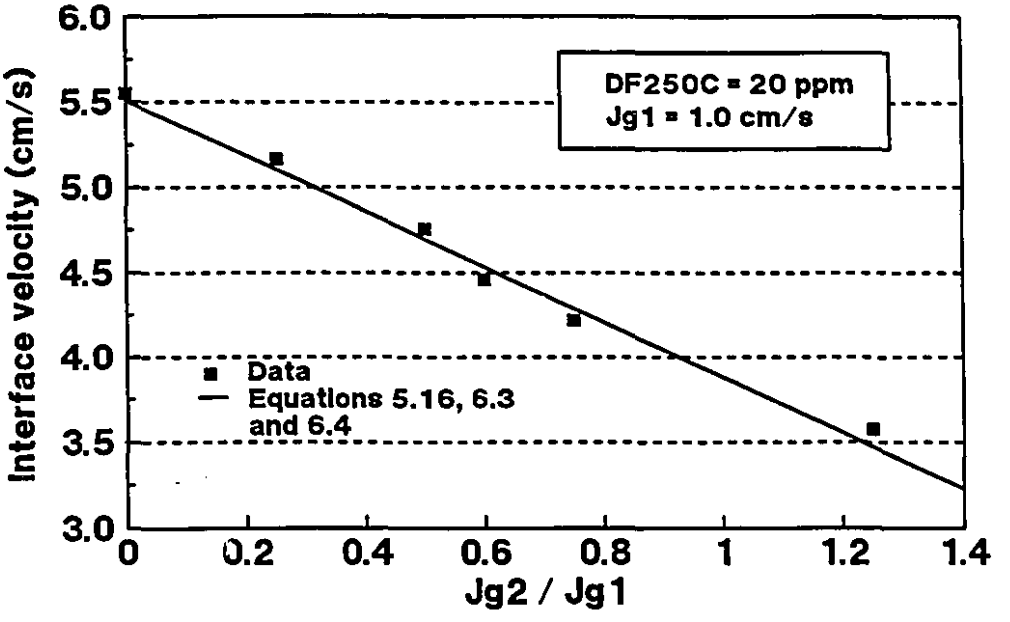

Figure 6.25 Example of model fit: model and measured u_{in} in Cell 6 at J_{g1} = 1.0 cm/s with DF250C = 20 ppm.

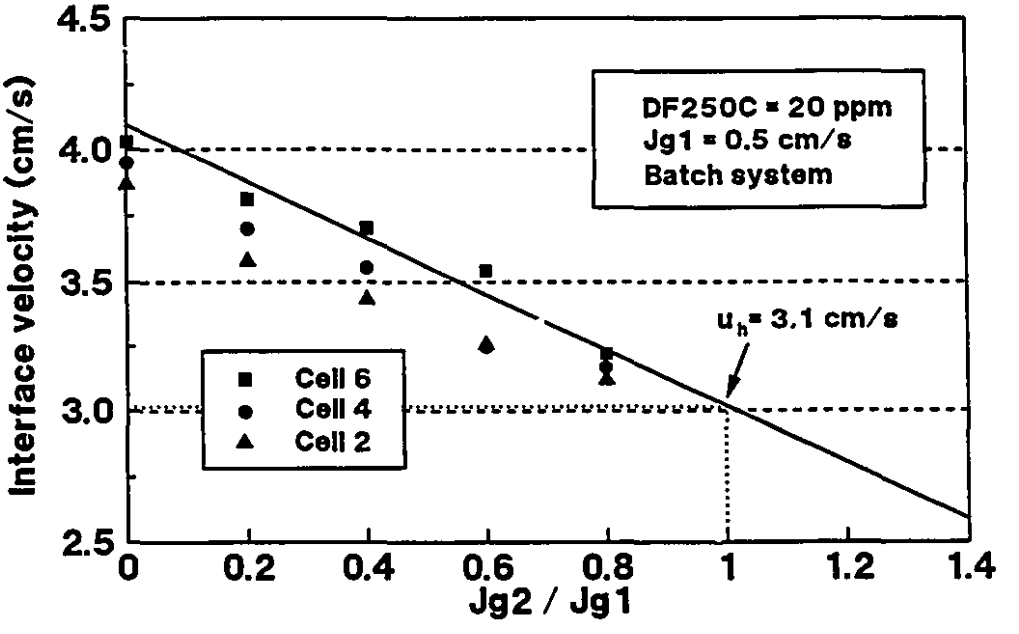

Figure 6.26 Measurement of u_{in} in Cells 6, 4 and 2 at J_{g1} = 0.50 cm/s with DF250C = 20 ppm. The u_h quoted is for Cell 6.

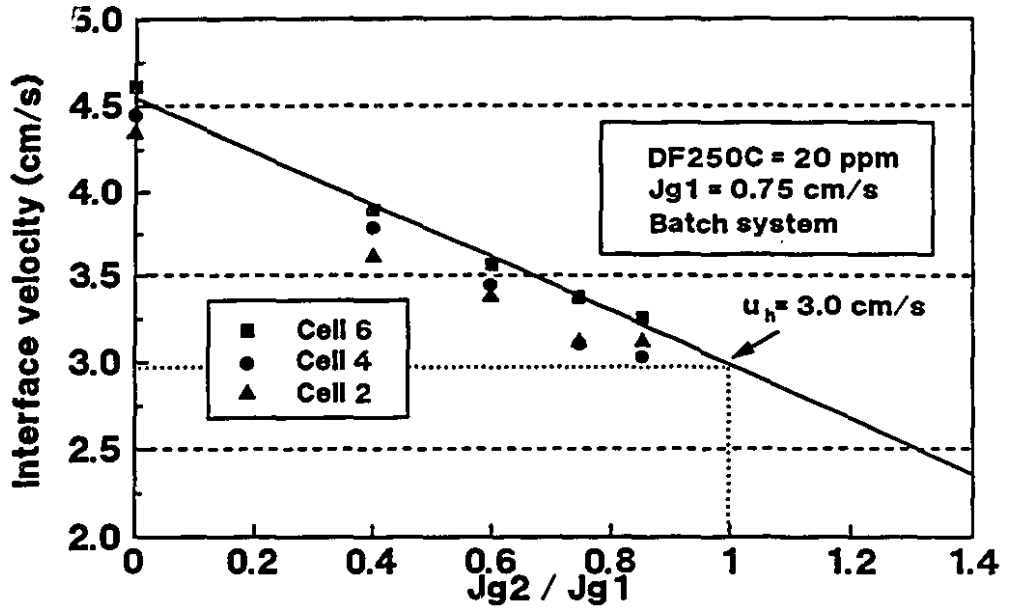

Figure 6.27 Measurement of u_{in} in Cells 6, 4 and 2 at J_{gl} = 0.75 cm/s with DF250C = 20 ppm. The u_h quoted is for Cell 6.

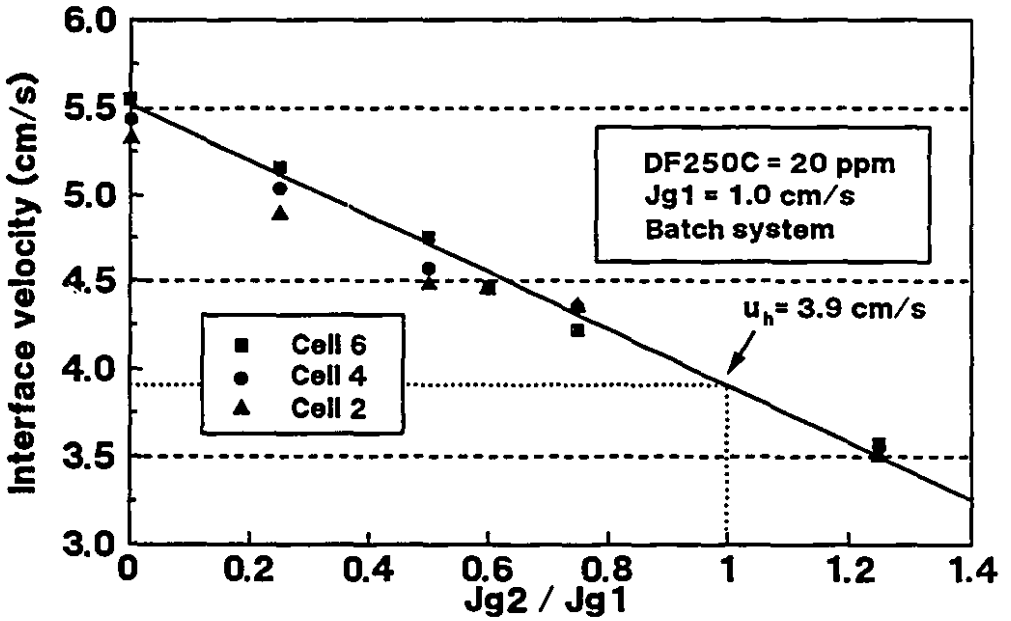

Figure 6.28 Measurement of u_{in} in Cells 6, 4 and 2 at J_{gl} = 1.0 cm/s with DF250C = 20 ppm. The u_h quoted is for Cell 6.

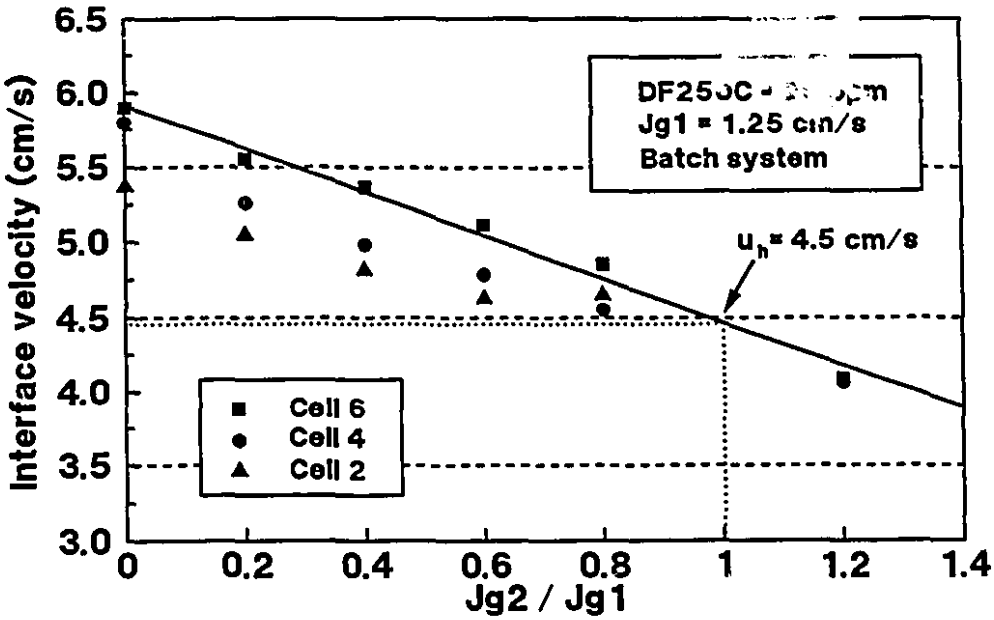

Figure 6.29 Measurement of u_{in} in Cells 6, 4 and 2 at J_{gl} = 1.25 cm/s with DF250C = 20 ppm. The u_h quoted is for Cell 6.

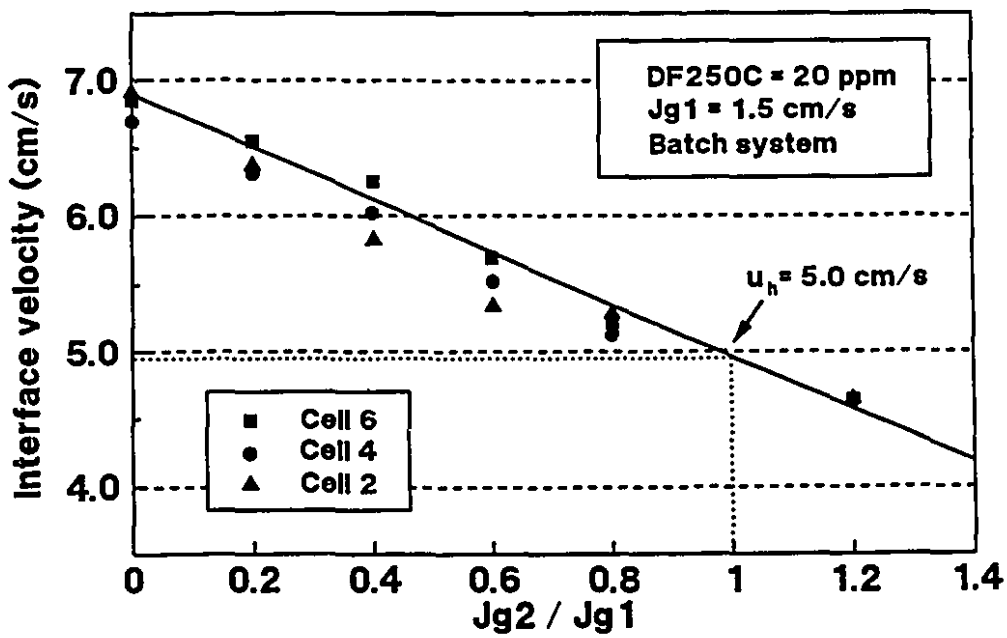

Figure 6.30 Measurement of u_{in} in Cells 6, 4 and 2 at J_{gl} = 1.5 cm/s with DF250C = 20 ppm. The u_h quoted is for Cell 6.

6.3 Experiments with DF250C = 20 ppm in Countercurrent System

The experiments presented in this section were carried out in a countercurrent system ($J_l > 0$) at room temperature with DF250C = 20 ppm. The countercurrent liquid flow was introduced at the top of the column through a distributor, which is the wash water inlet in column flotation. The flowrate of the underflow pump was equal to that of the wash water pump and both flowrates were kept constant during an experiment. The experimental procedure was the same as that described in Section 6.1.1.

6.3.1 u_0 in Cell 6 in Countercurrent System

For all experiments, J_{g2} was set to zero, i.e. J_{g2} / J_{gl} was equal to zero. In this particular case, the interface velocity, u_{in}, is equal to the buoyancy velocity, u_0. In Table 6.13, the ε_{gl} and u_0 are calculated by using Equations 5.9 and 5.10, respectively. Based on eight replicates for each experiment, the maximum relative standard deviation for u_0 was 2.66% and the maximum relative standard deviation for ε_g was 3.56%.

Table 6.13 Measurement of u_0 with DF250C = 20 ppm in countercurrent system

J_{gl}(cm/s)	J_l (cm/s)	ε_{gl} (%)	u_0 (cm/s)	u_g (cm/s)	$u_0+J_g-J_l$
0.50	0.40	7.59	1.9	6.6	2.0
0.50	0.80	8.43	2.2	5.9	1.9
0.50	1.20	9.63	1.9	5.2	1.2
0.75	0.40	13.22	2.3	5.7	2.7
0.75	0.80	14.39	2.1	5.2	2.0
0.75	1.20	14.54	1.8	5.2	1.4
1.00	0.40	18.94	2.2	5.3	2.8
1.00	0.80	19.15	2.2	5.2	2.4
1.00	1.20	23.94	1.7	4.2	1.5

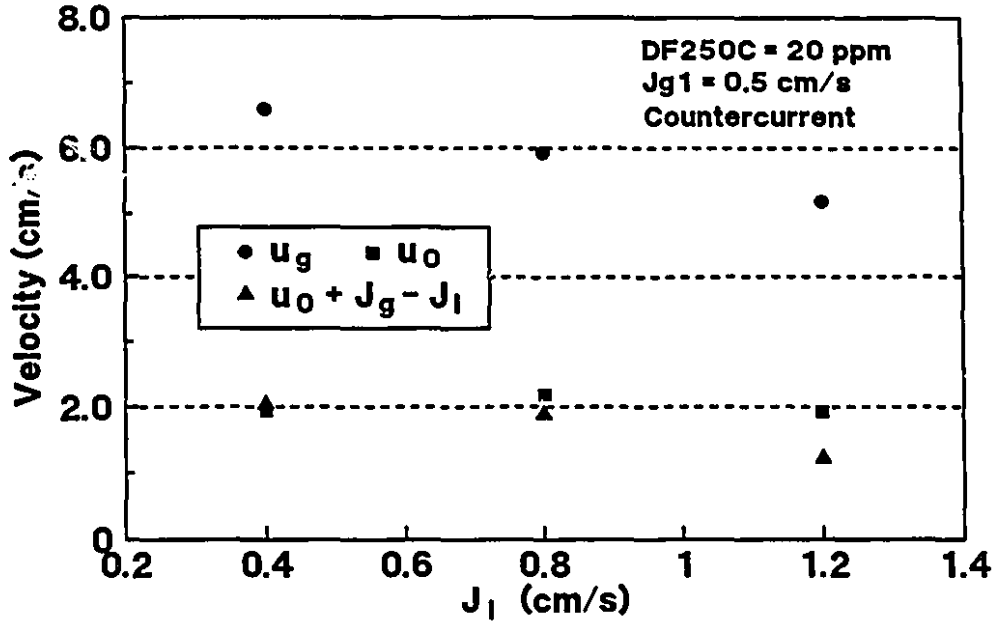

Figure 6.31 u_g, u_o and $u_o+J_g-J_l$ at J_{gl} = 0.5 cm/s with DF250C = 20 ppm.

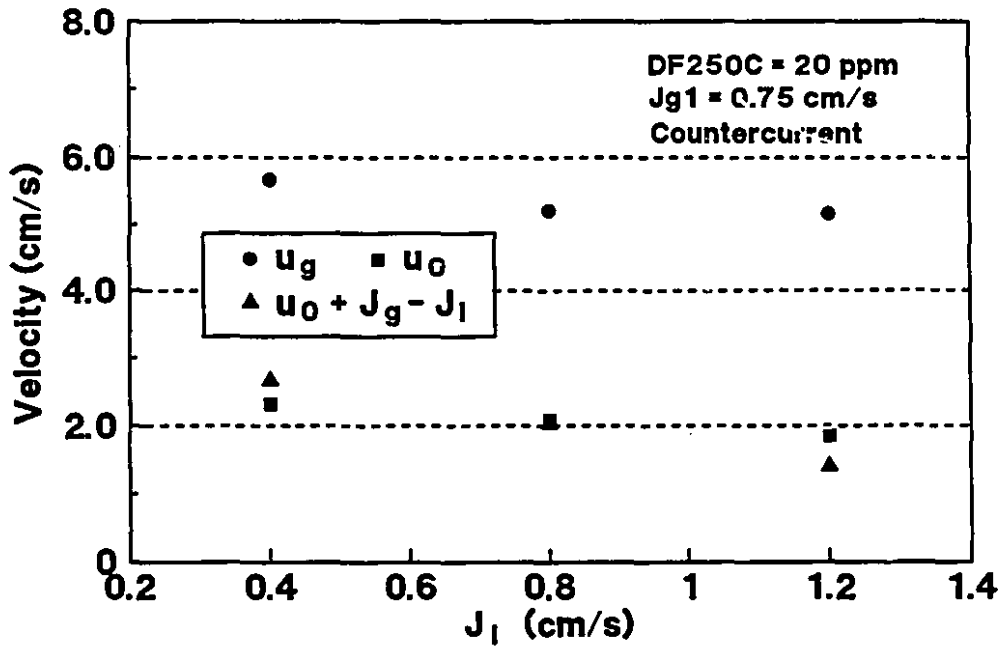

Figure 6.32 u_g, u_o and $u_o+J_g-J_l$ at J_{gl} = 0.75 cm/s with DF250C = 20 ppm.

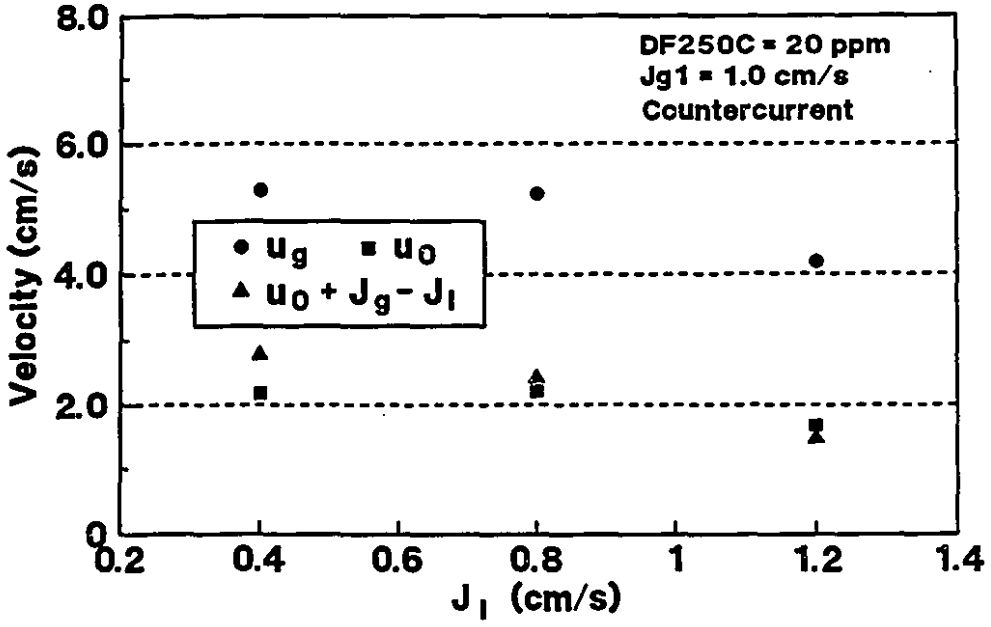

Figure 6.33 u_g, u_0 and $u_0+J_g-J_l$ at J_{gl} = 1.0 cm/s with DF250C = 20 ppm.

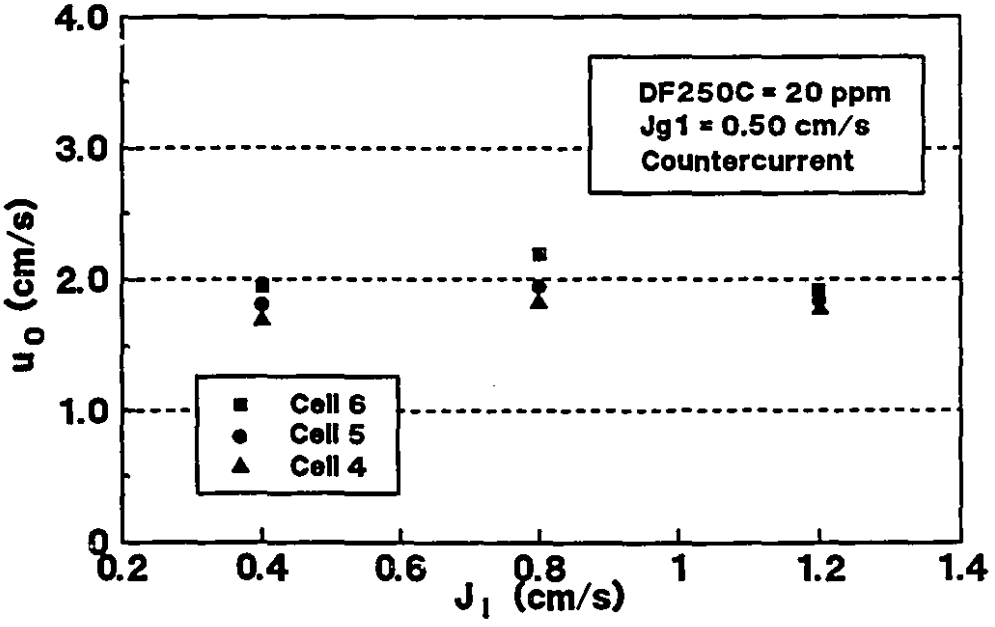

Figure 6.34 Measurement of u_0 in Cells 6, 5 and 4 at J_{gl} = 0.5 cm/s with DF250C = 20 ppm.

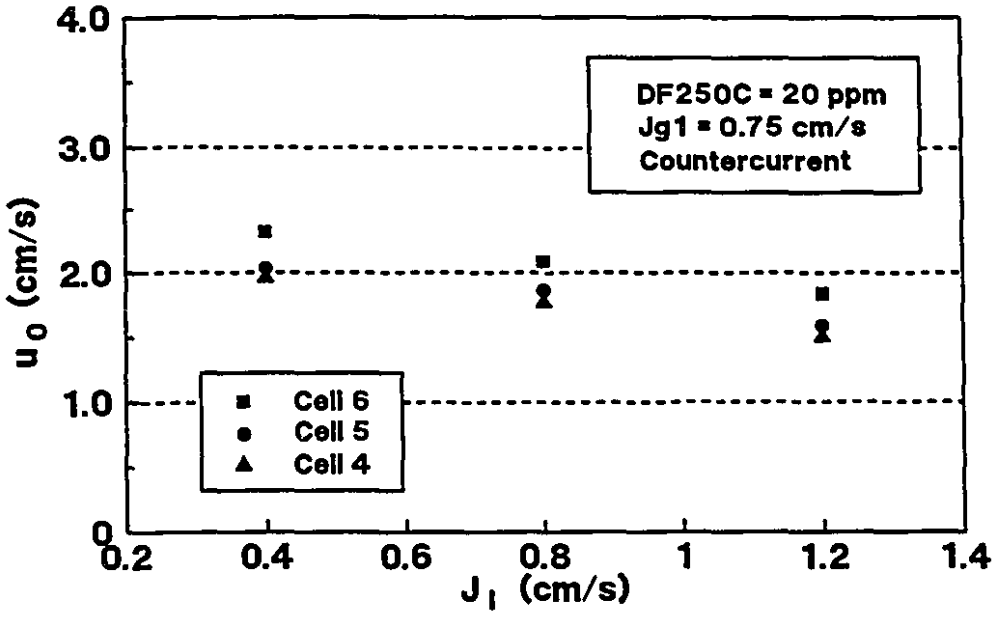

Figure 6.35 Measurement of u_0 in Cells 6, 5 and 4 at J_{gl} = 0.75 cm/s with DF250C = 20 ppm.

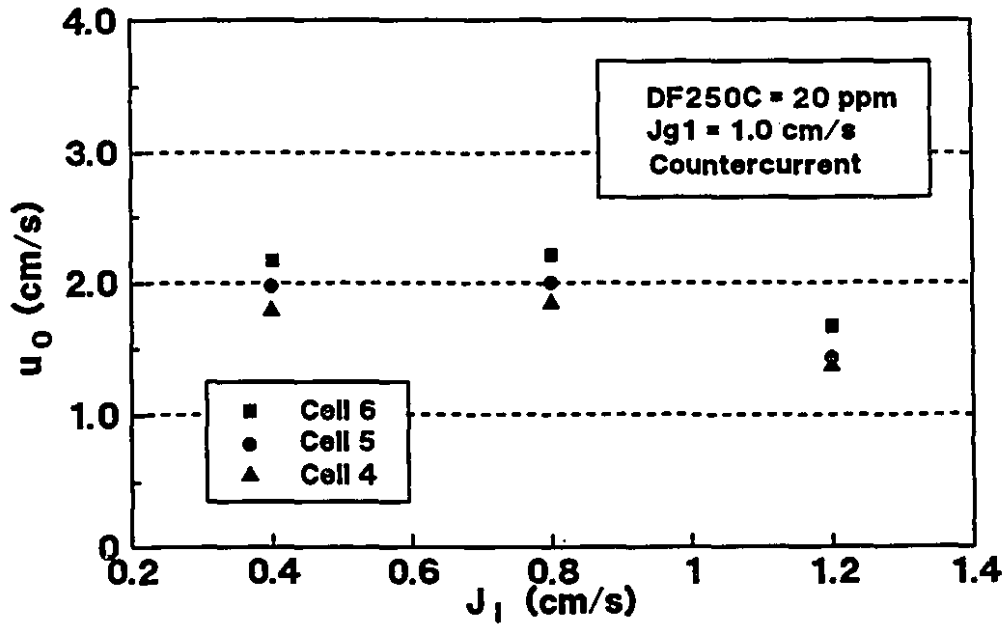

Figure 6.36 Measurement of u_0 in Cells 6, 5 and 4 at J_{gl} = 1.0 cm/s with DF250C = 20 ppm.

Figures 6.31 - 6.33 illustrate u_g, u_0 and $u_0+J_g-J_l$ at J_{gl} = 0.5, 0.75 and 1.0 cm/s, respectively. By Nicklin's derivation, u_g should be equal to $u_0+J_g-J_l$. However, a large difference between u_g and $u_0+J_g-J_l$ is evident in the Figures.

6.3.2 Axial Profile of u_0

Figures 6.34, 6.35 and 6.36 illustrate u_0 measured in Cells 6, 5 and 4 at various J_l for J_{gl} = 0.5, 0.75 and 1.0 cm/s, respectively. Cells 3, 2 and 1 were not include in the analysis because these cells did not remain full and the water addition caused a variation in conductance in these cells.

6.3.3 Experiments with a step change of J_g

In the countercurrent system, the distribution of the downward liquid velocity over the cross section of the column was probably not homogeneous. This, in turn, caused liquid circulation to develop and the interface became unstable.

Figure 6.37 illustrates an experiment at J_{gl} = 0.75 cm/s, J_{g2} = 0.5 cm/s and J_l = 0.4 cm/s with DF250C = 20 ppm. In the experiment, the attempt to obtain u_{in} failed due to the unstable interface between the upper bubble swarm and lower bubble swarm.

6.4 Experiments with DF1263 in Batch System

The experiments to measure u_{in} failed with frother DF1263 even in batch operation. The procedure of the experiment was the same as that described in Section 6.1. Figure 6.38 illustrates a typical result under batch operation at J_{gl} = 1.25 cm/s stepped to J_{g2} = 0 cm/s with DF1263 = 20 ppm. In the experiment, the gas flow was terminated at 10 s but the step change in gas flow did not form an interface in this case. After termination of the gas flow, a white, milk-like colour reduced gradually in the whole column. Finally, around 80 s, the column was clear. At no time, unlike the case with batch air - water only or batch air - water - Dowfroth 250C, did an interface form.

In Figure 6.38, the plot of the resistance versus time in Cell 6 illustrates that the gas holdup decreased gradually. The R_l represents the resistance of the mixture of air bubbles and water and R_0 represents the resistance of water. In the experiment, R_l was to 10800 Ω and R_2 was 7450 Ω. Substituting R_l and R_2 into Equation 5.9, the gas holdup, ε_g, is equal to 23.1%. Table 6.7 in

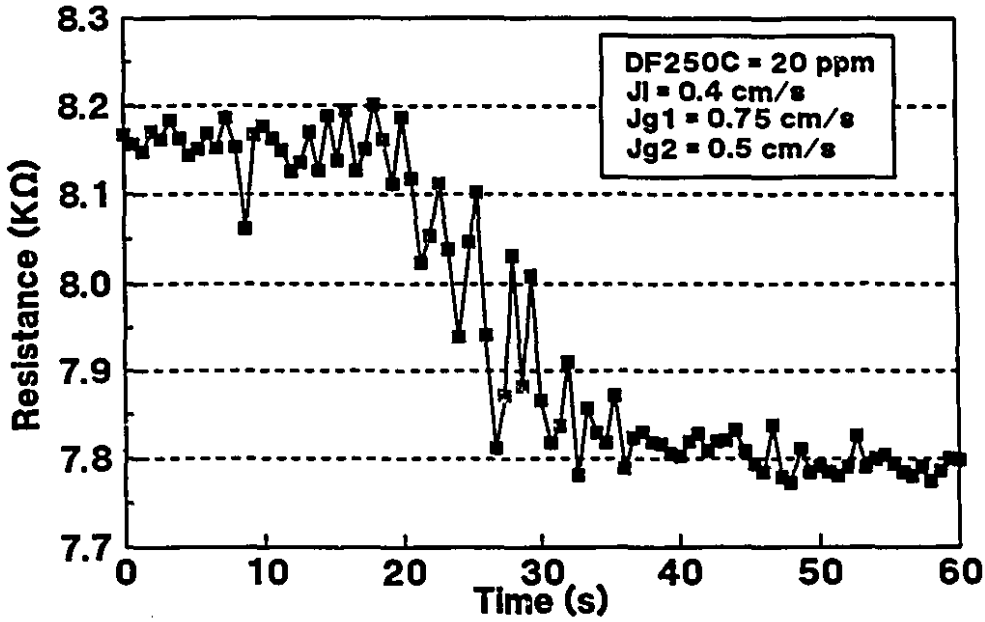

Figure 6.37 Resistance versus time in Cell 6 for a step change of J_g at J_l = 0.4 cm/s with DF250C = 20 ppm.

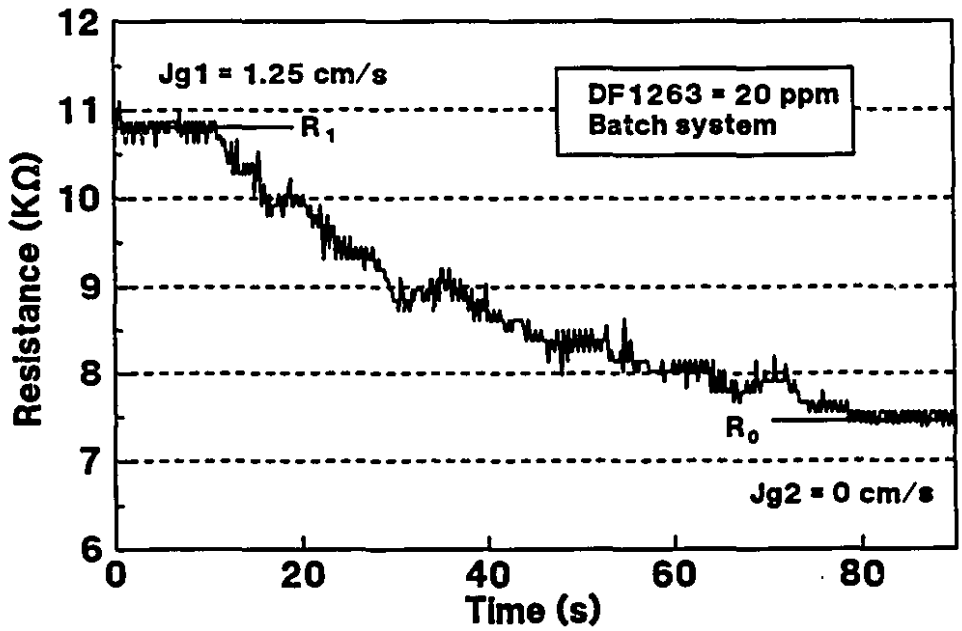

Figure 6.38 Resistance versus time in Cell 6 with DF1263 = 20 ppm.

Section 6.2.1 showed the ε_g was 11.7% at J_g = 1.25 cm/s with DF250C = 20 ppm. It can be concluded, therefore, that the frother DF1263 generates finer bubbles than DF250C.

Since bubble size and bubble size distribution vary with the type and concentration of the frother, in this case, it seems that the size and distribution of bubbles makes the formation of the interface impossible. It would appear that a wide size distribution of bubbles finer than 1 mm, where a wide range in bubble velocity results (Clift et al.,1978), causes the lack of interface formation.

CHAPTER 7

DISCUSSION

7.1 Axial Profiles in Columns

7.1.1 Axial Profile of Gas Holdup

An axial profile of gas holdup exists in the collection zone of a flotation column because of the hydrostatic pressure drop (Finch et al., 1994; Uribe-Salas et al., 1992). (A profile also exists in the froth zone but this is due to coalescence and water drainage rather than hydrostatic pressure changes (Yianatos et al., 1986).)

Theoretical examination suggests that the gas holdup will decrease with depth (Finch and Dobby, 1990a). Uribe-Salas et al. (1992) verified this experimentally from pressure gradient measurements in the air - water - frother system. The experimental results showed that the gas holdup decreased by about 50% over a depth of 10 m in the collection zone of a 0.91 m X 13.5 m column with 20 ppm of Dowfroth 250C.

To predict the gas holdup profile, three models have been presented (Finch et al., 1994). The first model assumes that the gas holdup is proportional to bubble volume, which is inversely proportional to pressure

$$\varepsilon_g = \varepsilon_{go} \frac{P_o}{P_{loc}} \tag{7.1}$$

where ε_{go} and P_o are the gas holdup and pressure on the top of the column, respectively, and P_{loc} is the local pressure where ε_g is measured. The second model is the drift flux approach which has the approximate analytical form (Finch and Dobby, 1990a)

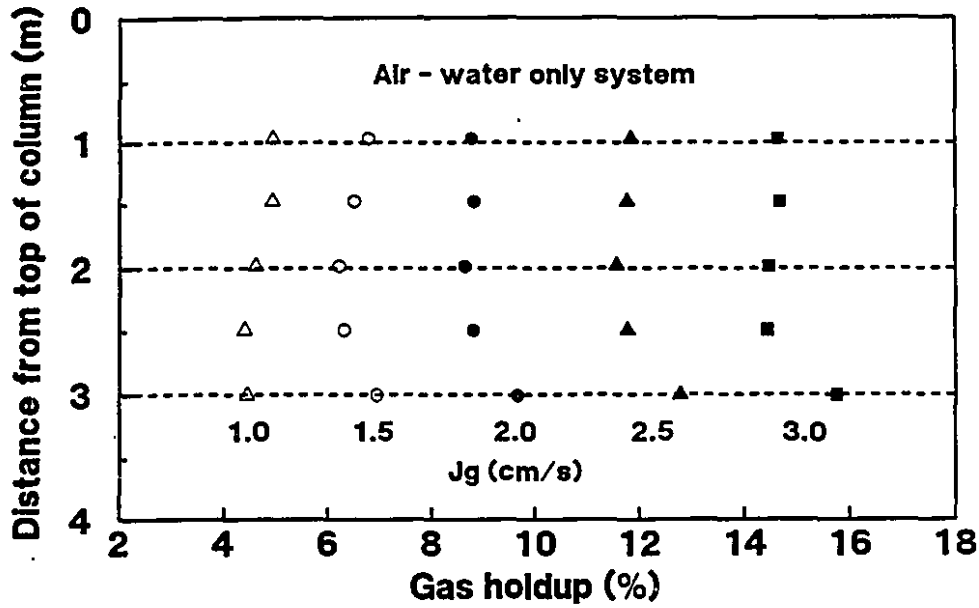

Figure 7.1 Axial profile of ε_g in air - water only system.

$$\varepsilon_g (1 - \varepsilon_g) = \varepsilon_{go} (1 - \varepsilon_{go}) (\frac{P_o}{P_{loc}})^{1/3} \qquad (7.2)$$

And, the third model is one of two models from Zhou and Egiebor (1993)

$$\varepsilon_g = \varepsilon_{go} \exp [\frac{0.455 (-H) \beta g}{u_{go}^2}] \qquad (7.3)$$

where H is the distance from the top of the column in meters, u_{go} is J_{go}/ε_{go} in m/s which is assumed constant along the collection zone and β is dimensionless and obtained by data fitting. Here β is linked to a reduced bubble buoyancy due to adsorbed frother. For the gas - water - frother system, the third model gave the best fitting to the data (Finch et al., 1994).

Table 7.1 gives the mean of the gas holdup measured in each cell in the air - water only system. For example, the ε_g of 4.45% in Cell 6 at J_{gl} = 1.0 cm/s, is the mean of the ε_{gl}'s in Cell 6 reported in Tables 1 - 10 of Appendix 3. Figure 7.1 illustrates the axial profile of gas holdup. The differences of ε_g among Cells 5 - 2 are not significant and ε_g in Cell 6 is slightly larger than that in Cells 5 - 2. Equations 7.1, 7.2 and 7.3 were used to examine the data in Table 7.1; however, none was applicable.

Table 7.1 Profile of ε_g at various J_{gl} in air - water only system

J_{gl} (cm/s)	ε_g (%)				
	Cell 6	Cell 5	Cell 4	Cell 3	Cell 2
1.0	4.45	4.41	4.62	4.93	4.95
1.5	6.94	6.32	6.22	6.52	6.79
2.0	9.66	8.82	8.65	8.82	8.78
2.5	12.79	11.79	11.57	11.76	11.85
3.0	15.76	14.45	14.47	14.68	14.65

7.1.2 $J_{g,loc}$ and P_{loc} in Air - Water Only System

The J_g is defined as the superficial gas velocity under a standard atmosphere. In this study, the equipment used for the gas rate measurement was a thermal-type gas mass flowmeter. The indicated gas flowrate, which is independent of gas density, viscosity and pressure, was calibrated under a standard atmosphere. The length of the column is 391 cm and the effect of the pressure has to be taken into account when gas rate is measured inside the column.

Assuming the temperature in the column is constant, the local superficial gas velocity, $J_{g,loc}$, is given by

$$J_{g,loc} = J_g \frac{P_o}{P_{loc}} \qquad (7.4)$$

If ε_g throughout the column is constant, P_{loc}, at a depth h below the top of the column, is given by

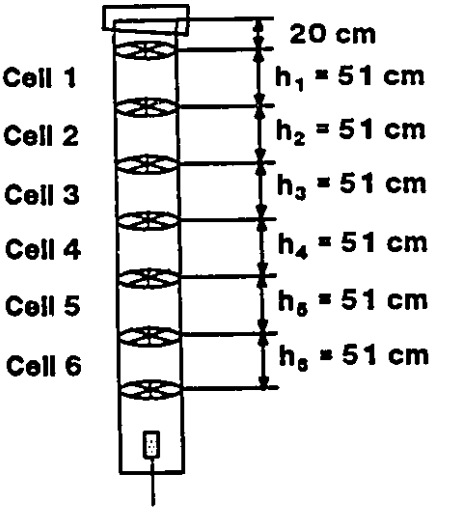

Figure 7.2 Diagram of Cells 6 - 1 in column

$$P_{loc} = P_o + [\ \rho_l (1 - \varepsilon_g)\, gh + \rho_g \varepsilon_g\, gh\ ] \tag{7.5}$$

Because $\rho_g << \rho_l$, the term including ρ_g can be ignored, yielding

$$P_{loc} = P_o + \rho_l (1 - \varepsilon_g)\, gh \tag{7.6}$$

Since an axial profile of gas holdup exists in the column, $P_{loc,i}$, the local pressure at the centre of Cell i, is actually given by (in cgs system)

$$P_{loc,2} = P_o + \rho_l g [(20 + h_1) (1 - \varepsilon_{g,1}) + 0.5\, h_2 (1 - \varepsilon_{g,2})] \tag{7.7}$$

$$P_{loc,3} = P_o + \rho_l g [(20 + h_1) (1 - \varepsilon_{g,1}) + h_2 (1 - \varepsilon_{g,2}) + 0.5\, h_3 (1 - \varepsilon_{g,3})] \tag{7.8}$$

$$P_{loc,4} = P_o + \rho_l g [(20 + h_1) (1 - \varepsilon_{g,1}) + h_2 (1 - \varepsilon_{g,2}) + h_3 (1 - \varepsilon_{g,3}) + 0.5\, h_4 (1 - \varepsilon_{g,4})] \tag{7.9}$$

$$P_{loc,5} = P_o + \rho_l g [(20 + h_1) (1 - \varepsilon_{g,1}) + h_2 (1 - \varepsilon_{g,2}) + h_3 (1 - \varepsilon_{g,3}) + h_4 (1 - \varepsilon_{g,4}) + 0.5\, h_5 (1 - \varepsilon_{g,5})] \tag{7.10}$$

$$P_{loc,6} = P_o + \rho_l g [(20 + h_1) (1 - \varepsilon_{g,1}) + h_2 (1 - \varepsilon_{g,2}) + h_3 (1 - \varepsilon_{g,3}) + h_4 (1 - \varepsilon_{g,4}) + h_5 (1 - \varepsilon_{g,5}) + 0.5\, h_6 (1 - \varepsilon_{g,6})] \tag{7.11}$$

where h_i is the length of Cell i (Figure 7.2) and $\varepsilon_{g,i}$ is the gas holdup in Cell i.

Table 7.2 gives the ratio of $P_{loc,i}$ to P_o in Cells 6 - 2 in the air - water only system. It can be seen that $P_{loc,i} / P_o$ decreases slightly as J_{gl} increases in a given cell. The $J_g / J_{g,loc}$ in the cell can be calculated using the ratio of $P_{loc,i}$ to P_o. In the previous chapters, the analysis was based on the relationship between the velocity and J_{g2} / J_{gl}. It is necessary to examine the difference between J_{g2} / J_{gl} and $J_{g2,loc} / J_{gl,loc}$. From Table 7.2, $J_{g2,loc} / J_{gl,loc}$ is equal to 0.4953 in Cell 6 at $J_{g2} / J_{gl} = 0.5$ ($J_{gl} = 2.0$ and $J_{g2} = 1.0$ cm/s). For all ratios of J_{g2} to J_{gl} ($0 < J_{g2} / J_{gl} < 2$), the relative difference between J_{g2} / J_{gl} and $J_{g2,loc} / J_{gl,loc}$ is less than 2 %. Instead of $J_{g2,loc} / J_{gl,loc}$, therefore, J_{g2} / J_{gl} can be used for the analysis of the results with only a small loss in accuracy.

Table 7.2 $P_{loc,i}$ / P_o at various J_{gl} in air - water only system

J_{gl} (cm/s)	$P_{loc,i}$ / P_o				
	Cell 6	Cell 5	Cell 4	Cell 3	Cell 2
1.0	1.2766	1.2295	1.1824	1.1355	1.0886
1.5	1.2713	1.2253	1.1791	1.1329	1.0869
2.0	1.2647	1.2200	1.1750	1.1300	1.0851
2.5	1.2560	1.2128	1.1692	1.1257	1.0822
3.0	1.2478	1.2059	1.1638	1.1217	1.0796

7.1.3 $u_{g,loc}$ in Air - Water Only System

In the column, ε_g is measured as the local gas holdup and the average gas velocity, u_g, is given by

$$u_g = \frac{J_g}{\varepsilon_g} \tag{4.8}$$

In this equation, while ε_g is the local gas holdup, i.e. the gas holdup under P_{loc}, J_g is the superficial gas velocity under a standard atmosphere. The local average gas velocity, $u_{g,loc}$, is defined as

$$u_{g,loc} = \frac{J_{g,loc}}{\varepsilon_g} \tag{7.12}$$

Tables 7.3 and 7.4, respectively, give the u_g and $u_{g,loc}$ at various J_{gl} in the air - water only system. From Figures 7.3 and 7.4, it can be seen that there is a large difference between u_g and $u_{g,loc}$. In fact, the $u_{g,loc}$ represents the real condition in the column.

7.1.4 u_0 and Nicklin's Assumption in Air - Water Only System

Figure 7.5 illustrates the profile of u_0 in Cells 6 - 2 for the air - water only system. It can be seen that the buoyancy velocity, u_0, is a linear function of J_g given by

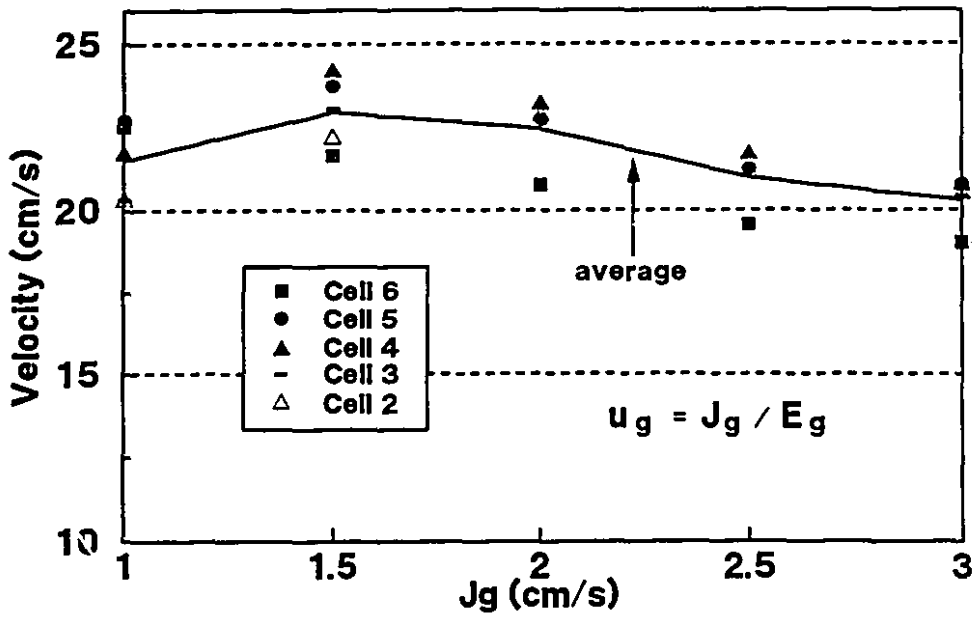

Figure 7.3 Average gas velocity, u_g, in Cells 6 - 2 in air - water only system.

Table 7.3 Average gas velocity, u_g, at various J_{gl} in air - water only system

J_{gl} (cm/s)	u_g (cm/s)					Average
	Cell 6	Cell 5	Cell 4	Cell 3	Cell 2	
1.0	22.49	22.68	21.65	20.29	20.27	21.5
1.5	21.62	23.73	24.14	23.03	22.13	22.9
2.0	20.73	22.70	23.16	22.70	22.81	22.4
2.5	19.56	21.21	21.63	21.27	21.11	21.0
3.0	19.04	20.77	20.73	20.44	20.48	20.3

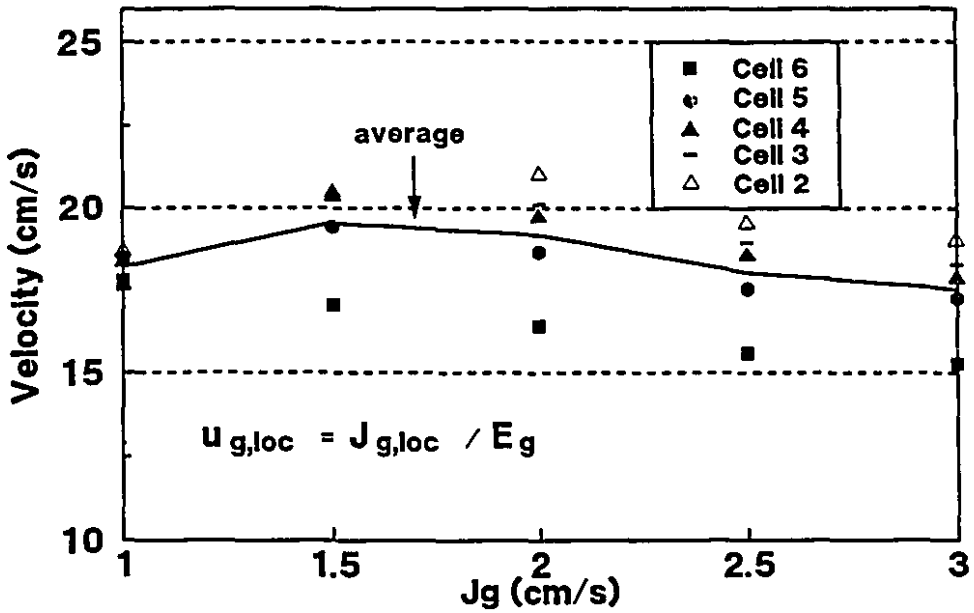

Figure 7.4 Local average gas velocity, $u_{g,loc}$, in Cells 6 - 2 in air - water only system.

Table 7.4 Local average gas velocity, $u_{g,loc}$, at various J_{gl} in air - water only system

J_{gl} (cm/s)	$u_{g,loc}$ (cm/s)					Average
	Cell 6	Cell 5	Cell 4	Cell 3	Cell 2	
1.0	17.62	18.44	18.31	17.87	18.62	18.2
1.5	17.01	19.37	20.47	20.33	20.36	19.5
2.0	16.39	18.61	19.71	20.09	21.02	19.2
2.5	15.57	17.49	18.50	18.90	19.50	18.0
3.0	15.26	17.22	17.81	18.23	18.97	17.5

$$u_0 = 23.4 - 2.13\,J_g \tag{7.13}$$

where units are cm/s.

Nicklin (1962) related u_g with u_0 and J_g in a batch system

$$u_g = u_0 + J_g \tag{4.61}$$

For the local values, we should have

$$u_{g,loc} = u_0 + J_{g,loc} \tag{7.14}$$

In Figure 7.6, the u_g, $u_{g,loc}$, u_0+J_g and $u_0+J_{g,loc}$ are the averages in Cells 6 - 2. From Figure 7.6, it can be seen that u_g approximates u_0+J_g, but $u_{g,loc}$ is not equal to $u_0+J_{g,loc}$. This suggests that Nicklin's derivation can be apparently correct, but only under restrictive conditions, i.e. u_g and J_g must be measured at atmospheric pressure. For comparison, u_h is included in Figure 7.6. Comparing $u_0+J_{g,loc}$ or u_0+J_g with u_h, we see the same tendency: they linearly decrease as J_g increases.

7.1.5 Axial Profile of ε_g in Air - Water - Frother System

Tables 7.5 and 7.6 give the ε_g in Cells 6 - 2 and Figures 7.7 and 7.8 illustrate the axial profiles of ε_g with DF250C = 10 ppm and 20 ppm under batch operation, respectively.

From the models used to predict the gas holdup profile in the column (Equations 7.1, 7.2 and 7.3), it can be seen that the gas holdup should increase from the bottom to the top of the column. However, in both of the air - water only system and the air - water - frother system, there exists a high gas holdup zone near the sparger (Figures 7.1, 7.7 and 7.8). This high gas holdup region was also reported in a 0.91 m X 13.5 m column with DF250C = 20 ppm (Uribe-Salas et al., 1992). Due to this high gas holdup region, the data shown in Tables 7.5 and 7.6 are not suitable for fitting by the three models.

The increment of ε_g in the high gas holdup region should be a function of the superficial gas velocity, the bubble sizes and the column diameter. The possible impact of this high gas holdup region on column flotation could be studied in the future.

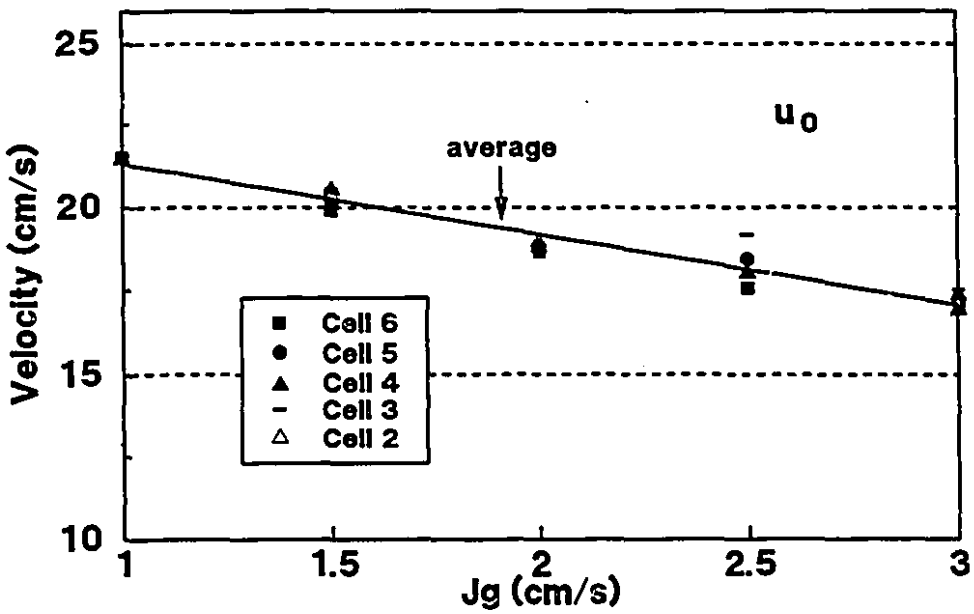

Figure 7.5 Variation of u_0 with J_g in air - water only system.

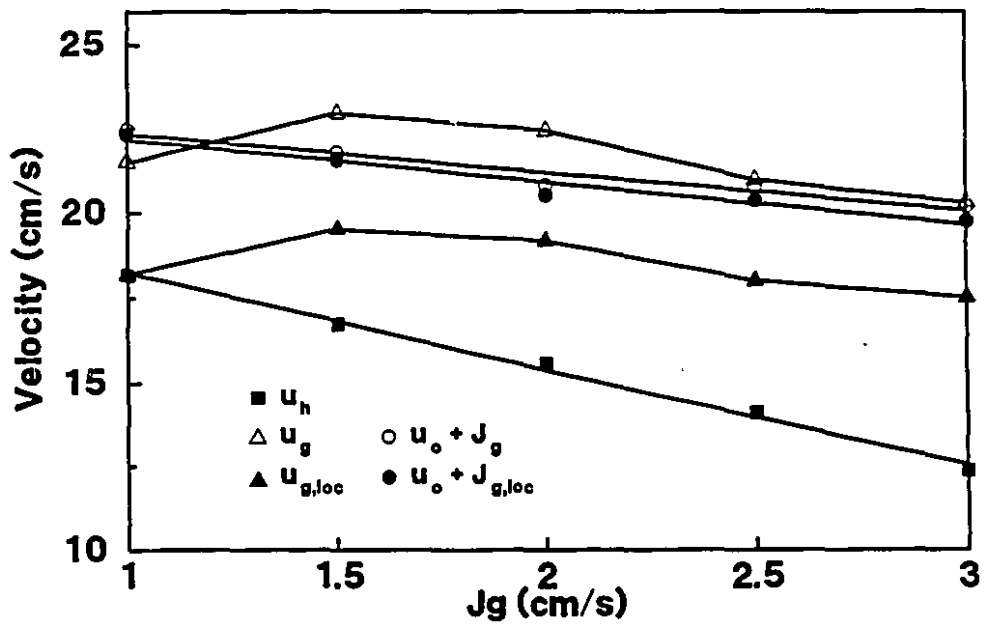

Figure 7.6 Comparison among u_g, $u_{g,loc}$, u_0+J_g and $u_0+J_{g,loc}$.

7.1.6 $u_{g,loc}$ in Air - Water - Frother System

The pressure in the column was taken into account to calculate the local average gas velocity, $u_{g,loc}$, in the air - water - frother system. Following the method used in Section 7.1.3, $u_{g,loc}$ and u_g, shown in Figures 7.9 and 7.10, are the averages for Cells 6 - 2.

In Figures 7.9 and 7.10, the $u_{g,loc}$ is larger than u_h in the air - water - frother system. Comparing with Figure 7.6, it can be seen that the relative difference between u_h and $u_{g,loc}$ in the presence of frothers is greater than that in the absence of frother. The reason appears to be bubble circulation in the air - water - frother system, which will be discussed later. By considering the bubble swarm velocity in a three-dimensional domain, instead of a one-dimensional domain, the difference between u_h and $u_{g,loc}$ is explained in the next section.

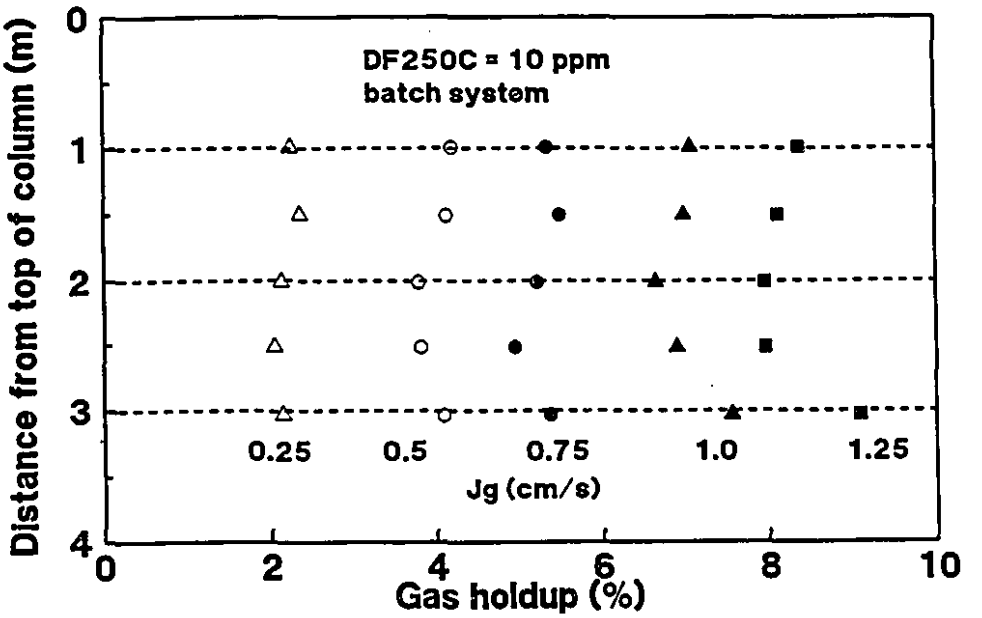

Figure 7.7 Axial profile of ε_g with DF250C = 10 ppm under batch operation.

Table 7.5 ε_g at various J_{gl} with DF250C = 10 ppm under batch operation

J_{gl} (cm/s)	ε_g (%)				
	Cell 6	Cell 5	Cell 4	Cell 3	Cell 2
0.25	2.14	2.04	2.13	2.36	2.24
0.50	4.09	3.80	3.78	4.13	4.19
0.75	5.37	4.95	5.22	5.50	5.34
1.00	7.56	6.90	6.65	7.00	7.08
1.25	9.09	7.96	7.96	8.13	8.38

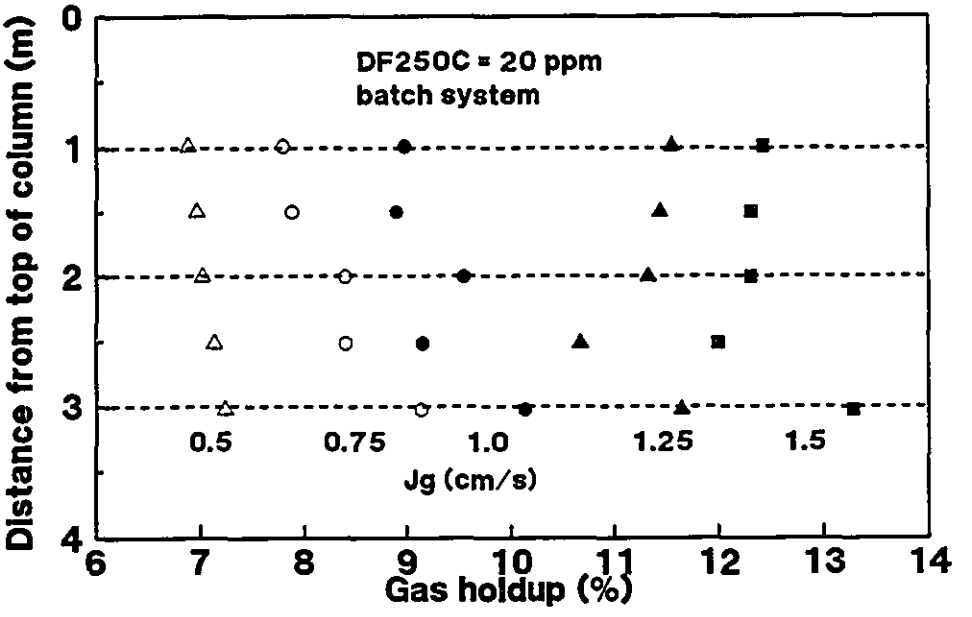

Figure 7.8 Axial profile of ε_g with DF250C = 20 ppm under batch operation.

Table 7.6 ε_g at various J_{gl} with DF250C = 20 ppm under batch operation

J_{gl} (cm/s)	ε_g (%)				
	Cell 6	Cell 5	Cell 4	Cell 3	Cell 2
0.50	7.24	7.14	7.02	6.97	6.88
0.75	9.14	8.41	8.40	7.89	7.80
1.00	10.14	9.16	9.55	8.90	8.98
1.25	11.65	10.68	11.33	11.41	11.50
1.50	13.29	12.00	12.31	12.32	12.42

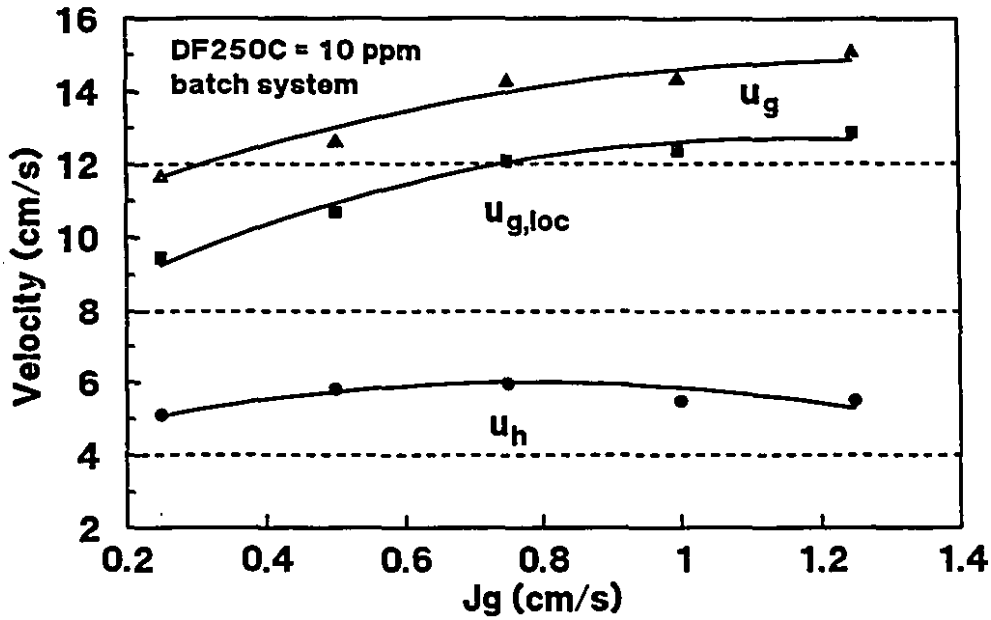

Figure 7.9 Comparison among u_g, $u_{g,loc}$ and u_h with DF250C = 10 ppm under batch operation.

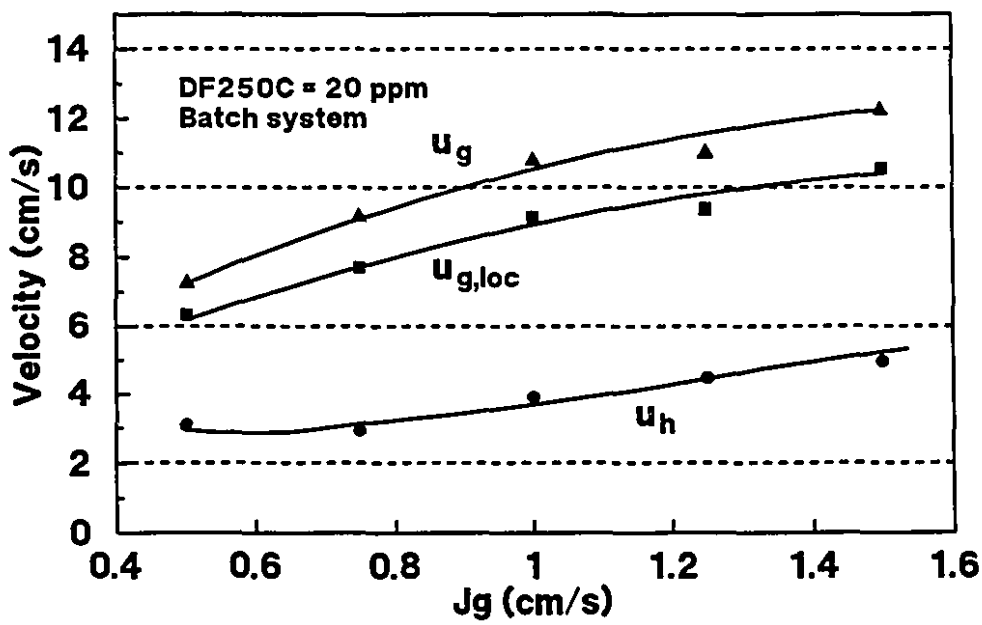

Figure 7.10 Comparison among u_g, $u_{g,loc}$ and u_h with DF250C = 20 ppm under batch operation.

7.2 u_h - Bubble Swarm Velocity in Columns

7.2.1 Nicklin's Expression

In two phase gas - liquid flow, the average gas velocity, u_g, is used as a measure of the velocity of the gas phase. Most researchers have defined u_g as the bubble swarm velocity in a column.

Nicklin (1962) obtained an expression equating the bubble rising velocity in a bubble swarm, u_B, to u_g

$$u_B = \frac{Q_g}{A_c \varepsilon_g} = u_g \tag{4.56}$$

with the following assumptions: the bubbles all have the same diameter, are spaced uniformly and rise at the same velocity, u_B. Because every bubble has the same velocity, the bubble swarm velocity should be equal to u_g.

In this study, u_g is corrected to $u_{g,loc}$ to obtain the real average gas velocity under the local pressure conditions at a given vertical position in the column. In Section 7.1, Equation 4.56 was rewritten as

$$u_{g,loc} = \frac{J_{g,loc}}{\varepsilon_g} \tag{7.12}$$

In fact, Nicklin simplified the bubble swarm velocity from a three-dimensional velocity to a one-dimensional velocity. Here the $u_{g,loc}$ is equal to the one-dimensional bubble swarm velocity. It will be argued here that the three-dimensional bubble swarm velocity is u_h. In Section 7.1, the difference between u_h and $u_{g,loc}$ was clearly evident.

It can be seen that Nicklin's expression does not contain some important characteristics of a real system. First, there are interactions with the walls and between the bubbles and liquid. Second, there is a bubble size distribution. Third, there is a nonuniform bubble concentration over the cross section of the column. All these characteristics will cause more complex motion of the phases than allowed for in Nicklin's model.

It is difficult to give a complete theoretical analysis for bubble swarm velocity in a three-dimensional domain. If the bubble swarm velocity can be simplified from the three-dimensional domain to the two-dimensional domain, we can define the u_h as the average velocity of the bubbles over the cross section of the column, and may obtain an expression for u_h.

7.2.2 Two-dimensional Average Velocity over Cross Section of Column

The one-dimensional theory is widely used in the study of bubble columns. The one-dimensional theory, however, does not account for the variation in the concentration and velocity of the two (or more) phases across the cross section of the column. The average value of a quantity X over the cross-sectional area is defined by

$$\langle X \rangle = \frac{\int_{A_c} X \, dA_c}{A_c} \tag{7.15}$$

In practice, the $u_{g,loc}$ is given by (Wallis, 1969)

$$u_{g,loc} = \frac{\langle J_{g,loc} \rangle}{\langle \varepsilon_g \rangle} \tag{7.16}$$

where $\langle J_{g,loc} \rangle$ is the overall average given by

$$\langle J_{g,loc} \rangle = \frac{Q_{g,loc}}{A_c} \tag{7.17}$$

where $Q_{g,loc}$ is the local volume gas flowrate under the local pressure condition.

The overall gas holdup ε_g without $\langle\ \rangle$ has been used to represent the average gas holdup, $\langle \varepsilon_g \rangle$, over the cross section of the column because ε_g is a convenient value that can be measured experimentally. There are three classical methods used for the evaluation of the gas holdup: the isolation method, pressure method and conductivity method (Fan, 1989). All three measure physical values related to the ratio of the volume occupied by gas to the volume occupied by the mixture of the liquid and gas. The ε_g measured by these three methods agree with the definition of $\langle \varepsilon_g \rangle$ physically and mathematically.

In the two-dimensional domain, u_h is the average of the bubble velocities over the cross

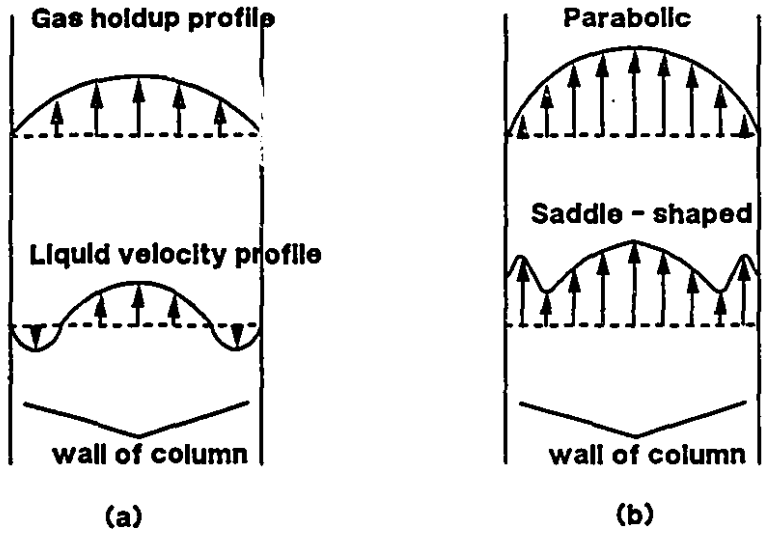

Figure 7.11 Profiles of gas holdup and liquid circulation in columns: (a) gulf-stream circulation; (b) parabolic radial gas holdup profile and saddle-shaped radial gas holdup profile.

section of the column given by (Wallis, 1969)

$$u_h = \langle u_{g,loc} \rangle = \langle \frac{J_{g,loc}}{\varepsilon_g} \rangle \tag{7.18}$$

It can be seen that the u_h is not equal to $u_{g,loc}$ since u_h is related to the profiles of the fluid velocity and gas holdup. To solve for u_h, knowledge of the gas holdup profiles and liquid velocity profiles over the cross section of the column is necessary.

7.2.3 Radial Gas Holdup Profile and Liquid Circulation Velocity

For application of the one-dimensional bubbly flow model, uniform distributions over the cross section for the gas and liquid have to be assumed. However, non-uniform gas holdups and liquid circulation have been reported in columns (Nassos and Bankoff, 1967; Freedman and Davidson, 1969; Hills, 1974; Lockett and Kirkpatrick, 1975; Xu and Finch, 1992). Because the density differences caused by the non-uniform gas holdup provide the driving force for liquid circulation, non-uniform gas holdup and liquid circulation are intimately related.

Figure 7.11 (a) illustrates the 'gulf-stream' circulation, which is the most common type of

the liquid circulation in a bubble column, i.e. in absence of frothers, and the associated radial gas holdup profile (Freedman and Davidson, 1969; Clark et al., 1987).

The shapes of radial gas holdup profiles can be complex and depend on the bubble generation system, gas rate, frother concentration and column size. Two axisymmetrical profiles are well-known, the parabolic or radial power law distribution and the saddle-shaped distribution (Figure 7.11 (b)). The parabolic radial gas holdup profiles are easily described mathematically, but the saddle-shaped profiles are more difficult. Therefore, most liquid circulation models are related to parabolic radial gas holdup profiles.

(i) Parabolic gas holdup profile $\varepsilon_g(\phi)$

The parabolic radial gas holdup profile is given by

$$\varepsilon_g(\phi) = (\varepsilon_{gc} - \varepsilon_{gw}) (1 - \phi^n) \tag{7.19}$$

where $\phi = r/R$, the dimensionless radial position (r is the radial distance from the centre to a point and R is the radius of the column), ε_{gc} and ε_{gw} are the gas holdup at the centre and the wall of the column, respectively, and n is a constant to describe the power law curve. The usual assumption is that $\varepsilon_{gw} = 0$ and $n > 1$. The average gas holdup over the cross section of the column, i.e. the measured gas holdup, is given by

$$\overline{\varepsilon_g} = \varepsilon_g = \frac{1}{\pi R^2} \int_0^R \varepsilon_{gc} [1 - (\frac{r}{R})^n] 2\pi r dr = \frac{n}{n+2} \varepsilon_{gc} \tag{7.20}$$

(ii) Liquid circulation velocity $u_l(\phi)$

The following model was developed by Ueyama and Miyauchi (1979) for a bubble column in the air - water only system. Under steady state conditions, the equation of motion for a liquid is given by

$$-\frac{1}{r}\frac{d}{dr}(r\tau) = \frac{dp}{dz} + (1 - \varepsilon_g) \rho_l g \tag{7.21}$$

where dp/dz is the axial pressure drop and τ is the shear stress given by

$$\tau = -(\nu_M + \nu_t) \rho_l \frac{d}{dr} u_l(\phi) \tag{7.22}$$

where $u_l(\phi)$ is the liquid circulation velocity, ν_M is the molecular viscosity, and ν_t is the turbulent

kinematic viscosity. Compared with ν_t, ν_M can be neglected (Ueyama and Miyauchi, 1979). Two assumptions are made to solve the above equations: ν_t is constant in the turbulent region, and the radial distribution of gas holdup can be approximated by Equation 7.19. The solution for $u_l(\phi)$ is given by

$$u_l(\phi) = [\, A\,(\,1 - \phi^2\,) - 1\,]\,|u_{lw}| - \frac{R^2 g}{\nu_t}[\, B\,(\,1 - \phi^2\,) - C\,] \pm A\,(\,1 - \phi^2\,)\frac{|J_l|}{1 - \varepsilon_g} \tag{7.23}$$

with

$$|u_{lw}| = 135.3\,\frac{\nu_t A}{R}\,[\,-1 + D^{0.5}\,] \tag{7.24}$$

$$A = \frac{2\,(\,1 - \varepsilon_g\,)}{1 - \dfrac{n+6}{n+4}\,\varepsilon_g} \tag{7.25}$$

$$B = \frac{\varepsilon_g}{4}\,\frac{n+6}{n+4}\,\frac{1 - \dfrac{n^2 + 10n + 20}{(\,n+2\,)(\,n+6\,)}\,\varepsilon_g}{1 - \dfrac{n+6}{n+4}\,\varepsilon_g(\phi)} \tag{7.26}$$

$$C = \frac{n+2}{n}\left[\frac{1 - \phi^2}{4} - \frac{1 - \phi^{n+2}}{(\,n+2\,)^2}\right]\varepsilon_g \tag{7.27}$$

$$D = 1 + \frac{1}{135.3A}\left[\frac{(2B - 0.5\,\varepsilon_g\,)R^3 g}{A\,\nu_t^{\,2}} - \frac{\pm|J_l|}{1 - \varepsilon_g}\frac{2R}{\nu_t}\right] \tag{7.28}$$

where u_{lw} is the liquid circulation velocity at the column wall. The superficial liquid velocity, designated by $\pm|J_g|$, has a positive sign for concurrent flows and a negative sign for

countercurrent flows.

(iii) Turbulent viscosity ν_t

Based on experimental data (Ueyama et al., 1977; Hills, 1974; Miyauchi and Shyu, 1970; Yamagoshi, 1969; Yoshitome, 1967; Pavlov, 1965), the relationship between the turbulent viscosity, ν_t, and the column diameter, D, can be expressed as (Ueyama and Miyauchi, 1979)

$$\nu_t = 0.0486\, D^{1.84} \qquad (D < 0.4\ m) \tag{7.29}$$

where the unit for ν_t is m^2/s. In the air - water only system, ν_t is considered to be independent of J_g.

7.2.4 n in Parabolic Profile Models

The usual value for n is larger than 1 in the models of gas holdup and liquid circulation velocity. Before the work of Ueyama and Miyauchi (1979), n was reported in the range 1.3 - 2.3 by fitting experimental data. Ueyama and Miyauchi (1979) re-examined those data and found that by using ν_t from Equation 7.29, $n = 2$ was an acceptable compromise for bubble columns. Based on their work, $n = 2$ is used for the simulations of u_h in the air - water only system.

7.2.5 Simulations of u_h in Air - Water Only System

Combining Equations 4.13 and 4.49, yields

$$u_g = \frac{J_g}{\varepsilon_g} = u_b\,(\,1 - \varepsilon_g\,)^{m-1} + u_l \tag{7.30}$$

Using this expression over the cross section of the column gives

$$u_g(\phi) = \frac{J_g(\phi)}{\varepsilon_g(\phi)} = u_b\,(\,1 - \varepsilon_g(\phi)\,)^{m_c-1} + u_l(\phi) \tag{7.31}$$

where $u_g(\phi)$ and $J_g(\phi)$ are defined as the bubble velocity and local superficial gas velocity over the cross section of the column, respectively, $\varepsilon_g(\phi)$ and $u_l(\phi)$ are given by Equations 7.19 and 7.23, respectively, and m_c is a coefficient that depends on the characteristics of the bubbles. For u_h, we have

$$u_h = \left\langle \frac{J_{g,loc}}{\varepsilon_g} \right\rangle = \frac{1}{A_c} \int_{A_c} \left(\frac{J_{g,loc}}{\varepsilon_g} \right) dA_c = \frac{1}{\pi} \int_0^1 \frac{J_g(\phi)}{\varepsilon_g(\phi)} 2\pi\phi \, d\phi \qquad (7.32)$$

Substituting Equations 7.31 into 7.32, yields

$$u_h = \frac{1}{\pi} \int_0^1 [\, u_b (1 - \varepsilon_g(\phi))^{m_c - 1} + u_l(\phi) \,] \, 2\pi\phi \, d\phi \qquad (7.33)$$

Using u_h measured in the experiments, the m_c was calculated by numerical integration of Equation 7.33 at various J_{gl} and the results are shown in Table 7.7. The three parameters used in the calculations were: (a) $n = 2$ for $\varepsilon_g(\phi)$ and $u_l(\phi)$, (b) $u_b = 0.21$ m/s as $J_{gl} = 1.0$ - 3.0 cm/s (see Section 5.1), and (c) $\nu_t = 2.49 \times 10^{-4}$ m^2/s by substituting $D = 0.057$ m into Equation 7.29. The $J_{g,loc}$ and the average ε_g of Cells 6 - 2 were used. Figure 7.12 illustrates the $\varepsilon_g(\phi)$ and Figure 7.13 shows $u_g(\phi)$, $u_l(\phi)$ and $u_{g,loc}$ at $J_{gl} = 2.0$ cm/s in the air - water only system.

Table 7.7 Calculated m_c in air - water only system

J_{gl} (cm/s)	$u_{g,loc}$ (cm/s)	u_h (cm/s)	m_c
1.0	18.2	18.2	4.23
1.5	19.5	16.7	4.60
2.0	19.2	15.6	4.46
2.5	18.0	14.1	4.35
3.0	17.5	12.4	4.38

From Table 7.7, it can be seen that the m_c varies over a small range as J_{gl} increases from 1.0 to 3.0 cm/s. The m_c should be a function of the bubble diameter and the bubble Reynolds number. Substituting u_b, $u_{g,loc}$, $J_{g,loc}$ and the average gas holdup into Equation 7.30, the average m is 2.1. The difference between m_c and m shows that Equations 7.30 and 7.33 apply to different domains. All variables in Equation 7.30 are the one-dimensional averages. For example, in Equation 7.30, the u_l is equal to zero because there is no net liquid flow in the column under batch operation. However, $u_l(\phi)$ in Equation 7.31 indicates that the local liquid velocity is not equal to zero. Because of the effects of $\varepsilon_g(\phi)$ and $u_l(\phi)$, $u_g(\phi)$ is not constant over the cross section of the column, and consequently, u_h, i.e. the average of the bubble velocities over the cross section, is less than $u_{g,loc}$. A mathematical proof of this follows.

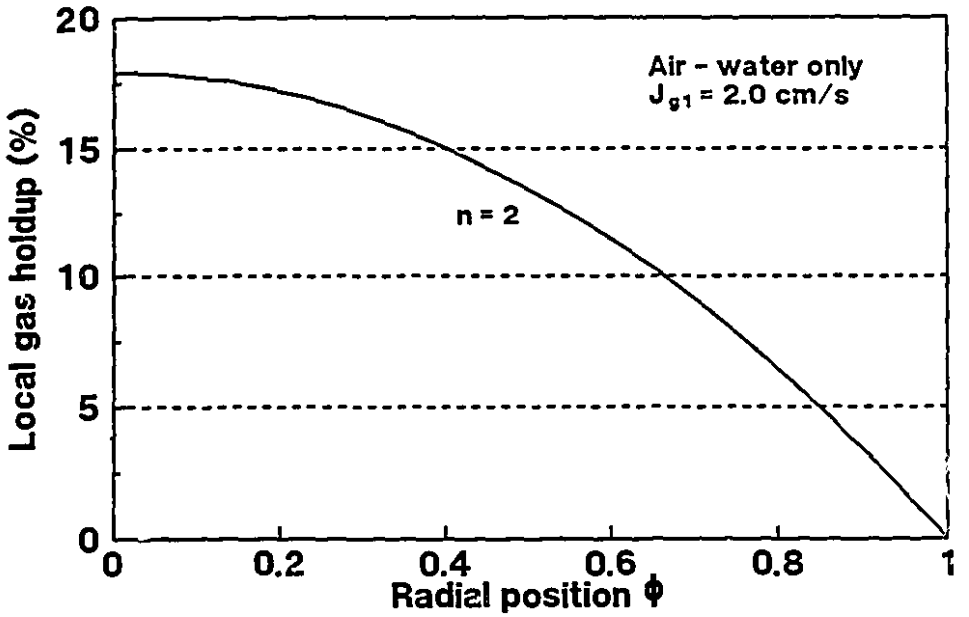

Figure 7.12 Local gas holdup at $n = 2$ and $J_{g1} = 2.0$ cm/s in air - water only system.

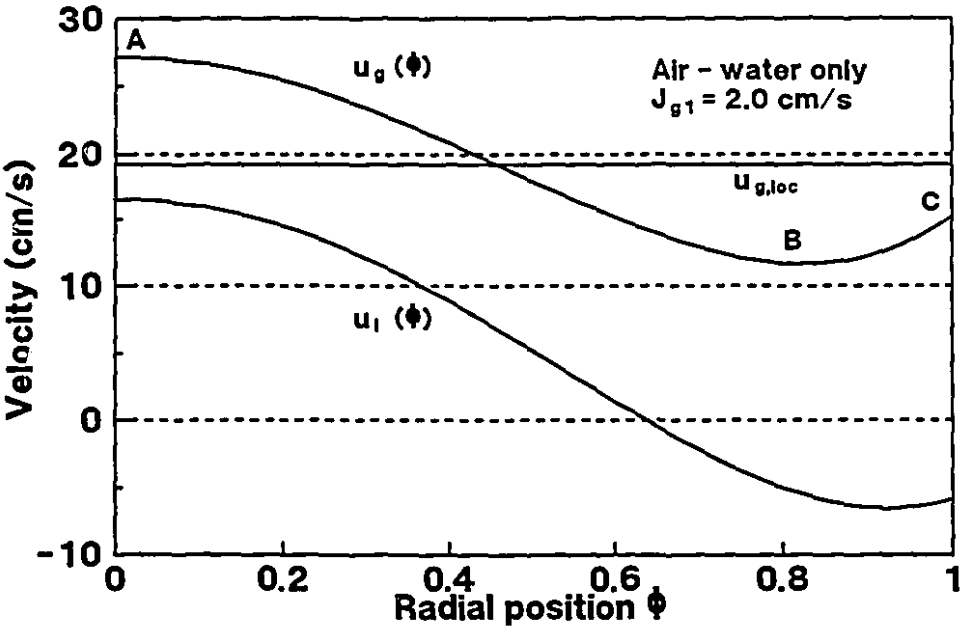

Figure 7.13 $u_g(\phi)$, $u_l(\phi)$ and $u_{g,loc}$ at $n = 2$, $m_c = 4.46$ and $J_{g1} = 2.0$ cm/s in air - water only system.

7.2.6 A Mathematical Proof of $u_h < u_{g,loc}$

In general, it is difficult to build a complete theoretical relationship for u_h and $u_{g,loc}$. Using a mathematical inequality, however, it can be proved that u_h is less than $u_{g,loc}$ for $n = 2$.

(i) A mathematical inequality

Assume $f(x)$ and $g(x)$ are two real functions with $0 \le x \le 1$. If

$$[\, f(x_2) - f(x_1) \,][\, g(x_2) - g(x_1) \,] \ge 0 \tag{7.34}$$

which means that $f(x)$ and $g(x)$ should increase or decrease at the same position for $0 \le x \le 1$, then we have

$$\int_0^1 f(x)\, g(x)\, dx \ge \int_0^1 f(x)\, dx \cdot \int_0^1 g(x)\, dx \tag{7.35}$$

Conversely, if

$$[\, f(x_2) - f(x_1) \,][\, g(x_2) - g(x_1) \,] \le 0 \tag{7.36}$$

then we have

$$\int_0^1 f(x)\, g(x)\, dx \le \int_0^1 f(x)\, dx \cdot \int_0^1 g(x)\, dx \tag{7.37}$$

The proof of the inequality is shown in Appendix 5.

(ii) Relationship between u_h and $u_{g,loc}$ for $n = 2$

Over the cross section of the column, with $n = 2$, $\varepsilon_g(\phi)$ is a function of ϕ^2 and $J_g(\phi)$ is also assumed as a function of ϕ^2 . For the averages over the cross section, we have

$$\langle J_{g,loc} \rangle = \frac{1}{\pi} \int_0^1 J_g(\phi^2)\, 2\pi\phi\, d\phi = \int_0^1 J_g(\phi^2)\, d(\phi^2) \tag{7.38}$$

$$\langle \varepsilon_g \rangle = \frac{1}{\pi} \int_0^1 \varepsilon_g(\phi^2)\, 2\pi\phi\, d\phi = \int_0^1 \varepsilon_g(\phi^2)\, d(\phi^2) \tag{7.39}$$

For $0 \le \phi \le 1$, we set

$$\left\langle \frac{J_{g,loc}}{\varepsilon_g} \right\rangle = \frac{1}{\pi} \int_0^1 \frac{J_g(\phi^2)}{\varepsilon_g(\phi^2)} 2\pi\phi \, d\phi = \int_0^1 \frac{J_g(\phi^2)}{\varepsilon_g(\phi^2)} \, d(\phi^2) \tag{7.40}$$

$$f(\phi^2) = \frac{J_g(\phi^2)}{\varepsilon_g(\phi^2)} \tag{7.41}$$

and

$$g(\phi^2) = \varepsilon_g(\phi^2) \tag{7.42}$$

Consequently, we have

$$f(\phi^2)\, g(\phi^2) = \frac{J_g(\phi^2)}{\varepsilon_g(\phi^2)} \cdot \varepsilon_g(\phi^2) = J_g(\phi^2) \tag{7.43}$$

If Equation 7.34 is satisfied with $f(\phi^2)$ and $g(\phi^2)$ in $0 \le \phi \le 1$, from Equation 7.35, we obtain

$$\int_0^1 J_g(\phi^2)\, d(\phi^2) \ge \int_0^1 \frac{J_g(\phi^2)}{\varepsilon_g(\phi^2)} \, d(\phi^2) \cdot \int_0^1 \varepsilon_g(\phi^2)\, d(\phi^2) \tag{7.44}$$

Because the second term on the right hand side is greater than zero, the inequality can be rearranged as

$$\frac{\int_0^1 J_g(\phi^2)\, d(\phi^2)}{\int_0^1 \varepsilon_g(\phi^2)\, d(\phi^2)} \ge \int_0^1 \frac{J_g(\phi^2)}{\varepsilon_g(\phi^2)} \, d(\phi^2) \tag{7.45}$$

Substituting Equations 7.38, 7.39 and 7.40 into 7.45, yields

$$u_{g,loc} = \frac{\langle J_{g,loc} \rangle}{\langle \varepsilon_g \rangle} \ge \left\langle \frac{J_{g,loc}}{\varepsilon_g} \right\rangle = u_h \tag{7.46}$$

For $n = 2$, this inequality indicates that $u_{g,loc}$ is larger than u_h when the $\varepsilon_g(\phi)$ and $u_g(\phi)$ increase or decrease at the same position of $0 \le \phi \le 1$. However, if $\varepsilon_g(\phi)$ increases as $u_g(\phi)$ decreases at the same position, we will have $u_{g,loc} \le u_h$ (Equation 7.37).

In $0 \le \phi \le 1$, Figures 7.12 and 7.13 illustrate that $\varepsilon_g(\phi)$ is a decreasing function and $u_g(\phi)$ also decreases from A ($\phi = 0$) to B ($\phi_B = 0.82$, at which the slope of $u_g(\phi)$ changes from

negative to positive), but then increases from B to C ($\phi = 1$). In this case, two regions must be considered: (a) in $0 \le \phi \le 0.82$, where u_h is less than $u_{g,loc}$, and (b) in $0.82 < \phi \le 1$, where u_h is larger than $u_{g,loc}$. R_B is introduced as the ratio of the gas volume in $0 \le \phi \le \phi_B$ to the total gas volume in unit height of the column given by

$$R_B = \frac{\int_0^{\phi_B} \varepsilon_g(\phi)\, 2\pi\phi\, d\phi}{\int_0^1 \varepsilon_g(\phi)\, 2\pi\phi\, d\phi} = \frac{1}{\pi\varepsilon_g} \int_0^{\phi_B} 2\varepsilon_g(\, 1 - \phi^2\,)\, 2\pi\phi\, d\phi = 2\phi_B^2 - \phi_B^4 \qquad (7.47)$$

Table 7.8 gives the values of R_B at various J_{gl}. It can be seen that most of the air bubbles are in the range $0 \le \phi \le \phi_B$. Therefore, we can conclude that, in a column, $u_h \le u_{g,loc}$ for n=2.

Table 7.8 R_B at various J_{gl} in air - water only system

J_{gl} (cm/s)	1.0	1.5	2.0	2.5	3.0
ϕ_B	0.88	0.84	0.82	0.80	0.76
R_B	0.9491	0.9133	0.8927	0.8704	0.8216

7.2.7 u_h and $u_{g,loc}$ in Air - Water Only System

Figure 7.6 compares u_h with $u_{g,loc}$ at various J_{gl}. The u_h is equal to $u_{g,loc}$ at J_{gl} = 1.0 cm/s (see also Table 7.7), probably because at this relatively low gas rate a flat gas holdup profile and weak liquid circulation occur. When J_g increases, non-uniform distribution of gas holdup occurs and liquid circulation velocity is increased. Consequently, u_h decreases and the difference between u_h and $u_{g,loc}$ becomes apparent.

The experimental results in Section 5.3 showed the effect of the liquid circulation flow on the bubble swarm velocity in the column. Figure 5.23 illustrates $u_{2,C6}$, i.e. the velocity of the top of bubble swarm, decreases as the duration of the air pulse increases, asymptotically approaching 25.5 cm/s, when the single bubble terminal velocity is 21 cm/s (Section 5.1). In the experiments, it was observed that a convex front of the bubble swarm formed by faster moving bubbles rising along the centre of the column. In fact, the $u_{2,C6}$ was the velocity of the convex front of the bubble swarm. Figure 7.13 illustrates that the calculated $u_g(\phi)$ is 27 cm/s at the centre of the column ($\phi = 0$) due to the effect of the upward liquid flow. Comparing $u_{2,C6}$ (25.5 cm/s) with $u_g(\phi)$ (27 cm/s) at $\phi = 0$, it can be seen that the bubble swarm velocity is affected by liquid circulation in the column.

Based on the experiments, an empirical relationship between u_h and $u_{g,loc}$ is given by

$$u_h = C_{hg}\, u_{g,loc} \tag{7.48}$$

where C_{hg} is a function of ε_g (in fraction) for $1.0 < J_g < 3.0$ cm/s

$$C_{hg} = 1.90 - 30.99\, \varepsilon_g + 293.6\, \varepsilon_g^2 - 937.4\, \varepsilon_g^3 \tag{7.49}$$

7.2.8 u_h and $u_{g,loc}$ in Air - Water - Frother System

In the presence of frother, the hydrodynamic conditions inside the column are more complex than that of the air - water only system. The simulations for u_h and m_c were not successful. Substituting reasonable m_c (< 10) and n (< 10) values into Equation 7.33, the calculated u_h is less than $u_{g,loc}$ but larger than u_h obtained from the experiments. The reason is that in the presence of frother, by observation, the air bubbles adopted a circulatory flow pattern.

In the air - water only system, there was no bubble circulation seen in the column at $J_g <$ 4.0 cm/s. Figure 7.13 illustrates this condition: the $u_g(\phi)$ has a positive value from the centre to the wall of the column. From observation, however, in the presence of frother, the bubbles were always circulating. Because the effect of bubble circulation is not accounted for, Equation 7.33 failed to describe the u_h in the air - water - frother system.

Although a theoretical model is not available for the air - water - frother system, qualitatively the larger relative difference between u_h and $u_{g,loc}$ in the presence of frother compared to that of the air - water only system does fit the observed increase in bubble circulation and the attendant large distribution in bubble velocities across the cross section of the column. Figures 7.9 and 7.10 illustrate that the u_h is only 40 - 55% of $u_{g,loc}$ with DF250C = 10 and 20 ppm. In the presence of frother an empirical relationship between u_h and $u_{g,loc}$ can be determined using Equation 7.48. With DF250C = 10 ppm for $0.25 < J_g < 1.25$ cm/s , C_{hg} is given by

$$C_{hg} = 0.478 + 3.988\, \varepsilon_g - 94.84\, \varepsilon_g^2 + 490.8\, \varepsilon_g^3 \tag{7.50}$$

and with DF250C = 20 ppm for $0.50 < J_g < 1.50$ cm/s, C_{hg} is

$$C_{hg} = -1.667 + 0.7432\, \varepsilon_g^{-1} - 0.08107\, \varepsilon_g^{-2} + 0.002784\, \varepsilon_g^{-3} \tag{7.51}$$

7.3 Analysis of Momentum for Properties of u_h and u_{in}

7.3.1 Momentum Equations

The overall momentum balance for a fluid system moving with nonaccelerating coordinates is given by (Parker et al., 1969; Zheng et al., 1979; Olson, 1980)

$$\Sigma F = \frac{d}{dt}(mu) \tag{7.52}$$

where ΣF is the sum of the forces acting on the system and mu is the momentum of the system. The time rate of change of momentum of the system can be written as

$$\frac{d}{dt}(mu) = \frac{\partial}{\partial t}\iiint_V u_V \rho_V dV + \iint_S (u_S \rho_S) u_{Sr} \cdot dS \tag{7.53}$$

where ρ_V and u_V are the density and velocity of the fluid in the control volume, ρ_S and u_S are the density and velocity of the fluid on the control surface, and u_{Sr} is the velocity of the fluid on the control surface relative to the control surface. The first term on the right hand side is the time rate of the momentum change of the fluid in the control volume; the second term is the time rate of the momentum change of the fluid leaving and entering the control surface. Assuming the velocity of the control volume is U, we have

$$u_V = U + u_{Vr} \tag{7.54}$$

$$u_S = U + u_{Sr} \tag{7.55}$$

where u_{Vr} is the velocity of the fluid in the control volume relative to the control volume. Combining Equations 7.54 and 7.55 with Equations 7.52 and 7.53, yields

$$\Sigma F = \frac{\partial}{\partial t}\iiint_V \rho_V (U + u_{Vr}) dV + \iint_S \rho_S (U + u_{Sr}) u_{Sr} \cdot dS \tag{7.56}$$

Rearranging Equation 7.56, we obtain the overall momentum equation

$$\Sigma F = \frac{d}{dt}(mu) = m_V \frac{\partial U}{\partial t} + \frac{\partial}{\partial t}\iiint_V u_{Vr} \rho_V dV + \iint_S (u_{Sr} \rho_S) u_{Sr} \cdot dS \tag{7.57}$$

where m_V is the mass of the fluid in the control volume. Equation 7.57 is the general equation used for momentum analysis. In Equation 7.57, the second term on the right hand side means that in the control volume the fluid may be accelerating relative to the control volume, and the third term means that the momentum of the fluid entering the control surface may not be equal to the momentum of the fluid leaving the control surface.

The ΣF, the net external force acting on the fluid, includes: (a) normal forces due to pressure; (b) body forces due to fields, such as gravity, electric, or magnetic; (c) shear or friction forces due to viscous shear; and, (d) externally applied forces.

If the values of the properties in a fluid are known to vary with time and location, the differential form of the momentum equation is particular useful. The one dimensional differential equation for a fluid system in direction z is given by

$$\Sigma F_{diff} = \rho_f \frac{\partial U}{\partial t} + \rho_f \frac{\partial u_{fr}}{\partial t} + \rho_f u_{fr} \frac{\partial u_{fr}}{\partial z} \tag{7.58}$$

where ΣF_{diff} is the sum of the forces in direction z on the control volume, per unit volume of the fluid, ρ_f is the density of the fluid and u_{fr} is the velocity of the fluid relative to the control volume.

7.3.2 Control Volume and Momentum Balance

Figure 7.14 shows the control volume for the momentum analysis of a bubble swarm rising in a column. This moving control volume is located immediately above the interface formed by the step change of the gas flowrate. In this case, the system is treated as a separated flow and the three dimensional momentum equations for the gas phase and liquid phase are reduced to one dimensional equations. The momentum equations, in the vertical direction z, are given by

$$\rho_g \frac{\partial U}{\partial t} + \rho_g \frac{\partial u_{gr}}{\partial t} + \rho_g u_{gr} \frac{\partial u_{gr}}{\partial z} = b_g + f_g + w_g - \frac{\partial p}{\partial z} \tag{7.59}$$

$$\rho_l \frac{\partial U}{\partial t} + \rho_l \frac{\partial u_{lr}}{\partial t} + \rho_l u_{lr} \frac{\partial u_{lr}}{\partial z} = b_l + f_l + w_l - \frac{\partial p}{\partial z} \tag{7.60}$$

where the subscript g indicates the gas phase and l indicates the liquid phase. The b's are the body forces, per unit volume of that phase. The $\partial p / \partial z$ is the average gradient of the pressure.

The f_g is the force acting on the gas phase from the liquid, per unit volume of the gas phase. The f_l is the force acting on the liquid phase from the gas phase, per unit volume of the liquid phase. The w's are simply the remaining forces per unit volume of that phase (i.e. "forces left over" that are not contained in b's, f's and $\partial p/\partial z$).

F_l and F_g are defined as the equivalent of the f_l and f_g, per unit volume of the whole control volume. Thus (Wallis, 1969 and Whalley, 1987)

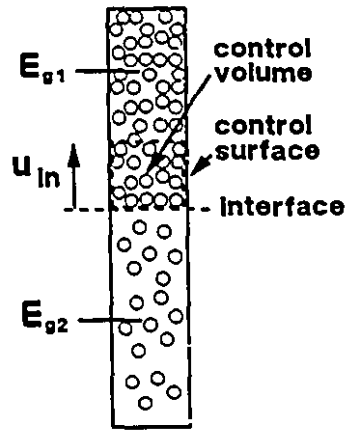

Figure 7.14 Control volume of bubble swarm.

$$F_l = f_l (1 - \varepsilon_g) \tag{7.61}$$

$$F_g = f_g \varepsilon_g \tag{7.62}$$

If these forces are entirely due to mutual hydrodynamic drag, action and reaction are equal and we have

$$F_l = - F_g \tag{7.63}$$

Therefore, the relationship between f_l and f_g is given by

$$f_g = - f_l \frac{1 - \varepsilon_g}{\varepsilon_g} \tag{7.64}$$

7.3.3 Conditions for Control Volume

Based on the experimental observations, the following conditions were assumed for the moving control volume (Figure 7.14):

(a) the velocity of the control volume, i.e. U in Equations 7.59 and 7.60, is equal to the interface velocity, u_{in};

(b) the velocity of the bubbles in the control volume, u_{gc}, is equal to u_h at the corresponding J_{gl};
(c) the gas holdup in the control volume is equal to ε_{gl}; and,
(d) as shown in Section 5.6,

$$u_{lop} (1 - \varepsilon_{gl}) = (\varepsilon_{g2} - \varepsilon_{gl}) u_{in} \tag{5.27}$$

In fact, the left hand side is equal to the liquid velocity across the interface. Neglecting the small difference in velocity between the control volume and the interface, the liquid velocity in the control volume, u_{lc}, is given by

$$u_{lc} = (\varepsilon_{g2} - \varepsilon_{gl}) u_{in} \tag{7.65}$$

7.3.4 Forces on Gas and Liquid Phases

The forces on the gas phase and liquid phase are:

(i) b_g and b_l

The body force included here is only that due to gravity and other forces, such as the electric force and the magnetic force, are not considered. The b_g is given by

$$b_g = - \rho_g g \tag{7.66}$$

and b_l is given by

$$b_l = - \rho_l g \tag{7.67}$$

(ii) $\partial p / \partial z$

The pressure gradient is given by

$$\frac{\partial p}{\partial z} = - \left[\rho_g g \varepsilon_{gl} + \rho_l g (1 - \varepsilon_{gl}) \right] \tag{7.68}$$

(iii) w_g and w_l

The w_g and w_l are determined experimentally.

(iv) f_g and f_l

The Ergun equation is widely used to model fluidization in gas - solids and liquid - solids systems (Fan, 1989; Clift and Grace, 1985; Tien, 1983; Harriott and Simone, 1983). In this

case, the f_s and f_l will be derived from the Ergun equation.

The Ergun equation (Ergun, 1952; Kunii and Levenspiel, 1969), for the frictional pressure drop during viscous flow through fixed beds of uniformly sized solids, is given by (in cgs system)

$$-\left[\frac{\partial p}{\partial z}\right]_F = 150\,\frac{\mu_f J_f}{(\phi_s d_p)^2}\,\frac{(1-\varepsilon_f)^2}{\varepsilon_f^3} + 1.75\,\frac{\rho_f J_f^2}{\phi_s d_p}\,\frac{1-\varepsilon_f}{\varepsilon_f^3} \qquad (7.69)$$

where μ_f and ρ_f are the viscosity and density of the fluid, ε_f is the fluid holdup, J_f is the superficial fluid velocity, d_p is the volumetric diameter of the solid particles, and ϕ_s is the sphericity of the solid particles given by

$$\phi_s = \left[\frac{surface\ of\ sphere}{surface\ of\ particle}\right]_{both\ of\ same\ volume} \qquad (7.70)$$

In the Ergun equation, the first term on the right hand side represents the pressure drop due to viscous energy loss and the second term shows the pressure drop due to kinetic energy loss. When the particle Reynolds number, $Re_p < 20$, the second term on the right hand side of Equation 7.36 can be neglected, and the first term can be dropped if $Re_p > 1000$. When $20 < Re_p < 1000$, both terms have to be used. The Reynolds number of the particle is defined as

$$Re_p = \frac{d_p \rho_f J_f}{\mu_f} \qquad (7.71)$$

When the Ergun equation is used for beds containing particles of different sizes, the d_p is replaced by the mean diameter of the particles (Kunii and Levenspiel, 1969).

To choose the fixed bed as the control volume, the inertial and gravitational terms are neglected in the steady state condition and the momentum equation for the fluid is given by

$$f_f = \left[\frac{\partial p}{\partial z}\right]_F = -\,150\,\frac{\mu_f J_f}{(\phi_s d_p)^2}\,\frac{(1-\varepsilon_f)^2}{\varepsilon_f^3} - 1.75\,\frac{\rho_f J_f^2}{\phi_s d_p}\,\frac{1-\varepsilon_f}{\varepsilon_f^3} \qquad (7.72)$$

Substituting $u_f = J_f / \varepsilon_f$ into this equation, yields

$$f_f = -150 \frac{\mu_s u_f}{(\phi_s d_p)^2} \frac{(1-\varepsilon_f)^2}{\varepsilon_f^2} - 1.75 \frac{\rho_s u_f^2}{\phi_s d_p} \frac{1-\varepsilon_f}{\varepsilon_f} \tag{7.73}$$

Comparing the conditions in the control volume shown in Figure 7.14 with that in a fixed bed, clearly the bubbles move upwards in the air - water system while the solid particles are stationary in the fixed bed. In the case of the column, the fluid velocity, u_f, should be replaced with the relative velocity in the control volume, $u_{r,c}$, given by

$$u_{r,c} = u_{lc} - u_{gc} = u_{in}(\varepsilon_{g2} - \varepsilon_{g1}) - u_h \tag{7.74}$$

To use Equation 7.73 in the column, 1.0 is selected for ϕ_s (bubbles are essentially spherical), and μ_f, ρ_f, d_p and ε_s are replaced by μ_l, ρ_l, d_{bs} and ε_{gl}, respectively. The f_l is given by

$$f_l = -150 \frac{\mu_l}{d_{bs}^2} u_{r,c} \frac{\varepsilon_{gl}^2}{(1-\varepsilon_{gl})^2} - 1.75 \frac{\rho_l}{d_{bs}} u_{r,c}^2 \frac{\varepsilon_{gl}}{1-\varepsilon_{gl}} \tag{7.75}$$

and the f_g can be calculated using Equation 7.64.

7.3.5 Momentum Equation for Two Phases

Equation 7.59 is added to Equation 7.60 to give

$$\rho_g \frac{\partial U}{\partial t} + \rho_g \frac{\partial u_{gr}}{\partial t} + \rho_g u_{gr} \frac{\partial u_{gr}}{\partial z} + \rho_l \frac{\partial U}{\partial t} + \rho_l \frac{\partial u_{lr}}{\partial t} + \rho_l u_{lr} \frac{\partial u_{lr}}{\partial z} = b_g + b_l + f_g + f_l + w_g + w_l - 2\frac{\partial p}{\partial z} \tag{7.76}$$

The inertial terms on the left hand side are the change of the momentum, and the forces on the right hand side are the net force acting on the control volume. Rearranging the terms on the right hand side, yields

$$w = w_g + w_l \tag{7.77}$$

$$b = b_g + b_l - 2\frac{\partial p}{\partial z} = (\rho_g - \rho_l) g (1 - 2\varepsilon_{gl}) \tag{7.78}$$

$$f = f_g + f_l = \left(- f_l \frac{1 - \varepsilon_{gl}}{\varepsilon_{gl}} \right) + f_l = f_l \left(2 - \frac{1}{\varepsilon_{gl}} \right) \tag{7.79}$$

Consequently, the net force on the control volume is given by

$$\sum F_{diff} = w + (\rho_g - \rho_l) g (1 - 2 \varepsilon_{gl}) + f_l \left(2 - \frac{1}{\varepsilon_{gl}} \right) \tag{7.80}$$

where f_l is expressed in Equation 7.75.

7.3.6 Properties of u_h

Based on the conditions in the control volume shown in Section 7.3.3, we have

$$U = u_{in} \tag{7.81}$$

$$u_{gr} = u_{gc} - U = u_h - u_{in} \tag{7.82}$$

$$u_{lr} = u_{lc} - U = (\varepsilon_{g2} - \varepsilon_{gl}) u_{in} - u_{in} = (\varepsilon_{g2} - \varepsilon_{gl} - 1) u_{in} \tag{7.83}$$

Substituting these three equations into the inertial terms, yields

$$\rho_g \frac{\partial U}{\partial t} = \rho_g \frac{\partial u_{in}}{\partial t} \tag{7.84}$$

$$\rho_g \frac{\partial u_{gr}}{\partial t} = \rho_g \frac{\partial}{\partial t} (u_h - u_{in}) = - \rho_g \frac{\partial u_{in}}{\partial t} \tag{7.85}$$

$$\rho_g u_{gr} \frac{\partial u_{gr}}{\partial z} = \rho_g (u_h - u_{in}) \frac{\partial}{\partial z} (u_h - u_{in}) = - \rho_g (u_h - u_{in}) \frac{\partial u_{in}}{\partial z} \tag{7.86}$$

$$\rho_l \frac{\partial U}{\partial t} = \rho_l \frac{\partial u_{in}}{\partial t} \tag{7.87}$$

$$\rho_l \frac{\partial u_{lr}}{\partial t} = \rho_l \frac{\partial}{\partial t} [(\varepsilon_{g2} - \varepsilon_{gl} - 1) u_{in}] = \rho_l (\varepsilon_{g2} - \varepsilon_{gl} - 1) \frac{\partial u_{in}}{\partial t} \tag{7.88}$$

$$\begin{aligned} \rho_l u_{lr} \frac{\partial u_{lr}}{\partial z} &= \rho_l (\varepsilon_{g2} - \varepsilon_{gl} - 1) \frac{\partial}{\partial z} [(\varepsilon_{g2} - \varepsilon_{gl} - 1) u_{in}] \\ &= \rho_l (\varepsilon_{g2} - \varepsilon_{gl} - 1)^2 \frac{\partial u_{in}}{\partial z} \end{aligned} \tag{7.89}$$

Consequently, we obtain

$$\begin{aligned} \textit{change of momentum} = {} & \rho_l (\varepsilon_{g2} - \varepsilon_{gl}) \frac{\partial u_{in}}{\partial t} \\ & + [\rho_l u_{in} (\varepsilon_{g2} - \varepsilon_{gl} - 1)^2 - \rho_g (u_h - u_{in})] \frac{\partial u_{in}}{\partial z} \end{aligned} \tag{7.90}$$

When the column is operating under steady state, the net force on the control volume is zero (i.e. the change of momentum is equal to zero), and $\varepsilon_{g2} = \varepsilon_{gl}$, $u_{in} = u_h$. Substituting these conditions into Equation 7.90, yields

$$\rho_l u_{in} \frac{\partial u_{in}}{\partial z} = \rho_l u_h \frac{\partial u_h}{\partial z} = 0 \tag{7.91}$$

It can be seen that $\partial u_h/\partial z$ is zero. On the other hand, $\partial u_h/\partial t$ is zero because J_g and J_l do not vary with time in this steady state condition. Therefore, the total differential of the hindered velocity, u_h, is given by

$$du_h = \frac{\partial u_h}{\partial t} dt + \frac{\partial u_h}{\partial z} dz = 0 \tag{7.92}$$

This equation theoretically predicts that u_h should be constant and independent of time and position in the column when the column is operating under steady state. As shown in Section 6.5, the measurements of u_{in} in Cells 6 - 2, empirically illustrated that u_h is a constant no matter where it is measured. Comparing with $u_{g,loc}$ which varies with the position in the column, we can conclude that u_h is an important characteristic of the system.

7.3.7 Change of Momentum and Properties of u_{in}

As discussed by many researchers, it is hard to use fundamental models to calculate the

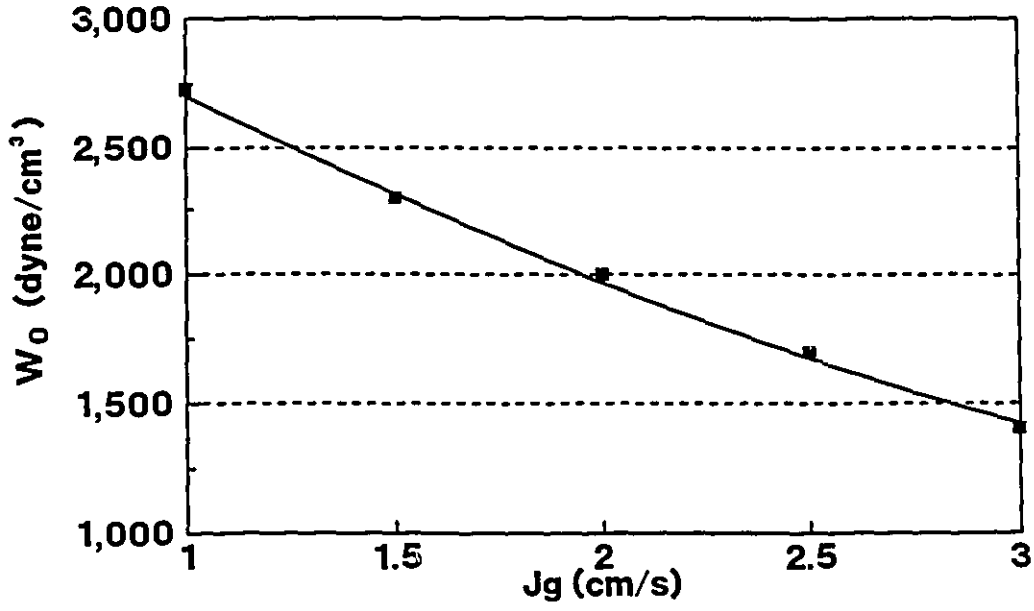

Figure 7.15 w_0 at various J_g.

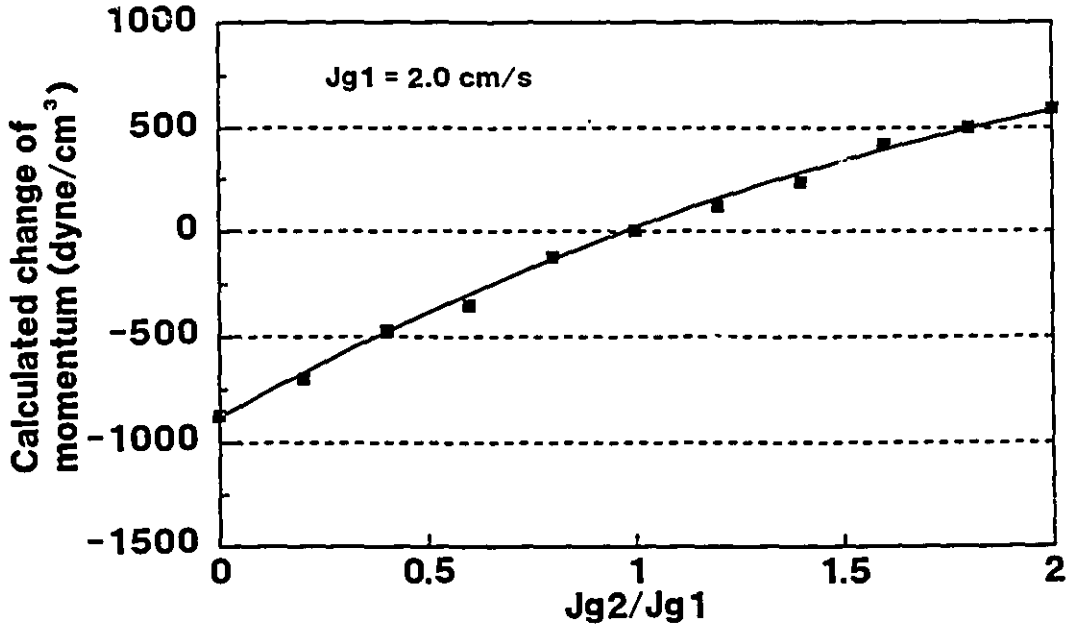

Figure 7.16 Calculations for change of momentum in Cell 6 at J_{g1} = 2.0 cm/s.

change of momentum in the control volume because of the complexity of the system. In this section, the numerical values of the calculations may not match the experimental data, but the trend in the results will give useful information.

(i) w_0

When the column is operating under steady state, the net force on the control volume is equal to zero. Equation 7.80 becomes

$$w_0 + (\rho_g - \rho_l) g (1 - 2 \varepsilon_{gl}) + f_l (2 - \frac{1}{\varepsilon_{gl}}) = 0 \qquad (7.93)$$

where w_0 is w in the control volume as the column is operating at steady state. In this particular case, $u_{r,c}$ is equal to $-u_h$. Substituting the experimental data into the equation, the w_0 can be calculated and the results are illustrated in Figure 7.15.

(ii) Calculations for change of momentum at J_{gl} = 2.0 cm/s

In an experiment, we assume that w is a constant and equal to w_0 at a certain J_{gl}. The change of momentum is given by

$$change\ of\ momentum = w_0 + (\rho_g - \rho_l) g (1 - 2 \varepsilon_{gl}) + f_l (2 - \frac{1}{\varepsilon_{gl}}) \qquad (7.94)$$

Figure 7.16 illustrates the calculated results for the change of momentum in Cell 6 at J_{gl} = 2.0 cm/s. It can be seen that the calculated change of momentum is negative for $J_{g2}/J_{gl} < 1$ and is positive for $J_{g2}/J_{gl} > 1$.

Because $\rho_l >> \rho_g$, Equation 7.90 can be simplified as

$$change\ of\ momentum = \rho_l (\varepsilon_{g2} - \varepsilon_{gl}) \frac{\partial u_{ln}}{\partial t} + \rho_l u_{ln} (\varepsilon_{g2} - \varepsilon_{gl} - 1)^2 \frac{\partial u_{ln}}{\partial z} \qquad (7.95)$$

For convenience in the discussion, we set

$$C_t = \rho_l (\varepsilon_{g2} - \varepsilon_{gl}) \qquad (7.96)$$

$$C_z = \rho_l u_{ln} (\varepsilon_{g2} - \varepsilon_{gl} - 1)^2 \qquad (7.97)$$

When $J_{g2} / J_{gl} < 1$, Figure 6.51 illustrates that there is no the significant deceleration on

the interface velocity, u_{in}, at J_{gl} = 2.0 cm/s in the air - water only system; however, Figure 7.16 illustrates that the inertia momentum is negative at $J_{g2} / J_{gl} < 1$.

Because u_{in} is a function of time and location in the column, we have

$$du_{in} = \frac{\partial u_{in}}{\partial t} dt + \frac{\partial u_{in}}{\partial z} dz \qquad (7.98)$$

From this equation, it can be seen that the proper combination of the positive $\partial u_{in}/\partial t$ and negative $\partial u_{in}/\partial z$ could give a constant u_{in}. At $J_{g2} / J_{gl} < 1$ (i.e. $\varepsilon_{g2} < \varepsilon_{gl}$), $C_t < 0$ and $C_z > 0$. If the positive $\partial u_{in}/\partial t$ and negative $\partial u_{in}/\partial z$ are substituted into Equation 7.96, the value of the change of momentum is negative, which agrees with the results shown in Figure 7.16.

When $J_{g2} / J_{gl} > 1$, there is a significant acceleration on u_{in} (Figure 6.51) and the calculated change of momentum is positive (Figure 7.16). In this case, $\varepsilon_{g2} > \varepsilon_{gl}$ causes a positive C_t and C_z. The proper combination of $\partial u_{in}/\partial t$ and $\partial u_{in}/\partial z$ can give positive values for du_{in} and the change of momentum.

Because $\partial u_{in} /\partial t$ and $\partial u_{in} /\partial z$ can not be measured individually in the present work, the above analysis only gives a qualitative explanation. The $\partial u_{in} /\partial t$ and $\partial u_{in} /\partial z$ should be measured separately in future.

(iii) u_{in} in a tall column at $J_{g2} / J_{gl} > 1$

At $J_{g2} / J_{gl} > 1$, the difference between ε_{g2} and ε_{gl} decreases as the interface rises from the bottom to the top of the column. For example, in the air - water only system at J_{gl} = 2.0 cm/s and J_{g2} = 4.0 cm/s, the difference between ε_{g2} and ε_{gl}, i.e. the difference of the gas holdup across the interface, is 11.55% in Cell 6 and 6.46% in Cell 2 (Table 30 in Appendix 3).

It can be argued that the interface is formed between the faster moving bubbles in the lower bubble swarm and the slower moving bubbles in the upper bubble swarm. As the interface rises in a tall column at $J_{g2} / J_{gl} > 1$, the faster moving bubbles from the lower bubble swarm move into the upper bubble swarm, and the number of bubbles in this "fast group" decreases. Finally, the fastest bubbles from the lower bubble swarm will "disappear" into the upper bubble swarm, i.e. the interface will "disappear" and the difference in gas holdup across the interface will be zero. At this moment, the "final" u_{in} should be equal to the u_h of the upper bubble swarm.

Actually, there is no need to build an extremely tall column to verify this argument. At J_{gl}

= 2.0 cm/s, Figure 6.51 illustrates that the acceleration in u_{in} is nearly complete when the interface has risen from Cell 6 to Cell 2. At J_{g2} / J_{gl} = 1.2, 1.4, 1.6, 1.8 and 2.0, u_{in} in Cell 2 is equal to 15.4, 15.3, 15.2, 15.0 and 15.0 cm/s, respectively (Tables 26 - 30 in Appendix 3). It can be seen that these values are close to u_h (15.6 cm/s) at J_{gl} = 2.0 cm/s. In the air - water only system at J_{gl} = 1.0, 1.5, 2.5 and 3.0 cm/s, all the experimental data agree with the statement of equivalence (Figures 5.47, 5.49, 5.53 and 5.55).

In the air - water only system, we find that u_h can be roughly estimated from the u_{in} measured in the top zone of a tall column by a step increment in J_g. In the presence of frothers the acceleration in u_{in} was not observed from experimental data. For the air - water - frother system, further information of the interactions between bubble, frother and liquid, is needed to explain the hydrodynamic conditions in the column.

CHAPTER 8

CONCLUSIONS AND SUGGESTIONS FOR FUTURE WORK

8.1 Conclusions

1. A new fast response conductivity meter was developed. The "five time constant" in this new conductivity meter is 0.08 s. Comparing with 2.3 s in a commercial conductivity meter (Tacussel Model CD 810), the response time of the new conductivity meter meets the requirement for measurements under dynamic conditions.

u_h and u_{in}

2. A bubble interface (or front) was created by introducing a step change of gas flow in a vertical column, and the rising velocity of this bubble interface, u_{in}, was measured using the new conductivity meter.

3. The three-dimensional bubble swarm velocity in the column was obtained by interpolation from the u_{in} measured at various J_{g2} / J_{g1}, where J_{g1} and J_{g2} are the superficial gas velocities before and after the step change of gas flowrate, respectively. This velocity was referred to as the hindered velocity, u_h.

4. An empirical relationship between u_{in} and u_h was given by

$$u_{in} = u_h \left[1 + A \left(\frac{J_{g2}}{J_{g1}} - 1 \right) \right]$$

For the air - water only system at $J_g < 4.0$ cm/s, u_h and A were given by

$$u_h = 21.1 - 2.84 J_{g1}$$

$$A = -0.170 - 0.00162 J_{gl}^{4.4}$$

For the air - water - frother system with DF250C = 10 ppm in the range $0.25 < J_g < 1.25$ cm/s, u_h and A were given by

$$u_h = 3.23 + 9.99 J_{gl} - 11.6 J_{gl}^2 + 3.95 J_{gl}^3$$

$$A = 0.167 - 0.928 J_{gl} + 0.365 J_{gl}^2$$

For the air - water - frother system with DF250C = 20 ppm in the range $0.5 < J_g < 1.25$ cm/s, u_h and A were given by

$$u_h = -14.1 + 4.61 J_{gl}^{-1} + 18.7 J_{gl} - 5.33 J_{gl}^2$$

$$A = -7.36 + 1.99 J_{gl}^{-1} + 7.33 J_{gl} - 2.38 J_{gl}^2$$

5. For the air - water only system under batch operation, the relationship between u_{in} and u_{top}, which can be used to predict the level variation due to a change in the air flowrate, was given by

$$u_{top} = \frac{\varepsilon_{g2} - \varepsilon_{gl}}{1 - \varepsilon_{gl}} u_{in}$$

In a column, the variation of ε_g with height makes its application to level change prediction difficult.

u_h and $u_{g,loc}$

6. The average gas velocity, u_g, was corrected to the local average gas velocity, $u_{g,loc}$, to obtain the average gas velocity under the local pressure conditions at a given vertical position in the column

$$u_{g,loc} = \frac{J_{g,loc}}{\varepsilon_g} = \frac{J_g}{\varepsilon_g} \frac{P_o}{P_{loc}}$$

7. The u_h is the three-dimensional bubble swarm velocity and $u_{g,loc}$ is the one-dimensional bubble swarm velocity in the column. The experimental results showed that u_h was significantly less than $u_{g,loc}$ (and u_g).

8. Comparing with $u_{g,loc}$, u_h is constant along the column, which was supported by theoretical momentum analysis. The u_h is characteristic of the system.

9. For the air - water only system in the two-dimensional domain, using the models of parabolic gas holdup profile and liquid circulation velocity profile over the cross section of the column, the simulated u_h agreed with the u_h obtained from the experiments.

10. For the air - water - frother system, the simulation of u_h did not fit the experimental data because the air bubbles adopted a circulatory flow pattern.

11. Using an inequality, $u_{g,loc} \geq u_h$ was mathematically proved for a column in the two-dimensional domain with a parabolic gas holdup profile of $n = 2$.

12. An empirical relationship between u_h and $u_{g,loc}$ was given by

$$u_h = C_{hg}\, u_{g,loc}$$

In the air - water only system for $1.0 < J_g < 3.0$ cm/s, C_{hg} was expressed as

$$C_{hg} = 1.90 - 30.99\, \varepsilon_g + 293.6\, \varepsilon_g^2 - 937.4\, \varepsilon_g^3$$

With DF250C = 10 ppm for $0.25 < J_g < 1.25$ cm/s, C_{hg} was expressed as

$$C_{hg} = 0.478 + 3.988\, \varepsilon_g - 94.84\, \varepsilon_g^2 + 490.8\, \varepsilon_g^3$$

and with DF250C = 20 ppm for $0.50 < J_g < 1.50$ cm/s, C_{hg} was expressed as

$$C_{hg} = -1.667 + 0.7432\, \varepsilon_g^{-1} - 0.08107\, \varepsilon_g^{-2} + 0.002784\, \varepsilon_g^{-3}$$

Nicklin's derivation

13. In the air - water only system, by changing duration of the gas pulse injected into the column, Nicklin's assumption was confirmed by experiments: the buoyancy velocity, u_0, can be obtained by measuring the velocity of the bottom of a bubble swarm.

14. In the air - water only system, by stopping and restarting gas flow, the experiments showed that there was no effect on the bottom velocity of the upper bubble swarm at J_g = 2.0 cm/s (bubbly flow conditions) contrary to the prediction of Nicklin. There was a small effect at J_g = 5.0 cm/s (non-bubbly flow), however, it was much smaller than that suggested by Nicklin.

15. Nicklin's derivation gave

$$u_g = u_0 + J_g + J_l$$

for countercurrent flow, and for $u_{g,loc}$ and $J_{g,loc}$, the above equation becomes

$$u_{g,loc} = u_0 + J_{g,loc} + J_l$$

In the air - water only system under batch operation, Nicklin's derivation is apparently correct but only under restrictive conditions, namely u_g and J_g must be measured at atmospheric pressure. Considering the local values, the experiments showed that $u_{g,loc}$ was not equal to $u_0+J_{g,loc}$. In the air - water - frother system with DF250C = 10 ppm and 20 ppm under batch operation or with countercurrent liquid flow, the experiments showed that Nicklin's derivation was not applicable even if atmospheric values of u_g and J_g were used.

8.2 Claims for Original Research

1. A new conductivity meter was developed with a sufficiently short response time to permit the measurement of bubble swarm velocity in a column. This new conductivity meter can be used for other conductivity based process measurements, such as dynamic gas holdup and interface detection in flotation columns.

2. A new method based on a conductivity technique was developed for the measurement of the three-dimensional bubble swarm velocity, u_h, in a column.

3. The u_h is shown to be invariant with position in the column and is proposed as the key characteristic swarm velocity of the system.

4. The experimental results showed there is a significant deference between the three-dimensional bubble swarm velocity, u_h, and u_g obtained from Nicklin's derivation. Particularly, for a flotation column, u_g gives a large error for estimating bubble swarm velocity in the presence of frothers.

8.3 Suggestions for Future Work

1. Experiments on u_h are recommended for the air - water - solids system with and without frothers. This could be used to check the conclusion of Banisi (1994) that bubble swarm velocity increases in the presence of solids.

2. The measurement of u_h and u_{in} is recommended in pilot and industrial columns. The relationship between u_{in} and u_{top} obtained in the laboratory column should be re-examined in an industrial column. Differences between predicted and actual level position changes could permit some estimation of water flow across the interface.

3. For the measurement of u_h in large-size pilot and industrial columns with the new conductivity meter, the grid electrode for the laboratory column can not be used. A new conductivity electrode, which is removable and is isolated from the wall of the column, should be designed and tested.

4. The bubble swarm velocity model needs to be expanded from the two-dimensional domain treated here to the three-dimensional domain to explore u_h with bubble circulatory flow patterns.

REFERENCES

Adamson, A.W., 1979; *A Textbook of Physical Chemistry*; Academic Press, pp.953

Andrews, D.H., 1970; *Introductory Physical Chemistry*; McGraw Hill Book Co., pp.689

Atkins, P.W., 1982; *Physical Chemistry*, W.H. Freeman and Company, pp.1095

Banisi, S., 1994; *On-Line Phase Holdup Measurement and Analysis in Flotation Columns*; Ph.D. thesis, McGill University, Canada

Barrow, G.M., 1973; *Physical Chemistry*, McGraw Hill Book Co., pp.787

Boutin, P. and Wheeler, D.A., 1967; Column Flotation; *Mining World*, vol.20, No.3, pp.47-50

Braunstein, J., and Robbins, G.D., 1971; Electric Conductance Measurements and Capacitive Balance; *J. Chem. Ed.*, vol.48, No.1, pp.52-59

Bridge, A.G., Lapidus, L. and Elgin, J.C., 1964; The Mechanics of Vertical Gas-Liquid Fluidized System 1: Countercurrent Flow; *AIChE J.*, vol.10, pp.819-826

Clark, N.N., Atkinson, C.M. and Flemmer, R.L.C., 1987; Turbulent Circulation in Bubble Columns; *AIChE J.*, vol.33, No.3, pp.515-518

Clift, R., Grace, J.R., and Weber, M.E., 1978; *Bubbles, Drops, and Particles*; Academic Press, New York

Clift, R. and Grace, J.R., 1985; Continuous Bubbling and Slugging; in *Fluidization*, 2nd Edition, (eds. Davidson, J.F., Clift, R. and Harrison, D.), Academic, London, pp.73-132

Cole. R.H., and Coles, J.S., 1964; *Physical Principles of Chemistry*; W.H. Freeman and Company, pp.795

Collins, R., 1967; The Effect of a Containing Cylindrical Boundary on the Velocity of a Large Gas Bubble in a Liquid; *J. Fluid Mech.*, vol.28, pp.97

Condon, E.U. (Ed.), 1967; *Handbook of Physics*, Chapter 9; McGraw Hill Book Co., pp.146-169

Crozier, R.D. 1992; *Flotation - Theory, Reagents and Ore Testing*; Pergamon Press

Davidson, J.F. and Harrison, D., 1966; The Behaviour of a Continuity Bubbling Fluidized Bed; *Chem. Eng. Sci.*, vol.21, pp.273

Davies, R.M. and Taylor, G.I., 1950; The Mechanics of Large Bubbles Rising Through Extended Liquids and Through Liquids in Tubes; *Proc. Roy. Soc.*, vol.A200, pp.375-390

Dobby, G.S. and Finch, J.A., 1985; Mixing Characteristics of Industrial Flotation Columns; *Chem. Eng. Sci.*, vol.40, No.7, pp.1061-1068

Dobby, G.S. and Finch, J.A., 1986; Particle Collection in Columns - Gas Rate and Bubble Size Effects; *Canadian Metall. Q.*, Vol.25, No.1, pp.9-13

Dobby, G.S., Yianatos, J.B. and Finch, J.A., 1988; Estimation of Bubble Diameter in Flotation Columns from Drift Flux Analysis; *Canadian Metall. Q.*, vol.27, No.2, pp.85-90

Dow Chemical Company, 1976; *Flotation Fundamentals and Mining Chemicals*; Dow Chemical Company

Edgar, C.B.Jr., 1966; *AEC Report* No.NYO-3114-14 by G.B.Wallis, pp.19-21

Ergun, S., 1952; Fluid Flow Through Packed Columns; *Chem. Eng. Prog.*, vol.48, No.2, pp.89-94

Fan, L.S., 1989; *Gas - Liquid - Solid Engineering*; Butterworths, Boston

Finch, J.A. and Dobby, G.S., 1990a; *Column Flotation*; Pergamon Press, New York

Finch, J.A. and Dobby, G.S., 1990b; Column Flotation: A Selected Review; in *Workshop on Sulphide Flotation*, Lulea, Sweden, pp.149-160

Finch, J.A., Uribe-Salas, A. and Xu, M., 1994; Column Flotation: A Selected Review Part 3; in *Flotation (Science and Engineering)*, (Ed. Kostas Matis), to be published

Flint, I.M., MacPhail, P. and Dobby, G.S., 1988; Aerosol Frother Addition Column Flotation; *C.I.M. Bulletin*, vol.81, No.913, pp.81-84

Freedman, W. and Davidson, J.B., 1969; Holdup and Liquid Circulation in Bubble Columns; *Trans. Instn. Chem. Engrs.*, vol.47, pp.251-262

Gahl, R., 1916; History of the Flotation Process at Inspiration; *Trans. A.I.M.E.*, vol.37, pp.577-630

Gaudin, A.M., 1957; *Flotation* (2nd ed.); McGraw-Hill, New York

Gilmont, R., and Walton, R.F., 1956; New Design of an Electrolytic Cell for the Study of Electroplating Phenomena; *Jour. Electrochem. Soc.*, vol.103, No.10, pp.549-552

Glasstone, S., 1930; *The Electrochemistry of Solutions*; Methuen & Co. Ltd. pp.476

Glasstone, S., 1942; *An Introduction to Electrochemistry*; D Van Nostrand Company, Inc. pp.557

Hadamard, J., 1911; *Compl. Rend. Acad. Sci. Paris*, vol.152, pp.1735-1738

Harriott, P. and Simone, S., 1983; Fluidizing Fine Powders; in *Handbook of Fluids in Motion*, (eds. Cheremisinoff, N.P., and Gupta, R.), Ann Arbor Science, Michigan, pp.653 - 664

Hewitt, G.G., 1978; *Measurement of Two Phase Flow Parameters*; Academic Press, chpt.XI, pp.120-127

Hills, J.H., 1974; Radial Non-uniformity of Velocity and Voidage in a Bubble Column; *Trans. Instn. Chem. Engrs.*, vol.52, pp.1-9

Hills, J.H., 1976; The Operation of a Bubble Column at High Throughput, I. Gas Holdup Measurements; *Chem. Eng. J.*, vol.12, No.89

Hills, J.H. and Darton, R.C., 1976; The Rising Velocity of a Large Bubble in a Bubble Swarm; *Trans. Instn. Chem. Engrs.*, vol.54, 256-264

Kasper, C., 1940; The Theory of the Potential and the Technical Practice of Electrodeposition; *Trans. Electrochem. Soc.*, vol.77, pp.353-384; vol.78, pp.131-161

Klassen, V.I. and Mokrousov, V.A., 1963; *An Introduction to the Theory of Flotation*; Butterworths, London

Kunii, D. and Levenspiel, O., 1969; *Fluidization Engineering*; Robert E. Krieger, Florida

Ladenburg, R., 1907; *Ann. Physik*, vol.23, pp.447

Levine, I.N., 1988; *Physical Chemistry*; McGraw Hill Book Co., pp.920

Lockett, M.J. and Kirkpatrick, R.D., 1975; Ideal Bubbly Flow and Actual Flow in Bubble Columns; *Trans. Instn. Chem. Engrs.*, vol.53, pp.267-273

Lord Rayleigh, 1892; On the Influence of Obstacles Arranged in Rectangular Order Upon the Properties of a Medium; *Phil. Mag.*, Vol.34, pp.481-502

Marchese, M.M., 1991; *Hydrodynamic Study of a Downwards concurrent Bubble Column*; Master thesis, McGill University, Canada

Marrucci, G., 1965; Rising Velocity of a Swarm of Spherical Bubbles; *Ind. Eng. Chem. Fund.*, vol.4, pp.224

Maxwell, J.C., 1892; *A Treatise of Electricity and Magnetism*, 3rd Edn.; Vol.1, Part II, Chapter IX, pp.435-449; Oxford University Press, London.

Meredith, R.E., and Tobias, C.W., 1960; Resistance to Potential Flow through a Cubical Array of Spheres; *J. Appl. Phys.*, vol.31, No.7, pp.1270-1273

Miller, D.N., 1980; Gas Holdup and Pressure Drop in Bubble Column Reactors; *Ind. Eng. Chem. Process Des. Dev.*, vol.19, pp.371-376

Miyauchi, T. and Shyu, C.N., 1970; Flow of Fluid in Gas Bubble Columns; *Kagaku Kogaku*, vol.34, pp.958

Nassos, G.P. and Bankoff, S.G., 1967; Slip Velocity Ratios in An Air-Water System under Steady-State and Transient Conditions; *Chem. Eng. Sci.*, Vol.22, pp.661-667

Nicklin, D.J., 1962; Two-Phase Bubble Flow; *Chem. Eng. Sci.*, Vol.17, pp.693-702

Olson, R.M., 1980; *Essential of Engineering Fluid Mechanics*, 4th Edition; Harper & Row, New York

Parker, J.D., Boggs, J.H. and Blick, E.F., 1969; *Introduction to Fluid Mechanics and Heat Transfer*; Addison - Wesley, Massachusetts

Pavlov, V.P., 1965; *Khim. Prom.*, No.9, pp.698

Radovich, N.A. and Moissis, R.; 1962; The Transition from Two-Phase Bubble Flow to Slug Flow; *MIT Report* 7-7673-22

Richardson, J.F. and Zaki, W.N., 1954; Sedimentation and Fluidization: part I; *Trans. Insl. Chem. Engrs.*, vol.32, pp.35-53

Rybezynski, W., 1911; On the Translatory Motion of a Fluid Sphere in a Viscous Medium (in German); *Bull. Int. Acad. Pol. Sci. Leff. Cl. Sci. Math. Natur.*, Ser.A, pp.40

Schiller, L. and Naumann, A., 1933; *Z. Ver. Dtsch. Ing.*, vol.77, pp.318

Shah, Y.T. and Deckwer, W.D., 1981; Scale-up Aspects of Fluid-Fluid Reaction; in *Scale-up in Chemical Process Industries* (ed. Kabel, R. and Bisio, A.), John Wiley

Shah, Y.T., Kelkar, B.G. and Godbole, S.P., 1982; Design Parameters Estimation for Bubble Column Reactors; *AIChE Jorlrnal*, vol.28, No.3, 353-379

Shames, I., 1962; *Mechanics of Fluids*; McGraw - Hill, New York

Shen, G., Uribe-Salas, A., Ahmed, N. and Finch, J.A., 1991; Measurement of Dynamic Gas Holdup in a Bubble Column; in *Computer Applications in the Mineral Industry*, vol.2 (eds. Poulin, R., Pakalnis, R.C.T., and Mular, A.L.), Proceedings of the Second Canadian Conference on Computer Applications in the Mineral Industry, Vancouver, Canada, Sept. 15-18, 1991, pp.287-298

Stokes, G.G., 1880; *Mathematical and Physical Papers*; vol.1, Cambridge University Press, London

Summers, A., Xu, M. and Finch, J.A., 1992; *Jameson Cell testwork*; report to Falconbridge Ltd., McGill University, Canada

Tien, C., 1983; Deep Bed Filtration; in *Handbook of Fluids in Motion*, (eds. Cheremisinoff, N.P., and Gupta, R.), Ann Arbor Science, Michigan, pp.969-1000

Turner, J.C.R., 1966; On Bubble Flow in Liquids and Fluidized Beds; *Chem. Eng. Sci.*, vol.21, pp.971

Turner, J.C.R., 1976; Two-Phase Conductivity- The Electrical Conductance of Liquid Fluidized Beds of Spheres; *Chem. Eng. Sci.*, vol.31, pp.487-492

Ueyama, K. and Miyauchi, T., 1977; Behavior of Bubbles and Liquid in a Bubble Column; *Kagaku Kogaku Ronbunshu*, vol.3, pp.19

Ueyama, K. and Miyauchi, T., 1979; Properties of Recirculating Turbulent Two Phase Flow in Gas Bubble Columns; *AIChE J.*, vol.25, pp.258-266

Uribe-Salas, A., 1991; *Process Measurements in Flotation Columns Using Electrical Conductivity*; Ph.D. thesis, McGill University, Canada

Uribe-Salas, A., Gomez, C.O. and Finch, J.A., 1991; Gas holdup measurement in flotation columns using electrical conductivity; *Can. Met. Ouart.*, vol.30, No.4, pp.201

Uribe-Salas, A., Gomez, C.O. and Finch, J.A., 1992; Axial Gas Holdup Profiles in Flotation Columns; in *Proceedings of 42nd. Canadian Chemical Engineering Conference*, Toronto, Ontario, Canada, Oct. 18-21, 1992

Wagner, C., 1962; The Scope of Electrochemical Engineering; in *Advances in Electrochemistry and Electrochemical Engineering*, Vol.2, (ed. Tobias, C.W.), pp.1-14; Inerscience Publishers, New York

Wallis, G.B., 1962; *Proceedings of the Symposium on the Interaction between Fluids and Particles*; (ed. Rottenberg, P.A.); London: Institution of Chemical Engineers

Wallis, G.B., 1969; *One Dimensional Two-Phase Flow*; McGraw-Hill, New York

Whalley, P.B. and Davidson, J.F., 1974; Liquid Circulation in Bubble Columns; *Inst. Chem. Eng. Symp. Ser.*, No.38

Whalley, P.B., 1987; *Boiling, Condensation, and Gas - Liquid Flow*; Oxford University Press, Oxford

Wheeler, D.A., 1966; Big Flotation Column Mill Tested; *E & MJ*, vol.167, No.11, pp.98-99

Wheeler, D.A., 1988; Historical View of Column Flotation Development; in *Column Flotation '88* (ed., Sastry, K.V.S.), SME Annual Meeting Phoenix, Arizona, pp.3-4

Xu, M. and Finch, J.A., 1989; Effect of Sparger Surface Area on Bubble Diameter in Flotation Columns; *Canadian Metall. Q.*, vol.28, No.1, pp.1-6

Xu, M., Uribe-Salas, A., Finch, J.A. and Gomez, C.O., 1989; Gas Rate Limitation in Column Flotation; in *Processing of Complex Ores* (Eds. Dobby, G.S. and Rao, S.R.), pp.387-407

Xu, M., 1990; *Radial Gas Holdup Profile and Mixing in the Collection Zone of Flotation Columns*; Ph.D. thesis, McGill University, Canada

Xu, M., Uribe-Salas, A. and Finch, J.A., 1991; Maximum Gas and Bubble Surface Rates in Flotation Columns; *Int. J. Min. Proc.*, vol.32, pp.233

Xu, M. and Finch, J.A., 1992; Measurement of Radial Gas Holdup Profiles in Flotation Columns; *Int. J. Min. Proc.*, vol.36, No.3/4, pp.229

Yamagoshi, T., 1969; B.S. thesis; University of Tokyo, Japan

Yianatos, J.B., Laplante, A.R. and Finch, J.A, 1985; Estimation of Local Gas Holdup in the Bubbly and Froth Zones; *Chem. Engng. Sci.*, vol.40, No.10, pp.1965-1968

Yianatos, J.B., Finch, J.A. and Laplante, A.R., 1986; Holdup Profile and Bubble Size Distribution of Flotation Column Froths; *Can. Met. Quart.*, vol.25, No.1, pp.23-29

Yianatos, J.B., 1987; *Column Flotation Froths*; Ph.D. thesis, McGill University, Canada

Yianatos, J.B., Finch, J.A. and Laplante, A.R., 1987; *Cleaning Action in Column Flotation Froths*; Trans. I.M.M., vol.96, pp.C199-C205

Yianatos, J.B., Finch, J.A., Dobby, G.S. and Xu, M., 1988; Bubble Size Estimation in a Bubble Swarm; *J. Colloid & Interface Sci.*, vol 126, No.1, pp.37-44

Yianatos, J.B. and Finch, J.A., 1990; Gas Holdup vs. Gas Rate in the Bubbly Regime; *Int. J. Min. Process.*, vol.29, pp.141-146

Yoshitome, H., 1967; Dr. Eng. Dissertation, Tokyo Inst. Technol., Japan

Zheng, Q.Y. and Lu, Z.Q., 1979; *Fluid Mechanics* (in Chinese); Mechanical Engineering Press, Beijing, China

Zhou, Z.A. and Egiebor, N.O., 1993; Prediction of axial gas holdup profiles in flotation columns; *Minerals Eng.*, vol.6, No.3, pp.307-312

Zhou, Z.A., Egiebor, N.O. and Plitt, L.R., 1993a; Frother Effects on Bubble Size Estimation in a Flotation Column; *Minerals Eng.*, vol.6, No.1, pp.55-67

Zhou, Z.A., Egiebor, N.O. and Plitt, L.R., 1993b; Frother Effects on Bubble Motion in a Swarm; *Canadian Metallurgical Quarterly*, vol.32, No.2, pp.89-96

APPENDIX 1

Computer Control and Data Acquisition Program

The following BASIC program was used for the control and data acquisition of the experiments. In the program, the resistances in Cells 1 - 6 and pressure are measured and recorded in the files, which can be inputted and analyzed by the data analysis program shown in Appendix 2. The program was compiled using QuickBASIC 4.0 under DOS system.

```
'*****************************************************************
'*    Control and Data Acquisition Program (QuickBASIC 4.0)
'*                    Gang Shen
'*                McGill University
'*****************************************************************
'
DECLARE SUB Initial ()
DECLARE SUB linear (mint, maxt, A, B, rxy)
DECLARE SUB DrawFram (xmin%, xmax%, ymin!, ymax!, xx!, YY!)
DECLARE SUB DrawLine (ymin!, xx!, YY!, tt1!, gg1!, c)
DECLARE SUB pump (PCH%, PD%())
DECLARE SUB Trans (c$, num)
DECLARE SUB flow (flowrate)
DECLARE SUB speedpump ()
DECLARE SUB show (B, R1, AP1, BP1, AP2, BP2)
DECLARE SUB das8 (mode%, BYVAL dummy%, flag%)
DECLARE SUB GetFileName (FTemp$)
'
'*****************************
'*      Main program
'*****************************
'
DIM D%(6), A%(10)
DIM A1%(2000), A2%(2000), A3%(2000), A4%(2000)
DIM A5%(2000), A6%(2000), A7%(2000), A8%(2000)
DIM A9%(2000), A10%(2000), A11%(2000), A12%(2000)
DIM P%(2, 2000), PD%(10)
DIM res!(2000), t!(2000), rs(10)
DIM AR(40), BR(40), rxy(40)

COMMON SHARED D%(), A%(), res!(), t!()

CLS
SCREEN 9
COLOR 11, 7

R1 = 5766! / 1.056          'resistor between convertor and ground
light = 32                  'light for record of VHS
```

```
B = 185

AP1 = .005748              'pressure - voltage for pressure sensor
BP1 = -.02571
AP2 = .001745
BP2 = .2151

c% = 2
CLS                        'Make an experiment
LOCATE 9, 15
PRINT "*************************************************************";
LOCATE 10, 15
PRINT "*.        Welcome to Data Acquisition System          *";
LOCATE 11, 15
PRINT "*************************************************************";

CALL Initial
OUT &H40D, 128             'Switch on V1

LOCATE 14, 20
PRINT "Do you want to adjust the PUMP SPEEDS ";
INPUT PS$

IF PS$ = "y" OR w$ = "Y" THEN
  CALL speedpump
END IF

CLS
LOCATE 10, 22
PRINT "Do you want to SEE conditions of column ";
INPUT w$
IF w$ = "y" OR w$ = "Y" THEN
  CALL show(B, R1, AP1, BP1, AP2, BP2)
END IF

CLS
LOCATE 10, 20
PRINT "The sampling rate is 1.5 samples per second per cell."
LOCATE 12, 20
PRINT "The maximum sampling time is 1200 seconds (20 min.)."

DO
LOCATE 14, 20
INPUT "Please enter the sampling time (seconds): "; NS%
LOOP WHILE NS% < 1 OR NS% > 1200

FOR i% = 1 TO INT(NS% * 3 / 2) + 1          'calculate time array
  k = i% - 1
  t!(i%) = .666666 * k
  IF k = INT(k / 3) * 3 THEN t!(i%) = 2! * k / 3
NEXT i%

'Set mode 5 going and acquire data
NC = 8                     'conversions from channel 0 to 7
MD% = 5                      'Mode 5, do conversions direct to array
D%(0) = VARPTR(A%(1))      'Starting location of array
```

```
D%(1) = NC                'Number of conversions

CLS
LOCATE 9, 12
INPUT "Do you want to use the REMOTE control? (Y/N) ", R$
IF R$ = "Y" OR R$ = "y" THEN
  LOCATE 11, 12
  PRINT "The data acquisition system STANDS BY.";
  DO
     CALL das8(MD%, VARPTR(D%(0)), flag%)
     IF flag% <> 0 THEN PRINT "Error in acquiring data": STOP
     digi = A%(8)
  LOOP WHILE (digi > 400)              'read signal from the remote switch
END IF

CLS
LOCATE 8, 20
PRINT "Data Acquisition starts at "; TIME$
LOCATE 10, 20
PRINT "Please wait!"

OUT &H40D, 128 + light                'V1 + light

FOR i = 1 TO INT(NS% * 3 / 2) + 1     'Beginning of data acquisition

  IF i = 16 THEN OUT &H40D, 64 + light    'V2 = 64
  'At the 10th V2 on and V1 off

  IF i = 46 THEN OUT &H40D, light
  'At the 30th V2 and V1 off

  'reading data from the electrode 1, 2 (cell 1)
  OUT &H40C, 5                    'switch on relay No.1, 3
     FOR j = 1 TO B - 1
     NEXT j

  CALL das8(MD%, VARPTR(D%(0)), flag%)
  IF flag% <> 0 THEN PRINT "Error in acquiring data": STOP

  A1%(i) = A%(1)
  A2%(i) = A%(2)

  'reading data from the electrode 2, 3 (cell 2)
  OUT &H40C, 18                   'switch on relay No.2, 5
     FOR j = 1 TO B - 1
     NEXT j

  CALL das8(MD%, VARPTR(D%(0)), flag%)
  IF flag% <> 0 THEN PRINT "Error in acquiring data": STOP

  A3%(i) = A%(1)
  A4%(i) = A%(2)

  'reading data from the electrode 3, 4 (cell 3)
  OUT &H40C, 72                   'switch on relay No.4, 7
     FOR j = 1 TO B - 1
```

```
        NEXT j

    CALL das8(MD%, VARPTR(D%(0)), flag%)
    IF flag% <> 0 THEN PRINT "Error in acquiring data": STOP

    A5%(i) = A%(1)
    A6%(i) = A%(2)

    'reading data from the electrode 4, 5 (cell 4)
    OUT &H40C, 32                'switch on relay No.6
    OUT &H40E, 1                 'switch on relay No.9
        FOR j = 1 TO B - 1
        NEXT j

    CALL das8(MD%, VARPTR(D%(0)), flag%)
    IF flag% <> 0 THEN PRINT "Error in acquiring data": STOP

    A7%(i) = A%(1)
    A8%(i) = A%(2)

    'reading data from the electrode 5, 6 (cell 5)
    OUT &H40C, 128               'switch on relay No.8
    OUT &H40E, 4                 'switch on relay No.11
        FOR j = 1 TO B - 1
        NEXT j

    CALL das8(MD%, VARPTR(D%(0)), flag%)
    IF flag% <> 0 THEN PRINT "Error in acquiring data": STOP

    A9%(i) = A%(1)
    A10%(i) = A%(2)

    OUT &H40C, 0                 'switch off first group of relay

    'reading data from the electrode 6, 7 (cell 6)
    OUT &H40E, 10                'switch on relay No.10, 12
        FOR j = 1 TO B - 1
        NEXT j

    CALL das8(MD%, VARPTR(D%(0)), flag%)
    IF flag% <> 0 THEN PRINT "Error in acquiring data": STOP

    A11%(i) = A%(1)
    A12%(i) = A%(2)

    P%(1, i) = A%(3)
    P%(2, i) = A%(4)

    OUT &H40E, 0                 'switch off second group of relay

NEXT i

OUT &H40C, 0        'switch off relay boards
OUT &H40E, 0        '(first and second groups)

OUT &H40D, 0        'switch off the light and valves
```

```
   LOCATE 12, 20
   PRINT "Data Acquisition terminates at "; TIME$

   LOCATE 14, 20
   INPUT "Do you want to save it without analysis ?", c$
   IF c$ = "Y" OR c$ = "y" THEN GOTO S

   '———— Data processing ————
A:
   CLS
   DO
   LOCATE 6, 2
   PRINT "Which cell do you";
   LOCATE 7, 2
   PRINT "want to read";
   LOCATE 8, 2
   INPUT "(cell 1-6): ", cell%
   LOOP WHILE cell% < 1 OR cell% > 6
   LOCATE 2, 30
   PRINT USING "Cell number: #"; cell%

   FOR i% = 1 TO INT(NS% * 3 / 2) + 1          'calculate R(cell 1-6)
     IF cell% = 1 THEN res!(i%) = R1 * (A2%(i%) * 1! / A1%(i%) - 1!)
     IF cell% = 2 THEN res!(i%) = R1 * (A4%(i%) * 1! / A3%(i%) - 1!)
     IF cell% = 3 THEN res!(i%) = R1 * (A6%(i%) * 1! / A5%(i%) - 1!)
     IF cell% = 4 THEN res!(i%) = R1 * (A8%(i%) * 1! / A7%(i%) - 1!)
     IF cell% = 5 THEN res!(i%) = R1 * (A10%(i%) * 1! / A9%(i%) - 1!)
     IF cell% = 6 THEN res!(i%) = R1 * (A12%(i%) * 1! / A11%(i%) - 1!)
   NEXT i%

   ' End of processing data

   IF c% = 1 THEN NS% = INT((Linenum - 2) / 3 * 2)

   xmin% = 0
   xmax% = NS%

   ymin! = res!(1)                    'find max. and min. values of y axis
   ymax! = res!(1)
   FOR i = 2 TO INT(NS% * 3 / 2) + 1
     IF res!(i) > ymax! THEN ymax! = res!(i)
     IF res!(i) < ymin! THEN ymin! = res!(i)
   NEXT i
   ymax! = INT((ymax! + 1500!) / 1000!) * 1000!
   ymin! = INT((ymin! - 1500!) / 1000!) * 1000!
   IF ymax! > 90000! THEN ymax! = 90000!
   IF ymin! < 0 OR ymin! > ymax! THEN ymin! = 0!

   CALL DrawFram(xmin%, xmax%, ymin!, ymax!, xx!, YY!)

   FOR i = 1 TO INT(NS% * 3 / 2) + 1                  'draw data points
     tt1! = t!(i)
     gg1! = res!(i)
     CALL DrawLine(ymin!, xx!, YY!, tt1!, gg1!, 11)
   NEXT i
```

```
LOCATE 10, 2
PRINT "Do you want";
LOCATE 11, 2
PRINT "to SEE another";
LOCATE 12, 2
INPUT "cell"; H$
IF H$ = "Y" OR H$ = "y" THEN GOTO A

IF c% = 2 THEN
  LOCATE 10, 2
  PRINT "Do you want";
  LOCATE 11, 2
  PRINT "to SAVE this  ";
  LOCATE 12, 2
  INPUT "file and leave"; H$
  IF H$ = "Y" OR H$ = "y" THEN GOTO S
END IF

LOCATE 14, 2
PRINT "Input START";
LOCATE 15, 2
PRINT "point of First";
DO
  LOCATE 16, 2
  INPUT "line :"; firstrp%
LOOP WHILE firstrp% < 1 OR firstrp% > (INT(NS% * 3 / 2) + 1)

LOCATE 18, 2
PRINT "Input END";
LOCATE 19, 2
PRINT "point of First";
DO
  LOCATE 20, 2
  INPUT "line :"; endrp%
LOOP WHILE endrp% < firstrp% OR endrp% > (INT(NS% * 3 / 2) + 1)

fr = 0!
FOR i = firstrp% TO endrp%
  fr = fr + res!(i)
NEXT i
fr = fr / (endrp% - firstrp% + 1)

LINE (1, 180)-(154, 310), 0, BF
LOCATE 14, 2
PRINT "Input START";
LOCATE 15, 2
PRINT "point of Second";
DO
  LOCATE 16, 2
  INPUT "line :"; sdrp%
LOOP WHILE sdrp% < 1 OR sdrp% > (INT(NS% * 3 / 2) + 1)

LOCATE 18, 2
PRINT "Input END";
LOCATE 19, 2
PRINT "point of Second";
```

```
DO
  LOCATE 20, 2
  INPUT "line :"; edsdrp%
LOOP WHILE edsdrp% < sdrp% OR edsdrp% > (INT(NS% * 3 / 2) + 1)

sr = 0!
FOR i = sdrp% TO edsdrp%
  sr = sr + res!(i)
NEXT i
sr = sr / (edsdrp% - sdrp% + 1)

LINE (1, 22)-(154, 310), 0, BF
LOCATE 4, 2
PRINT "Ave. resistance in";
LOCATE 5, 2
PRINT "First line =";
LOCATE 6, 2
PRINT "  "; fr; " ohm";

LOCATE 7, 2
PRINT "Ave. resistance in";
LOCATE 8, 2
PRINT "Second line =";
LOCATE 9, 2
PRINT "  "; sr; " ohm";

IF sr <= fr THEN
  lr = sr
  hr = fr
ELSE
  lr = fr
  hr = sr
END IF

GA = lr / hr                    'Conductance = 1 / Resistance
EG = (1 - GA) / (1 + .5 * GA) * 100!
LOCATE 11, 2
PRINT USING "Eg =##.###%"; EG

LOCATE 12, 2
PRINT "Do you want to";
LOCATE 13, 2
INPUT "do REGRESSION"; H$
IF H$ = "N" OR H$ = "n" THEN GOTO B

mid = .5 * (fr + sr)
mindif = 1!
j = 1
FOR i = firstrp% TO edsdrp%
  aa = ABS((res!(i) - mid) / fr)
  IF aa < mindif THEN
      mindif = aa
      j = i
  END IF
NEXT i
```

```
tt1! = t!(j)
gg1! = res!(j)
CALL DrawLine(ymin!, xx!, YY!, tt1!, gg1!, 12)

LOCATE 12, 2
PRINT "The mid. point";
LOCATE 13, 2
PRINT USING "number = ####    "; j

LOCATE 15, 2
PRINT "Do you want to";
LOCATE 16, 2
PRINT "CHOSE A POINT ";
LOCATE 17, 2
INPUT "as FIRST point"; pt$
IF pt$ = "Y" OR pt$ = "y" THEN
  LOCATE 19, 2
  PRINT "Please input ";
  LOCATE 20, 2
  INPUT "POINT NUMBER: ", pt
  fr = res!(pt)
END IF

LINE (1, 180)-(154, 310), 0, BF
LOCATE 15, 2
PRINT "Please input  ";
LOCATE 16, 2
PRINT "the BEGINNING  ";
LOCATE 17, 2
INPUT "point: ", begp
LOCATE 19, 2
PRINT "Please input ";
LOCATE 20, 2
INPUT "the END point: ", endp

LINE (1, 22)-(154, 310), 0, BF
LOCATE 4, 2
PRINT "Regression: ";

LOCATE 6, 2
PRINT "Begin at :"; begp;
LOCATE 7, 2
PRINT "End at   :"; endp;

CALL linear(begp, endp, aa, bb, rr)

LOCATE 9, 2
PRINT "Rxy = "; rr;

t1 = (fr - aa) / bb
t2 = (sr - aa) / bb
time = t2 - t1
LOCATE 11, 2
PRINT "First point=";
LOCATE 12, 2
PRINT "   "; t1; "s";
```

```
   LOCATE 13, 2
   PRINT "Second point=";
   LOCATE 14, 2
   PRINT "   "; t2; "s";

   LOCATE 15, 2
   PRINT "Diff. ="; time; "s";
   LOCATE 16, 2
   PRINT "Velocity =";
   LOCATE 17, 2
   PRINT "   "; 51! / time; "cm/s";

B: LOCATE 19, 2
   PRINT "Would you like";
   LOCATE 20, 2
   PRINT "to see another";
   LOCATE 21, 2
   INPUT "CELL (Y/N)? ", c$

   IF c$ = "Y" OR c$ = "y" THEN GOTO A

   IF c% = 1 THEN
    LOCATE 19, 2
    PRINT "Would you like";
    LOCATE 20, 2
    PRINT "to READ another";
    LOCATE 21, 2
    INPUT "FILE (Y/N)? ", c$
    IF c$ = "Y" OR c$ = "y" THEN
        CLS
        CALL GetFileName(FileN$)        ' Input file name.
        GOTO A
    END IF
   END IF

   '-------- Generate a .PRN file --------
   CLS
   LOCATE 11, 20
   INPUT "Do you want to save data files? ", c$
   IF c$ = "N" OR c$ = "n" THEN
    OUT &H40D, 0            'Switch on the valve of air flow
    SCREEN 0
    END
   END IF

S: CLS
   LOCATE 12, 20
   INPUT "Enter NAME of output file (auto. PRN ext.) : "; FILE$

   FOR j% = 1 TO 6                          'Data output for Cell 1-6

   F$ = FILE$ + "C" + CHR$(j% + 48) + ".PRN"
   OPEN F$ FOR OUTPUT AS #2

   FOR i% = 1 TO INT(NS% * 3 / 2) + 1
    IF j% = 1 THEN res!(i%) = R1 * (A2%(i%) * 1! / A1%(i%) - 1!)
```

```
  IF j% = 2 THEN res!(i%) = R1 * (A4%(i%) * 1! / A3%(i%) - 1!)
  IF j% = 3 THEN res!(i%) = R1 * (A6%(i%) * 1! / A5%(i%) - 1!)
  IF j% = 4 THEN res!(i%) = R1 * (A8%(i%) * 1! / A7%(i%) - 1!)
  IF j% = 5 THEN res!(i%) = R1 * (A10%(i%) * 1! / A9%(i%) - 1!)
  IF j% = 6 THEN res!(i%) = R1 * (A12%(i%) * 1! / A11%(i%) - 1!)
NEXT i%

FOR i% = 1 TO INT(NS% * 3 / 2) + 1
  PRINT #2, USING "####.###  ########.#"; t!(i%); res!(i%)
NEXT i%

CLOSE #2
NEXT j%

F$ = FILE$ + "P.PRN"
OPEN F$ FOR OUTPUT AS #3

FOR i% = 1 TO INT(NS% * 3 / 2) + 1
  pre1 = (P%(1, i%) / 4096! - BP1) / AP1
  pre2 = (P%(2, i%) / 4096! - BP2) / AP2
  PRINT #3, USING "####.###  ####.# ####.#"; t!(i%); pre1; pre2
NEXT i%

CLOSE #3

OUT &H40D, 0              'Switch off valves of air flow

PD%(0) = 0
PD%(1) = 0
CALL pump(PCH%, PD%())

SCREEN 0

END

SUB DrawFram (xmin%, xmax%, ymin!, ymax!, xx!, YY!)
'**************************************
'*      diagram frame drawing         *
'**************************************
'
DIM xlable%(10)
DIM ylable!(10)

LINE (156, 38)-(638, 310), 0, BF        'clean the graphic window
LINE (210, 49)-(631, 275), 1, B         'draw the diagram frame

'draw the y axis intervale
FOR i% = 1 TO 4
  LINE (210, 275 - i% * 45)-(214, 275 - i% * 45), 1
NEXT i%

'draw the x axis intervale
FOR i% = 1 TO 4
  LINE (210 + i% * 84, 275)-(210 + i% * 84, 49), 1
NEXT i%
```

```
'calculate x axis divition
XL% = (xmax% - xmin%) / 5
xlable%(1) = xmin%
FOR i% = 1 TO 5
  xlable%(i% + 1) = xlable%(i%) + XL%
NEXT i%

'calculate y axis division
yl! = (ymax! - ymin!) / 5
ylable!(1) = ymin!
FOR i% = 1 TO 5
  ylable!(i% + 1) = ylable!(i%) + yl!
NEXT i%

'print y lables on the frame
LOCATE 4, 22
PRINT USING "#####"; ylable!(6)
LOCATE 7, 22
PRINT USING "#####"; ylable!(5)
LOCATE 11, 22
PRINT USING "#####"; ylable!(4)
LOCATE 14, 22
PRINT USING "#####"; ylable!(3)
LOCATE 17, 22
PRINT USING "#####"; ylable!(2)
LOCATE 20, 22
PRINT USING "#####"; ylable!(1)

'print x lables on the frame
LOCATE 21, 25
PRINT USING "####"; xlable%(1)
LOCATE 21, 36
PRINT USING "####"; xlable%(2)
LOCATE 21, 46
PRINT USING "####"; xlable%(3)
LOCATE 21, 57
PRINT USING "####"; xlable%(4)
LOCATE 21, 67
PRINT USING "####"; xlable%(5)
LOCATE 21, 76
PRINT USING "####"; xlable%(6)

'print y axis title
  LOCATE 10, 21: PRINT "O";
  LOCATE 11, 21: PRINT "h";
  LOCATE 12, 21: PRINT "m";

'print x axis title
LOCATE 22, 48
PRINT "Time (s)";

xmax% = xlable%(6)
ymax! = ylable!(6)

'calculate xx - x pixels / per unit
'          YY - y pixels / per unit
```

```
xx! = (631! - 210!) / (xmax% - xmin%)
YY! = (275! - 49!) / (ymax! - ymin!)

END SUB

SUB DrawLine (ymin!, xx!, YY!, tt1!, gg1!, c)
'*************************************
'*       draw a point sub.           *
'*************************************
'
'calculate x and y pixel of a point on the diagram
xpixel% = 210 + INT(tt1! * xx!)
ypixel% = 275 + INT(ymin! * YY!) - INT(gg1! * YY!)

'limit a point in the diagram frame
IF ypixel% < 49 THEN ypixel% = 49
IF ypixel% > 275 THEN ypixel% = 275

'draw a point
PSET (xpixel%, ypixel%), c

END SUB

SUB flow (flowrate)
'*******************************
'*   Read liquid flowrate
'*******************************
'
OPEN "COM1: 2400, N, 7, 1, ASC" FOR RANDOM AS #1
FOR i = 1 TO 666: NEXT i

c$ = INPUT$(LOC(1), #1)
bt = TIMER
CALL Trans(c$, dtf)

FOR i = 1 TO 5666: NEXT i

c$ = INPUT$(LOC(1), #1)
et = TIMER
CALL Trans(c$, dte)

flowrate = (dte - dtf) / (et - bt) * 60! / 1000!

LOCATE 2, 20
PRINT USING "W(f)= ######.### g; W(s)= ######.### g;"; dtf; dte
LOCATE 3, 20
PRINT USING "T(f)= #######.## s; T(s)= #######.## s;"; bt; et

CLOSE #1
END SUB

SUB GetFileName (FTemp$)
'*******************************
'*      Get a file name
'*******************************
'
```

```
LOCATE 1, 20
INPUT "Enter a file name (press ENTER to quit): ", FTemp$

END SUB

SUB Initial
'*****************************************
'*    Initiation for A/D and D/A
'*****************************************
'
OUT &H40F, &H80          'Initialize PA, PB and PC all outputs

'------- Set address of DAS-8 with mode 0 ----------------
D%(0) = &H300        'I/O address of DAS-8 (change to suit)
MD% = 0              'initialize mode
flag% = 0            'declare error variable
CALL das8(MD%, VARPTR(D%(0)), flag%)
IF flag% <> 0 THEN PRINT "Error in initialization": STOP

'------- Set PGA of DAS-8 with mode 19 ----------------
R = 11                       'Gain code is 9, range 0 - 10 V
VL = 0!: VH = 1!             '          11, range 0 - 1 V
MD% = 19                     '          13, range 0 - 0.1 V
D%(0) = R                    '          0, range -5 - +5 V
CALL das8(MD%, VARPTR(D%(0)), flag%)
IF flag% <> 0 THEN PRINT "Error in setting PGA": STOP

'------- Set timer rate with mode 10 ----------------
MD% = 10             'Mode 10 for setting counter configuration
D%(0) = 2            'Operate on counter #2
D%(1) = 3            'Configuration #2 = rate generator
CALL das8(MD%, VARPTR(D%(0)), flag%)
IF flag% <> 0 THEN PRINT "Error in setting counter 2 configuration": STOP
'
'Prompt user for desired sample rate
F = 4000             'sampling frequency, samples / per second
N = 1000! / F * 1000!
MD% = 11             'Mode 11 to load counter
D%(0) = 2            'Operate on counter #2
IF N < 32767 THEN D%(1) = N ELSE D%(1) = N - 65536!  'correct for integer
CALL das8(MD%, VARPTR(D%(0)), flag%)
IF flag% <> 0 THEN PRINT "Error in loading counter 2": STOP

'------- Set the channels with mode 1 ----------------
MD% = 1              'Set scan limits, mode 1
LL% = 0: D%(0) = LL%     'Set channel 0 to channel 7
UL% = 7: D%(1) = UL%
CALL das8(MD%, VARPTR(D%(0)), flag%)
IF flag% <> 0 THEN PRINT "Error in setting channel scan limits": STOP

END SUB

SUB linear (mint, maxt, A, B, rxy)
'*************************************
'*        Linear regression
'*************************************
```

```
'
DIM x(100), y(100)

nn = maxt - mint + 1
IF mint = 0 THEN mint = 1
IF nn > 100 THEN nn = 100
FOR i = 1 TO nn
  y(i) = res!(mint + i - 1)
  x(i) = t!(mint + i - 1)
NEXT i

xs = 0!
xxs = 0!
ys = 0!
yys = 0!
xys = 0!
FOR i = 1 TO nn
  xs = xs + x(i)
  xxs = xxs + x(i) * x(i)
  ys = ys + y(i)
  yys = yys + y(i) * y(i)
  xys = xys + x(i) * y(i)
NEXT i

lxx = xxs - xs * xs / nn
lyy = yys - ys * ys / nn
lxy = xys - xs * ys / nn
B = lxy / lxx
A = ys / nn - xs / nn * B
rxy = ABS(lxy / SQR(lxx * lyy))

END SUB

SUB pump (PCH%, PD%())
'*******************************
'*     Adjust pump speed
'*******************************
'
B% = 1024
FOR i% = 0 TO PCH%
  XH% = INT(PD%(i%) / 256)          'work out high byte
  XL% = PD%(i%) - 256 * XH%          'remainder = low byte
  OUT B% + 2 * i%, XL%              'write low byte to D/A
  OUT B% + 1 + 2 * i%, XH%           'write high byte & load D/A
NEXT i%

END SUB

SUB show (B, R1, AP1, BP1, AP2, BP2)
'*****************************************
'*    show resistances in Cells 1 - 6
'*****************************************
'
DIM rs(10)
tf = 0!
xmin% = 0
```

```
xmax% = 300
ymin! = 3000!
ymax! = 12000!
CALL DrawFram(xmin%, xmax%, ymin!, ymax!, xx!, YY!)

LOCATE 2, 28
PRINT "Press ENTER key to leave!"

LOCATE 6, 8: COLOR 9, 7: PRINT "Cell 1"
LOCATE 7, 8: COLOR 10, 7: PRINT "Cell 2"
LOCATE 8, 8: COLOR 11, 7: PRINT "Cell 3"
LOCATE 9, 8: COLOR 12, 7: PRINT "Cell 4"
LOCATE 10, 8: COLOR 13, 7: PRINT "Cell 5"
LOCATE 11, 8: COLOR 14, 7: PRINT "Cell 6"

COLOR 11, 7          'Set mode 5 going and acquire data
NC = 8               'conversions from channel 0 to 7
MD% = 5              'Mode 5, do conversions direct to array
D%(0) = VARPTR(A%(1))  'Starting location of array
D%(1) = NC           'Number of conversions


DO                   'Beginning of displaing the gas holdups
onechar$ = UCASE$(INKEY$)

 'reading data from the electrode 1, 2 (cell 1)
 OUT &H40C, 5                  'switch on relay No.1, 3
     FOR j = 1 TO B - 1
     NEXT j

 CALL das8(MD%, VARPTR(D%(0)), flag%)
 IF flag% <> 0 THEN PRINT "Error in acquiring data": STOP

 D1 = A%(1)
 D2 = A%(2)

 'reading data from the electrode 2, 3 (cell 2)
 OUT &H40C, 18                 'switch on relay No.2, 5
     FOR j = 1 TO B - 1
     NEXT j

 CALL das8(MD%, VARPTR(D%(0)), flag%)
 IF flag% <> 0 THEN PRINT "Error in acquiring data": STOP

 D3 = A%(1)
 D4 = A%(2)

 'reading data from the electrode 3, 4 (cell 3)
 OUT &H40C, 72                 'switch on relay No.4, 7
     FOR j = 1 TO B - 1
     NEXT j

 CALL das8(MD%, VARPTR(D%(0)), flag%)
 IF flag% <> 0 THEN PRINT "Error in acquiring data": STOP

 D5 = A%(1)
```

```
D6 = A%(2)

'reading data from the electrode 4, 5 (cell 4)
OUT &H40C, 32                    'switch on relay No.6
OUT &H40E, 1                     'switch on relay No.9
    FOR j = 1 TO B - 1
    NEXT j

CALL das8(MD%, VARPTR(D%(0)), flag%)
IF flag% <> 0 THEN PRINT "Error in acquiring data": STOP

D7 = A%(1)
D8 = A%(2)

'reading data from the electrode 5, 6 (cell 5)
OUT &H40C, 128                   'switch on relay No.8
OUT &H40E, 4                     'switch on relay No.11
    FOR j = 1 TO B - 1
    NEXT j

CALL das8(MD%, VARPTR(D%(0)), flag%)
IF flag% <> 0 THEN PRINT "Error in acquiring data": STOP

D9 = A%(1)
D10 = A%(2)

OUT &H40C, 0                     'switch off first group of relay

'reading data from the electrode 6, 7 (cell 6)
OUT &H40E, 10                    'switch on relay No.10, 12
    FOR j = 1 TO B - 1
    NEXT j

CALL das8(MD%, VARPTR(D%(0)), flag%)
IF flag% <> 0 THEN PRINT "Error in acquiring data": STOP

D11 = A%(1)
D12 = A%(2)

OUT &H40E, 0                     'switch off second group of relay

pre1 = (A%(3) / 4096! - BP1) / AP1
pre2 = (A%(4) / 4096! - BP2) / AP2
rs(7) = pre1 * 35
rs(8) = pre2 * 30

inter = 500
rs(1) = R1 * (D2 * 1! / D1 - 1!) + 3 * inter
rs(2) = R1 * (D4 * 1! / D3 - 1!) + 2 * inter
rs(3) = R1 * (D6 * 1! / D5 - 1!) + 1 * inter
rs(4) = R1 * (D8 * 1! / D7 - 1!) - 0 * inter
rs(5) = R1 * (D10 * 1! / D9 - 1!) - 1 * inter
rs(6) = R1 * (D12 * 1! / D11 - 1!) - 2 * inter

FOR i = 1 TO 6
    co = 8 + i
```

```
        gpt = rs(i)
        CALL DrawLine(ymin!, xx!, YY!, tf, gpt, co)
    NEXT i

    co = 15: gpt = rs(7)
        CALL DrawLine(ymin!, xx!, YY!, tf, gpt, co)
    co = 8: gpt = rs(8)
        CALL DrawLine(ymin!, xx!, YY!, tf, gpt, co)

LOCATE 14, 3: COLOR 15, 7: PRINT USING "P1 = ###.# cm H2O"; pre1
LOCATE 15, 3: COLOR 8, 7: PRINT USING "P2 = ###.# cm H2O"; pre2
COLOR 11, 7

    tf = tf + .6666

LOOP WHILE onechar$ = ""            'End of display

END SUB

SUB speedpump
    '************************************************
    '* Read liquid flowrate and adjust pump speed
    '************************************************
    '
    'PD% = data (range 0-4095), PCH% = channel (0-3), BASE% = I/O address
    DIM PD%(10)
    CLS
    B% = 1024
    PCH% = 1

    DO
        LOCATE 8, 20
        PRINT "Enter the pump speed (200 - 4090) :";
        INPUT speed%
    LOOP WHILE speed% > 4090 OR speed% < 200
    PD%(0) = speed%
    PD%(1) = speed%

    LOCATE 9, 20
    PRINT "1. Press U to increase pump speeds."
    LOCATE 10, 20
    PRINT "2. Press D to decrease pump speeds."
    LOCATE 11, 20
    PRINT "3, Press F to see flowrate."
    LOCATE 12, 20
    PRINT "4. Press Q to leave the pump control."

    k = 0!
    trate = 0!

    DO

    LOCATE 14, 20
    PRINT USING "Pump 1: Tailings ####."; PD%(0)
    LOCATE 15, 20
    PRINT USING "Pump 2: Wash water ####."; PD%(1)
```

```
    one$ = UCASE$(INKEY$)
    SELECT CASE one$

    CASE "F"
    CALL flow(rate)
    LOCATE 17, 20
    PRINT USING "Flowrate: ##.#### L/min."; rate
    trate = trate + rate
    k = k + 1!
    LOCATE 19, 20
    PRINT USING "Flowrate (avg) = ##.#### L/min. (##)"; trate / k; k

    CASE "U"
    IF PD%(0) < 4094 THEN
        PD%(0) = PD%(0) + 2
        PD%(1) = PD%(1) + 2
        CALL pump(PCH%, PD%())
    END IF

    CASE "D"
    IF PD%(1) > 2 THEN
        PD%(0) = PD%(0) - 2
        PD%(1) = PD%(1) - 2
        CALL pump(PCH%, PD%())
    ELSE
        PD%(0) = 0
        PD%(1) = 0
        CALL pump(PCH%, PD%())
    END IF

    CASE ELSE
    CALL pump(PCH%, PD%())

    END SELECT

    LOOP WHILE one$ <> "Q"

  END SUB

SUB Trans (c$, num)
'*****************************************
'*     Convert readings from balance
'*****************************************
'
E$ = RIGHT$(c$, 32)
FOR j = 1 TO 32
  i = 32 - j + 1
  R$ = MID$(E$, i, 1)
  IF R$ = "+" AND i < 25 THEN       'pick up the last number and
    w$ = MID$(E$, i + 1, 8)         'check if it is a complete number.
    num = VAL(w$)
    EXIT FOR
  END IF
NEXT j

END SUB
```

APPENDIX 2

Computer Data Analysis Program

The following BASIC computer program was used for the data analysis of the gas holdup, ε_g, and the interface velocity, u_{in}, in Cells 1 - 6. In this program, the input data files are the files generated by the control and data acquisition program shown in Appendix 1, and the calculated results can be saved in a file named by the user. The program was compiled using QuickBASIC 4.0 under DOS system.

```
'*************************************************************
'*        Data Analysis Program (QuickBASIC 4.0)
'*                  Gang Shen
'*               McGill University
'*************************************************************
'
DECLARE SUB FileSub (aa!(), t!(), FileN$, FileR$, linenum)
DECLARE SUB QuitProgram ()
DECLARE SUB RestoreW (x1%, y1%)
DECLARE SUB SaveW (x1%, y1%, x2%, y2%)
DECLARE SUB invert (lin%, col%, nchars%)
DECLARE SUB Drawinit ()
DECLARE SUB DrawFram (xmin%, xmax%, ymin!, ymax!, xx!, YY!)
DECLARE SUB DrawP (xbeg!, ymin!, xx!, YY!, xval!, yval!, C)
DECLARE SUB GetFileName (S$, GFN$)
DECLARE SUB Diagram (aa!(), t!(), linenum, ymin!, xx!, YY!)
DECLARE SUB clean (C$)
DECLARE SUB GetCell (C$, celln%, l$)
DECLARE SUB FindY (aa!(), cell%, linenum, ymax!, ymin!)
DECLARE SUB FindX (S1$, S2$, linenum, xmin%, xmax%, l$)
DECLARE SUB PrintC ()
DECLARE SUB Reg (aa!(), t!(), FileR$, linenum, ymin!, xx!, YY!)
DECLARE SUB Eg (aa!(), p(), E(), fr, sr, tr, FileR$)
DECLARE SUB V (aa!(), t!(), p(), fr, sr, tr, ymin!, xx!, YY!, FileR$)
DECLARE SUB linear (aa!(), t!(), cell%, mint%, maxt%, A, B, rxy)
DECLARE SUB First (aa!(), t!(), p(), cell%, fr, sr, ymin!, xx!, YY!, range, FileR$)
'
'************************************
'*        Main program
'************************************
'
DIM aa!(8, 1200)
DIM t!(1200)

'$DYNAMIC
DIM SHARED gwindow!(10)
```

```
ERASE gwindow!                  'window array for the help information

SCREEN 9
COLOR 11, 7

CLS

'get a menu selection from the user
DO
 CALL Drawinit

 DO                                'DO-LOOP for the menu selection
  onechar$ = UCASE$(INKEY$)
 LOOP WHILE onechar$ = ""

 SELECT CASE onechar$

  'read a file
  CASE "F"
   CALL FileSub(aa!(), t!(), FileN$, FileR$, linenum)

  'view the diagram
  CASE "D"
   IF FileN$ = "" THEN
        COLOR 4, 7
        LOCATE 6, 2
        PRINT "Please Read A";
        LOCATE 7, 2
        PRINT "Data File First!"
        COLOR 11, 7
        BEEP
        FOR i = 1 TO 3600: NEXT i
        CALL clean("D")
   ELSE
        CALL Diagram(aa!(), t!(), linenum, ymin!, xx!, YY!)
   END IF

  'begin the regression
  CASE "R"
   IF FileN$ = "" THEN
        COLOR 4, 7
        LOCATE 6, 2
        PRINT "Please Read A";
        LOCATE 7, 2
        PRINT "Data File First!"
        COLOR 11, 7
        BEEP
        FOR i = 1 TO 3600: NEXT i
        CALL clean("D")
   ELSEIF FileR$ = "" THEN
        COLOR 4, 7
        LOCATE 6, 2
        PRINT "Please Set A";
        LOCATE 7, 2
        PRINT "File Name for"
        LOCATE 8, 2
```

```
        PRINT "Recording!";
        COLOR 11, 7
        BEEP
        FOR i = 1 TO 3600: NEXT i
        CALL clean("D")
    ELSE
        CALL Reg(aa!(), t!(), FileR$, linenum, ymin!, xx!, YY!)
    END IF

  'quit the program
  CASE "Q"
    CALL QuitProgram

  'warning with pushing the wrong key
  CASE ELSE
    BEEP

 END SELECT

LOOP

END

REM $STATIC
SUB clean (C$)
'*************************************
'*          Clean screen
'*************************************
'
  C$ = UCASE$(C$)
  SELECT CASE C$

    'Whole screen
    CASE "A"
      CLS

    'Menu
    CASE "M"
    LINE (8, 3)-(425, 30), 0, BF

    'Data window
    CASE "D"
    LINE (3, 38)-(154, 310), 0, BF

    'Graphic window
    CASE "G"
    LINE (156, 38)-(638, 310), 0, BF

    'Note window
    CASE "N"
    LOCATE 24, 2
    PRINT SPACE$(78);

    'warning with the wrong key word
    CASE ELSE
```

```
  END SELECT

END SUB

DEFINT A
SUB Diagram (aa!(), t!(), linenum, ymin!, xx!, YY!)
'*************************************
'*      Draw a disgram  sub.
'*************************************
'
'draw the top-line menu with highlights
   CALL clean("M")
   LOCATE 2, 2
   PRINT "All  OneCell  AddonE  enLarge  P1&P2  eXit";
   CALL invert(2, 2, 1)
   CALL invert(2, 7, 1)
   CALL invert(2, 21, 1)
   CALL invert(2, 26, 1)
   CALL invert(2, 33, 1)
   CALL invert(2, 41, 1)

DO
   DO                                'DO-LOOP for the menu selection
    onechar$ = UCASE$(INKEY$)
   LOOP WHILE onechar$ = ""

   SELECT CASE onechar$

   'print all cells
   CASE "A"
    CALL clean("G")
    cell% = 1
    NS% = INT((linenum - 1) / 3 * 2)
    xmin% = 0
    xmax% = NS%
    CALL FindY(aa!(), cell%, linenum, ymax!, yyy!)
    cell% = 6
    CALL FindY(aa!(), cell%, linenum, yyy!, ymin!)
    CALL DrawFram(xmin%, xmax%, ymin!, ymax!, xx!, YY!)

    CALL PrintC
    bb = 1
    ee = linenum - 1
    tb = xmin%
    FOR j = 1 TO 6
        co = j + 8
        FOR i = bb TO ee                'draw data points
          tval! = t!(i)
          rval! = aa!(j, i)
          CALL DrawP(tb, ymin!, xx!, YY!, tval!, rval!, co)
        NEXT i
    NEXT j

   'print one cell only
   CASE "O"
    C$ = " ||   Please enter the cell number : "
```

```
    CALL GetCell(C$, cell%, "H")
    CALL clean("G")
    COLOR 8, 7
    LOCATE 2, 70
    PRINT USING "Cell : #"; cell%
    COLOR 11, 7

    NS% = INT((linenum - 1) / 3 * 2)
    xmin% = 0
    xmax% = NS%
    CALL FindY(aa!(), cell%, linenum, ymax!, ymin!)
    CALL DrawFram(xmin%, xmax%, ymin!, ymax!, xx!, YY!)

    CALL PrintC
    bb = 1
    ee = linenum - 1
    tb = xmin%
    co = cell% + 8
    FOR i = bb TO ee                    'draw data points
        tval! = t!(i)
        rval! = aa!(cell%, i)
        CALL DrawP(tb, ymin!, xx!, YY!, tval!, rval!, co)
    NEXT i

  'print one cell which covers on the previous cell
  CASE "E"
    C$ = " ||   Please enter the cell number : "
    CALL GetCell(C$, cell%, "L")
    COLOR 8, 7
    LOCATE 2, 70
    PRINT USING "Cell : #"; cell%
    COLOR 11, 7

    co = cell% + 8
    FOR i = bb TO ee                    'draw data points
        tval! = t!(i)
        rval! = aa!(cell%, i)
        CALL DrawP(tb, ymin!, xx!, YY!, tval!, rval!, co)
    NEXT i

  'enlarge one cell
  CASE "L"
    C$ = " ||   Please enter the cell number : "
    CALL GetCell(C$, cell%, "L")
    CALL FindY(aa!(), cell%, linenum, ymax!, ymin!)

    S1$ = " ||   Input Beginning TIME on X axis: "
    S2$ = " ||   Input End TIME on X axis: "
    CALL FindX(S1$, S2$, linenum, xmin%, xmax%, "L")
    CALL clean("G")

    CALL DrawFram(xmin%, xmax%, ymin!, ymax!, xx!, YY!)

    CALL PrintC
    bb = INT(xmin% / 2 * 3 + 1)
    ee = INT(xmax% / 2 * 3 + 1)
```

```
    tb = xmin%
    co = cell% + 8
    FOR i = bb TO ee                    'draw data points
        tval! = t!(i)
        rval! = aa!(cell%, i)
        CALL DrawP(tb, ymin!, xx!, YY!, tval!, rval!, co)
    NEXT i

  'print two pressure signals
  CASE "P"
    CALL clean("G")
    COLOR 8, 7
    LOCATE 2, 70
    PRINT "P1 and P2";
    COLOR 11, 7

    NS% = INT((linenum - 1) / 3 * 2)
    xmin% = 0
    xmax% = NS%
    cell% = 8
'    CALL FindY(aa!(), cell%, linenum, pymax!, pymin!)
    pymin! = 0
    pymax! = 800!
    CALL DrawFram(xmin%, xmax%, pymin!, pymax!, xx!, YY!)

    bb = 1
    ee = linenum - 1
    tb = xmin%
    FOR cell% = 7 TO 8
     IF cell% = 7 THEN co = 15
     IF cell% = 8 THEN co = 8
    FOR i = bb TO ee                    'draw data points
        tval! = t!(i)
        rval! = aa!(cell%, i)
        CALL DrawP(tb, pymin!, xx!, YY!, tval!, rval!, co)
    NEXT i
    NEXT cell%



  'ends the sub.
  CASE "X"

  'warning with pushing the wrong key
  CASE ELSE
    BEEP

 END SELECT

LOOP WHILE onechar$ <> "X"

END SUB

DEFINT B-C
SUB DrawFram (xmin%, xmax%, ymin!, ymax!, xx!, YY!)
'*************************************
```

```
'*      diagram frame drawing
'*************************************
'
DIM xlable%(10)
DIM ylable!(10)

CALL clean("G")
LINE (210, 49)-(631, 275), 1, B          'draw the diagram frame

'draw the y axis intervale
FOR i% = 1 TO 4
  LINE (210, 275 - i% * 45)-(214, 275 - i% * 45), 1
NEXT i%

'draw the x axis intervale
FOR i% = 1 TO 4
  LINE (210 + i% * 84, 275)-(210 + i% * 84, 49), 1
NEXT i%

'calculate x axis divition
xl% = (xmax% - xmin%) / 5
xlable%(1) = xmin%
FOR i% = 1 TO 5
  xlable%(i% + 1) = xlable%(i%) + xl%
NEXT i%

'calculate y axis division
yl! = (ymax! - ymin!) / 5
ylable!(1) = ymin!
FOR i% = 1 TO 5
  ylable!(i% + 1) = ylable!(i%) + yl!
NEXT i%

'print y lables on the frame
LOCATE 4, 22
PRINT USING "#####"; ylable!(6)
LOCATE 7, 22
PRINT USING "#####"; ylable!(5)
LOCATE 11, 22
PRINT USING "#####"; ylable!(4)
LOCATE 14, 22
PRINT USING "#####"; ylable!(3)
LOCATE 17, 22
PRINT USING "#####"; ylable!(2)
LOCATE 20, 22
PRINT USING "#####"; ylable!(1)

'print x lables on the frame
LOCATE 21, 25
PRINT USING "####"; xlable%(1)
LOCATE 21, 36
PRINT USING "####"; xlable%(2)
LOCATE 21, 46
PRINT USING "####"; xlable%(3)
LOCATE 21, 57
PRINT USING "####"; xlable%(4)
```

```
LOCATE 21, 67
PRINT USING "####"; xlable%(5)
LOCATE 21, 76
PRINT USING "####"; xlable%(6)

'print y axis title
IF ymax! > 1000 THEN
  LOCATE 10, 21: PRINT "O";
  LOCATE 11, 21: PRINT "H";
  LOCATE 12, 21: PRINT "M";
ELSE
  LOCATE 9, 21: PRINT "H";
  LOCATE 10, 21: PRINT "E";
  LOCATE 11, 21: PRINT "A";
  LOCATE 12, 21: PRINT "D";
END IF

'print x axis title
LOCATE 22, 48
PRINT "TIME (s)";

xmax% = xlable%(6)
ymax! = ylable!(6)

'calculate xx - x pixels / per unit
'          YY - y pixels / per unit
xx! = (631! - 210!) / (xmax% - xmin%)
YY! = (275! - 49!) / (ymax! - ymin!)

END SUB

SUB Drawinit
'*************************************
'*        topic menu drawing
'*************************************
'
'draw the window boundaries
LINE (0, 37)-(639, 37), 15
LINE (0, 312)-(639, 312), 15
LINE (155, 37)-(155, 312), 15
LINE (0, 0)-(639, 349), 9, B
LINE (1, 1)-(638, 348), 9, B

'initialize the data window
CALL clean("D")
LOCATE 4, 2
PRINT "    Data Window";

'draw the top-line menu with highlights
CALL clean("M")
LOCATE 2, 2
PRINT "File   view Diagram   Regression   Quit";
CALL invert(2, 2, 1)
CALL invert(2, 14, 1)
CALL invert(2, 24, 1)
CALL invert(2, 37, 1)
```

```
CALL clean("N")
LOCATE 24, 6
PRINT "Please press a highlighted key !";

END SUB

DEFSNG A-C
SUB DrawP (xbeg!, ymin!, xx!, YY!, xval!, yval!, C)
'*************************************
'*        draw a point sub.
'*************************************
'
'calculate x and y pixel of a point on the diagram
xpixel% = 210 + INT((xval! - xbeg!) * xx!)
ypixel% = 275 + INT((ymin! - yval!) * YY!)

'limit a point in the diagram frame
IF ypixel% < 49 THEN ypixel% = 49
IF ypixel% > 275 THEN ypixel% = 275

'draw a point
PSET (xpixel%, ypixel%), C

END SUB

DEFINT A
SUB Eg (aa!(), p(), E(), fr, sr, tr, FileRS)
'*************************************
'*          Calculation of Eg
'*************************************
'
   C$ = " ||    Input BASIC LINE number (1 or 3): "
   DO
     CALL GetCell(C$, bnum%, "H")
   LOOP WHILE bnum% <> 1 AND bnum% <> 3

   C$ = " ||    Input CELL number (0 for total): "
   DO
     CALL GetCell(C$, mm%, "H")
   LOOP WHILE mm% < 0 OR mm% > 6

   FileNum = FREEFILE
   OPEN FileR$ FOR APPEND AS FileNum

     PRINT #FileNum, "P(B-1) = "; p(1, 1)
     PRINT #FileNum, "P(E-1) = "; p(1, 2)
     PRINT #FileNum, "P(B-2) = "; p(2, 1)
     PRINT #FileNum, "P(E-2) = "; p(2, 2)
     PRINT #FileNum, "P(B-3) = "; p(3, 1)
     PRINT #FileNum, "P(E-3) = "; p(3, 2)
     PRINT #FileNum,

   IF mm% <> 0 THEN
     cbe = mm%
     ced = mm%
   ELSE
```

```
  cbc = 1
  ced = 6
END IF

CALL clear("D")
FOR cell% = cbc TO ced

fr = 0!
FOR i = p(1, 1) TO p(1, 2)
  fr = fr + aa!(cell%, i)
NEXT i
fr = fr / (p(1, 2) - p(1, 1) + 1)
IF fr < .000001 THEN fr = .000001

sr = 0!
FOR i = p(2, 1) TO p(2, 2)
  sr = sr + aa!(cell%, i)
NEXT i
sr = sr / (p(2, 2) - p(2, 1) + 1)
IF sr < .000001 THEN sr = .000001

tr = 0!
FOR i = p(3, 1) TO p(3, 2)
  tr = tr + aa!(cell%, i)
NEXT i
tr = tr / (p(3, 2) - p(3, 1) + 1)
IF tr < .000001 THEN tr = .000001

COLOR 4, 7
ll = 4 + (cell% - 1) * 3
LOCATE ll, 2
PRINT USING "Cell #:"; cell%
IF bnum% = 1 THEN
  GA = fr / sr        'Conductance = 1 / Resistance
ELSE
  GA = tr / sr
END IF
Egn = (1 - GA) / (1 + .5 * GA) * 100!
LOCATE ll + 1, 2
PRINT USING "Eg1 = ##.##%"; Egn
E(cell%, 1) = Egn

PRINT #FileNum, "Cell "; cell%; ":"
PRINT #FileNum, "Eg(1) = "; Egn; "%"

IF bnum% = 1 THEN
  GA = fr / tr                    'Conductance = 1 / Resistance
ELSE
  GA = tr / fr
END IF
Egn = (1 - GA) / (1 + .5 * GA) * 100!
LOCATE ll + 2, 2
PRINT USING "Eg2 = ##.##%"; Egn
E(cell%, 2) = Egn

PRINT #FileNum, "Eg(2) = "; Egn; "%"
```

```
    PRINT #FileNum,

    NEXT cell%
    COLOR 11, 7

    CLOSE FileNum               ' Close the file.

END SUB

DEFSNG A
SUB FileSub (aa!(), t!(), FileN$, FileR$, linenum) STATIC
'*************************************
'*          Read a file
'*************************************
'
'draw the top-line menu with highlights
    CALL clean("M")
    LOCATE 2, 2
    PRINT "Read data   Set a file name for results   eXit";
    CALL invert(2, 2, 1)
    CALL invert(2, 14, 1)
    CALL invert(2, 45, 1)

DO
    CALL clean("N")
    LOCATE 24, 6
    PRINT "Please press a highlighted key !";

    DO                              'DO-LOOP for the menu selection
      onechar$ = UCASE$(INKEY$)
    LOOP WHILE onechar$ = ""

    SELECT CASE onechar$

    'read a data file
    CASE "R"

      'message window and beep
      CALL clean("N")
      LOCATE 24, 6
      PRINT "Read a set of files from the disk.";

      S$ = " ||    Please enter the file name : "
      CALL GetFileName(S$, FileN$)

      COLOR 8, 7
      LOCATE 2, 55
      PRINT USING "File: &"; FileN$
      COLOR 11, 7

      CALL clean("N")
      LOCATE 24, 6
      PRINT "Please wait!  Reading: ";

    FOR cell% = 1 TO 6
```

```
PRINT USING "Cell#."; cell%;                    'read cell files
FileName$ = FileN$ + "C" + CHR$(cell% + 48) + ".PRN"
FileNum = FREEFILE
OPEN FileName$ FOR INPUT AS FileNum

linenum = 1
DO WHILE NOT EOF(FileNum)
  INPUT #FileNum, tt!, aa!(cell%, linenum)
  linenum = linenum + 1
LOOP

CLOSE FileNum                ' Close the file.

NEXT cell%

PRINT "P1&P2.";                    'read pressure files
FileName$ = FileN$ + "P.PRN"
FileNum = FREEFILE
OPEN FileName$ FOR INPUT AS FileNum

linenum = 1
DO WHILE NOT EOF(FileNum)
  INPUT #FileNum, t!(linenum), aa!(7, linenum), aa!(8, linenum)
  linenum = linenum + 1
LOOP

CLOSE FileNum                ' Close the file.

'input a file name for recording results
CASE "S"
 IF FileN$ = "" THEN
       COLOR 4, 7
       LOCATE 6, 2
       PRINT "Please Read A";
       LOCATE 7, 2
       PRINT "Data File First!"
       COLOR 11, 7
       BEEP
       FOR i = 1 TO 3600: NEXT i
       CALL clean("D")
 ELSE
       CALL clean("N")
       LOCATE 24, 6
       PRINT "Enter a file name for recording the analysis results.";

       A$ = " ||    Please enter the FILE name : "
       CALL GetFileName(A$, FileR$)
       FileR$ = FileR$ + ".DAT"
       FileRec = FREEFILE
       OPEN FileR$ FOR OUTPUT AS FileRec
         S$ = "The analysis results for " + FileN$
         PRINT #FileRec, S$
         PRINT #FileRec, "The file for each cell has "; linenum - 1; " data."
         PRINT #FileRec,
       CLOSE FileRec                'Close the file.
 END IF
```

```
  'ends this subroutine
  CASE "X"

  'wrong key
  CASE ELSE
    BEEP


END SELECT

LOOP WHILE onechar$ < > "X"

END SUB

SUB FindX (S1$, S2$, linenum, xmin%, xmax%, l$)
'*************************************
'*     Get min. & max. on X axis
'*************************************
'
IF l$ < > "L" THEN
  column = 20
  row = 10
ELSE
  column = 30
  row = 2
END IF

'save a window which is covered by the question
CALL SaveW(140, 10, 639, 220)

COLOR 14, 7
LOCATE row, column
PRINT "╔═══════════════════════════════════════════════════════════════════════╗ ";
LOCATE row + 1, column
PRINT "‖                                       ‖ ";
LOCATE row + 2, column
PRINT "‖                                       ‖ ";
LOCATE row + 3, column
PRINT "╚═══════════════════════════════════════════════════════════════════════╝ ";
DO
  LOCATE row + 1, column
  PRINT S1$;
  INPUT xmin%
LOOP WHILE xmin% < 0 OR xmin% > linenum - 3
DO
  LOCATE row + 2, column
  PRINT S2$;
  INPUT xmax%
LOOP WHILE xmax% < = xmin% + 3 OR xmax% > = linenum - 1

'restore the window when the user does not leave the program
CALL RestoreW(140, 10)
'
COLOR 11, 7
END SUB
```

```
SUB FindY (aa!(), cell%, linenum, ymax!, ymin!)
'****************************************
'*     Find max. and min. on y axis
'****************************************
'
   ymin! = aa!(cell%, 1)
   ymax! = aa!(cell%, 1)

   FOR i = 2 TO linenum - 1
     IF aa!(cell%, i) > ymax! THEN ymax! = aa!(cell%, i)
     IF aa!(cell%, i) < ymin! THEN ymin! = aa!(cell%, i)
   NEXT i

   IF ymax! < 1000 THEN
     ymax! = INT(ymax! + 100!)
   ELSE
     ymax! = INT((ymax! + 2000!) / 1000!) * 1000!
   END IF

   ymin! = INT((ymin! - 1500!) / 1000!) * 1000!
   IF ymax! > 90000! THEN ymax! = 90000!
   IF ymin! < 0 OR ymin! > ymax! THEN ymin! = 0!

END SUB

SUB First (aa!(), t!(), p(), cell%, fr, sr, ymin!, xx!, YY!, range, FileR$)
'*************************************
'*       regre. for first range
'*************************************
'
DIM AR(60), BR(60), rxy(60)

     'draw the top-line menu with highlights
      CALL clean("M")
      LOCATE 2, 2
      PRINT "mid. Point   Auto   Manual   eXit";
      CALL invert(2, 7, 1)
      CALL invert(2, 15, 1)
      CALL invert(2, 22, 1)
      CALL invert(2, 32, 1)

          mid = .5 * (fr + sr)
          mindif = 1!
          j = 1

          IF range = 1 THEN
            p1 = p(1, 1)              'range on line 1 and 2
            p2 = p(2, 2)
          ELSE
            p1 = p(2, 1)              'range on line 2 and 3
            p2 = p(3, 2)
          END IF

          FOR i = p1 TO p2
            d = ABS((aa!(cell%, i) - mid) / fr)
            IF d < mindif THEN
```

```
            mindif = d
            j = i
          END IF
        NEXT i

        tb = 0
        tval! = t!(j)
        rval! = aa!(cell%, j)
        CALL DrawP(tb, ymin!, xx!, YY!, tval!, rval!, 8)

        COLOR 8, 11
        LOCATE 22, 60
        PRINT USING "( mid. P = #### )"; j
        COLOR 11, 7

FileNum = FREEFILE
OPEN FileR$ FOR APPEND AS FileNum
PRINT #FileNum, "Linear regression for Cell "; cell%; " :"
IF range = 1 THEN
    PRINT #FileNum, " The First Range:"
ELSE
    PRINT #FileNum, " The Second Range:"
END IF
PRINT #FileNum,

DO
 DO                                'DO-LOOP for the menu selection
    onechar$ = UCASE$(INKEY$)
 LOOP WHILE onechar$ = ""

 SELECT CASE onechar$

 'change the mid. point
 CASE "P"
    C$ = " ||    Please enter MID. POINT number : "
    CALL GetCell(C$, pt%, "L")
    j = pt%
    tval! = t!(j)
    rval! = aa!(cell%, j)
    CALL DrawP(tb, ymin!, xx!, YY!, tval!, rval!, 12)
    COLOR 12, 11
    LOCATE 22, 60
    PRINT USING "( mid. P = #### )"; j
    COLOR 11, 7

 'auto scane
 CASE "A"
    C$ = " ||    Input regre. POINT number : "
    CALL GetCell(C$, regp%, "L")

    CALL clean("D")
    COLOR 4, 7
    LOCATE 4, 2
    PRINT " P    Rxy    V(s)";

    PRINT #FileNum, "Auto. scan process:"
```

```
PRINT #FileNum, " The mid. point = "; j
PRINT #FileNum, " P     Rxy      V(s)"

l% = 5
FOR i = 1 TO regp%
  mint% = j - i
  maxt% = j + i
  CALL linear(aa!(), t!(), cell%, mint%, maxt%, AR(i), BR(i), rxy(i))
  t1 = (fr - AR(i)) / BR(i)
  t2 = (sr - AR(i)) / BR(i)
  swarm = 51 / (t2 - t1)
  LOCATE l%, 2
  PRINT USING "##   "; i;
  PRINT USING "#.####"; rxy(i);
  PRINT USING "###.##"; swarm;

  PRINT #FileNum, i; rxy(i); swarm
  l% = l% + 1

NEXT i

PRINT #FileNum,

LOCATE l%, 2
PRINT "(Press any key";
l% = l% + 1
LOCATE l%, 2
INPUT "to continue.)", any$
COLOR 11, 7

C$ = " ||    Input POINTS number you like: "
CALL GetCell(C$, p%, "L")

CALL clean("D")
t1 = (fr - AR(p%)) / BR(p%)
t2 = (sr - AR(p%)) / BR(p%)
time = t2 - t1

COLOR 4, 7
LOCATE 4, 2
PRINT "Begin at :"; j - p%;
LOCATE 5, 2
PRINT "End at   :"; j + p%;

LOCATE 7, 2
PRINT "First TIME =";
LOCATE 8, 2
PRINT "   "; t1; "s";
LOCATE 9, 2
PRINT "Second TIME =";
LOCATE 10, 2
PRINT "   "; t2; "s";

LOCATE 12, 2
PRINT "Diff. ="; time; "s";
LOCATE 13, 2
```

```
        PRINT "Velocity =";
        LOCATE 14, 2
        PRINT "   "; 51! / time; "cm/s";
        COLOR 11, 7

        PRINT #FileNum, "One choice from auto. scan process:"
        PRINT #FileNum, "Cell "; cell%; " :"
        PRINT #FileNum, "Begin at :"; j - p%
        PRINT #FileNum, "End at   :"; j + p%
        PRINT #FileNum, "First TIME ="; t1; "s"
        PRINT #FileNum, "Second TIME ="; t2; "s"
        PRINT #FileNum, "Diff. ="; time; "s"
        PRINT #FileNum, "Velocity ="; 51! / time; "cm/s"
        PRINT #FileNum,

    'manual choice
    CASE "M"
        S1$ = " ||    Input Beginning POINT on X : "
        S2$ = " ||    Input End POINT on X : "
        CALL FindX(S1$, S2$, p(2, 2), begp%, endp%, "L")

        CALL clean("D")
        COLOR 4, 7
        LOCATE 6, 2
        PRINT "Begin at :"; begp%;
        LOCATE 7, 2
        PRINT "End at   :"; endp%;

        CALL linear(aa!(), t!(), cell%, begp%, endp%, aa, bb, rr)

        LOCATE 9, 2
        PRINT "Rxy = "; rr;

        t1 = (fr - aa) / bb
        t2 = (sr - aa) / bb
        time = t2 - t1
        LOCATE 11, 2
        PRINT "First TIME =";
        LOCATE 12, 2
        PRINT "   "; t1; "s";
        LOCATE 13, 2
        PRINT "Second TIME =";
        LOCATE 14, 2
        PRINT "   "; t2; "s";

        LOCATE 15, 2
        PRINT "Diff. ="; time; "s";
        LOCATE 16, 2
        PRINT "Velocity =";
        LOCATE 17, 2
        PRINT "   "; 51! / time; "cm/s";
        COLOR 11, 7

        PRINT #FileNum, "Manual choice process:"
        PRINT #FileNum, "Cell "; cell%; " :"
        PRINT #FileNum, "Begin at :"; begp%
```

```
            PRINT #FileNum, "End at   :"; endp%
            PRINT #FileNum, "First TIME ="; t1; "s"
            PRINT #FileNum, "Second TIME ="; t2; "s"
            PRINT #FileNum, "Diff. ="; time; "s"
            PRINT #FileNum, "Velocity ="; 51! / time; "cm/s"
            PRINT #FileNum,

        'ends the sub.
        CASE "X"
            CLOSE #FileNum

        'warning with pushing the wrong key
        CASE ELSE
            BEEP

        END SELECT
      LOOP WHILE onechar$ < > "X"

END SUB

SUB GetCell (C$, celln%, l$)
'************************************
'*      Get the cell number sub.
'************************************
'
IF l$ < > "L" THEN
  column = 20
  row = 10
ELSE
  column = 30
  row = 22
END IF

'save a window which is covered by the question
CALL SaveW(140, 120, 620, 340)

COLOR 14, 7
LOCATE row, column
PRINT "╔═══════════════════════════════════════════════════════════════════════════╗";
LOCATE row + 1, column
PRINT "‖                                                                           ‖";
LOCATE row + 2, column
PRINT "╚═══════════════════════════════════════════════════════════════════════════╝";
LOCATE row + 1, column
PRINT C$;
INPUT celln%
COLOR 11, 7
'
'restore the window when the user does not leave the program
CALL RestoreW(140, 120)
'
END SUB

DEFINT A
SUB GetFileName (S$, GFN$)
' ************************************
```

```
' *    Get a file name from user
' ************************************
'save a window which is covered by the question
CALL SaveW(140, 120, 540, 220)

COLOR 14, 7
LOCATE 10, 20
PRINT "╔═══════════════════════════════════════════════════════════════════════╗";
LOCATE 11, 20
PRINT "‖                                                                       ‖";
LOCATE 12, 20
PRINT "╚═══════════════════════════════════════════════════════════════════════╝";
LOCATE 11, 20
PRINT SS;
INPUT GFN$
COLOR 11, 7
'
'restore the window when the user does not leave the program
CALL RestoreW(140, 120)
'
END SUB

DEFINT B-C
SUB invert (lin%, col%, nchars%)
'**************************************
'*     character inverting sub.
'**************************************
'
'calculate the position of characters to be inverted
x1% = col% * 8 - 9
x2% = (col% + nchars% - 1) * 8 - 2
y1% = lin% * 14 - 15
y2% = lin% * 14 - 1

'calculate the size of array
arraysize% = 1 + INT((x2% - x1% + 8) / 8) * (y2% - y1% + 1)

REDIM myarray!(arraysize%)
GET (x1%, y1%)-(x2%, y2%), myarray!
PUT (x1%, y1%), myarray!, PRESET
ERASE myarray!
'
END SUB

DEFSNG A-C
SUB linear (aa!(), t!(), cell%, mint%, maxt%, A, B, rxy)
'**************************************
'*    Linear regression of a line
'**************************************
'  where  mint = begin point of regression
'         maxt = end point of regression
'         a and b = parameters in y = ax + b
'         rxy = coeffitiant
'
DIM x(100), y(100)
```

```
nn = maxt% - mint% + 1
IF mint% = 0 THEN mint% = 1
IF nn > 100 THEN nn = 100
FOR i = 1 TO nn
  y(i) = aa!(cell%, mint% + i - 1)
  x(i) = t!(mint% + i - 1)
NEXT i

xs = 0!
xxs = 0!
ys = 0!
yys = 0!
xys = 0!
FOR i = 1 TO nn
  xs = xs + x(i)
  xxs = xxs + x(i) * x(i)
  ys = ys + y(i)
  yys = yys + y(i) * y(i)
  xys = xys + x(i) * y(i)
NEXT i

lxx = xxs - xs * xs / nn
lyy = yys - ys * ys / nn
lxy = xys - xs * ys / nn
B = lxy / lxx
A = ys / nn - xs / nn * B
rxy = ABS(lxy / SQR(lxx * lyy))

END SUB

SUB PrintC
'*************************************
'*        Print cell color
'*************************************
'
   LOCATE 6, 70: COLOR 9, 7: PRINT "Cell 1"
   LOCATE 7, 70: COLOR 10, 7: PRINT "Cell 2"
   LOCATE 8, 70: COLOR 11, 7: PRINT "Cell 3"
   LOCATE 9, 70: COLOR 12, 7: PRINT "Cell 4"
   LOCATE 10, 70: COLOR 13, 7: PRINT "Cell 5"
   LOCATE 11, 70: COLOR 14, 7: PRINT "Cell 6"
   COLOR 11, 7
END SUB

DEFINT A-C
SUB QuitProgram
'*************************************
'*          End program sub.
'*************************************
'
'save a window which is covered by the question
CALL SaveW(1?2, 120, 480, 220)

'message window and beep
LOCATE 24, 2
PRINT SPACE$(78);
```

```
LOCATE 24, 6
PRINT "Warning ! Warning !! Warning !!!";
BEEP

COLOR 12, 7
LOCATE 10, 20
PRINT " ╔═══════════════════════════════════════════════════════════════╗ ";
LOCATE 11, 20
PRINT " ‖   Do you really want to quit ? (Y/N)     ‖ ";
LOCATE 12, 20
PRINT " ╚═══════════════════════════════════════════════════════════════╝ ";
COLOR 11, 7

DO
  B$ = UCASE$(INKEY$)
LOOP WHILE B$ = ""

IF B$ = "Y" THEN
  SCREEN 0
  WIDTH 80
  CLS
  END
END IF

'restore the window when the user does not leave the program
CALL RestoreW(140, 120)
'
END SUB

DEFSNG A-C
SUB Reg (aa!(), t!(), FileR$, linenum, ymin!, xx!, YY!)
'*************************************
'*    Regression of Eg & V(swarm)
'*************************************
'
DIM p(3, 2), E(6, 2)

CALL clean("D")
DO
'draw the top-line menu with highlights
    CALL clean("M")
    LOCATE 2, 2
    PRINT "First  Second  Third  Eg  V(swarm)  eXit";
    CALL invert(2, 2, 1)
    CALL invert(2, 9, 1)
    CALL invert(2, 17, 1)
    CALL invert(2, 24, 1)
    CALL invert(2, 28, 1)
    CALL invert(2, 39, 1)

    DO                              'DO-LOOP for the menu selection
      onechar$ = UCASE$(INKEY$)
    LOOP WHILE onechar$ = ""

    SELECT CASE onechar$
```

```
'get beginning and end points for FIRST line
CASE "F"
  S1$ = " ||  Input START point of First line: "
  S2$ = " ||  Input END point of First line: "
  CALL FindX(S1$, S2$, linenum, firstrp%, endrp%, "L")
  COLOR 4, 7
  LOCATE 4, 2
  PRINT "P(B-1): "; firstrp%
  LOCATE 5, 2
  PRINT "P(E-1): "; endrp%
  COLOR 11, 7
  p(1, 1) = firstrp%
  p(1, 2) = endrp%


'get beginning and end points for SECOND line
CASE "S"
  S1$ = " ||  Input START point of Second line: "
  S2$ = " ||  Input END point of Second line: "
  CALL FindX(S1$, S2$, linenum, sdrp%, edsdrp%, "L")
  COLOR 4, 7
  LOCATE 7, 2
  PRINT "P(B-2): "; sdrp%;
  LOCATE 8, 2
  PRINT "P(E-2): "; edsdrp%
  COLOR 11, 7
  p(2, 1) = sdrp%
  p(2, 2) = edsdrp%


'get beginning and end points for THIRD line
CASE "T"
  S1$ = " ||  Input START point of Third line: "
  S2$ = " ||  Input END point of Third line: "
  CALL FindX(S1$, S2$, linenum, tdrp%, edtdrp%, "L")
  COLOR 4, 7
  LOCATE 10, 2
  PRINT "P(B-3): "; tdrp%;
  LOCATE 11, 2
  PRINT "P(E-3): "; edtdrp%
  COLOR 11, 7
  p(3, 1) = tdrp%
  p(3, 2) = edtdrp%

CASE "E"
  CALL Eg(aa!(), p(), E(), fr, sr, tr, FileR$)

CASE "V"
  CALL V(aa!(), t!(), p(), fr, sr, tr, ymin!, xx!, YY!, FileR$)

'save results into the file and end the sub.
CASE "X"
  CALL SaveW(140, 120, 540, 320)
  COLOR 14, 7
  LOCATE 10, 20
  PRINT" ╔═══════════════════════════════════════════════════════════════════════╗ ";
```

```
    LOCATE 11, 20
    PRINT " ||    If exit, the initials will be lost !      || ";
    LOCATE 12, 20
    PRINT " ||                                              || ";
    LOCATE 13, 20
    PRINT" ╚═══════════════════════════════════════════════════════════════════════╝ ";
    LOCATE 12, 20
    INPUT " ||    Do you rellay want to EXIT ? (Y/N) ", ans$

    IF ans$ = "N" OR ans$ = "n" THEN
        onechar$ = "N"
        CALL RestoreW(140, 120)
    ELSE
        CALL clean("G")
    END IF
    COLOR 11, 7

  'warning with pushing the wrong key
  CASE ELSE
   BEEP

 END SELECT

LOOP WHILE onechar$ < > "X"

END SUB

DEFINT A
SUB RestoreW (x1%, y1%)
'*************************************
'*      restoring graphic area
'*************************************
'
PUT (x1%, y1%), gwindow!, PSET
ERASE gwindow!
'
END SUB

SUB SaveW (x1%, y1%, x2%, y2%)
'*************************************
'*      saving graphic area sub.
'*************************************
'
arraysize% = 1 + INT((x2% - x1% + 8) / 8) * (y2% - y1% + 1)
REDIM gwindow!(arraysize%)
GET (x1%, y1%)-(x2%, y2%), gwindow!
'
END SUB

DEFSNG A
SUB V (aa!(), t!(), p(), fr, sr, tr, ymin!, xx!, YY!, FileR$)
'*************************************
'*      Calculation of V(swarm)
'*************************************
'
DIM AR(60), BR(60), rxy(60)
```

```
DO
'draw the top-line menu with highlights
   CALL clean("M")
   LOCATE 2, 2
   PRINT "Cell   First (Line 1-2)   Second (Line 2-3)   eXit";
   CALL invert(2, 2, 1)
   CALL invert(2, 9, 1)
   CALL invert(2, 28, 1)
   CALL invert(2, 49, 1)
   CALL clean("D")

   DO                                'DO-LOOP for the menu selection
     onechar$ = UCASE$(INKEY$)
   LOOP WHILE onechar$ = ""

   cell% = 6                         'the defult cell number is 6

   SELECT CASE onechar$

   'get the cell number
   CASE "C"
     C$ = " ||    Please enter the cell number : "
     CALL GetCell(C$, cell%, "H")

   'calculate the regression between line 1 and 2
   CASE "F"
     COLOR 8, 7
     LOCATE 4, 60
     PRINT "The First Regre."
     COLOR 11, 7
     range = 1
     CALL First(aa!(), t!(), p(), cell%, fr, sr, ymin!, xx!, YY!, range, FileR$)

   'calculate the regression between line 2 and 3
   CASE "S"
     COLOR 8, 7
     LOCATE 4, 60
     PRINT "The Second Regre."
     COLOR 11, 7
     range = 2
     CALL First(aa!(), t!(), p(), cell%, sr, tr, ymin!, xx!, YY!, range, FileR$)

   'ends the sub.
   CASE "X"

   'warning with pushing the wrong key
   CASE ELSE
     BEEP

  END SELECT

LOOP WHILE onechar$ <> "X"

END SUB
```

APPENDIX 3

Measurements of u_{in} and ε_g in Cells 6 - 2 in Air - Water Only System

In this appendix, the measurements of u_{in} and ε_g in Cells 6, 5, 4, 3 and 2 are given for the 48 experiments in the air - water only system. In these Tables, the interface velocity, u_{in}, and the gas holdups, ε_{g1} and ε_{g2}, are calculated using Equations 5.9 and 5.10 found in Section 5.2.2. For a total of 48 experiments, based on ten replicates for each experiment, the maximum relative standard deviation for u_{in} was 1.68%, and the maximum relative standard deviation for ε_{g1} and ε_{g2} was 2.86%.

Index for Tables

No. of Table	J_{g1} (cm/s)	J_{g2} (cm/s)	J_{g2}/J_{g1}	No. of Table	J_{g1} (cm/s)	J_{g2} (cm/s)	J_{g2}/J_{g1}
Table 1	1.0	0.0	0.0	Table 25	2.0	1.6	0.8
Table 2	1.0	0.2	0.2	Table 26	2.0	2.4	1.2
Table 3	1.0	0.4	0.4	Table 27	2.0	2.8	1.4
Table 4	1.0	0.6	0.6	Table 28	2.0	3.2	1.6
Table 5	1.0	0.8	0.8	Table 29	2.0	3.6	1.8
Table 6	1.0	1.2	1.2	Table 30	2.0	4.0	2.0
Table 7	1.0	1.4	1.4	Table 31	2.5	0.0	0.0
Table 8	1.0	1.6	1.6	Table 32	2.5	0.5	0.2
Table 9	1.0	1.8	1.8	Table 33	2.5	1.0	0.4
Table 10	1.0	2.0	2.0	Table 34	2.5	1.5	0.6
Table 11	1.5	0.0	0.0	Table 35	2.5	2.0	0.8
Table 12	1.5	0.3	0.2	Table 36	2.5	3.0	1.2
Table 13	1.5	0.6	0.4	Table 37	2.5	3.25	1.3
Table 14	1.5	0.9	0.6	Table 38	2.5	3.50	1.4

No. of Table	J_{g1} (cm/s)	J_{g2} (cm/s)	J_{g2}/J_{g1}	No. of Table	J_{g1} (cm/s)	J_{g2} (cm/s)	J_{g2}/J_{g1}
Table 15	1.5	1.2	0.8	Table 39	2.5	3.7	1.5
Table 16	1.5	1.8	1.2	Table 40	2.5	4.0	1.6
Table 17	1.5	2.1	1.4	Table 41	3.0	0.0	0.0
Table 18	1.5	2.4	1.6	Table 42	3.0	0.6	0.2
Table 19	1.5	2.7	1.8	Table 43	3.0	1.2	0.4
Table 20	1.5	3.0	2.0	Table 44	3.0	1.8	0.6
Table 21	2.0	0.0	0.0	Table 45	3.0	2.4	0.8
Table 22	2.0	0.4	0.2	Table 46	3.0	3.3	1.1
Table 23	2.0	0.8	0.4	Table 47	3.0	3.6	1.2
Table 24	2.0	1.2	0.6	Table 48	3.0	3.9	1.3

Tables 1 - 48

Table 1 Profile of u_{in} at $J_{g1} = 1.0$ cm/s and $J_{g2} = 0$

Cell	ε_{g1} (%)	ε_{g2} (%)	ε_{g2}-ε_{g1} (%)	u_{in} (cm/s)
6	4.40	0.00	-4.40	21.5
5	4.37	0.00	-4.37	21.5
4	4.64	0.00	-4.64	21.5
3	5.05	0.00	-5.05	21.4
2	5.17	0.00	-5.17	21.4

Table 2 Profile of u_{in} at J_{g1} = 1.0 cm/s and J_{g2} = 0.2 cm/s

Cell	ε_{g1} (%)	ε_{g2} (%)	ε_{g2}-ε_{g1} (%)	u_{in} (cm/s)
6	4.33	0.86	-3.47	20.2
5	4.33	0.85	-3.49	21.0
4	4.57	0.98	-3.59	21.0
3	4.86	1.03	-3.84	21.0
2	5.18	1.25	-3.93	21.0

Table 3 Profile of u_{in} at J_{g1} = 1.0 cm/s and J_{g2} = 0.4 cm/s

Cell	ε_{g1} (%)	ε_{g2} (%)	ε_{g2}-ε_{g1} (%)	u_{in} (cm/s)
6	4.35	1.85	-2.50	20.0
5	4.22	1.79	-2.44	19.7
4	4.51	1.95	-2.56	19.5
3	4.89	2.20	-2.69	20.1
2	5.18	2.33	-2.86	19.8

Table 4 Profile of u_{in} at J_{g1} = 1.0 cm/s and J_{g2} = 0.6 cm/s

Cell	ε_{g1} (%)	ε_{g2} (%)	ε_{g2}-ε_{g1} (%)	u_{in} (cm/s)
6	4.45	2.86	-1.59	19.4
5	4.49	2.90	-1.58	19.4
4	4.69	3.06	-1.63	18.9
3	5.02	3.42	-1.61	18.8
2	4.73	3.47	-1.26	18.5

Table 5 Profile of u_{in} at J_{g1} = 1.0 cm/s and J_{g2} = 0.8 cm/s

Cell	ε_{g1} (%)	ε_{g2} (%)	ε_{g2}-ε_{g1} (%)	u_{in} (cm/s)
6	4.50	3.74	-0.76	18.9
5	4.41	3.72	-0.69	19.2
4	4.68	4.02	-0.66	18.5
3	4.82	4.20	-0.62	18.5
2	4.51	4.15	-0.37	18.5

Table 6 Profile of u_{in} at J_{g1} = 1.0 cm/s and J_{g2} = 1.2 cm/s

Cell	ε_{g1} (%)	ε_{g2} (%)	ε_{g2}-ε_{g1} (%)	u_{in} (cm/s)
6	4.38	5.94	1.56	17.7
5	4.49	6.02	1.52	17.4
4	4.54	5.92	1.37	18.2
3	4.95	6.00	1.05	18.2
2	4.49	5.31	0.83	18.2

Table 7 Profile of u_{in} at J_{g1} = 1.0 cm/s and J_{g2} = 1.4 cm/s

Cell	ε_{g1} (%)	ε_{g2} (%)	ε_{g2}-ε_{g1} (%)	u_{in} (cm/s)
6	4.47	6.75	2.28	16.9
5	4.44	6.82	2.38	17.3
4	4.70	6.86	2.16	18.0
3	4.85	6.71	1.86	18.2
2	4.91	6.11	1.20	18.2

Table 8 Profile of u_{in} at J_{g1} = 1.0 cm/s and J_{g2} = 1.6 cm/s

Cell	ε_{g1} (%)	ε_{g2} (%)	ε_{g2}-ε_{g1} (%)	u_{in} (cm/s)
6	4.54	7.98	3.44	16.6
5	4.51	7.91	3.40	17.2
4	4.63	7.97	3.33	17.9
3	4.94	8.05	3.11	18.1
2	5.00	7.51	2.51	18.1

Table 9 Profile of u_{in} at J_{g1} = 1.0 cm/s and J_{g2} = 1.8 cm/s

Cell	ε_{g1} (%)	ε_{g2} (%)	ε_{g2}-ε_{g1} (%)	u_{in} (cm/s)
6	4.52	9.34	4.82	15.6
5	4.45	9.02	4.57	16.4
4	4.60	9.17	4.57	17.2
3	4.93	9.39	4.46	17.9
2	5.19	8.81	3.62	18.1

Table 10 Profile of u_{in} at J_{g1} = 1.0 cm/s and J_{g2} = 2.0 cm/s

Cell	ε_{g1} (%)	ε_{g2} (%)	ε_{g2}-ε_{g1} (%)	u_{in} (cm/s)
6	4.53	10.32	5.79	14.9
5	4.40	9.87	5.48	15.6
4	4.62	10.23	5.61	17.0
3	4.99	10.35	5.36	17.7
2	5.12	9.59	4.47	18.0

Table 11 Profile of u_{in} at J_{g1} = 1.5 cm/s and J_{g2} = 0

Cell	ε_{g1} (%)	ε_{g2} (%)	ε_{g2}-ε_{g1} (%)	u_{in} (cm/s)
6	6.80	0.00	-6.80	19.9
5	6.12	0.00	-6.12	20.1
4	5.96	0.00	-5.96	20.5
3	6.24	0.00	-6.24	20.5
2	6.68	0.00	-6.68	20.3

Table 12 Profile of u_{in} at J_{g1} = 1.5 cm/s and J_{g2} = 0.3 cm/s

Cell	ε_{g1} (%)	ε_{g2} (%)	ε_{g2}-ε_{g1} (%)	u_{in} (cm/s)
6	7.17	1.08	-6.09	19.2
5	6.48	0.60	-5.88	19.4
4	6.20	0.62	-5.58	19.5
3	6.37	0.65	-5.72	19.3
2	6.62	0.72	-5.90	19.0

Table 13 Profile of u_{in} at J_{g1} = 1.5 cm/s and J_{g2} = 0.6 cm/s

Cell	ε_{g1} (%)	ε_{g2} (%)	ε_{g2}-ε_{g1} (%)	u_{in} (cm/s)
6	7.04	2.53	-4.51	18.9
5	6.31	1.94	-4.38	18.9
4	6.09	1.64	-4.46	18.6
3	6.43	1.65	-4.77	18.6
2	6.6i	1.82	-4.78	18.1

Table 14 Profile of u_{in} at J_{g1} = 1.5 cm/s and J_{g2} = 0.9 cm/s

Cell	ε_{g1} (%)	ε_{g2} (%)	ε_{g2}-ε_{g1} (%)	u_{in} (cm/s)
6	7.05	4.00	-3.05	17.7
5	6.35	3.29	-3.06	18.1
4	6.22	3.27	-2.95	18.0
3	6.42	3.23	-3.19	18.1
2	6.67	3.50	-3.18	17.8

Table 15 Profile of u_{in} at J_{g1} = 1.5 cm/s and J_{g2} = 1.2 cm/s

Cell	ε_{g1} (%)	ε_{g2} (%)	ε_{g2}-ε_{g1} (%)	u_{in} (cm/s)
6	6.93	5.39	-1.54	16.9
5	6.27	4.74	-1.53	17.5
4	6.11	4.55	-1.57	17.6
3	6.25	4.60	-1.65	17.5
2	6.46	4.87	-1.60	17.4

Table 16 Profile of u_{in} at J_{g1} = 1.5 cm/s and J_{g2} = 1.8 cm/s

Cell	ε_{g1} (%)	ε_{g2} (%)	ε_{g2}-ε_{g1} (%)	u_{in} (cm/s)
6	6.91	8.08	1.17	15.9
5	6.20	7.41	1.21	16.0
4	6.14	7.32	1.18	16.2
3	6.50	7.68	1.18	16.1
2	6.74	7.89	1.15	16.5

Table 17 Profile of u_{in} at J_{g1} = 1.5 cm/s and J_{g2} = 2.1 cm/s

Cell	ε_{g1} (%)	ε_{g2} (%)	ε_{g2}-ε_{g1} (%)	u_{in} (cm/s)
6	6.89	10.51	3.62	15.9
5	6.39	9.50	3.11	15.6
4	6.38	9.62	3.24	15.8
3	6.75	10.04	3.29	16.1
2	6.95	10.42	3.47	16.2

Table 18 Profile of u_{in} at J_{g1} = 1.5 cm/s and J_{g2} = 2.4 cm/s

Cell	ε_{g1} (%)	ε_{g2} (%)	ε_{g2}-ε_{g1} (%)	u_{in} (cm/s)
6	6.84	11.94	5.10	15.2
5	6.35	11.12	4.77	15.0
4	6.41	11.21	4.80	15.4
3	6.73	11.57	4.84	15.9
2	7.11	11.70	4.58	16.1

Table 19 Profile of u_{in} at J_{g1} = 1.5 cm/s and J_{g2} = 2.7 cm/s

Cell	ε_{g1} (%)	ε_{g2} (%)	ε_{g2}-ε_{g1} (%)	u_{in} (cm/s)
6	6.93	13.56	6.63	14.0
5	6.33	12.39	6.06	14.7
4	6.40	12.43	6.03	15.2
3	6.83	12.92	6.10	15.7
2	7.10	12.96	5.87	16.1

Table 20 Profile of u_{in} at J_{g1} = 1.5 cm/s and J_{g2} = 3.0 cm/s

Cell	ε_{g1} (%)	ε_{g2} (%)	ε_{g2}-ε_{g1} (%)	u_{in} (cm/s)
6	6.82	15.56	8.74	13.5
5	6.41	14.26	7.85	14.5
4	6.25	13.91	7.66	15.1
3	6.68	14.18	7.50	15.6
2	6.91	13.69	6.79	16.0

Table 21 Profile of u_{in} at J_{g1} = 2.0 cm/s and J_{g2} = 0

Cell	ε_{g1} (%)	ε_{g2} (%)	ε_{g2}-ε_{g1} (%)	u_{in} (cm/s)
6	9.88	0.00	-9.88	18.6
5	9.02	0.00	-9.02	18.8
4	9.35	0.00	-9.35	18.8
3	9.63	0.00	-9.63	18.9
2	9.78	0.00	-9.78	18.9

Table 22 Profile of u_{in} at J_{g1} = 2.0 cm/s and J_{g2} = 0.4 cm/s

Cell	ε_{g1} (%)	ε_{g2} (%)	ε_{g2}-ε_{g1} (%)	u_{in} (cm/s)
6	10.08	1.73	-8.35	18.1
5	9.21	1.68	-7.53	18.1
4	8.87	1.13	-7.74	18.1
3	8.86	1.11	-7.75	18.1
2	8.74	1.46	-7.28	17.8

Table 23 Profile of u_{in} at J_{g1} = 2.0 cm/s and J_{g2} = 0.8 cm/s

Cell	ε_{g1} (%)	ε_{g2} (%)	ε_{g2}-ε_{g1} (%)	u_{in} (cm/s)
6	10.02	3.45	-6.57	17.3
5	9.10	2.73	-6.37	17.3
4	8.78	2.46	-6.32	17.4
3	8.82	2.35	-6.47	17.2
2	8.50	2.25	-6.25	17.0

Table 24 Profile of u_{in} at J_{g1} = 2.0 cm/s and J_{g2} = 1.2 cm/s

Cell	ε_{g1} (%)	ε_{g2} (%)	ε_{g2}-ε_{g1} (%)	u_{in} (cm/s)
6	9.94	5.54	-4.40	17.0
5	9.06	4.89	-4.17	16.8
4	8.84	4.70	-4.15	16.8
3	8.93	4.62	-4.31	16.6
2	8.60	4.81	-3.79	16.6

Table 25 Profile of u_{in} at J_{g1} = 2.0 cm/s and J_{g2} = 1.6 cm/s

Cell	ε_{g1} (%)	ε_{g2} (%)	ε_{g2}-ε_{g1} (%)	u_{in} (cm/s)
6	10.04	7.71	-2.33	16.0
5	9.22	7.03	-2.20	16.2
4	8.81	6.69	-2.12	16.2
3	9.07	6.96	-2.10	16.1
2	8.78	6.92	-1.85	16.1

Table 26 Profile of u_{in} at J_{g1} = 2.0 cm/s and J_{g2} = 2.4 cm/s

Cell	ε_{g1} (%)	ε_{g2} (%)	ε_{g2}-ε_{g1} (%)	u_{in} (cm/s)
6	9.21	11.55	2.34	15.1
5	8.55	10.76	2.21	14.9
4	8.40	10.63	2.23	15.1
3	8.69	10.93	2.24	15.1
2	8.63	10.65	2.02	15.4

Table 27 Profile of u_{in} at J_{g1} = 2.0 cm/s and J_{g2} = 2.8 cm/s

Cell	ε_{g1} (%)	ε_{g2} (%)	ε_{g2}-ε_{g1} (%)	u_{in} (cm/s)
6	9.57	13.93	4.36	14.6
5	8.55	12.86	4.31	14.5
4	8.39	12.63	4.23	14.6
3	8.78	13.01	4.23	15.0
2	9.00	12.76	3.76	15.3

Table 28 Profile of u_{in} at J_{g1} = 2.0 cm/s and J_{g2} = 3.2 cm/s

Cell	ε_{g1} (%)	ε_{g2} (%)	ε_{g2}-ε_{g1} (%)	u_{in} (cm/s)
6	9.35	16.08	6.73	13.5
5	8.53	14.69	6.16	14.2
4	8.34	14.24	5.91	14.6
3	8.61	14.14	5.53	14.9
2	8.68	13.63	4.95	15.2

Table 29 Profile of u_{in} at J_{g1} = 2.0 cm/s and J_{g2} = 3.6 cm/s

Cell	ε_{g1} (%)	ε_{g2} (%)	ε_{g2}-ε_{g1} (%)	u_{in} (cm/s)
6	9.25	18.47	9.22	13.1
5	8.54	16.68	8.15	13.9
4	8.36	16.01	7.64	14.3
3	8.49	15.59	7.10	14.8
2	8.76	14.59	5.83	15.0

Table 30 Profile of u_{in} at J_{g1} = 2.0 cm/s and J_{g2} = 4.0 cm/s

Cell	ε_{g1} (%)	ε_{g2} (%)	ε_{g2}-ε_{g1} (%)	u_{in} (cm/s)
6	9.27	20.82	11.55	12.5
5	8.43	18.27	9.84	13.7
4	8.33	17.04	8.72	14.2
3	8.34	15.69	7.34	14.8
2	8.36	14.82	6.46	15.0

Table 31 Profile of u_{in} at J_{g1} = 2.5 cm/s and J_{g2} = 0

Cell	ε_{g1} (%)	ε_{g2} (%)	ε_{g2}-ε_{g1} (%)	u_{in} (cm/s)
6	12.39	0	-12.39	17.6
5	11.42	0	-11.42	18.4
4	10.86	0	-10.86	18.0
3	11.08	0	-11.08	19.2
2	12.31	0	-12.31	18.0

Table 32 Profile of u_{in} at J_{g1} = 2.5 cm/s and J_{g2} = 0.5 cm/s

Cell	ε_{g1} (%)	ε_{g2} (%)	ε_{g2}-ε_{g1} (%)	u_{in} (cm/s)
6	12.91	2.23	-10.68	17.3
5	11.79	1.83	-9.96	17.2
4	11.16	2.20	-8.96	17.2
3	11.59	2.52	-9.07	16.5
2	11.99	2.84	-9.15	17.0

Table 33 Profile of u_{in} at J_{g1} = 2.5 cm/s and J_{g2} = 1.0 cm/s

Cell	ε_{g1} (%)	ε_{g2} (%)	ε_{g2}-ε_{g1} (%)	u_{in} (cm/s)
6	12.98	4.59	-8.39	16.6
5	11.88	3.79	-8.09	16.4
4	11.39	3.50	-7.89	16.4
3	11.45	4.90	-6.55	16.1
2	11.66	5.27	-6.39	15.8

Table 34 Profile of u_{in} at J_{g1} = 2.5 cm/s and J_{g2} = 1.5 cm/s

Cell	ε_{g1} (%)	ε_{g2} (%)	ε_{g2}-ε_{g1} (%)	u_{in} (cm/s)
6	12.65	7.22	-5.43	15.3
5	11.52	6.46	-5.05	15.5
4	11.98	6.24	-5.74	15.5
3	11.36	6.33	-5.03	15.1
2	11.41	6.28	-5.13	15.3

Table 35 Profile of u_{in} at J_{g1} = 3.0 cm/s and J_{g2} = 2.0 cm/s

Cell	ε_{g1} (%)	ε_{g2} (%)	ε_{g2}-ε_{g1} (%)	u_{in} (cm/s)
6	12.80	10.03	-2.77	14.8
5	11.76	9.17	-2.59	14.7
4	11.17	8.91	-2.26	14.7
3	11.58	8.85	-2.73	14.6
2	11.98	8.63	-3.35	14.6

Table 36 Profile of u_{in} at J_{g1} = 2.5 cm/s and J_{g2} = 3.0 cm/s

Cell	ε_{g1} (%)	ε_{g2} (%)	ε_{g2}-ε_{g1} (%)	u_{in} (cm/s)
6	12.72	15.62	2.90	13.6
5	11.90	14.35	2.45	13.7
4	11.79	13.96	2.17	13.5
3	12.08	14.30	2.22	14.0
2	12.16	13.71	1.55	13.9

Table 37 Profile of u_{in} at J_{g1} = 2.5 cm/s and J_{g2} = 3.25 cm/s

Cell	ε_{g1} (%)	ε_{g2} (%)	ε_{g2}-ε_{g1} (%)	u_{in} (cm/s)
6	12.81	16.73	3.92	12.9
5	11.97	15.36	3.39	13.3
4	11.85	14.85	3.00	13.4
3	12.13	14.71	2.58	13.8
2	11.88	14.02	2.15	14.0

Table 38 Profile of u_{in} at J_{g1} = 2.5 cm/s and J_{g2} = 3.5 cm/s

Cell	ε_{g1} (%)	ε_{g2} (%)	ε_{g2}-ε_{g1} (%)	u_{in} (cm/s)
6	12.92	18.61	5.69	12.6
5	11.91	16.68	4.77	13.0
4	11.99	16.12	4.13	13.3
3	12.14	15.88	3.74	13.7
2	11.85	14.64	2.79	13.9

Table 39 Profile of u_{in} at J_{g1} = 2.5 cm/s and J_{g2} = 3.75 cm/s

Cell	ε_{g1} (%)	ε_{g2} (%)	ε_{g2}-ε_{g1} (%)	u_{in} (cm/s)
6	12.83	19.68	6.85	12.3
5	11.89	17.57	5.68	12.7
4	11.68	16.48	4.81	13.3
3	11.93	15.71	3.78	13.7
2	11.45	14.67	3.22	13.9

Table 40 Profile of u_{in} at J_{g1} = 2.5 cm/s and J_{g2} = 4.0 cm/s

Cell	ε_{g1} (%)	ε_{g2} (%)	ε_{g2}-ε_{g1} (%)	u_{in} (cm/s)
6	12.84	21.06	8.22	11.8
5	11.86	18.69	6.84	12.7
4	11.86	17.21	5.35	13.0
3	12.30	16.51	4.21	13.5
2	11.82	16.38	4.57	13.9

Table 41 Profile of u_{in} at $J_{g1} = 3.0$ cm/s and $J_{g2} = 0$

Cell	ε_{g1} (%)	ε_{g2} (%)	ε_{g2}-ε_{g1} (%)	u_{in} (cm/s)
6	15.35	0	-15.35	16.9
5	14.34	0	-14.34	17.1
4	14.26	0	-14.26	17.3
3	14.58	0	-14.58	17.5
2	14.88	0	-14.88	16.9

Table 42 Profile of u_{in} at $J_{g1} = 3.0$ cm/s and $J_{g2} = 0.6$ cm/s

Cell	ε_{g1} (%)	ε_{g2} (%)	ε_{g2}-ε_{g1} (%)	u_{in} (cm/s)
6	15.69	2.63	-13.06	15.8
5	14.11	2.48	-11.63	16.0
4	14.72	2.63	-12.09	15.8
3	14.74	3.04	-11.70	16.8
2	14.63	3.21	-11.42	15.8

Table 43 Profile of u_{in} at $J_{g1} = 3.0$ cm/s and $J_{g2} = 1.2$ cm/s

Cell	ε_{g1} (%)	ε_{g2} (%)	ε_{g2}-ε_{g1} (%)	u_{in} (cm/s)
6	15.89	5.56	-10.33	15.3
5	14.21	4.87	-9.34	14.9
4	14.27	5.66	-8.61	15.1
3	14.50	6.29	-8.21	14.5
2	14.81	6.64	-8.17	14.7

Table 44 Profile of u_{in} at J_{g1} = 3.0 cm/s and J_{g2} = 1.8 cm/s

Cell	ε_{g1} (%)	ε_{g2} (%)	ε_{g2}-ε_{g1} (%)	u_{in} (cm/s)
6	16.01	9.05	-6.96	14.1
5	14.32	8.12	-6.20	14.0
4	14.29	7.87	-6.42	13.8
3	14.54	7.95	-6.59	13.6
2	14.51	7.72	-6.79	14.4

Table 45 Profile of u_{in} at J_{g1} = 3.0 cm/s and J_{g2} = 2.4 cm/s

Cell	ε_{g1} (%)	ε_{g2} (%)	ε_{g2}-ε_{g1} (%)	u_{in} (cm/s)
6	15.84	12.5	-3.34	13.2
5	14.24	11.35	-2.89	13.2
4	14.31	10.97	-3.34	13.0
3	14.72	10.95	-3.77	12.9
2	14.71	10.76	-3.95	-

Table 46 Profile of u_{in} at J_{g1} = 3.0 cm/s and J_{g2} = 3.3 cm/s

Cell	ε_{g1} (%)	ε_{g2} (%)	ε_{g2}-ε_{g1} (%)	u_{in} (cm/s)
6	15.75	17.72	1.97	12.0
5	14.74	16.35	1.61	12.0
4	14.60	16.03	1.43	12.2
3	14.84	15.95	1.11	12.4
2	14.95	16.08	1.13	-

Table 47 Profile of u_{in} at J_{g1} = 3.0 cm/s and J_{g2} = 3.6 cm/s

Cell	ε_{g1} (%)	ε_{g2} (%)	ε_{g2}-ε_{g1} (%)	u_{in} (cm/s)
6	15.80	19.66	3.86	11.7
5	14.71	17.91	3.20	11.6
4	14.61	17.14	2.54	11.6
3	14.78	16.82	2.04	12.2
2	14.39	16.53	2.14	-

Table 48 Profile of u_{in} at J_{g1} = 3.0 cm/s and J_{g2} = 3.9 cm/s

Cell	ε_{g1} (%)	ε_{g2} (%)	ε_{g2}-ε_{g1} (%)	u_{in} (cm/s)
6	15.72	21.17	5.45	10.7
5	14.93	19.21	4.28	11.5
4	14.73	18.05	3.32	11.7
3	14.71	17.00	2.30	12.0
2	14.34	16.79	2.45	-

APPENDIX 4

Properties of Frothers DF250C and DF1263

The full names for DF250C and DF1263 are Dowfroth 250C and Dowfroth 1263, respectively. As flotation frothers, they are manufactured by Dow Chemical Company. The DF250C and DF1263 are methoxy polypropylene glycols (polypropylene glycol methyl ethers), with the general formula:

$$CH_3 - (O - C_3 H_6)_n - OH$$

where n is about 4 for DF250C and is about 5 for DF1263. The following table gives the properties for the two frothers (Dow Chemical Company, 1976; Crozier, 1992).

Table 1 Properties of DF250C and DF1263

Dowfroth	Molecular weight	Density (25°C)	Boiling Pt. °C	Freeze Pt. °C	pH
250C	250	0.98	252	< -50	7.2
1263	348	0.978	299	< -41	-

APPENDIX 5

Proof for an Inequality

If f and g are continuous on a closed interval $[a,b]$, and f and g increase or decrease at the same point in $[a,b]$, for x and y in the interval $[a,b]$, we have

$$[\,f(x) - f(y)\,]\,[\,g(x) - g(y)\,] \geq 0 \tag{A.1}$$

The definite integral of this inequality for x from a to b is given by

$$\int_a^b [\,f(x) - f(y)\,]\,[\,g(x) - g(y)\,]\,dx \geq 0 \tag{A.2}$$

and we obtain

$$\int_a^b f(x)\,g(x)\,dx - f(y)\int_a^b g(x)\,dx - g(y)\int_a^b f(x)\,dx + f(y)\,g(y)\int_a^b dx \geq 0 \tag{A.3}$$

The definite integral of the inequality A.3 for y from a to b is given by

$$\begin{aligned}&\int_a^b f(x)\,g(x)\,dx\int_a^b dy - \int_a^b f(y)\,dy\int_a^b g(x)\,dx\\ &- \int_a^b g(y)\,dy\int_a^b f(x)\,dx + \int_a^b f(y)\,g(y)\,dy\int_a^b dx \geq 0\end{aligned} \tag{A.4}$$

and we have

$$\begin{aligned}&(b-a)\int_a^b f(x)\,g(x)\,dx - \int_a^b f(y)\,dy\int_a^b g(x)\,dx\\ &- \int_a^b g(y)\,dy\int_a^b f(x)\,dx + (b-a)\int_a^b f(y)\,g(y)\,dy \geq 0\end{aligned} \tag{A.5}$$

Note $f(y)$ is the equivalent of $f(x)$ and $g(y)$ is the equivalent of $g(x)$. The inequality A.5 can be rearranged as

$$2\,(b-a)\int_a^b f(x)\,g(x)\,dx \geq 2\int_a^b f(x)\,dx\int_a^b g(x)\,dx \tag{A.6}$$

Finally, we obtain

$$(b - a) \int_a^b f(x)\, g(x)\, dx \geq \int_a^b f(x)\, dx \int_a^b g(x)\, dx \qquad \textbf{(A.7)}$$

If $a = 0$ and $b = 1$, the inequality A.7 becomes

$$\int_0^1 f(x)\, g(x)\, dx \geq \int_0^1 f(x)\, dx \int_0^1 g(x)\, dx \qquad \textbf{(A.8)}$$

Conversely, if f increases as g decreases, or f decreases as g increases in the interval $[a,b]$, we have

$$[f(x) - f(y)]\,[g(x) - g(y)] \leq 0 \qquad \textbf{(A.9)}$$

With the same method, we can prove

$$(b - a) \int_a^b f(x)\, g(x)\, dx \leq \int_a^b f(x)\, dx \int_a^b g(x)\, dx \qquad \textbf{(A.10)}$$